COLLAGEN TYPE I AND II BLEND HYDROGELS FOR ARTICULAR CARTILAGE TISSUE ENGINEERING

by

Claire Kilmer

A Dissertation

Submitted to the Faculty of Purdue University

In Partial Fulfillment of the Requirements for the degree of

Doctor of Philosophy

Davidson School of Chemical Engineering

West Lafayette, Indiana

August 2019

THE PURDUE UNIVERSITY GRADUATE SCHOOL
STATEMENT OF COMMITTEE APPROVAL

Dr. Julie C. Liu, Chair
Davidson School of Chemical Engineering

Dr. Alyssa Panitch, Chair
Weldon School of Biomedical Engineering

Dr. Gert J. Breur
Department of Veterinary Medicine

Dr. John Morgan
Davidson School of Chemical Engineering

Dr. Stephen Beaudoin
Davidson School of Chemical Engineering

Approved by:

Dr. Sangtae Kim
Head of the Graduate Program

To Mom, Dad, Katey, and Josh

ACKNOWLEDGMENTS

My journey here at Purdue would never have been possible without the support and encouragement from so many different people. First, I would like to thank my advisors Dr. Julie Liu and Dr. Alyssa Panitch for guidance and financial support during my time at Purdue. Without your mentorship I would never been able to become the scientist and researcher I am today. I would also like to thank Dr. Gert Breur for his constant encouragement throughout the animal study and many conversations about sea turtle shells. Meetings with you were always a bright spot in my week. I would also like to thank the rest of my committee, Dr. John Morgan and Dr. Stephen Beaudoin, for insightful questions at different points during my time researching cartilage.

I would like to extend a thank you to Dr. Abby Cox, Robyn McCain, Christa Crain, Victor Bernal-Crespo, Kris Kazmierczak, Shery Park, and Cheryl Anderson of the Purdue College of Veterinary Medicine for teaching me more than I ever thought I could learn about rabbits and bringing a few more puppies into my life.

There are so many other people that have helped me through graduate school including past and present Liu and Panitch laboratory members. I would like to thank Dr. Tanaya Walimbe for amazing conversation and collaboration as both a lab mate and friend. You are a special human, and I know I could have never done graduate school without you. To Celina Twitchell, thank you for walking through graduate school with me and always helping me troubleshoot. A huge thank you to Dr. Charng-yu Lin and Nelda Vázquez-Portalatín for training me in numerous experiments throughout the years and answering more questions than I ever thought was possible. To Carly, Bradley, and Jessica, I am so excited to see what these next few years have in store for you guys.

A special thank you is essential to my roommate Dr. Kelly Higgins. Thank you for being there when I needed you most. To my other amazing roommates, Elizabeth, Trace, Grim, and Julia, thank you for always cheering me up when I was down and making West Lafayette feel like home.

Finally, I would like to thank my Mom, Dad, and Katey for their constant love and support both throughout my childhood and during my time in graduate school. Josh Shepherd, thank you for sticking with me through these years, and I am excited for you to be by my side in our next adventure.

TABLE OF CONTENTS

LIST OF TABLES

LIST OF FIGURES

ABSTRACT

Author: Kilmer, Claire, E. PhD
Institution: Purdue University
Degree Received: August 2019
Title: Collagen Type I and II Blend Hydrogels for Articular Cartilage Tissue Engineering
Major Professor: Julie Liu

Osteoarthritis (OA) is a debilitating condition that affects over 27 million Americans and is defined by degradation in articular cartilage extracellular matrix. Patients suffer from pain and stiffness in the joints associated with the onset of OA. Tissue that is damaged by OA is a major health concern since cartilage tissue has a limited ability to self-repair due to the lack of vasculature in cartilage and low cell content. Tissue engineering seeks to repair damaged cartilage by introducing an optimized combination of cells, scaffold, and bioactive factors that can be transplanted into a patient.

Collagen type II is a promising material to repair cartilage defects since it is a major component of articular cartilage and plays a key role in chondrocyte function. This work harnesses the biological activity of collagen type II and the superior mechanical properties of collagen type I by characterizing gels made of collagen type I and II blends (1:0, 3:1, 1:1, 1:3, and 0:1). The collagen blend hydrogels were able to incorporate both types of collagen, chondroitin sulfate (CS), and hyaluronic acid. Cryo-scanning electron microscopy images showed that the 3:1 ratio of collagen type I to type II gels had a lower void space percentage (36.4%) than the 1:1 gels (46.5%). The complex modulus was larger for the 3:1 gels (G* = 5.0 Pa) compared to the 1:1 gels (G* = 1.2 Pa). The 3:1 blend consistently formed gels with superior mechanical properties compared to the other blends and showed the potential to be implemented as a scaffold for articular cartilage engineering.

Building on the characterization work, this study examined the chondrogenic differentiation of bone marrow-derived mesenchymal stem cells (MSCs) embedded within a 3:1 collagen type I to II blend (Col I/II) hydrogel or an all collagen type I (Col I) hydrogel. Glycosaminoglycan (GAG) production in Col I/II hydrogels was statistically higher than in Col I hydrogels or pellet culture, and these results suggested that adding collagen type II promoted GAG production. Col I/II hydrogels had statistically lower alkaline phosphatase (AP) activity than pellets cultured in

chondrogenic medium. The ability of MSCs encapsulated in Col I/II hydrogels to repair cartilage defects was investigated by creating two defects in the femurs of rabbits. After 13 weeks, histochemical staining suggested that Col I/II blend hydrogels provided favorable conditions for cartilage repair. Histological scoring revealed a statistically higher cartilage repair score for the Col I/II hydrogels compared to either the Col I hydrogels or empty defect controls. Results from this study suggest that there is clinical value in the cartilage repair capabilities of our Col I/II hydrogel with encapsulated MSCs.

There are many examples of collagen hydrogels with incorporated CS here the addition of CS has been shown to improve scaffolds for articular cartilage tissue engineering. Our final study investigated the use of CS with attached collagen binding peptides to retain, without the use of chemical crosslinking, matrix molecules and better recapitulate aspects of native cartilage in a Col I/II hydrogel with encapsulated MSCs. The number of SILY peptides attached to a CS backbone was varied to create 3 different molecules: CS-10SILY, CS-15SILY, and CS-20SILY, with 10, 15, and 20 denoting the number of SILY peptides attached to CS. As CS retention, average fibril diameter, and mechanical properties are altered by the addition of different CS-SILY molecules, the physical properties of the desired Col I/II hydrogel can be tuned by adjusting the amount of SILY peptides attached to the CS backbone. In addition, the scaffolds that contained CS-10SILY, CS-15SILY, and CS-20SILY had higher GAG production which suggests better differentiation of MSCs into chondrocytes in scaffolds that contain a CS-SILY molecule. Taken together, these results suggested that the addition of a CS-SILY molecule to a Col I/II hydrogel with encapsulated MSCs has the potential to promote cartilage repair.

1. INTRODUCTION

1.1 Motivation

Osteoarthritis (OA) is a debilitating condition that affects over 30 million Americans and is defined by degradation in articular cartilage extracellular matrix (ECM).[1] OA causes pain and stiffness in the joints of almost half of the population at some point in their life.[2] Tissue that is damaged by OA is a major health concern since cartilage tissue has a limited ability to self-repair due to low cell content and lack of vasculature.[3] Patients with OA suffer from pain and stiffness in the joints causing loss of mobility and the inability to work. Medical expenses directly related to OA total $13.2 billion per year in the United States.[4] Although there is no cure for OA, there are many treatment options including osteochondral grafts, autologous chondrocyte implantation, and marrow stimulation.[5] However, these invasive options are associated with long rehabilitation times for temporary results and usually promote the regrowth of fibrocartilage, which has mechanical properties inferior to native, hyaline cartilage.[5] Our tissue engineering approach seeks to repair damaged cartilage by introducing an optimized combination of cells, scaffold, and bioactive factors that can be transplanted into a patient.[6]

1.2 The Knee Joint

Although often thought of as a simple hinge, the knee joint is a complex combination of many different tissue types. The tibia, femur, and patella are the three bones that come together to form the knee joint. The knee is primarily supported by a network of ligaments, which connect bone to bone, while the muscles and tendons, which connect muscle to bone around the knee, provide secondary support.[7] The joint capsule is made up of a fibrous outer layer that surrounds the knee to keep joint fluid in position and provide stability.[8] Cells from the inner layer of synovial membrane secrete synovial fluid that lubricates articulating surfaces and nourishes the joint. Inside the joint, two menisci made of fibrocartilage distribute joint loads, stabilize movement of the joint, and create a more congruent space between the femur and tibia. Articular cartilage is weight-bearing connective tissue that covers the surfaces of diarthrodial joints. It is important to understand the form and function of articular cartilage to create an environment that will effectively regenerate damaged cartilage tissue.

1.3 Articular Cartilage

Articular cartilage, which can withstand excessive loading up to 8 to 10 times an individual's body weight, provides a low-friction, lubricated surface that dissipates the high stresses associated with joint motion.[9,10] The tissue is made up of one cell type, chondrocytes, embedded in a three-dimensional ECM. The ECM, which is 90% of the dry weight of cartilage, is made up of collagen fibrils, proteoglycans, glycoproteins, and water.[11,12] Mature articular cartilage is composed of dense connective tissue containing no blood vessels and is separated into four different zones (Figure 1-1).

Each cartilage zone consists of a different alignment of collagen fibers, which provide structural and elastic strength, and varied distribution of proteoglycans, which allow the tissue to withstand high compressive forces (Figure 1-1B) [13] The diverse ECM organization of cartilage leads to different mechanical properties including an increase in the ability to resist compressive strain deeper into the tissue.[14] In the deep zone, vertical collagen fibers protect against large strains experienced at the junction of bone and cartilage.[15] The middle, or transition, zone consists of randomly aligned collagen fibers. Horizontal fibers in the superficial tangential zone (STZ) resist tensile stresses parallel to the surface of articular cartilage.[16] Collagen fibril alignment also plays a fundamental role in cell biosynthesis of ECM components and phenotype.[17,18] Depending on the region of articular cartilage, the shape, number, and size of chondrocytes can also vary (Figure 1-1A). Compared to chondrocytes in deeper matrix, chondrocytes in the superficial zone are flatter, smaller, and greater in density.[19]

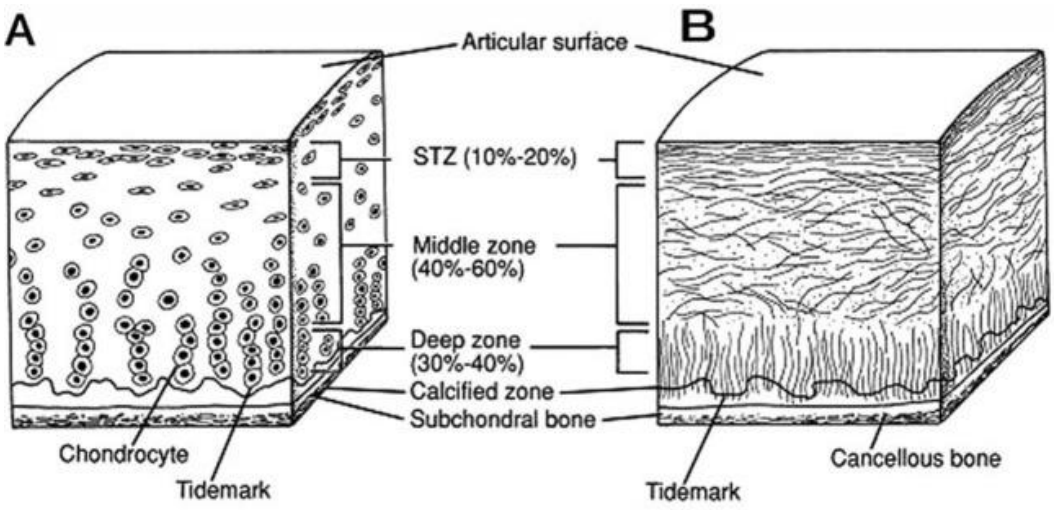

Figure 1-1. Cartilage Organization.

A cross-section of healthy articular cartilage to better understand the (A) cellular and (B) collagen fiber organization.[20]

1.3.1 The Cells of Articular Cartilage

Chondrocyte cells in cartilage are responsible for both producing and maintaining the ECM through a homeostatic balance of cartilage synthesis and degradation while only occupying 5% of the total tissue volume.[21] Each chondrocyte establishes its own microenvironment where it is responsible for matrix formation, degradation, and remodeling of its immediate surroundings. The chondrocyte is then entrapped in the matrix that it has produced which prevents migration and hinders cell-to-cell contact. Due to a lack of cell-to-cell contact, chondrocytes depend on several chemical and mechanical cues, including growth factors, mechanical loads, and hydrostatic pressures, from their environment to regulate their activity. Chondrocytes can survive in a hypoxic environment, due to the lack of vascularization, where oxygen levels are between 0.5% and 5%. Hypoxia has been shown to promote the synthesis of ECM molecules by chondrocytes.[22] Chondrocytes have limited replication potential, which hinders the tissue's response to injury, and the density of chondrocytes in articular cartilage diminish with age.

1.3.2 The Extracellular Matrix of Articular Cartilage

Collagen types II, IX, X, and XI impart the cartilage framework with its shape and strength. Collagen type II is the predominant collagen found in cartilage and consists of three identical α1(II) helical polypeptide units that are encoded by the *col2a1* gene and combine to form

tropocollagen.[23] The α chains of different collagen monomers are joined by intermolecular crosslinks forming a collagen network.[23] Collagen fibrillogenesis, the spontaneous self-assembly of collagen monomers into fibrils and then larger collagen fibers, occurs at physiological conditions (e.g., a temperature of 37°C and a pH of 7.4).[24,25] The collagen fibril network functions as the 3D architecture of the cartilage ECM and has high tensile strength. In addition, collagen networks undergo constant remodeling by chondrocytes and also entrap heavily glycosolated protein monomers known as proteoglycan molecules.[21,26,27] The negative charge of proteoglycans entrapped in collagen results in an influx and retention of water in the tissue, and this water retention gives cartilage a high compressive.[13,21]

Proteoglycans present in cartilage tissue include aggrecan, decorin, biglycan, lumican, and fibromodulin. Aggrecan is a large hyaluronic acid (HA)-binding proteoglycan that is made up of chondroitin sulfate (CS) and keratin sulfate (KS) glycosaminoglycans covalently attached to a protein core. It is the largest and most predominant proteoglycan by weight in cartilage and makes up between 5-15% of the dry weight.[28] The protein backbone of aggrecan is divided into three different segments, or globular domains, that together are ~230 kDa in molecular weight.[21] About 90% of the mass of aggrecan is composed of glycosaminoglycan (GAG) chains, including CS, KS, and N/O-linked oligosaccharides. The GAG chains bind to an area between G2, the second globular domain of aggrecan, and G3, the third globular domain of aggrecan.[29] On average, 100 CS and 30 KS molecules bind within the GAG-binding region.[30] Between G1, the first globular domain of aggrecan, and G2 lies the interglobular domain (IGD), which is the most susceptible region to proteolytic cleavage.[31]

The G1 domain is able to bind to HA through the link protein, which facilitates interactions between the two and can lead to the formation of aggregates.[32,33] The aggregates that form consist of over 100 molecules of aggrecan attached to a single HA chain via link proteins.[29] The aggrecan and HA aggregates have a high negative charge density due to the slightly negatively-charged HA chain and the charge contribution from the sulfate and carboxyl groups of GAG side chains of aggrecan.[21,34] The negatively-charged chains cause the aggregates to become hydrated. Osmotic pressure then builds up within the cartilage ECM due to mobile cations that are attracted to aggrecan.[35] These properties of aggrecan give cartilage its unique properties of high compressive strength and resilience during joint loading.[36] The second globular domain of aggrecan, G2, has many of the same structural features as G1 but lacks the ability to bind with HA.[37] Although the

final globular domain on the C-terminus region, G3, contains two epidermal growth factor-like domains and a complement regulatory protein module, the functions of these modules by themselves are unclear. The number of aggrecan monomers with an intact G3 domain decreases with age, and it is believed that this domain may facilitate attachment of GAGs.[21,38] Degradation of the native ECM architecture of cartilage, as discussed in the previous section, causes a condition known as osteoarthritis.

1.4 Osteoarthritis

There are many triggers, including mechanical injury that causes subsequent tissue damage or inflammation that triggers synthesis of cytokines such as interleukin-1 beta (IL-1β), that initiate degradation of articular cartilage during OA.[4,39] Different forms of OA are traditionally broken down into two categories: primary and secondary.[40] Primary OA is idiopathic, meaning the cause is unknown, and the condition arises spontaneously.[41] Patients with primary OA often have joints with abnormalities in the structural materials and biomechanics. Secondary OA is often known as post traumatic OA and results from injury or disease.[41] Progression of OA is due to both mechanical wear at the joint level and biochemical changes from enzymatic degradation.

1.4.1 Osteoarthritis Pathogenesis: Joint Level

OA causes changes to various parts of the knee joint including cartilage, bone, and synovium (Figure 1-2). Breakdown of articular cartilage, development of osteophytes, sclerosis of subchondral bone, formation of bone marrow lesions, and progression of synovial hyperplasia are all characteristics of the disorder.[41] Healthy cartilage is a smooth, white or yellow coating on articular surfaces (Figure 1-3A). In contrast, the cartilage of patients with OA is soft with a yellow or brown color, and the otherwise smooth articular cartilage surface becomes rough until fibrillation, or early splits in the cartilage occuring parallel to the surface, occurs. In later stages of the disease, vertical splits in cartilage penetrate deep into the tissue until they reach and expose the subchondral bone. As cartilage is lost overtime, the tissue becomes thinner starting from the superficial zone.

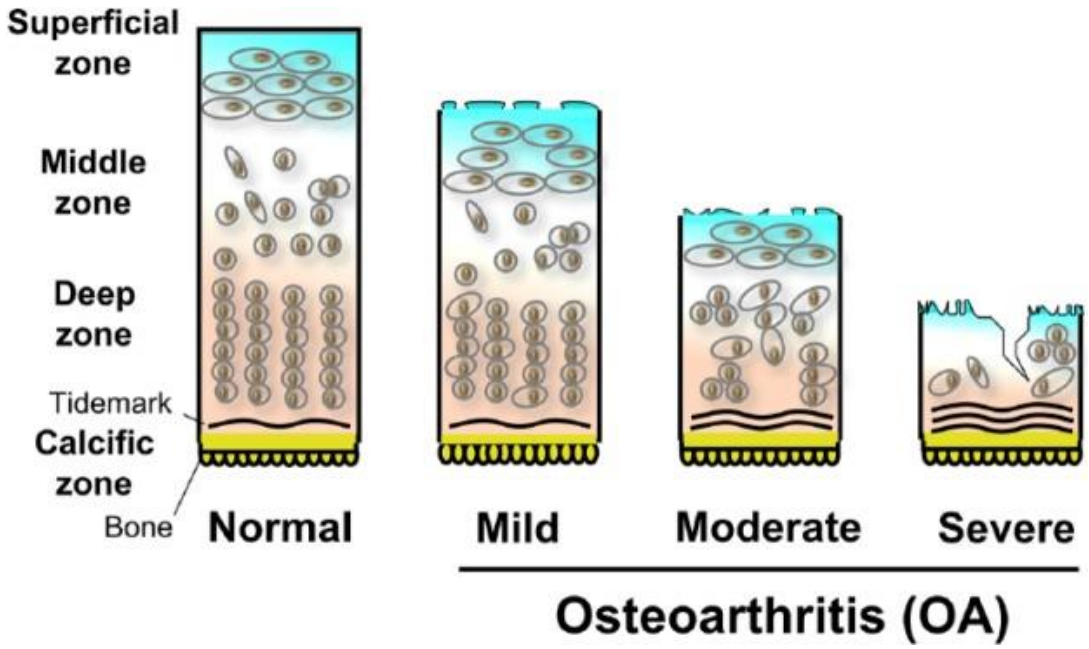

Figure 1-2. Osteoarthritic Degradation.

A comparison of normal articular cartilage to osteoarthritic cartilage at different stages (mild, moderate, and severe). [42]

In the development of OA, the stiffening and increase in the density of subchondral bone is known as sclerosis. Despite an increase in bone density, abnormal bone remodeling causes the subcentral bone to become hypomineralized. In areas where underlying bone is completely exposed, bone cysts can form when synovial fluid comes into contact with bone marrow.[43] Osteophytes, or bone projections, form along the margins of joints that are non-weight bearing regions (i.e. these regions do not take part in the process of articulating). Joint stiffness is often caused by a shortening and thickening to the joint capsule, and the synovial lining also becomes thicker due to synovial hyperplasia.[4445]

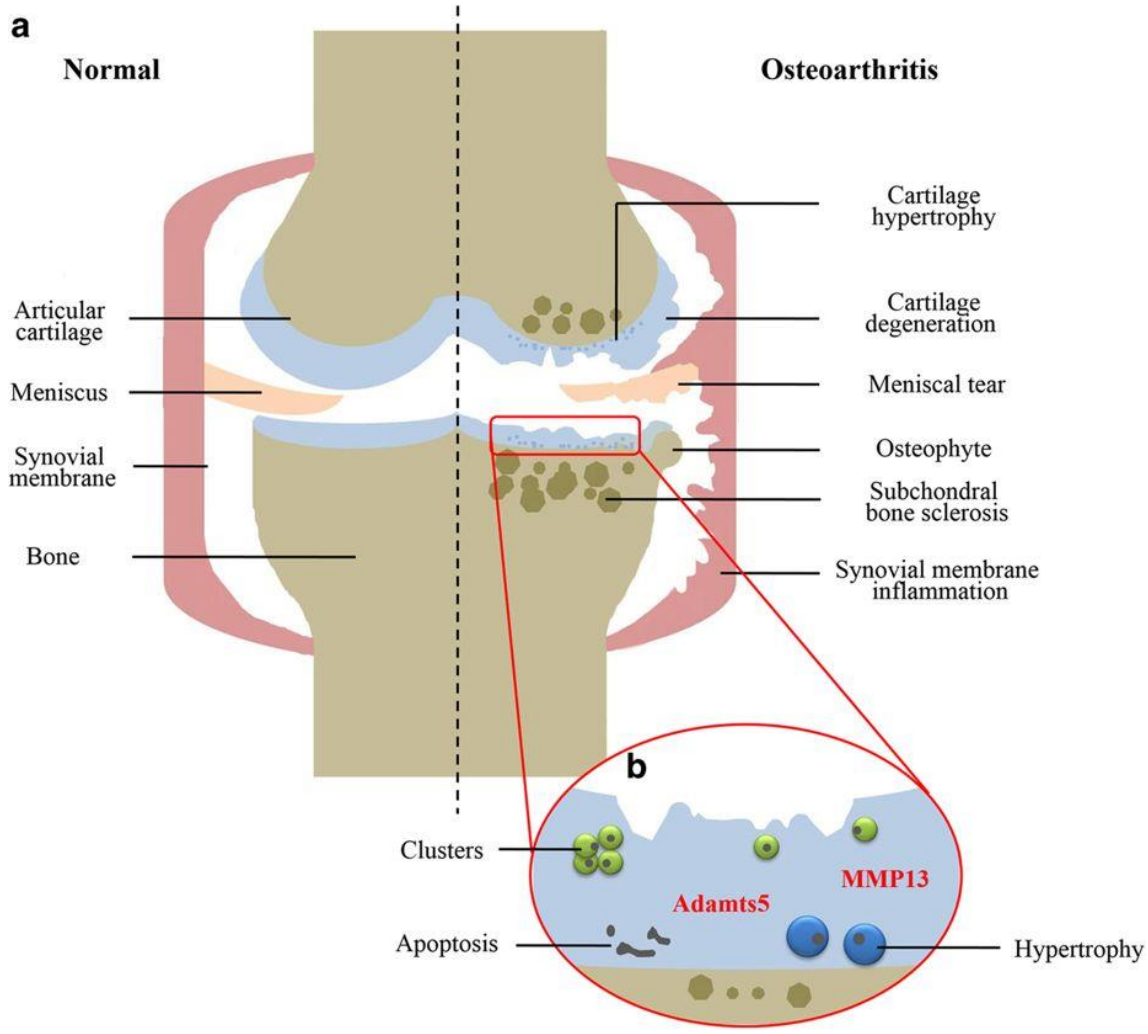

Figure 1-3. A Comparison of Healthy and Osteoarthritic Tissue.

A comparison of normal articular cartilage to osteoarthritic cartilage at a (a) joint and (b) biochemical level. [46]

1.4.2 Osteoarthritis Pathogenesis: Biochemical Changes

The pathogenesis of OA includes damage or alteration of the ECM network, response of chondrocytes to the damaged tissue, and failure of chondrocytes to restore cartilage followed by progressive loss of tissue.[39] The role of chondrocytes within articular cartilage is to maintain a state of homeostasis by keeping anabolic and catabolic activities in equilibrium.[39] Cytokines and growth factors are found in low concentrations in the synovial fluid and act as regulatory factors for chondrocytes during normal ECM turnover.[47] Careful regulation is required for proteolytic enzymes that mediate cartilage degradation.[30] For example, the key enzymes that mediate the

degradation of ECM molecules are matrix metalloproteinases (MMPs) that cleave collagen type II, aggrecanases that cleave aggrecan, and hyaluronidases that cleave hyaluronic acid (Figure 1-3B).[48] MMPs are overexpressed in the cartilage of patients suffering from OA.[49] In particular, MMP-1, MMP-3, and MMP-13 are thought to be the MMPs associated with lesion development in OA patients.[50] Early changes due to degradation begin in the superficial zone of articular cartilage where cartilage fragments are released into the joint space.[51,52] Synovial cells are recruited and become activated, producing catabolic and pro-inflammatory cytokines and growth factors, when they come into contact with the cartilage fragments.[53] The catabolic cytokines and growth factors activate chondrocytes to produce MMPs and other proteolytic enzymes, which result in further cartilage breakdown in the cycle of OA.[48]

Aggrecan, a glycosaminoglycan that plays an important structural role in cartilage as previously discussed, should be protected since degradation of this proteoglycan causes other components of the ECM to become susceptible to degradation. Aggrecan and HA take on a protective role by hindering diffusion of enzymes that can cleave ECM components.[54] However, aggrecan is one of the first matrix components to be degraded during the initial progression of OA. The protein core of aggrecan is cleaved by two enzymes: a disintegrin and metalloproteinase with thrombospondin motifs (ADAMTS), ADAMTS-4 and ADAMTS-5. Cleavage of aggrecan causes a loss of negative charges associated with the molecule.[49] The loss of negative charge causes an loss of water, and this decreases the compressive strength of cartilage. Members of the ADAMTS family cleave aggrecan within its IGD domain and release the portion containing GAGs.[31] The influx of aggrecan fragments into the synovium increases the amount of pro-inflammatory cytokines and MMPs that are produced.[37] Therefore, it is important to reduce fragmentation of ECM components in the early progression of OA to disrupt the degradation cycle.[55] It is very difficult to extract native aggrecan, and a limited number of research groups have been able to produce enough aggrecan for testing in tissue engineering applications.[56,57]

1.4.3 Current Treatment Options

The current treatment options available for OA treat the symptoms of the disease without restoration of the damaged cartilage tissue, and only the symptoms are addressed due to the fact that the etiologies of OA are not fully understood.[58] Noninvasive treatments, which are used in early stages of OA when the disease is considered mild, include controlling weight and

participating in an exercise program (Table 1-1). As the disease progresses to a moderate form, pharmacological drugs and injections into the joint space are used to manage symptoms (Table 1-1). The most common forms of pharmacological drugs taken for pain relief include analgesics, nonsteroidal anti-inflammatory drugs (NSAIDs), and cyclooxygense-2 (COX-2) inhibitors. However, these drugs should not be used for long term treatment due to serious side effects.[59] Injections of corticosteroids and hyaluronic acid (HA) supplements into the synovial space have also been shown to relieve pain. However, these injections require patients to receive multiple doses due to the short residence time of corticosteroids and HA supplements within the damaged tissue.[60,61] Supplementation with CS is also used because chondrocytes cannot replace proteoglycans degraded by OA even with an increased rate of synthesis.[35] Surgical methods can be used to restore the articular surfaces of cartilage, but these treatments require extensive rehabilitation and are only used for severe cases of OA (Table 1-1). Based on the severity of OA, the types of surgical approaches a patient may take to manage the disease are classified as palliative, reparative, and restorative.[62]

Table 1-1. Current treatment options to treat the symptoms of OA for patients at different stages of the disease defined by pathology.

Clinical Symptoms	Pathology	Presently Available Treatments
Mild/Early	• Superficial fibrillation and pannus • Diffuse hypercellularity • Slight reduction in proteoglycans	Exercise and Nutrition
Moderate	• Fissures to the middle zone • Cell clusters • Moderate reduction in proteoglycans	Medications (HA, CS, NSAIDS, corticosteroids)
Severe	• Fissures to the deep or calcified zone • Hypocellularity • Severe reduction in proteoglycans	ACI, Mosaicplasty, Arthroplasty

The main surgical treatments to repair damaged articular cartilage include arthroscopic lavage and debridement, marrow stimulating techniques, microfracture, osteochondral autografts/allografts, autologous chondrocyte implantation (ACI), and total knee arthroplasty.[5,10,59,63–65] An allograft, or tissue transplant taken from a donor, is limited by the tissue that is available to be transplanted, and there also is the possibility that the patient may reject the implant.[10] In contrast, a patient's own tissue used in an autograft has lower rejection risk but can lead to problems with donor site morbidity.[10,65] Total knee arthroplasty has shown successful results but severely limits the activity level of the patient.[66] In addition, a total knee arthroplasty precludes a patient from treatment options that may be offered in the future. Although current therapeutics and surgical methods are able to help alleviate the pain from OA, current treatment methods are not able to regenerate degraded cartilage.[4] We propose a tissue engineered solution to cartilage regeneration by combining cells, bioactive factors, and a scaffold.

1.5 Tissue Engineered Articular Cartilage

The main challenge of cartilage tissue regeneration through a tissue engineering approach is to regenerate tissue that closely matches the composition, structure, and function of native cartilage tissue to replace an area that has lost these aspects of healthy tissue.[67] Some studies have taken a scaffold free approach, but it is difficult and time-consuming to generate the amount of ECM that is required to confer mechanical properties in a cartilage defect.[68,69] The traditional tissue engineering approach seeks to repair damaged cartilage by introducing an optimized combination of cells, scaffold, and bioactive factors that can be transplanted into a patient.[6] The following sections will introduce cells and scaffolds used in the field of cartilage tissue engineering and discuss the rationale for the cell type and scaffold materials we used for our constructs in subsequent chapters.

1.5.1 The Cells of Tissue Engineered Articular Cartilage

A number of different cells types, including chondrocytes and different varieties of stems cells, have been encapsulated into scaffolds for cartilage tissue engineering.[6] For tissue engineered cartilage, it is important to choose a cell source that is abundant or easily expanded in 2D culture. In addition, the cells must be able to produce the ECM of hyaline cartilage without dedifferentiating to another cell type.[70,71] Chondrocytes in healthy cartilage are responsible for both producing and maintaining the ECM through a homeostatic balance of cartilage synthesis and degradation. However, chondrocytes are difficult to harvest due to the fact that a biopsy removes very few viable cells and donor sites often become unhealthy after cartilage removal.[72] Further expansion of biopsied chondrocytes *in vitro* is required due to the low yield of harvested cells, but the expansion of chondrocytes in a 2D monolayer induces dedifferentiation.[73]

Stem cells are a promising cell source for engineering cartilage tissue due to their ability to differentiate into chondrocytes under certain environmental conditions.[74] Many popular cell source choices for chondrocyte differentiation include mesenchymal stem cells (MSCs) from adipose tissue,[75] synovial fluid,[76] or bone marrow.[74] Although adipose tissue is relatively easy to extract, the chondrogenic potential of adipose derived stem cells is low compared to MSCs derived from synovial fluid or bone marrow.[77,78] Koga *et al.* found that both bone marrow- and synovium-derived MSCs showed greater chondrogenic potential compared to adipose- and muscle-derived

stem cells.[79] MSCs derived from synovial fluid have shown high chondrogenic potential and self-renewal capacity, but there is a very limited source of tissue.[76] Stem cells isolated from bone marrow are a promising source of cells for cartilage tissue engineering due to ease of isolation, abundance of tissue to extract from, and high chondrogenic potential.[6]

MSCs can be directed to differentiate at a certain time and to a specific phenotype based on a number of different biological and physical cues.[80] It is well known that many different biological cues, including growth factors, hormones, extracellular matrix, and other small chemicals, can direct the fate of stem cells to a certain differentiation lineage.[81–83] A number of both natural and synthetic molecules have been shown to be useful for guiding stem cells through chondrogenesis.[84,85] For example, soluble growth factors secreted by cells direct stem cell differentiation *in vivo*, but they can also be added to a culture *in vitro* and similarly affect stem cells.[84] The most popular growth factors that stimulate chondrogenesis are insulin-like growth factor (IGF) and members of the transforming growth factor beta (TGF-β) family. [86–88] The TGF-β family is known for inducing differentiation of MSCs to chondrocytes while preventing differentiation to osteocytes. Collagen type II expression and proteoglycan synthesis are increased in systems cultured with TGF-β3, a potent inducer of chondrogensis.[89] A subgroup of the TGF-β family, the bone morphogenetic proteins (BMPs), also plays a crucial role in cartilage repair. The growth factor bone morphogenetic protein-2 (BMP-2) is expressed during mesenchymal condensation, which is an important step in cartilage and embryonic development.[90] The ability to stimulate differentiation to chondrocytes can be amplified when BMP-2 is combined with TGF-β3.[87] However, as dosage is increased, the protein begins to promote differentiation to osteocytes.[87] Previous work has shown that when MSCs are grown in a matrix that is rich in proteoglycans and collagen type II, they favor differentiation to cartilage over bone when stimulated with BMP-2.[91] BMP-2 has also been used *in vivo* where it has been shown to regenerate hyaline-like cartilage and aid in the cartilage healing process.[92,93]

1.5.2 The Scaffolds of Tissue Engineered Articular Cartilage

It is important to consider the properties of a scaffold material as well as the properties of the target tissue since development of regenerated tissue depends on both set of criteria. Some important characteristics include nonimmunogenicity, sterility, and biodegradability. To prevent

rejection and to provide a favorable environment for the attachment of cells, it is important that the biomaterial used for the scaffold is biocompatible. In addition, the mechanical properties of a scaffold can induce the differentiation of encapsulated cells to a specific lineage as discussed in the previous section.[6,94] Biomaterials, including synthetic, natural, and composite, that provide signals present in the native extracellular matrix have been proposed as scaffolds to support improved cartilage regeneration.

Some widely used synthetic polymers include regulatory approved biodegradable and bioresorbable polymers such as polyglycolide (PGA), polylactides including poly(lactic acid) (PLA) and poly(lactic-*co*-glycolic acid) (PLGA), and polycaprolactone (PCL). Others, such as such as polyorthesters (POE), are not approved but are currently under investigation.[94,95] The ability to be formed into any desired shape and good mechanical strength are two advantages of synthetic polymers. The degradation profile can be varied by altering the molecular weight and copolymer ratios of utilized synthetic polymers. However, when degraded in the body, some of these synthetic materials do have potential side effects.[95] In addition, natural polymers are better able to mimic the native tissue environment.

Some of the natural polymers that are being used as scaffolds for cartilage tissue engineering include collagen, GAGs, alginate, chitosan, and a number of different polypeptides. These materials are able to mimic the intricate fibrillar architecture of cartilage and better interact with encapsulated cells. Collagen hydrogels are an attractive option for tissue-engineered scaffolds since collagen is found in many different tissues throughout the body and is also biocompatible.[96] In addition, collagen fibrillogenesis, the spontaneous self-assembly of collagen monomers into fibrils and then larger collagen fibers, occurs at physiological conditions.[97] In the next section we will explore different studies that utilize collagen as a 3D scaffold for tissue engineering.

1.5.3 Commercially Available Cartilage Tissue Engineering Collagen-Based Scaffolds

A number of different collagen-based scaffolds with autologous cells are currently available commercially and include matrix-induced autologous chondrocyte implantation (MACI), Novocart3D, and CaReS.[98,99] MACI, which is manufactured by Genzyme, is a membrane made up of both collagen type I and III on which biopsied chondrocytes are grown in monolayer for about 1 week prior to implantation. The membrane is cut into the shape of the cartilage defect and secured into place with a fibrin sealant. The collagen membrane is also sold separately, without cultured, autologous cells, under the name Chondro-Gide. Novocart3D, which is manufactured by

TeTeC, is a collagen type I sponge that has two distinct layers and contains chondroitin sulfate. A patient's chondrocytes are isolated and expanded in monolayer, without passage, before being seeded throughout the sponge. The cell-scaffold constructs are cultured for two days before implantation. In a two year follow up study, Novocart3D was shown to be appropriate for the treatment of large focal chondral and osteochondral defects when reviewing clinical and radiological results in both short- and medium-term studies.[100] CaReS, which is manufactured by Arthro Kinetics Biotechnology, is a collagen type I gel that is mixed with a patient's chondrocytes without growing the cells in monoculture. The cells are grown in 3D for about 4 weeks prior to implantation. CaReS gel has been shown to be a suitable treatment for both small and large cartilage defects of the knee.[99,101] A study that directly compared cartilage specific gene expression of cells cultured in MACI, Novocart3D, or CaReS scaffolds to native cartilage biopsies, found that cells cultured in these scaffolds had a significant decrease in collagen type II and aggrecan gene expression.[99] Of the three collagen scaffolds, the highest ratio of collagen type II to collagen type I was seen in CaReS, the collagen type I gel. Studies comparing collagen-based scaffolds for tissue engineered cartilage shown there is still room for improvement, especially in terms of long-term repair, before these scaffolds become a viable option for cartilage repair and regeneration. All of these commercially available collagen-based scaffolds are made only of collagen type I, and we believe that the addition of collagen type II to scaffolds can improve on cartilage regeneration capabilities.

1.5.4 Collagen-Based Scaffolds in Tissue Engineering

Collagen type I, which is abundantly available, continues to be the most utilized type of collagen in tissue engineered scaffolds, even though collagen type II is found in native cartilage tissue. The $\alpha_2\beta_1$ integrin receptor on the cell membrane of bone marrow cells interacts with collagen type I, an important component of bone, to induce osteoblastic differentiation.[102] MSCs encapsulated within collagen I hydrogels have been successfully differentiated into bone and used to repair bone in human and animal models.[103] On the other hand, many studies have used collagen I hydrogels for cartilage engineering. For example, to repair cartilage defects in humans, early studies encapsulated autologous chondrocytes within hydrogel scaffolds created using collagen type I from different species.[104,105] In another early study, porcine collagen type I hydrogel scaffolds with autologous bone marrow-derived MSCs were used in human osteoarthritic knees to repair cartilage defects more effectively than a cell-free scaffold.[106] Furthermore, autologous bone

marrow-derived MSCs were isolated, embedded within calf skin collagen type I, and used to repair cartilage defects into the weight-bearing region of a rabbit.[107] Better integration with surrounding tissue and surface splitting, fibrillation, and thinning are some limitations of collagen type I hydrogels used for articular cartilage repair that will need to be addressed as areas for improvement.[107]

Although collagen type I is found in fibrocartilage tissue such as the intervertebral disc and meniscus, articular cartilage contains little to no collagen type I.[108,109] In contrast, collagen type II makes up 90-95% of the collagen produced by chondrocytes in the ECM and is a promising scaffold material for use in articular cartilage.[20] It has been shown that collagen type II hydrogels promote the differentiation of embedded MSCs to chondrocytes more efficiently than collagen type I gels.[110,111] Despite some arthritogenic properties,[112] collagen type II is organized in a macromolecular structure that chondrocytes sense, and these cell-matrix interactions help to maintain chondrocyte phenotype.[113,114]

Compared to collagen type I, collagen type II exhibits poor mechanical properties when forming a physically crosslinked hydrogel. [115] In a study comparing fibrillogenesis of collagen type I and collagen type II, collagen hydrogels formed routinely in gels made of collagen type I but not in collagen type II hydrogels.[116] The same study also saw that the smaller fibers of collagen type II, as compared to collagen type I, were associated with more charged and hydrophobic residues that took part in more intramolecular interactions with fewer residues available for intermolecular interactions. The lack of intermolecular fibril interactions[116] and slower fibrillation process[117] are likely the reasons for lack of collagen type II gel formation.

Although a few papers have investigated collagen type II scaffolds, [111,118] the lack of robust hydrogels and inferior mechanical properties, as noted previously, have resulted in strategies, such as crosslinking scaffolds, using a recombinant collagen type II, or creating composite scaffolds, that address these concerns. Chemical crosslinkers, such as 3-(3-dimethylaminopropyl)carbodiimide (EDC), glutaraldehyde, and N-hydroxysuccinimide (NHS), have been utilized to modify scaffolds containing collagen type II,[119–126] but are not cytocompatible and cannot be used to encapsulate cells. Recombinant collagen type II has also been investigated as a scaffold, with encapsulated cells, for cartilage repair,[118,127,128] but it is expensive and difficult to scale.[129] Previous studies have combined collagen type II with a number of scaffold materials including poly(ethylene glycol) (PEG),[130,131] glycosaminoglycans

(GAGs),[120,132] alginate,[110,133] and chitosan.[124,134] Including collagen type II in composites increased ECM production specific to cartilage, regulated chondrocyte proliferation, and induced cartilage repair.[126,130,131,134–137] Blends of collagen type I and II have been studied without cells *in vivo,* [138] and with encapsulated chondrocytes *in vitro* and *in vivo.*[135,139] To date, our study is the first to encapsulate mesenchymal stem cells (MSCs) in a collagen type I and II hydrogel and investigate them in an *in vivo* model of cartilage defect repair.

1.5.5 Chondroitin Sulfate in Tissue Engineered Cartilage

As previously discussed, CS is a sulfated GAG made up of two repeating sugar units, N-acetyl-D-galactosamine and D-glucuronic acid. CS and KS attach to a protein core to form a molecule of aggrecan. Then multiple aggrecan molecules attach to a central filament of HA, which is negatively charged and trapped in a collagen network. The negative charge of the complex results in water influx and retention in the tissue, and the retention of water gives cartilage a high compressive strength and aids in joint lubrication. CS can be extracted from cartilage of several different animal sources including cows, pigs, and sharks.

CS is known to be both a symptomatic slow-acting drug in OA (SYSADOA), because it can influence symptoms like pain and inflammation, and a structure-modifying OA drug (SMOAD), because it has been shown to modify the course of OA.[140] In addition to being a molecule found naturally in cartilage and synovial fluid, CS can also be supplemented through diet or intra-articular injections. The addition of CS can aid in the fact that chondrocytes cannot replace proteoglycans degraded by enzymes when a patient suffers from OA.[35] It is hypothesized that CS, which stimulates the synthesis of proteoglycans and decreases the catabolic activity of chondrocytes, is also able to inhibit proteolytic enzymes.[141] CS has also been shown to increase the production of HA, which increases the viscosity of synovial fluid, by human synovial cells,.[142] The European League Against Rheumatism (EULAR) guidelines, which recommended certain treatment options for knee OA due to the fact that a large number of treatment options exist, gave CS the highest marks available in the recommendation strength and evidence grade categories.[140]

There are examples of hydrogels with incorporated CS where the addition of CS has been shown to improve scaffolds for articular cartilage tissue engineering. For example, when CS was added to a hydrogel made of PEG-RGD, embedded chondrocytes produced the highest level of GAG accumulation compared to PEG-RGD hydrogels alone and PEG-RGD hydrogels with added

HA.[143] In ECM-based cryogels made of either methacrylated CS or methacrylated HA crosslinked to poly (ethylene glycol) diacrylate (PEGDA), the addition of methacrylated CS stimulated gene expression of aggrecan and GAG accumulation.[144]

This thesis proposes that CS will be retained in our collagen type I and II blend hydrogel by crosslinking multiple collagen-binding peptides to a CS backbone through an amide bond using EDC crosslinking chemistry. Our lab has previously used the collagen-binding peptide (RRANAALKAGELYKSILYGSG) crosslinked to dermatan sulfate (DS), another example of a glycosaminoglycan, to design a mimic of decorin, a small proteoglycan that is associated with collagen fibrils.[145–148] The collagen-binding peptidoglycan (DS-SILY) has been shown to bind to and mask collagen from platelet activation in veins damaged from balloon angioplasty and inhibits collagen degradation by MMP-1 and MMP-13.[145,147] Although the same SILY peptide will be used, a CS molecule will be used as the backbone (CS-SILY) in this thesis to help retain CS in our Col I/II hydrogel.

1.5.6 Animal Studies for Investigating Tissue Engineered Cartilage

Several animal models of full thickness articular cartilage defects exist.[149] Sheep are a commonly used large animal model for translating research into cartilage repair.[150–152] Sheep are easy to house and handle; their stifle, or knee, joint is accessible for defect creation and repair; and they have low levels of spontaneous healing.[153,154] Furthermore, the sheep has been considered a scaled-down version of a human knee due to common anatomical characteristics.[155] Due to the age of skeletal maturity (2- to 3-years),[154] only female sheep will be used since current breeding practices are to maintain a large female population with relatively few males. Thus, male sheep that have reached skeletal maturity are rare and would be difficult to obtain or would require the researcher to raise and house them for a few years prior the cartilage studies.

Horse are the largest cartilage defect model, and their cartilage thickness that is similar to that of human cartilage.[156] Due to the thickness of cartilage, both partial and full thickness defects can be created. The large size of horses allows researchers to take a second look into cartilage defect repair using arthroscopic examinations. Since horses are also used for athletic racing, OA and joint degeneration is common in retired animals. Therefore, there is an interest in addressing the joint health of horses, but it also means that retired animals must be screened for pre-existing joint diseases.[149] Limitations of the species include ethical concerns because horses are considered

companion animals, which also makes them an expensive option. In addition, horses require large housing facilities and specialized surgical equipment.[149]

We chose a rabbit model for preliminary investigation due to the fact that they reach skeletal maturity in 9 months and require simple husbandry.[154] Rabbit have been widely used to research healing in cartilage defects, and they are the most commonly used small animal option used during the early stages of biomaterial testing..[157–162] In rabbit, the most commonly recommended critical defect size is ~3 mm in diameter since this size does not heal spontaneously.[163,164] It is important to note that healing has been described in rabbits as they have exceptional endogenous healing potential.[165,166] Due to the variability in intrinsic healing capabilities, cohort sizes of 13 to 16, or larger, are used in the early evaluation phase of a new therapy.[154,167]

1.6 Thesis Outline

The goal of this thesis was to create and investigate a biomimetic scaffold to replace damaged articular cartilage. Here, we harness the biological activity of collagen type II and the superior mechanical properties of collagen type I by blending the two types together into a composite hydrogel.

Chapter 2 characterizes hydrogels made of different blends of collagen type I and II by investigating whether the addition of collagen type I to a collagen type II hydrogel altered the amount of protein incorporated into the hydrogels, the mechanical properties of the hydrogels, and the structure of the collagen network. In addition, the effects of adding HA and/or CS on hydrogel formation were examined. The chapter consists of a manuscript by Nelda Vázquez-Portalatín, Claire E. Kilmer, Alyssa Panitch, and Julie C. Liu that was published in *Biomacromolecules*, 2016. Authors Nelda Vázquez-Portalatín and I contributed equally to the experimental execution, experimental design, and writing of this article. Nelda Vázquez-Portalatín performed the cryo-SEM imaging and mechanical testing experiments, and I performed all other experiments.

Chapter 3 explores the chondrogenic potential of collagen type I and II blend hydrogels both *in vitro* and in *vivo*. The chapter consists of a manuscript by Claire E. Kilmer, Abigail Cox, Gert Breur, Alyssa Panitch, and Julie C. Liu. Along with the co-authors, I designed and performed *in vitro* experiments and prepared all materials for use in the rabbit surgeries including bone marrow isolation and scaffold manufacture. I participated in the rabbit surgeries and bone marrow isolation that were performed by Dr. Gert Breur and his team, Robyn McCain, Christa Crain, and Kris

Kazmierczak. The histological preparation was done by Victor Bernal-Crespo and the Purdue Histology Research Laboratory. Histological evaluation was done by Dr. Abigail Cox and me.

Chapter 4 seeks to optimize collagen blend hydrogels using a biomimetic CS molecule with an attached collagen-binding peptide. The chapter consists of a manuscript by Claire E. Kilmer, Tanaya Walimbe, Alyssa Panitch, and Julie C. Liu. Along with the co-authors, I designed a new molecule, that contains a collagen type I binding peptide grafted to a chondroitin sulfate backbone, to help promote chondrogenesis and retain chondroitin sulfate into a collagen type I and II blend hydrogel. Tanaya Walimbe performed the cryo-SEM imaging. I designed and performed all cellular and characterization experiments and data analysis.

Chapter 5 summarizes the work completed in the previous three chapters and briefly outlines future experiments that could be done to further the work of this dissertation.

2. CHARACTERIZATION OF COLLAGEN TYPE I AND II BLENDED HYDROGELS FOR ARTICULAR CARTILAGE TISSUE ENGINEERING

Adapted with permission from Vazquez-Portalatin, N.; Kilmer, C. E.; Panitch, A.; Liu, J. C. Characterization of Collagen Type I and II Blended Hydrogels for Articular Cartilage Tissue Engineering. *Biomacromolecules* 2016. https://doi.org/10.1021/acs.biomac.6b00684.

2.1 Introduction

Osteoarthritis (OA) is a debilitating condition that affects over 27 million Americans and is defined by degradation in articular cartilage extracellular matrix (ECM).[1] Patients suffer from pain and stiffness in the joints associated with the onset of OA. Tissue that is damaged by OA is a major health concern since cartilage tissue has a limited ability to self-repair due to the lack of vasculature in cartilage and low cell content.[3] Tissue engineering seeks to repair damaged cartilage by introducing an optimized combination of cells, scaffold, and bioactive factors that can be transplanted into a patient.[6] To prevent rejection and to provide a favorable environment for the attachment of cells, it is important that the biomaterial used for the scaffold is biocompatible. In addition, the mechanical properties of a scaffold can induce the differentiation of encapsulated cells to a specific lineage.[6,94] Finally, the mechanical properties of the scaffold must match those of the surrounding tissue.

Many different biomaterial scaffolds are being studied as a way to repair damaged articular cartilage due to OA.[168] For example, hydrogel scaffolds made of collagen promote the formation of cartilage by encapsulating cells and mimicking native tissue.[169] The conservation of the structure and sequence of collagen across species has facilitated the biomedical application of collagen from many different sources.[170] Collagen type I hydrogels with embedded mesenchymal stem cells (MSCs) promote differentiation to chondrocytes and repair cartilage defects.[171] However, it has been shown that collagen type II hydrogels promote the differentiation of embedded MSCs to chondrocytes more efficiently than collagen type I gels.[172,173] Collagen type II stimulates a more rounded cell shape, which is an important determinant for stem cell

differentiation.[174] In addition, collagen type II and alginate hydrogels have been shown to initiate and maintain the differentiation of MSCs to chondrocytes without the addition of other bioactive molecules.[173]

Collagen type II makes up 90–95% of the collagen produced by chondrocytes in the ECM and is a promising scaffold material for use in articular cartilage.[175] However, when compared to collagen type I, collagen type II is glycosylated to a greater extent.[176,177] The high number of bulky disaccharide groups in collagen type II appears to hinder the formation of highly ordered fibrils.[176,177] Without cross-linking, collagen type II exhibits poor mechanical properties when forming a hydrogel on its own.[178] Previous studies have blended collagen types to change the mechanical properties of collagen hydrogels.[179]

During fibrillogenesis, collagen organization is affected by pH, ionic strength, and interactions with other components in the matrix. Previously, our lab created and characterized hydrogels made from collagen type I and III blends for use in skin and vasculature tissue engineering, and the addition of collagen type III increased the rate of collagen fibrillogensis.[179] Many different studies have investigated the effects of glycosaminoglycans (GAGs), an important nonfibrillar component of the native cartilage tissue ECM, on the rate of fibrillogenesis and collagen fibril diameter, and the conflicting data is summarized in the referenced paper.[180] GAGs attach to a protein core to form proteoglycans, which comprise 4–7% of the wet weight of healthy cartilage, and allow articular cartilage to withstand compressive forces.[13,181] Creating a collagen blend hydrogel with GAGs would thus more closely mimic the native structure of articular cartilage.[55] In this study, we sought to examine the effects of GAGs on collagen fibrillogenesis and to determine the amount of GAGs incorporated into the collagen hydrogel. Thus, we are interested in the interactions between a blend of collagen type I, collagen type II, and GAGs such as chondroitin sulfate (CS) and hyaluronic acid (HA).

The objective of this study was to create a hydrogel with a blend of collagen types I and II, and it was hypothesized that these blended hydrogels would have superior mechanical properties compared to gels made with collagen type II alone. We investigated whether the addition of collagen type I to a collagen type II hydrogel altered the amount of protein incorporated into the gels, the gel's mechanical properties, and the structure of the collagen network. In addition, we examined the effects of adding HA and/or CS on gel formation.

2.2 Materials and Methods

2.2.1 Gel Preparation

Collagen type I, which was extracted from rat tail, was purchased from BD Biosciences (Franklin Lakes, NJ). Lyophilized chicken sternal collagen type II and hyaluronic acid (1.5 - 1.8 x 10^6 Da) were purchased from Sigma-Aldrich (Saint Louis, MO). Sodium chondroitin sulfate from shark cartilage was purchased from Seikagaku (Tokyo, Japan). Stock solutions of both collagen types I and II were prepared in 20 mM acetic acid at a concentration of 5 mg/mL. The pH values of the solutions were raised to 7.4 with the addition of 10x phosphate buffered saline (PBS), 1 M NaOH, and 1x PBS, and the final concentrations of the collagen solutions were 4 mg/mL. The gels were prepared with collagen type I: collagen type II ratios of 1:0, 3:1, 1:1, 1:3, and 0:1 (Table 1). Glycosaminoglycans (e.g., CS or HA) were dissolved in 1x PBS to a concentration of 10 mg/mL and were added prior to polymerization. Gels were made with CS, HA, or a 1:1 ratio of CS to HA at a final concentration of 0.2 mg/mL of added glycosaminoglycans.

2.2.2 Collagen Incorporation into a Gel

The amount of collagen incorporated into the gels was determined using a previously described method.[179,182] Briefly, the samples were heated at 37°C overnight to ensure that the solutions had polymerized. The gel was centrifuged for 15 minutes at 11000*g*. The supernatant was separated from the pellet by decanting. The supernatant from each sample was tested (n = 3) for the total amount of collagen present using a bicinchoninic acid (BCA) assay (Pierce, Rockford, IL) following the manufacturer's protocol. Standard curves with different concentrations for each collagen type I to collagen type II ratio (1:0, 3:1, 1:1, 1:3, and 0:1) were used to determine the amount of collagen present within the supernatant. The amount of protein in the gel was calculated indirectly as the total amount of collagen prepared minus the amount of collagen in the supernatant.

A modified enzyme-linked immunosorbent assay (ELISA) was then performed to measure the amount of collagen type II in the supernatant (n = 3). A standard curve was created by adsorbing collagen with different ratios of collagen types I and II on a 96-well plate with a high binding surface (Corning, Corning, NY). The supernatant from the hydrogels and different ratio blends of collagen type I and II were diluted to a total protein concentration of 10 μg/mL. All samples and standards were then diluted 1:100 in 1x PBS and adsorbed onto the surface of a 96-well plate for

24 hours at 4˚C. The wells were rinsed three times with blocking buffer (5% non-fat powdered milk in 1x PBS), blocked with blocking buffer for 2 hours at room temperature, and rinsed three more times with blocking buffer. The plate was incubated for 24 hours at 4˚C with a primary antibody for collagen type II (Abcam 34712, Cambridge, MA). The wells were rinsed with blocking buffer before being incubated with an HRP-conjugated secondary antibody (Life Technologies 16035, Carlsbad, CA) for 2 hours at room temperature. A substrate reagent solution from a Substrate Reagent Pack (R&D Systems, Minneapolis, MN) was added to each well and incubated for 20 minutes at room temperature. A stopping solution of 2N H_2SO_4 was added to each well, and the absorbance was determined on a Spectromax M5 plate reader (Molecular Devices, Sunnyvale, CA) at 450 nm. Using the standard curves with the different collagen ratios, the ratios of collagen type I to collagen type II in our samples were quantified. The amounts of collagen types I and II in the gels were calculated indirectly by using the measured total protein concentration in the supernatant and the amounts of collagen types I and II in the supernatant.

2.2.3 CS and HA Incorporation into a Gel

A dimethylmethylene blue assay (DMMB) was performed to measure the amount of CS in the supernatant from gels made with varied amounts of HA or CS (n = 3). Specifically, 20 μL of the supernatant were mixed with 180 μL of DMMB reagent. The absorbance was measured on a plate reader at 525 nm. A standard curve of CS was created to quantify the amount of CS in the supernatants. The amount of CS retained in the gel was calculated indirectly.

A hyaluronic acid sandwich ELISA assay (Echelon Biosciences, Salt Lake City, UT) was performed following the manufacturer's protocol. Samples and standards were prepared in 1x assay buffer, and 100 μL was incubated in each well of the HA detection plate for 1 hour. The plate was washed three times with 1x tris buffered saline (TBS) before 100 μL of HA detector was incubated for 1 hour. After three more washes with 1x TBS, 100 μL of 3,3′,5,5′-Tetramethylbenzidine (TMB) solution was added and allowed to develop for 20 minutes. Finally, 50 μL of 1 N H_2SO_4 was added to stop the reaction before absorbance was read at 450 nm.

2.2.4 Cryo-Scanning Electron Microscopty (crySEM)

Samples for cryoSEM were prepared as previously described.[177] Briefly, collagen gels (n = 2 - 4) with different ratios of collagen type I to II were prepared on SEM holders and were incubated

overnight at 37°C to allow polymerization of the proteins. Samples with a 3:1 ratio of collagen type I to collagen type II with added CS, HA, or a 1:1 ratio of CS to HA were also prepared for cryoSEM imaging. The sample holders were then moved to the cryo holder, frozen in liquid nitrogen slush, moved to a Gatan Alto 2500 prechamber (Gatan Inc., Pleasanton, CA), cooled to -155°C, and fractured. The samples were sublimated at -90°C for 10-15 min and sputter coated for 120 s with platinum. Afterwards, the samples were transferred to the microscope cryo-stage, which had been cooled to -145°C, for imaging. All samples were imaged with an FEI NOVA nanoSEM field emission SEM (FEI, Hillsboro, OR) using the TLD (through the lens) or ET (Everhart-Thornley) detector operating at 5 kV accelerating voltage.

Fibril diameter measurements ($n \geq 782$) were analyzed using ImageJ software (National Institutes of Health, Bethesda, MD). As previously described, a perpendicular line was drawn across a fibril to obtain a measurement.[179] Three blinded individuals took 10 fibril diameter measurements per image, and each individual analyzed three or more images of each type of gel. ImageJ software was also used to obtain void space information ($n \geq 15$) from the cryoSEM images. A Diameter J plugin was used to segment the images and determine the fraction of image containing void space.

2.2.5 Rheology

An ARG2 rheometer (TA Instruments, New Castle, DE) was used to perform rheological analysis with a 20-mm cone geometry. Gels ($n = 4$) were subjected to frequency sweeps from 0.01 to 1 Hz using a controlled stress of 0.5 Pa.

2.2.6 Statistics

The data are represented as a mean with error bars corresponding to one standard deviation. Single factor analysis of variance (ANOVA) and Tukey's *post hoc* tests were performed for the total protein concentration in the gels, the percentage of CS retained, and rheology data. Nested factorial models were used to perform ANOVA and Tukey's *post hoc* tests to analyze the fibril diameter and void space percentage data. For all statistical tests, a value of $\alpha = 0.05$ was chosen, and significance was chosen to be a p-value at or below 0.05.

2.3 Results and Discussion

The total amount of protein in the supernatant was measured using a BCA assay and was used to calculate the total amount of protein in the gel. As the ratio of collagen type I to collagen type II decreased and thus the amount of collagen type II used to create the hydrogel increased, there was a statistical decrease in the final protein concentrations in the gels (Figure 2-1A). An ELISA was used to measure the amount of collagen type II in the supernatant, and this information was used to calculate the amounts of collagens type I and II in both the supernatant and gel. As the ratio of collagen type I to collagen type II in the starting solution decreased, the amounts of collagen types I and II incorporated in the gel respectively decreased and increased (Figure 2-1B and C). The amount of collagen type I in the gel decreased proportionally as the ratio of collagen type I to collagen type II decreased. However, the amount of collagen type II was not inversely proportional to the ratio of collagen type I to collagen type II. Instead, there was no statistically significant difference in the amount of collagen type II incorporated in the gel when the ratio of collagen type I to collagen type II was decreased from 1:3 to 0:1. A subset of the gels were immunostained for collagen type II to verify collagen type II incorporation in the gel (Figure 2-6). As expected, when more collagen type II was incorporated in the gel, an increase in fluorescence signal was observed. Since the amount of collagen type II incorporated in 0:1 gels did not differ from the 1:3 gels, the 0:1 gels were no longer considered in future experiments.

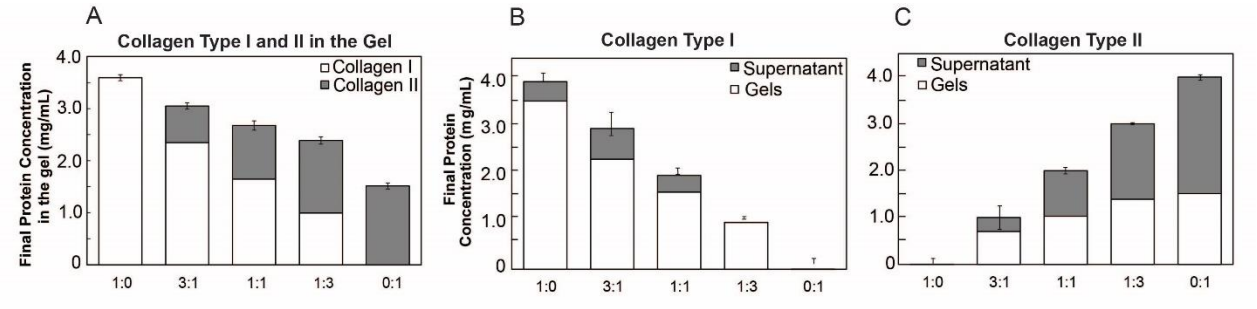

Figure 2-1. Final Protein Concentration.

(A) The final collagen concentration in the gel at different ratio blends uses white bars to represent collagen type I found in fibrillary form and gray bars to represent collagen type II measured in fibrillary form. Data (n = 3) are represented as the mean ± the standard deviation of the total concentration of collagen (both collagen types I and II) in the gel. An ANOVA and Tukey's honestly significant difference post hoc test were performed and indicate a significant difference in the total protein concentration in the gel between each ratio ($p < 0.05$). The final concentration of collagen in the gel and supernatant for (B) collagen type I and (C) collagen type II. The white bars represent collagen content in fibrillar form, whereas the gray bars represent collagen measured in the supernatant (n = 3). The error bars represent the standard deviation of the amount of collagen type II in the supernatant.

Next, we investigated whether the final protein concentrations in the blended collagen gels were altered due to the addition of HA and/or CS. The final protein concentration in the supernatant was measured for three different ratios of collagen type I to collagen type II (3:1, 1:1, and 1:3). Gels had no HA or CS added or were supplemented with HA, CS, or a combination of both HA and CS. When only HA or only CS was included, there was a significant increase in the total amount of protein incorporated into the gel. Thus, the addition of HA and/or CS did not negatively impact the total concentration of protein in the 3:1, 1:1, or 1:3 gels and therefore did not inhibit gel formation (Figure 2-2). The increase of protein incorporated into the gels upon addition of only CS is consistent with experiments performed by Stuart *et al.* using collagen type I gels.[179] Stuart and coworkers found that adding CS decreased the amount of collagen in the supernatant and thus resulted in more collagen incorporated into the gel.[179] In previous experiments, CS also increased the rate of fibrillogenesis of collagen type I and resulted in fibrils of smaller diameter.[182] These results also indicated that the addition of CS increased the number and shape of nucleation sites and promoted the aggregation of collagen molecules end-to-end.[183]

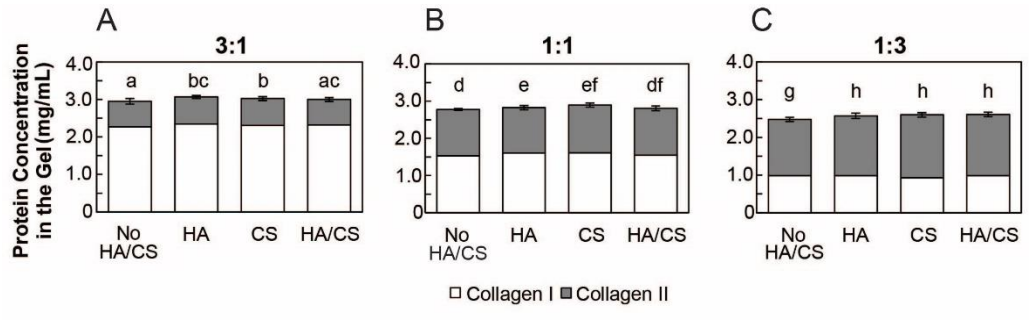

Figure 2-2. The final protein concentration in the fibrils at different ratio blends of collagen type I and collagen type II with the addition of HA, CS, or both HA and CS.

The gels were created containing a (A) 3:1, (B) 1:1, or (C) 1:3 ratio of collagen type I to collagen type II. An ANOVA and Tukey's honestly significant difference *post hoc* tests were performed. Different letters indicate groups with significantly different total protein concentrations incorporated in the gel ($p < 0.05$). Data ($n = 3$) are represented as the mean ± the standard deviation.

The percentage of CS retained in the gel was calculated using the supernatants from the gels supplemented with CS or both HA and CS (Figure 2-3A). There was a statistically significant difference in the percentage of CS retained when adding only CS to gels made with different ratios of collagen type I to II. In addition, there was a statistical difference in the percentage of CS retained when adding a 1:1 ratio of CS to HA to the different gel blends tested (3:1, 1:1, and 1:3). The interactions between CS and collagen are known to be ionic since increasing ionic strength reduces the binding of CS.[184,185] Furthermore, collagen type II is believed to bind more CS than collagen type I due to a stronger ionic interaction between collagen type II and GAGs. For example, Pieper *et al.* attempted unsuccessfully to remove GAGs from bovine tracheal cartilage collagen type II by washing with a high ionic strength solution.[186] In this study, the amount of collagen type II in the supernatant significantly increased with a decrease in the ratio of collagen I to collagen II (Figure 2-1), and these results could explain the significant decrease in the percentage of CS retained within the gel. When comparing the percentage of CS retained for gels with only CS added

to gels with CS and HA added, there were no statistical difference for the 3:1 gels, but there was a statistical difference for the 1:1 and 1:3 gels.

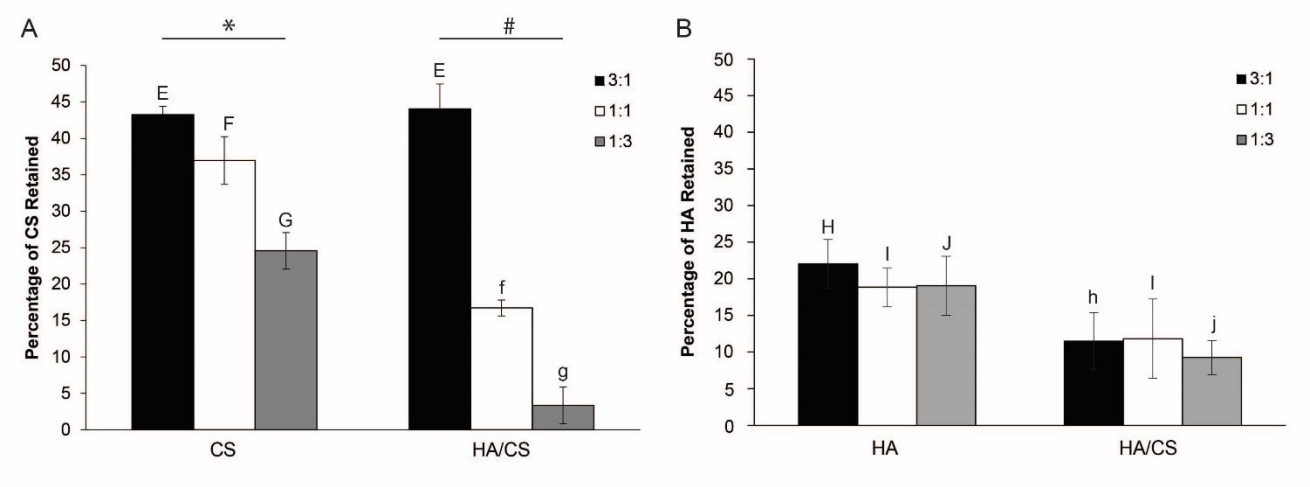

Figure 2-3. The percentage of (A) CS and (B) HA retained in the fibrils.

Gels were created using varying ratios of collagen type I to II (3:1, 1:1, and 1:3) with either CS, HA, or both CS and HA added into the gels. ANOVA and Tukey's honestly significant difference *post hoc* tests were performed. The * indicates significant differences ($p < 0.05$) between the three different hydrogel blends when CS is added. The # indicates significant differences ($p < 0.05$) between the three different hydrogel blends when HA and CS are added. EE indicates there is no statistical difference ($p > 0.05$) between the 3:1 gels. Ff and Gg indicate that there were statistical differences ($p < 0.05$) between the 1:1 and 1:3 gels, respectively. There is no significant difference ($p > 0.05$) between the three different hydrogel blends when either HA or HA and CS were added. Hh and Jj indicate that there were statistical differences ($p < 0.05$) between the 3:1 and 1:3 gels, respectively. II indicates there is no statistical difference ($p > 0.05$) between the 1:1 gels. Data ($n = 3$) are represented as the mean ± the standard deviation.

The percentage of HA retained in the gel was calculated using the supernatants from the gels supplemented with HA or both HA and CS (Figure 2-3B). There is no significant difference between the three different hydrogel blends when HA was added. When HA and CS is added, there was also no significant difference between the three different ratios. There were statistical differences between gels that had HA added and gels that had both CS and HA added for the 3:1 and 1:3 gels. However, there was no statistical difference between the 1:1 gels that had HA compared to 1:1 gels that had CS and HA. The HA that was used for these experiments was high molecular weight HA ($1.5 - 1.8 \times 10^6$ Da). High molecular weight HA chains form topological

interactions between chains that reduce their mobility.[187] Collagen molecules are separated from the HA molecules due to the reduction in mobility and topological hindrance. The separated collagen molecules then begin to nucleate and aggregate to form fibrils without interacting with the HA molecules. In addition, HA is known to form aggregates with ECM molecules. The aggregates of ECM molecules form a viscous barrier that inhibits the displacement of macromolecules in chondrocyte cultures.[188] These previous findings suggest that, in our experiments, supplemented HA interacts with the added CS and precludes the CS from being incorporated within the collagen gels. The 1:3 blend was not pursued in further experiments due to the significant decrease in CS incorporated into the gels when compared to the 3:1 and 1:1 gels.

CryoSEM was performed to observe the network and structure of the collagen fibrils in the gels. Figure 2-4A shows representative cryoSEM images of different ratio blends of collagen type I to collagen type II. In these images, collagen fibrils and the networks these fibrils form within the gels can be seen. Furthermore, qualitatively, the fibril diameters appear to be similar between the gels, but the void space seems to increase with the addition of collagen type II. Thick lamellar-like structures are also present in the SEM images, and similar structures have been observed in other SEM images of collagen hydrogels.[179]

To quantify our observations, the collagen fibril diameters were measured using ImageJ software, and the diameter distribution in the gels at different ratio blends is presented in Figure 2-4B. The 1:0, 3:1, and 1:1 gels showed unimodal distributions, and the average fibril diameter showed no significant differences among the different blends (Figure 2-7). ImageJ, along with a DiameterJ plugin, was used to obtain the void space percentage in the gels (Figure 2-4C). The 1:1 gels showed a significant increase in void space percentage (46.5%) compared to gels with ratios of 1:0 (35.1%) and 3:1 (36.4%).

CryoSEM images of 3:1 collagen type I to collagen type II gels with no GAGs or supplemented with CS, HA, or both CS and HA were also analyzed to examine the collagen fibril network within the gels (Figure 2-8A). The collagen fibril diameters (Figure 2-8B) and void space percentage (Figure 2-8C) were measured using ImageJ software, and there were no significant differences observed.

The unimodal distribution shape of fibrils (Figure 2-4B) obtained in this study is similar to what was previously shown for gels composed of collagen type I only and collagen type I and collagen type III blends.[179,180,189,190] However, gels composed of only collagen type I have also

shown bimodal distributions.[179,180,191] The fibril diameter ranges exhibited by collagen type I only gels (up to 0.65 μm) and collagen type I and II blends (up to 0.6 μm) were larger than those previously reported for gels composed of collagen type I only (up to 0.4 μm)[180,190] and collagen type I and III blends (up to 0.2 μm).[179] The addition of collagen type II to the blends did not significantly affect the average fibril diameter with or without the addition of GAGs (Figure 2-7 and Figure 2-8B)

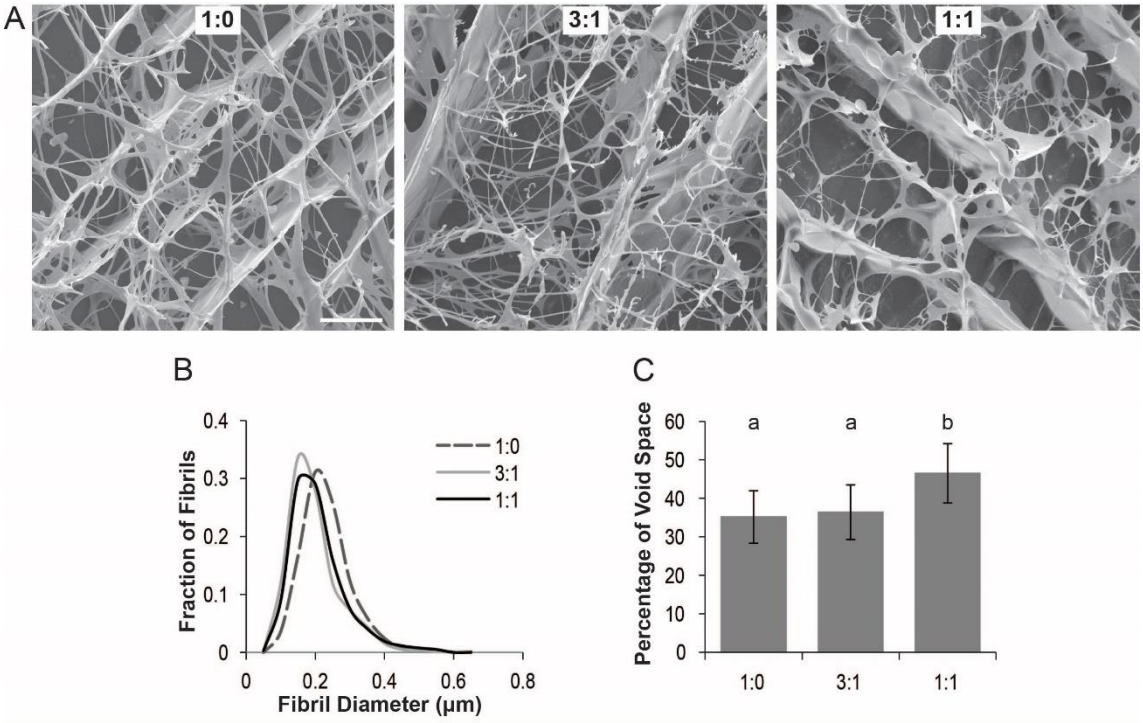

Figure 2-4. Collagen networks for different ratio blends.

(A) Representative cryoSEM images of different ratio blends of collagen type I to collagen type II show the collagen fibril network within the gels. Scale bar = 5 μm. (B) Distribution of collagen fibril diameters in the gels at different ratio blends. (C) Percentage of void space for the gels based on cryoSEM images obtained at 10,000x magnification. ANOVA and Tukey's *post hoc* tests were performed on the average fibril diameter and the percentage of void space data by using nested factorial models. For the average fibril diameter data, there were no significant differences observed between the different blends. The different letters indicate groups with a significant difference ($p < 0.05$) in the percentage of void space in the gels. Data ($n \geq 782$ for fibril diameter, $n \geq 15$ for void space percentage) are represented as the mean ± the standard deviation.

The void space percentage results obtained for the gels without GAGs (Figure 2-4C) are similar to previous studies that showed gels composed of 70% collagen type I and 30% collagen

type III or gels composed of 30% collagen type I and 70% collagen type III had an increase in void space percentage (~45-50%) compared to gels composed of collagen type I only (30%).[179] The significant increase in void space percentage as the ratio of collagen type I to collagen type II in the blends decreased suggests that the collagen type II addition limits fibril formation. Collagen type II may coat the fibrils formed by collagen type I and inhibit lateral aggregation of fibrils as has been shown for collagen type I and III gels.[192] This interaction between collagen type I and II could affect the stability of the gel and, thus, its mechanical properties.

Another explanation for the results seen from the analysis of the SEM images could be due to the fact that addition of collagen type II reduced the total collagen concentration in the gel (Figure 2-1A) and also reduced the collagen type I concentration (Figure 2-1B). A previous study showed that hydrogels have statistically similar fibril diameters when polymerized with varying collagen type I concentrations,[193] and these results are consistent with the results seen with the collagen type I and II blend hydrogels in this study. In addition, similar to the results seen for the blended collagen I and II hydrogels, another study showed that decreasing the collagen type I concentration increased the void space.[194]

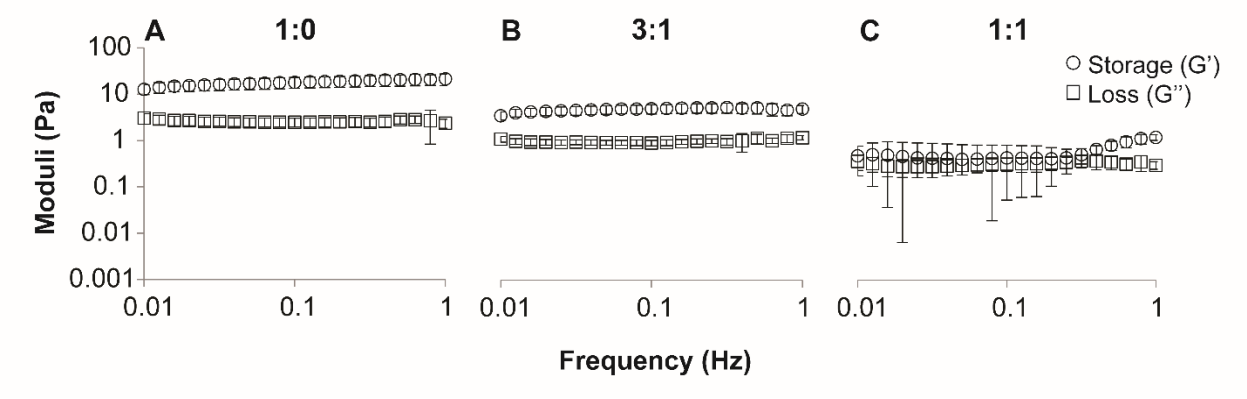

Figure 2-5. Frequency sweeps of storage and loss moduli of gels prepared from mixtures of (A) 1:0, (B) 3:1, and (C) 1:1 collagen type I to collagen type II.

Frequency sweeps of storage and loss moduli of gels prepared from mixtures of (A) 1:0, (B) 3:1, and (C) 1:1 collagen type I to collagen type II. ANOVA and Tukey's *post hoc* tests were performed. At 1 Hz, a significant difference ($p < 0.05$) was observed between the storage moduli for the three different gel blends. At 1 Hz, the loss modulus for the 1:1 gels was significantly different ($p < 0.05$) from the loss moduli of the 1:0 and 3:1 gels. Data ($n = 4$) are represented as the mean ± the standard deviation.

Frequency sweeps from 0.01 to 1 Hz were performed to characterize and understand the mechanical properties of these gels. The frequency sweeps showed that at 1 Hz, the 1:0, 3:1, and 1:1 gels respectively had average storage moduli (G') of 21.2 ± 5.9, 4.9 ± 1.0, and 1.2 ± 0.2 Pa (Figure 5); loss moduli (G'') of 2.4 ± 0.5, 1.2 ± 0.1, and 0.3 ± 0.1 Pa (Figure 2-5); and complex moduli (G*) of 21.4 ± 5.9, 5.0 ± 0.9, and 1.2 ± 0.2 Pa (Figure 2-9). The addition of collagen type II to the gels significantly decreased their stiffness, and this result could be attributed to a decrease in total protein concentration in the gel (Figure 2-1A) and the increase in void space (Figure 2-4C). Previously performed studies showed concentration-dependent changes in mechanical properties.[195,196] In particular, single collagen type I fibrils or collagen type I and agarose blend hydrogels demonstrated that higher collagen type I concentrations increased the mechanical properties.[195,196] Other studies with collagen type I membranes,[197] collagen type I hydrogels,[12] and collagen type I/III blended hydrogels[11] correlated an increase in porosity, or void space, with a decrease in the respective mechanical properties of tensile stress;[197] stiffness;[12] and storage, loss, and complex moduli.[11]

The decrease in stiffness with increasing collagen type II also suggests that the ability of collagen type II to alter network structure and fibril growth can affect the gels' mechanical properties. Previous work has shown that collagen type III also alters fibril formation of collagen I and, thus, the mechanical properties of the gel.[179] However, collagen gels composed of collagen type I and III blends exhibit higher mechanical properties than the gels composed of collagen types I and II shown here. At 1 Hz, gels composed of collagen type I and III blends exhibited a storage moduli range of 115-175 Pa and a loss moduli range of 15-25 Pa. Similarly, collagen type I gels had a storage moduli of ~170 Pa and loss moduli of ~24 Pa.[179] In another study, Stuart and coworkers found their collagen type I gels exhibited a storage modulus of ~145 Pa and a loss modulus of ~23 Pa.[180] While these collagen type I gels exhibited higher mechanical properties than the 1:0 gels presented herein, Shayegan *et al.* have also seen lower storage moduli (0.1 – 0.3 Pa) and loss moduli (0.7 – 1.0 Pa) for collagen type I gels at 4mg/ml to 5 mg/ml concentrations.[198] The difference in mechanical properties of these gels could be attributed to different collagen type I sources, gel preparation methods, and protein concentrations. Other studies have improved the mechanical properties of their gels by incorporating HA[187,191,199], dermatan sulfate[187], and other crosslinking agents.[199–201] Calderon *et al.* demonstrated that noncrosslinked collagen type II gels exhibited significantly lower compressive stress (27.6 ± 6.5 kPa) and compressive modulus (1.4 ±

0.35 kPa) than those that had been crosslinked (48.9-188.1 kPa and 2.4-10.3 kPa, respectively).[178] Halloran *et al.* have also presented similar results where noncrosslinked atelocollagen type II scaffolds showed lower storage moduli than gels that had been crosslinked with microbial transglutaminase.[199]

In this study, our goal was to develop and characterize collagen blend gels that harness the biological activity of collagen type II, which is the most abundant type of collagen produced by chondrocytes and has the ability to initiate and maintain the differentiation of MSCs to chondrocytes without added bioactive molecules.[174,175,202,203] There is a growing interest in making scaffolds for tissue engineered cartilage that utilizes collagen type II, and many current studies utilize collagen type II as a crosslinked sponge.[122,204,205] Due to the fact that collagen type II exhibits poor mechanical properties when forming a hydrogel on its own, studies have explored ways to enhance the mechanical properties of collagen type II hydrogels by developing composite scaffolds.[115,206,207] From the experiments conducted here, the 3:1 gels were able to incorporate both collagen type I and collagen type II within the gels. It is important to note that an antibody was able to detect collagen type II, and therefore it is likely that collagen type II would be accessible to cells embedded in the scaffolds. The 3:1 gels also retained a significantly higher amount of CS, which allows articular cartilage to withstand compressive forces, than the other blends. Adding GAGs to the collagen gels creates a more biologically relevant scaffold for articular cartilage tissue engineering. Moreover, compared to the 1:1 gels, the 3:1 gels exhibited lower void space percentages and higher storage, loss, and complex moduli. Thus, based on all these properties, the 3:1 collagen type I to collagen type II blend has the potential to be implemented as a scaffold to effectively engineer articular cartilage tissue.

2.4 Conclusion

In this study, we created hydrogels composed of different ratios of collagen type I to collagen type II to elucidate their unique properties. We demonstrated that the addition of collagen type II alters gel formation, network structure, and mechanical properties. From the five different blends we created, the 3:1 collagen type I to collagen type II ratio blend has the potential to be implemented effectively for use in tissue engineering.

2.5 Chapter 2 Supplementary Information

2.5.1 Supplemental Materials and Methods

Collagen type II in the gel was visualized using immunostaining with a primary antibody for collagen type II (Abcam 34712, Cambridge, MA). The gels were fixed in 3% paraformaldehyde for 1 hour. After fixation, the gels were rinsed three times with 1x PBS, blocked with blocking buffer (5% non-fat powdered milk in 1x PBS) for 1 hour at room temperature, and rinsed three times with 1x PBS. The gels were incubated with the primary antibody for 24 hours at 4˚C. The gels were rinsed with 1x PBS before being incubated with a goat anti-rabbit AlexaFluor® 555 (Cell Signaling Technology 4413S, Danvers, MA) for 24 hours at 4˚C. All confocal images were obtained using a 20x objective on a Nikon Ti-EC-1 Plus microscope (Nikon, Melville, NY). Nikon NIS-Elements AR software (version 3.2) was utilized to analyze fluorescence images.

2.5.2 Supplemental Figures

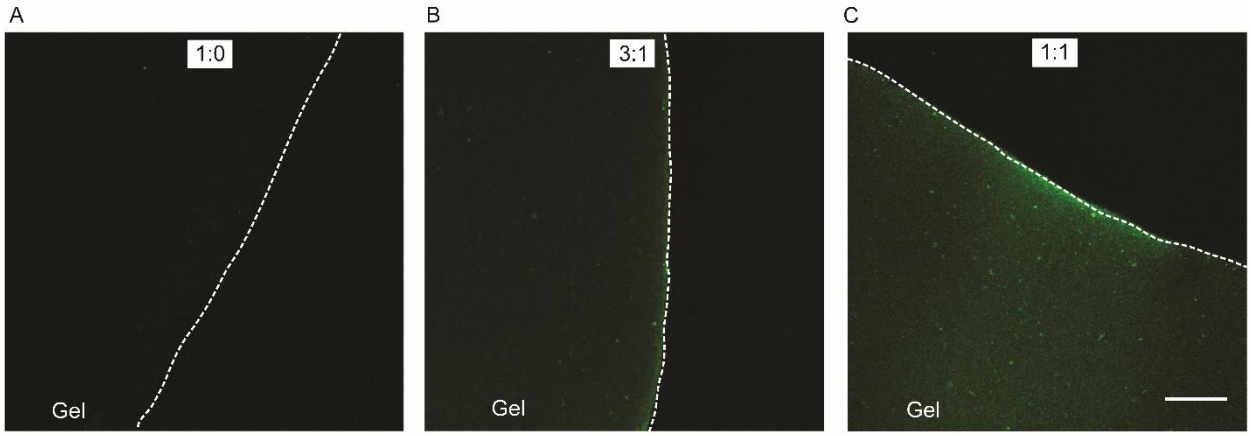

Figure 2-6. Representative images of immunostaining for collagen type II (green) hydrogels at different blends of (A) 1:0, (B) 3:1, and (C) 1:1 ratios of collagen type I to collagen type II. The boundary of the gel is indicated with the white, dashed lined, and the side containing the gel is notated in the figure. Scale bar represents 100 µm.

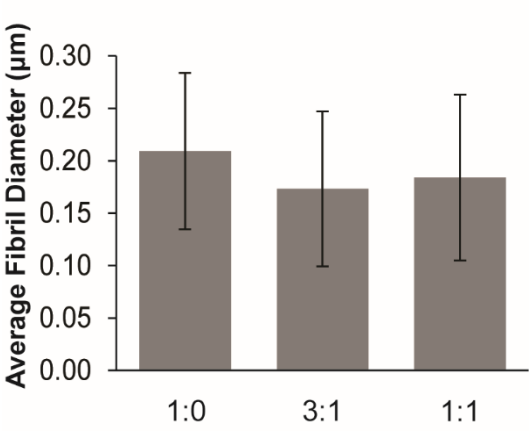

Figure 2-7. Average fibril diameter in the gels at different ratio blends.

ANOVA and Tukey's post hoc tests were performed on the average fibril diameter data by using nested factorial models. For the average fibril diameter data, there were no significant differences observed between the different blends. Data ($n \geq 782$) are represented as the mean ± the standard deviation.

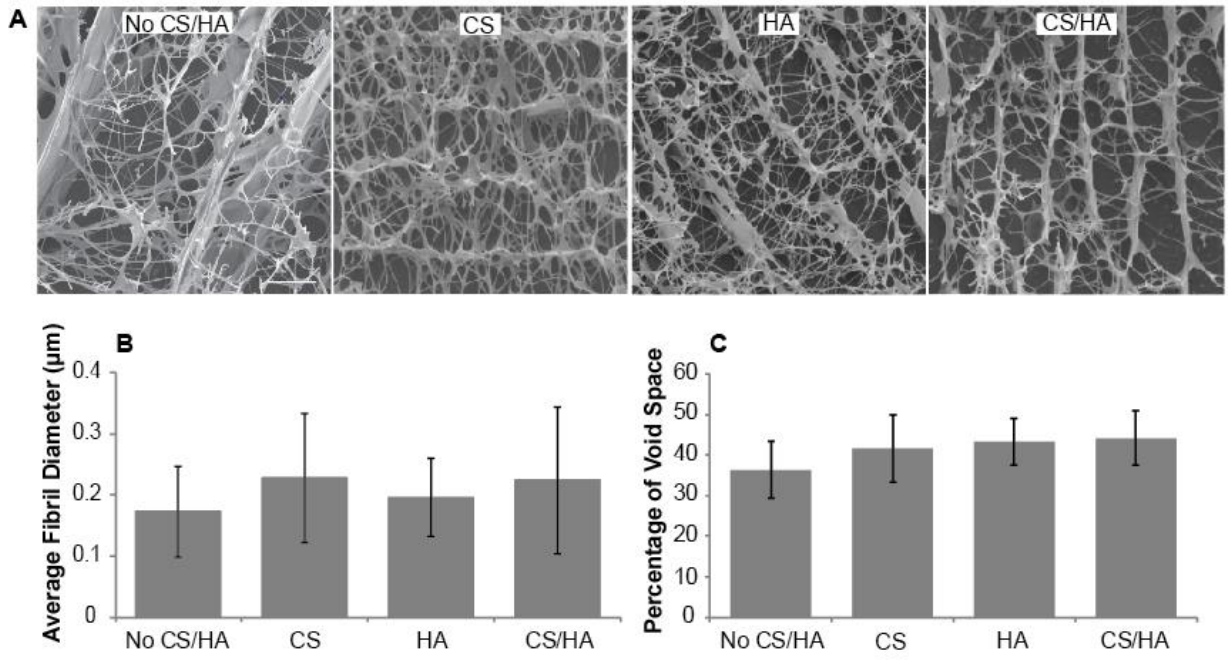

Figure 2-8. Effect of adding GAGs in collagen networks of different ratio blends.

(A) Representative cryoSEM images of 3:1 collagen type I to collagen type II gels with no GAGs added or supplemented with CS, HA, or both CS and HA show the collagen fibril network within the gels. Scale bar represents 5 μm. (B) Average fibril diameter and (C) percentage of void space for the gels based on cryoSEM images obtained at 10,000x magnification. ANOVA and Tukey's *post hoc* tests were performed on the average fibril diameter and the percentage of void space data by using nested factorial models. There were no significant differences observed between gels that had no GAGs added or gels supplemented with CS, HA, or both CS and HA ($p > 0.05$). Data ($n \geq 58$ for fibril diameter, $n \geq 8$ for void space percentage) are represented as the mean ± the standard deviation.

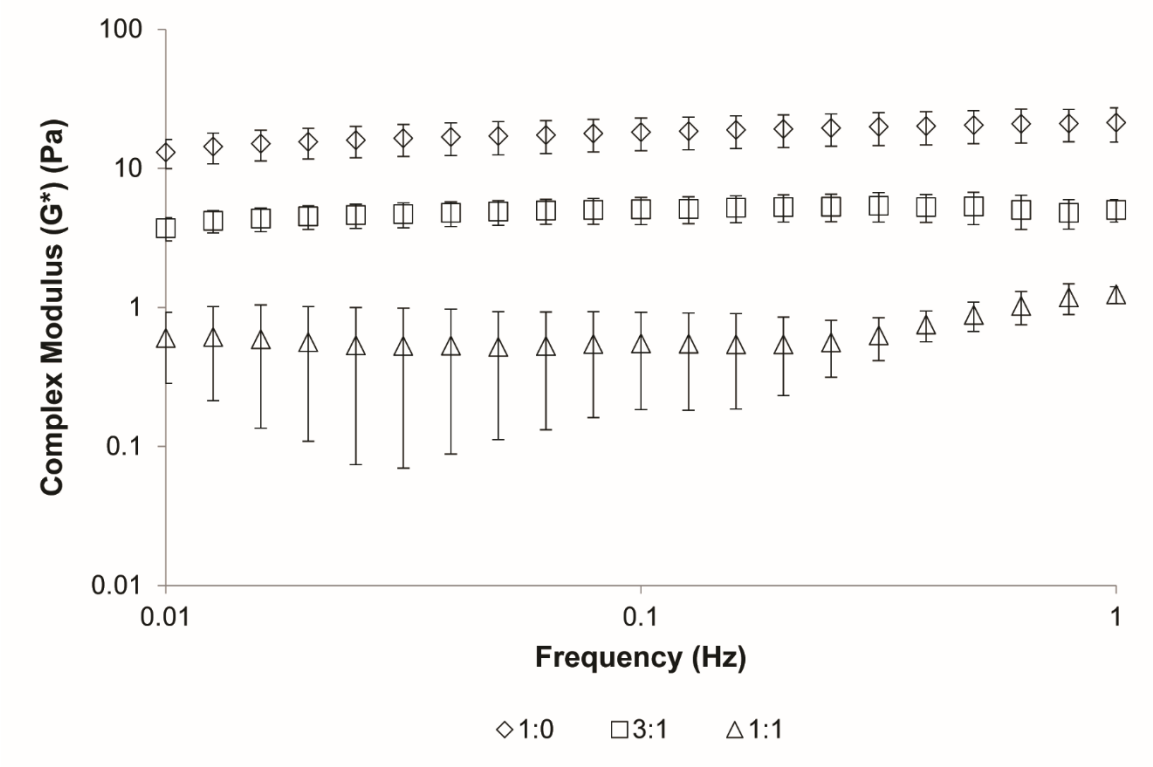

Figure 2-9. Complex modulus of gels prepared from mixtures of 1:0, 3:1, and 1:1 collagen type I to collagen type II. ANOVA and Tukey's *post hoc* tests were performed.

At 1 Hz, a significant difference ($p < 0.05$) was observed between the complex moduli for the three different ratios. Data ($n = 4$) are represented as the mean ± the standard deviation.

3. COLLAGEN TYPE I AND II BLEND HYDROGEL WITH AUTOLOGUS MESENCHYMAL STEM CELLS AS A SCAFFOLD FOR ARTICULAR CARTILAGE DEFECT REPAIR

3.1 Introduction

Osteoarthritis, a disease defined by the loss of articular cartilage due to wear and degradation, causes pain and stiffness in the joints of over 30 million adults in the United States.[208] Surgical procedures used to repair damaged articular cartilage are common in the United States, and their incidence rate grows at 5% annually.[209] Articular cartilage lacks the inherent ability for self-repair due to the fact that it is both avascular and has a low density of chondrocytes.[210] The avascular nature of articular cartilage hinders the native wound healing process due to limited delivery of nutrients and progenitor cells to damaged tissue. Although there is no cure for osteoarthritis, there are many surgical treatment options for focal cartilage defects, including osteochondral grafts, autologous chondrocyte implantation, and marrow stimulation.[211,212] However, these invasive options incur long rehabilitation times and usually promote the regrowth of fibrocartilage, which has mechanical properties inferior to native, hyaline cartilage.[213] Therefore, we take a tissue engineering approach to cartilage regeneration to restore the damaged tissue.

Tissue engineering seeks to repair damaged tissues by introducing an optimized combination of cells, scaffold, and bioactive factors that can be transplanted into a patient.[6] An ideal scaffold material should provide instructions to cells, which are either encapsulated in the material or recruited to the area, in order to maintain cell viability and regulate cell function.[214] Collagen hydrogels are attractive options for tissue-engineered scaffolds since collagen is found in many different tissues throughout the body and is also biocompatible.[96] In addition, collagen fibrillogenesis, the spontaneous self-assembly of collagen monomers into fibrils and then larger collagen fibers, occurs at physiological conditions.[97]

Although collagen type II is the main component found in native cartilage tissue, collagen type I, which is abundantly available, continues to be the most utilized type of collagen in tissue engineered scaffolds. The $\alpha_2\beta_1$ integrin receptor in the cell membrane of bone marrow cells interacts with collagen type I, an important component of bone, to induce osteoblastic differentiation.[102] MSCs encapsulated within collagen I hydrogels have been successfully

differentiated into bone and used to repair bone in animal models.[103] On the other hand, many studies have used collagen I hydrogels for cartilage engineering. For example, to repair cartilage defects in humans, early studies encapsulated autologous chondrocytes within hydrogel scaffolds created using collagen type I from different species.[104,105] In another early study, porcine collagen type I hydrogel scaffolds with autologous bone marrow-derived MSCs were used in human osteoarthritic knees to repair cartilage defects more effectively than a cell-free scaffold.[106] Furthermore, autologous bone marrow-derived MSCs were isolated, embedded within calf skin collagen type I, and used to repair cartilage defects into the weight-bearing region of a rabbit.[107] Better integration with surrounding tissue and surface splitting, fibrillation, and thinning are some limitations of collagen type I hydrogels used for articular cartilage repair that will need to be addressed as areas for improvement.[107]

Despite promising results from early studies investigating the differentiation of MSCs into chondrocytes in collagen type I based hydrogels, studies have also shown that collagen type II hydrogels promote the differentiation of embedded MSCs to chondrocytes more efficiently than collagen type I hydrogels.[110,111] Although collagen type I is found in fibrocartilage tissue such as the intervertebral disc and meniscus, articular cartilage contains little to no collagen type I.[108,109] In contrast, collagen type II makes up 90-95% of the ECM collagen produced by chondrocytes.[20] Despite some arthritogenic properties,[112] collagen type II is organized in a macromolecular structure that chondrocytes sense, and these cell-matrix interactions help to maintain chondrocyte phenotype.[114]

Compared to collagen type I, collagen type II exhibits poor mechanical properties when forming a physically crosslinked hydrogel.[115] In a study comparing fibrillogenesis of collagen type I and collagen type II, collagen hydrogels formed routinely in gels made of collagen type I but not in collagen type II hydrogels.[116] The same study also saw that the smaller fibers of collagen type II, as compared to collagen type I, were associated with more charged and hydrophobic residues that took part in more intramolecular interactions with fewer residues available for intermolecular interactions. The lack of intermolecular fibril interactions[116] and slower fibrillation process[117] are likely the reasons for lack of collagen type II gel formation.

Although a few papers have investigated collagen type II scaffolds,[111,118] the lack of robust hydrogels and inferior mechanical properties, as noted previously, have resulted in strategies, such as crosslinking scaffolds, using a recombinant collagen type II, or creating composite scaffolds,

that address these concerns. Chemical crosslinkers, such as 3-(3-dimethylaminopropyl)carbodiimide (EDC), glutaraldehyde, and N-hydroxysuccinimide (NHS), have been utilized to modify scaffolds containing collagen type II, [119–126] but are not cytocompatible and cannot be used to encapsulate cells. Recombinant collagen type II has also been investigated as a scaffold, with encapsulated cells, for cartilage repair,[118,127,128] but it is expensive and difficult to scale.[129] Previous studies have combined collagen type II with a number of scaffold materials including poly(ethylene glycol) (PEG),[130,131] glycosaminoglycans (GAGs),[120,132] alginate,[110,133] and chitosan.[124,134] Including collagen type II in composites increased ECM production specific to cartilage, regulated chondrocyte proliferation, and induced cartilage repair.[126,130,131,134–137] Blends of collagen type I and II have been studied without cells *in vivo,*[138] and with encapsulated chondrocytes *in vitro* and *in vivo.*[135,139] To date, our study is the first to encapsulate mesenchymal stem cells (MSCs) in a collagen type I and II hydrogel and investigate them in an *in vivo* model of cartilage defect repair.

A number of different cells types, including chondrocytes and different varieties of stem cells, have been encapsulated into scaffolds for cartilage tissue engineering.[6] Chondrocytes in healthy cartilage are responsible for both producing and maintaining the ECM through a homeostatic balance of cartilage synthesis and degradation. However, chondrocytes are difficult to harvest due to the fact that a biopsy removes very few viable cells and donor sites often become unhealthy after cartilage removal.[72] Further expansion of biopsied chondrocytes *in vitro* is required due to the low yield of harvested cells, but the chondrocytes often dedifferentiate.[73] Bone marrow-derived mesenchymal stems cells (MSCs) are a promising cell source for engineered articular cartilage due to their ease of isolation and ability to differentiate into chondrocytes under certain environmental conditions.[215,216]

Our lab previously developed and characterized hydrogel scaffolds made of a 3:1 collagen type I to collagen type II ratio (this formulation is hereafter referred to as Col I/II gels) to harness the biological activity of collagen type II and the superior gelation of collagen type I.[217] Hydrogels were prepared with collagen type I:type II ratios of 1:0, 3:1, 1:1, 1:3, and 0:1, and we demonstrated that the addition of collagen type II alters the amount of total collagen incorporated in the hydrogel, network structure, and storage modulus. From the five different ratio blends created, the 3:1 blend formed robust hydrogels with superior mechanical properties compared to the other blends investigated.[217] Building on the prior Col I/II blend characterization studies, the goal of the current

study was to evaluate the *in vitro* chondrogenic differentiation potential of bone marrow-derived MSCs embedded within Col I/II gels and the ability of Col I/II gels with encapsulated cells to repair cartilage defects *in vivo.* We used autologous MSCs to eliminate the possibility of an immune response following implantation. Of the many animal models that have been developed to assess the efficacy of tissue engineered cartilage scaffolds, a rabbit model was chosen for preliminary investigation due to the fact that rabbits reach skeletal maturity in 9 months and have a 3 mm critical sized defect.[154] The Col I/II hydrogel increased cartilage matrix GAG production and decreased unwanted phenotypes *in vitro*. In a rabbit model, the Col I/II hydrogel promoted integration with surrounding tissue and provided favorable conditions for cartilage repair. Results from this study suggest that there is a clinical value in the placement of a Col I/II hydrogel with encapsulated MSCs into a cartilage defect to aid in cartilage repair.

3.2 Materials and Methods

3.2.1 Reagents

Unless otherwise specified, all materials used were purchased from Sigma-Aldrich (St. Louis, MO).

3.2.2 Bone Marrow Collection

All animal experiments were performed using protocols approved by the Purdue Animal Care and Use Committee (PACUC). Bone marrow was collected from both femurs and humeri of skeletally mature, male New Zealand White rabbits (Covance, Princeton, NJ). The rabbits were 9 months of age prior to bone marrow collection and weighed 3.6 ± 0.2 kg. The rabbits were anesthetized by intramuscular injection with a mixture of ketamine, xylazine, and butorphanol (35 mg/kg, 5 mg/kg, and 0.01 mg/kg respectively) and were maintained on isoflurane and oxygen with a mask. Bone marrow was collected from four sites including both the left and right proximal femurs and proximal humeri. The bone marrow extraction sites were clipped and scrubbed with chlorhexidine using standard techniques. Bone marrow was aspirated using an 18-gauge needle

that was percutaneously inserted into the intertrochanteric fossa of the femur and the greater tubercle of the humerus. After the needle penetrated through the bone into the medullary cavity, the bone marrow was aspirated.

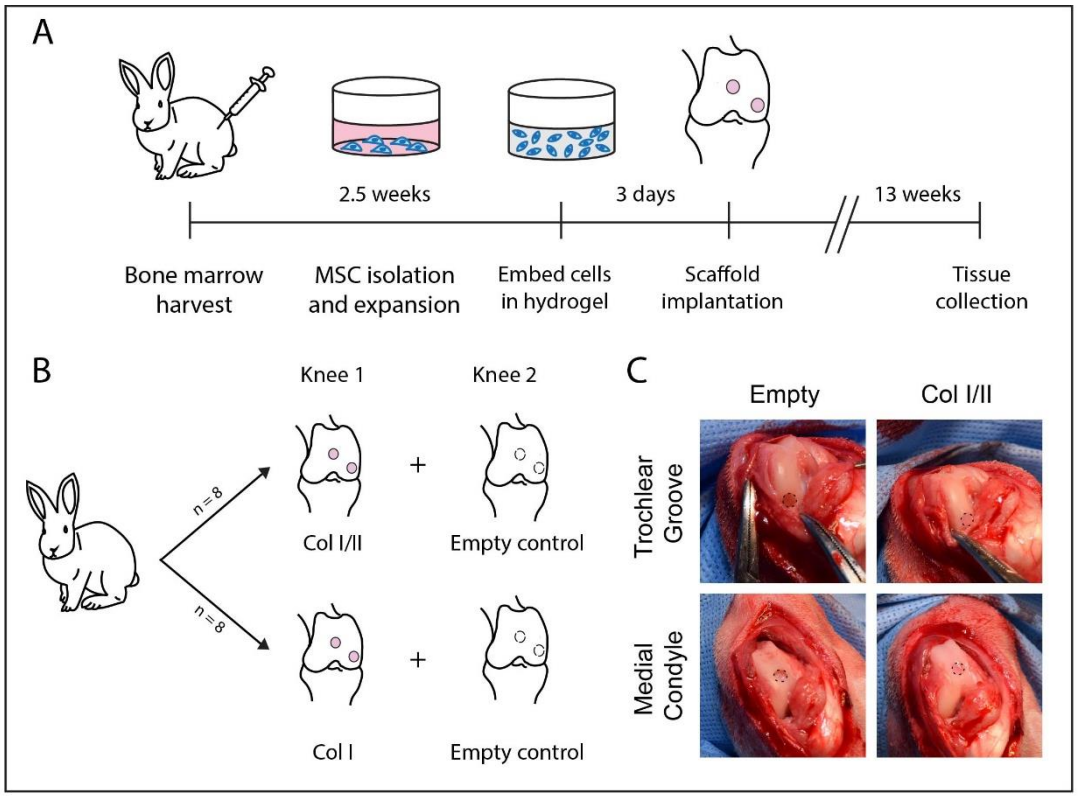

Figure 3-1. Overview of rabbit study.

(A) *In vivo* workflow timeline and (B) experimental design. (C) Defect preparation and scaffold implantation. Hydrogel scaffolds, which are surrounded by a dotted line, were press fit into defects that were drilled into the femoral trochlear groove and medial condyle.

3.2.3 Stem Cell Isolation and Culture

The marrow from each rabbit was pooled by rabbit, centrifuged for 10 minutes at 500*g* and resuspended in maintenance medium (low-glucose Dulbecco's modified Eagle's medium (DMEM) supplemented with 10% fetal bovine serum (Lonza, Walkersville, MD) and 1% penicillin-streptomycin. Autoclaved water was added to lyse the red blood cells. The marrow was gently mixed for 30 seconds before adding additional maintenance medium, and the suspension was centrifuged for 10 minutes at 500*g*. After the pellet was resuspended, the cells were counted, plated on 100-mm plates at a density of 10^7 cells per plate, and incubated at 37°C with 5% CO_2. The first

medium change was performed after four days of culture following a phosphate buffered saline (1x PBS) wash step, and subsequent medium changes were every three days. The cells were subcultured after 2.5 weeks upon reaching 70% - 80% confluency (Figure 3-1).

3.2.4 Collagen Scaffold Preparation

An 11 mg/mL stock solution of collagen type II from lyophilized chicken sternum (Sigma-Aldrich, Saint Louis, MO) was prepared in 20 mM acetic acid. Upon sterile filtration, the concentration of the collagen type II stock solution was measured using a bicinchoninic acid (BCA) assay (Pierce, Rockford, IL) following the manufacturer's protocol. The stock solution of collagen type II was then diluted to 8 mg/mL in 20 mM acetic acid prior to use. The collagen type I and II blend hydrogels were prepared using a modified protocol from Vazquez *et al.*[217] The stock solution of collagen type II was combined with acid-solubilized collagen type I from rat tail (Corning, Corning, NY). The pH of the solutions was raised to 7.4 with the addition of 10x PBS, 1 M NaOH, and 1x PBS and diluted to a final concentration of 4 mg/mL total collagen. The gels were prepared with a 3:1 collagen type I to collagen type II ratio (Col I/II) or all collagen type I (Col I). Passage 3 cells were resuspended in collagen pre-polymerization solutions at a cell density of 5 x 10^6 cells/mL and a final volume of 50 µL. The hydrogels were allowed to polymerize at 37°C for 2 hours before the addition of medium. After polymerization, chondrogenic medium with or without added growth factor was added to the scaffolds for *in vitro* analysis. Defined chondrogenic medium was formulated with high-glucose DMEM supplemented with 1% ITS+Premix (BD Biosciences, San Jose, CA), 1% penicillin-streptomycin, 1 mM sodium pyruvate, 50 µM proline, 4 mM L-glutamine, 50 µg/mL ascorbic acid, 100 nM dexamethasone, and 10 ng/mL transforming growth factor-β3 (TGF-β3) (Peprotech, Rocky Hill, NJ). Defined chondrogenic medium without added growth factor was formulated the same way as the chondrogenic media but lacked TGF-β3. Treatments grown in chondrogenic medium without added TGF-β3 growth factor are labeled with (-TGF) after the name of the treatment. For *in vitro* analysis, cell-hydrogel constructs were cultured for up to 4 weeks with 3 medium changes each week. MSCs grown in pellet culture served as a comparison in the study. To form the pellets, MSCs were centrifuged, washed, pelleted at a density of 2.5 x 10^5 cells/pellet, and cultured in a high-throughput culture system in a conical-bottom plate.[218] Both hydrogels and pellets were maintained in free-floating conditions. For the *in vivo* study, autologous MSCs were encapsulated into the collagen scaffolds, as previously discussed,

and were cultured for 3 days in maintenance medium prior to surgical implantation (Figure 3-1A).The medium was changed the day before implantation. After 3 days of culture, the cell-hydrogel constructs were press fit into the cartilage defects and filled the space without gaps or excess.

3.2.5 Papain Digestion

The pellets were rinsed with PBS and digested with 125 μg/mL of activated papain solution in a papain digestion buffer (5 mM ethylenediaminetetraacetic acid (EDTA), 5 mM L-cysteine (Alfa Aesar, Ward Hill, MA), and 100 mM NaH_2PO_4) at 60°C for 24 hours.[219] Cell-hydrogel constructs were lyophilized prior to digestion with papain solution. The digested product was then freeze-dried and resuspended in autoclaved water.

3.2.6 DNA Quantification

DNA was measured using Hoechst dye as previously described.[220] After combining the digested pellet or cell-hydrogel construct (n = 5 or 6 for cell-gel scaffolds and pellets) with the Hoechst dye solution, the fluorescence of the solution was read at a 340 nm excitation wavelength and a 465 nm emission wavelength. A standard curve was created using calf thymus DNA.

3.2.7 GAG Quantification

GAG content was measured using a dimethyl methylene blue (DMMB) assay where 20 μL of the digested pellets or cell-hydrogel constructs were combined with 30 μL of water and 250 μL DMMB dye solution (n = 5 or 6 for cell-gel scaffolds and pellets). The absorbance of the solution was read at 525 nm. A standard curve was created using chondroitin sulfate from shark cartilage (Seikagaku, Tokyo, Japan). The GAG values measured were normalized to the amount of DNA measured per sample.

3.2.8 AP Activity

The medium was collected from both the pellets and cell-hydrogel constructs (n = 8 or 9 for Col I hydrogels, Col I/II hydrogels, and pellets with TGF-β3 (Pel) and n = 3 for pellets without TGF-β3 (Pel (-TGF))) after each week following a previously described protocol and using proper background controls.[219] AP activity was measured by incubating 50 μL of the collected medium

with 50 μL of p-nitrophenylphosphate substrate solution (1 mM $MgCl_2$, 10 mg/mL p-nitrophenylphosphate, and 0.1 M glycine) for 2 hours at 37°C. A standard curve was created using p-nitrophenol in chondrogenic medium.

3.2.9 Gene Expression

Both the pellets and the gels were washed with PBS then homogenized in lysis buffer and β-mercaptoethanol using a syringe needle. For each sample (n=4), three cell-hydrogel constructs or pellets were combined for the Col I, Col I/II, and pellet with TGF-β3 (Pel) treatments. A total of 5 pellets cultured without TGF-β3 (Pel (-TGF)) were combined for use as qRT-PCR samples (n=4). The NucleoSpin RNA kit from Macherey-Nagel (Bethlehem, PA) was used to isolate RNA. A High Capacity cDNA Reverse Transcription kit from Applied Biosystems (Foster City, CA) was used to synthesize complementary DNA from the isolated RNA. Relative expression levels were measured using qRT-PCR with the primer sequences (Table 3-1) for collagen type I, II, and X, aggrecan, Sox9, and glyceraldehyde-3-phosphate dehydrogenase (GAPDH) (Integrated DNA Technologies, Skokie, IL). The samples were heated for 10 minutes at 95°C followed by 40 cycles for 15 seconds at 95°C, 15 seconds at 55 or 60°C, and 40 seconds at 68°C. All values were normalized to GAPDH levels with an average Ct value of 20.7 cycles and a standard deviation of 1.1 cycles. The differences in gene expression were calculated relative to negative controls using the ΔΔCt method.[221]

3.2.10 Surgical Implantation

The rabbits were randomly assigned, as seen in Figure 3-1B, into two groups to receive a Col I scaffold (n=8) or a Col I/II scaffold (n=8) with autologous MSCs. Each rabbit received treatment in one knee and one control knee was left empty. The knee that was chosen as the treatment knee was randomized so that that half of the rabbits received the treatment in the right knee and the other half received the treatment in the left knee. Rabbits were induced with a mixture of ketamine, xylazine, and butorphanol (35 mg/kg, 5 mg/kg, and 0.01 mg/kg IM, respectively) prior to intubation with isoflurane and oxygen. The joint was entered, using sterile surgical techniques and a medial parapatellar approach, and two 3.2-mm diameter and 2-mm deep defects (Figure 3-1C) in the femur were created with a Hall Power Pro5100M surgical drill (ConMed, Utica, NY). One defect was placed in the medial condyle (weight-bearing region) during maximum flexion of the

stifle, and the other was placed in the trochlear groove (the non-weight bearing region) 1 cm proximal to the origin of the cranial cruciate ligament. Within one knee, the same treatment was placed in the medial condyle and trochlear groove defect. The defects were rinsed with saline prior to treatment, and the control defects were rinsed with saline and left empty. Cell-hydrogel composites were washed with 1x PBS and press fit into both defects in one knee, and the defects in the other knee were left empty as a control. The surgical incision was closed in 3 separate layers using standard suturing techniques. All rabbits were given a subcutaneous injection of buprenorphine SR (ZooPharm, Windsor, CO) at 0.1 mg/kg. The rabbits were permitted time to recover before moving back to their cages and were allowed to move freely post operation. The rabbits were euthanized after 13 weeks with an overdose of barbiturate following guidelines from the American Veterinary Medical Association Panel on Euthanasia.

3.2.11 Defect Evaluation

Following euthanasia, the stifle joints were evaluated grossly for joint capsule inflammation and defect healing. After isolation of the distal femur, the defects were fixed in 10% neutral buffered formalin, decalcified in a 0.5 M EDTA solution, and embedded in paraffin. Radiographs confirmed total decalcification. Sagittal sections (4 μm thick) from the center of the defect were stained with hematoxylin and eosin (HE) or safranin-O/fast green (SOFG). HE and SOFG slides were evaluated under a light microscope. A semi-quantitative histochemical scoring system adapted from O'Driscoll *et al.* (Table 3-2) was used to evaluate tissue repair in 9 different categories with a total possible tissue repair score that ranged between 0 to 24 points.[222] All slides were examined and scored by two blinded observers, including one board-certified veterinary pathologist (A.C.). Independent histochemical scores by observers were averaged.

3.2.12 Statistical Analysis

All data were expressed as the mean ± standard deviation. An alpha level of 0.05 was selected for statistical significance. Unpaired t-tests were performed for normalized GAG content values between the same treatment at different timepoints for pellets without TGF-β3 (Pel (-TGF)) and the Col I hydrogels. Welch's t-tests were performed for normalized GAG content values between the same treatment at different timepoints for pellets with TGF-β3 (Pel) and the Col I/II hydrogels. A one-way ANOVA and Tukey's post hoc test were performed to analyze normalized

GAG content at a single timepoint ($p < 0.05$). A mixed-effect model and Tukey's post hoc test were performed to analyze AP activity ($p < 0.05$) at a single timepoint. A one-way ANOVA and Tukey's post hoc test were performed to analyze AP Activity of a treatment over time ($p < 0.05$). Single factor analysis of variance (ANOVA) and Tukey's post hoc tests were for gene expression analysis (sox9, aggrecan, collagen type I, and collagen type X) and histology scoring analysis. An ANOVA and Games Howell's post hoc test were performed for gene expression analysis of collagen type II.

3.3 Results

Collagen blend hydrogels increased GAG production

The GAG content normalized to DNA content in each scaffold with encapsulated MSCs or pellet was analyzed after a 14- and 28-day culture period with the results shown in Figure 3-2A and Figure 3-2B. GAG content, DNA content, and dry weight at 14 days are shown in Table 3-3, and GAG content, DNA content, and dry weight at 14 days are shown in Table 3-4. There was no statistical difference in normalized GAG content when comparing the Col I/II and Col I hydrogels when they were cultured in media with added TGF- β3 for 14 days. At 14 days there was a statistically greater ($p = 0.04$) amount of normalized GAG in the Col I hydrogels when compared to pellets with TGF- β3 (Pel). Normalized GAG content increased between days 14 and 28 in all treatments except for pellets cultured without TGF- β3 (Pel (-TGF)). After 28 days in culture, there was a statistically greater amount of normalized GAG in the Col I/II hydrogels compared to the Col I hydrogels, pellets with TGF- β3 (Pel), and pellets without TGF- β3 (Pel (-TGF)).

Collagen blend hydrogels did not promote an increase in AP activity

Medium aliquots were taken at 7, 14, 21, and 28 days and analyzed for AP activity. The Col I hydrogel and pellet with added TGF-β3 (Pel) each increased over time until a peak at about 14 days and 21 days, respectively (Figure 3-2C). A similar peak in AP activity was not seen in the Col I/II hydrogels or pellet without added TGF-β3 (Pel (-TGF)), and there was no significant increase in AP activity over time. Compared to the Col I/II hydrogel, the pellet with added TGF-β3 (Pel) had significantly higher AP activity at each time point, the Col I hydrogel had significantly

higher AP activity at days 7, 14, and 21, and the pellet without added TGF-β3 (Pel (-TGF)) had significantly higher AP activity at days 14 and 21.

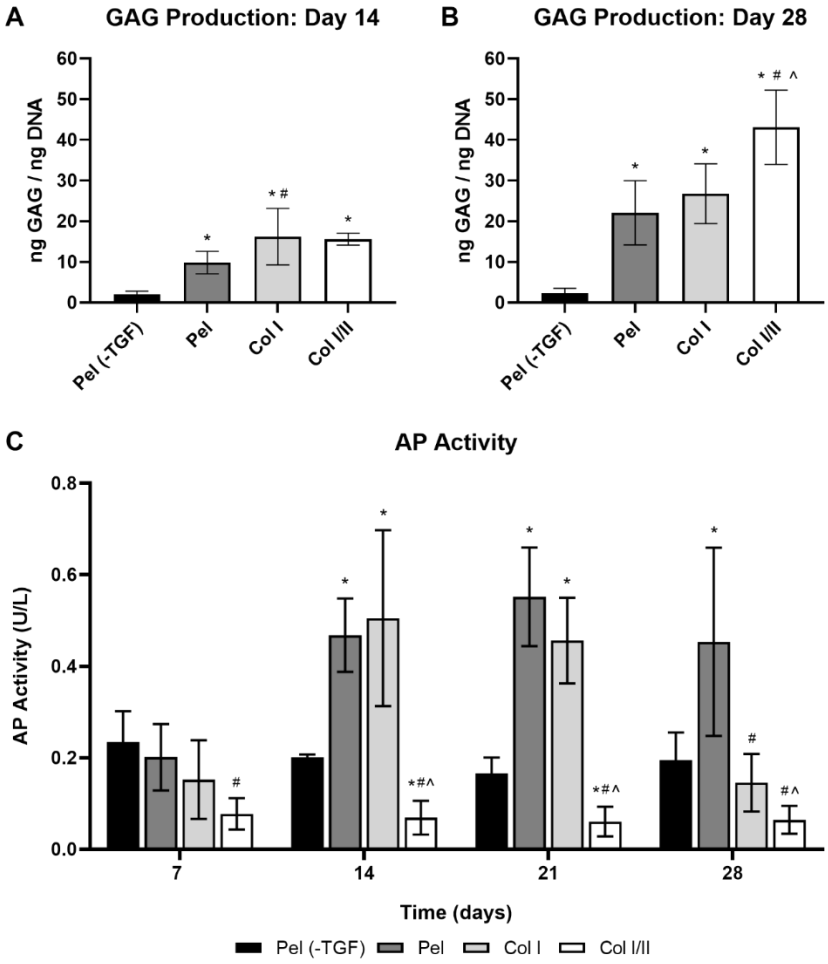

Figure 3-2. Collagen blend hydrogel increased GAG production when cultured with TGF-β and did not promote an increase in AP activity.

GAG/DNA ratio of the cell-hydrogel constructs and pellets after a (A) 14-day or (B) 28-dayculture period. Values are expressed as mean ± SD (n = 5 or 6 for cell-gel scaffolds and pellets). A one-way ANOVA and Tukey's post hoc test were performed within a timepoint ($p < 0.05$).* indicates a statistical difference in GAG production from pellets without TGF-β3 (Pel (-TGF)) within a timepoint, # indicates a statistical difference in GAG production from the pellets with TGF-β3 (Pel) within a timepoint, and ^ indicates a statistical difference in GAG production from the collagen type I hydrogels (Col I) within a timepoint. AP activity of rabbit MSCs over time assay in removed culture media at 7, 14, 21, or 28 days (n = 8 or 9 for Col I hydrogels, Col I/II hydrogels, and pellets with TGF-β3 (Pel) and n = 3 for pellets without TGF-β3 (Pel (-TGF))). A mixed-effect model and Tukey's post hoc test were performed ($p < 0.05$). * indicates a statistical difference in AP activity from pellets without TGF-β3 (Pel (-TGF)) within a timepoint, # indicates a statistical difference in AP activity from the pellets with TGF-β3 (Pel) within a timepoint, and ^ indicates a statistical difference in AP activity from the collagen type I hydrogels (Col I) within a timepoint.

Sox9 gene expression was upregulated in the Col I/II hydrogels compared to Col I gels

Gene expression levels were measured using qRT-PCR in cells cultured in Col I/II hydrogels, Col I hydrogels, pellets with TGF-β3 (Pel), and pellets without TGF-β3 (Pel (-TGF) after 14 days as seen in Figure 3-3. There was a statistical higher collagen type II gene expression in the pellets cultured with TGF-β3 (Pel) compared to Col I/II hydrogels, Col I hydrogels, and pellets without TGF-β3 (Pel (-TGF)). The collagen type II expression levels of both Col I/II hydrogels and Col I hydrogels were statistically higher than those of pellets cultured without TGF-β3 (Pel (-TGF)). Relative sox9 gene expression was upregulated in the Col I/II hydrogels and pellets cultured with TGF-β3 (Pel) when compared to either the Col I hydrogels or pellets cultured without TGF-β3 (Pel (-TGF)). The Col I/II hydrogels and pellets cultured with TGF-β3 (Pel) had statistically higher aggrecan and collagen type I gene expression levels than the pellets cultured without TGF-β3 (Pel (-TGF)). Finally, collagen type X gene expression was statistically upregulated in both Col I/II hydrogels and Col I hydrogels when compared to the pellets cultured without TGF-β3 (Pel (-TGF)).

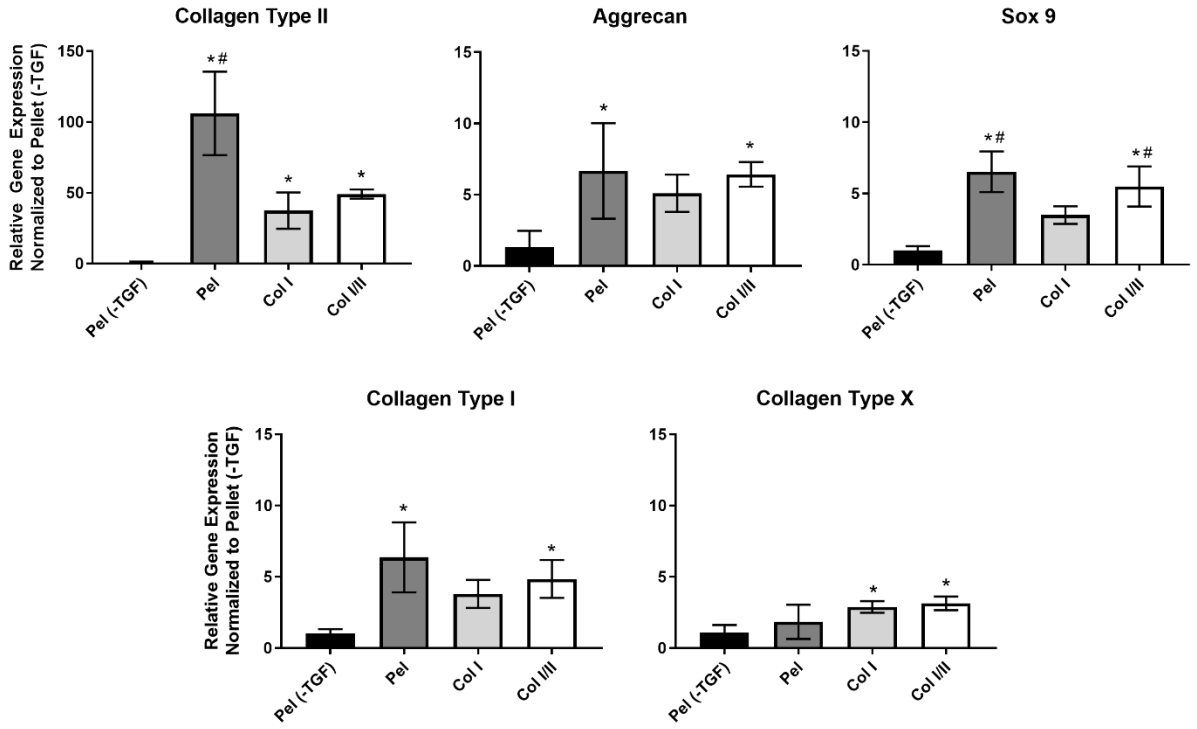

Figure 3-3. Relative gene expression of chondrogenic and collagen genes at 2 weeks.

Relative gene expression of sox9, the master transcription factor involved in chondrogenesis, was upregulated in the Col I/II hydrogels and pellets with TGF-β3 (Pel) compared to either the Col I hydrogels or pellets without TGF-β3 (Pel (-TGF)). An ANOVA and Tukey's post hoc tests were performed ($p < 0.05$) for gene expression analysis of sox9, aggrecan, collagen type I, and collagen type X (n=4). An ANOVA and a Games Howell post hoc test were performed ($p < 0.05$) for gene expression analysis of collagen type II. The * indicates statistical difference from the pellets without TGF-β3 (Pel (-TGF)), and the # indicates statistical difference from the Col I hydrogels.

Histological staining revealed that the repair tissue from Col I/II hydrogels with autologous MSCs matched surrounding articular cartilage

At 13 weeks post-operation, macroscopic examination during defect excision revealed no signs of joint capsule inflammation or degeneration around the defect. Osteoarthritis was not identified. After necropsy, the knees of the rabbits were dissected and photographed for macroscopic scoring (Table 3-5) using categories adapted from Van den Borne *et al.*[223] In addition, the scores were totaled to give an overall macroscopic score. As shown in Figure 3-8, there were no statistical differences between the three treatments investigated in any of the macroscopic

scoring categories (degree of defect repair, integration to border zone, and macroscopic appearance) for defects either in the trochlear groove and media condyle ($p < 0.05$). In addition, there were no statistical differences between the three treatments investigated when comparing overall repair assessment value for defects either in the trochlear groove and media condyle.

Upon excision, tissues were processed, sectioned, and stained with HE and SOFG. Histological analysis revealed differences between both the treatment groups and empty controls. Empty defects in both the trochlear groove and medial condyle lacked smooth surfaces and cellular morphologies expected in native cartilage tissue (Figure 3-4). Empty defects, which were devoid of collagen hydrogel, had a more fibrotic phenotype compared with the hydrogel-treated defects. When stained with SOFG, repair tissues of empty defects in both regions were nearly void of any proteoglycan staining (Figure 3-5).

The cartilage defects filled with the Col I hydrogel contained rounded cells in lacunar spaces with regions of eosinophilic matrix that matched surrounding articular cartilage (Figure 3-4). Spaces between the repair tissue and native cartilage on one or more edge were common in the defects filled with Col I hydrogel, and this finding indicated poor integration to adjacent tissue. Chondrocyte clustering was seen especially in areas on the edge of defects that were filled with the Col I hydrogel. In some defects filled with the Col I hydrogel, the superficial region had an irregular surface and areas with increased eosin in collagen fibers. In addition, some of the Col I hydrogel repair tissue contained bone fragments, which were adjacent to cartilage and did not integrate with the repair tissue. When stained with SOFG, the dark pink to red matrix staining seen in most of these defects was similar to native tissue, but there was a more fibrous superficial zone that lacked matrix staining (Figure 3-5).

The cellular morphology and proteoglycan staining for the Col I/II hydrogels matched that of the adjacent native articular cartilage and included chondrocytes in lacunar spaces (Figure 3-4). The defects in the medial condyle region had smooth and intact surfaces although some contained fissures. Compared to hypocellular regions in the defects filled with Col I hydrogels or left empty, the defects filled with the Col I/II hydrogels had more normal cellularity similar to the surrounding native tissue. However, some chondrocyte clusters were seen on the edge of the repair tissue. There were no major spaces lacking ECM between the surrounding cartilage and the Col I/II repair tissue. In the superficial zone, there were more flattened cells within a more organized ECM as seen in the surrounding native cartilage, but the defect area in the superficial zone also contained fibrous

tissue. There were larger lacunar spaces in the deeper repair tissue of the trochlear groove defects filled with Col I/II hydrogels. When stained with SOFG, the repair tissue in both the trochlear groove and medial condyle regions that were filled with a Col I/II hydrogel demonstrated proteoglycans staining (Figure 3-5).

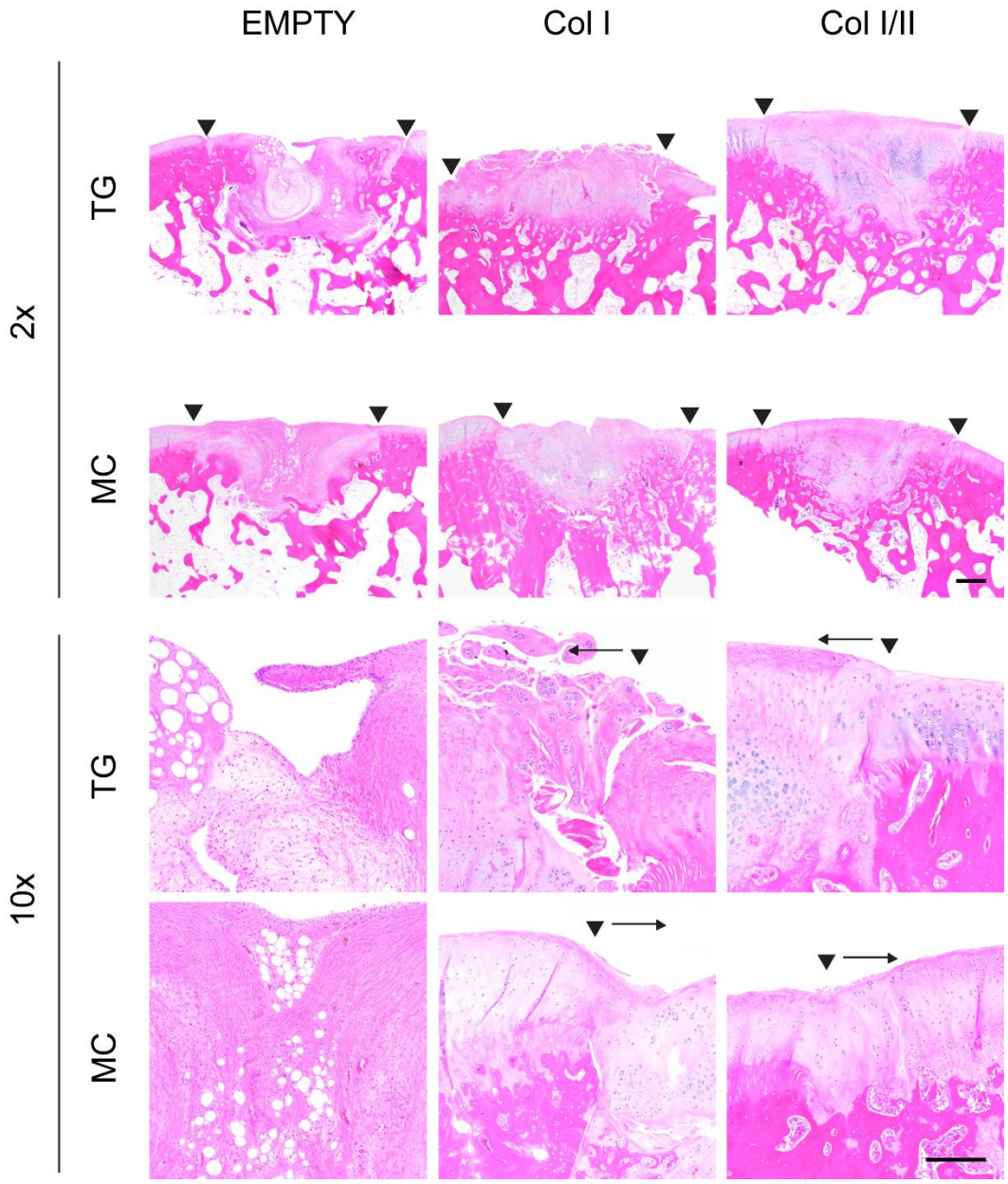

Figure 3-4. Col I/II hydrogel promoted cartilage tissue repair *in vivo*.

HE staining of repaired cartilage left empty or filled with either a Col I/II or Col I hydrogel in the trochlear groove (TG) or the medial condyle (MC) at two different magnifications (2x with a scale bar 500 µm and 10x with a 200 µm scale bar). Staining revealed that the cellular morphology in the Col I/II hydrogels matched that of articular cartilage tissue surrounding the repair tissue. The two arrowheads indicate the edges of the repair tissue. A single arrowhead with an arrow indicates the edge of the repair tissue and the direction of the repair tissue, respectively.

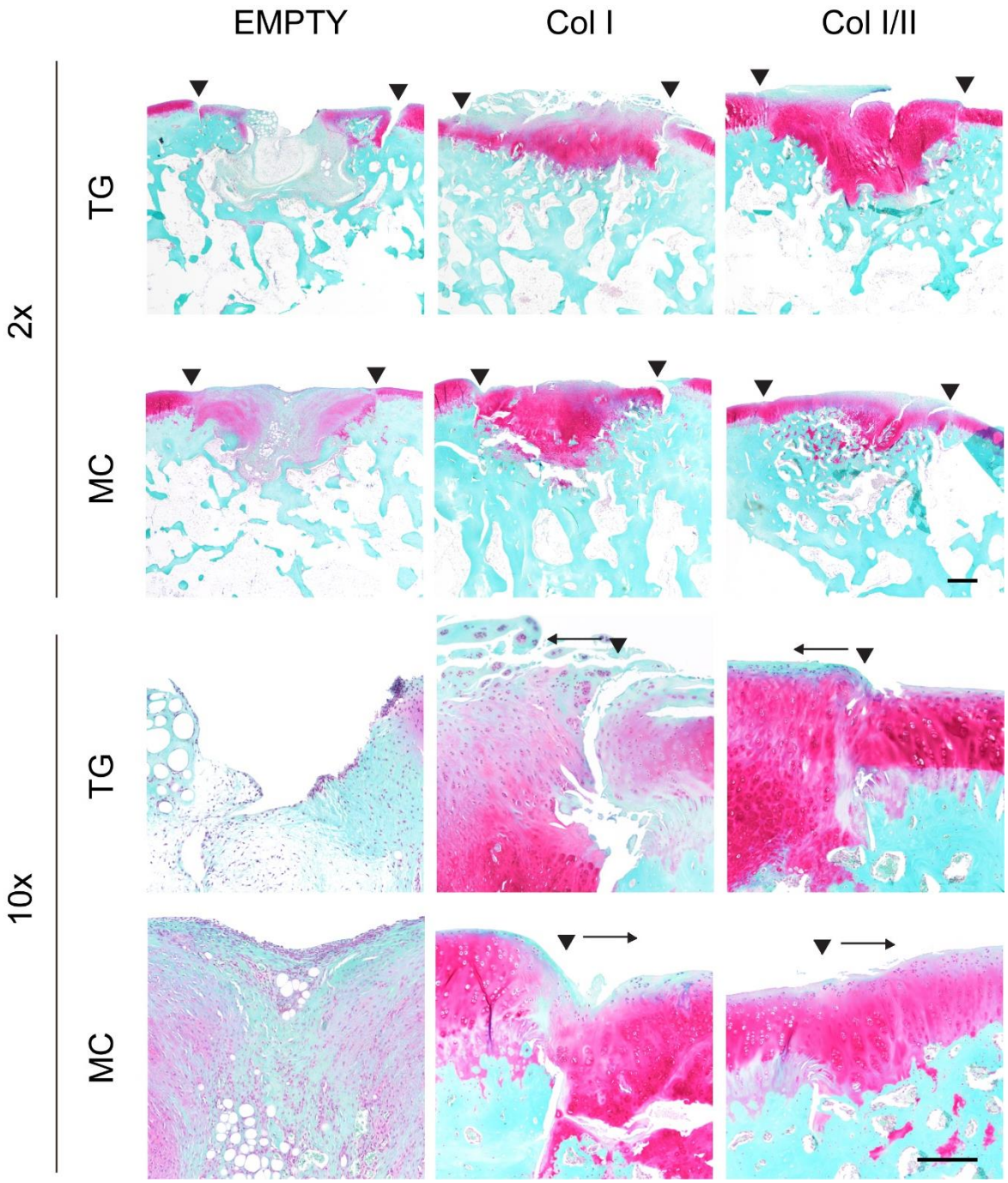

Figure 3-5. Col I/II hydrogel promoted cartilage matrix production *in vivo*.

SOFG staining of repaired cartilage left empty or filled with either a Col I/II or Col I hydrogel in the trochlear groove (TG) or the medial condyle (MC) at two different magnifications (2x with a scale bar 500 µm and 10x with a 200 µm scale bar). The Col I/II hydrogels had dark pink staining, which indicated the presence of proteoglycans. The two arrowheads indicate the edges of the repair tissue. A single arrowhead with an arrow indicates the edge of the repair tissue and the direction of the repair tissue, respectively.

Col I/II hydrogels repaired cartilage defects significantly better than Col I hydrogels or empty defects

In Figure 3-6, semiquantitative histological evaluation revealed that there was a statistically higher overall cartilage repair score for the Col I/II hydrogels compared to the Col I hydrogels and the empty defect controls in both the medial condyle (weight-bearing region) and the trochlear groove (non-weight bearing region). More specifically, the hypocellularity score for the Col I/II hydrogels, in the trochlear groove defects, was statistically higher than the repair scores of the Col I hydrogels and the empty defect controls (Figure 3-9). Trochlear groove defects had statistically higher repair scores in the Col I/II hydrogels compared to the empty defect controls in the categories of matrix staining, chondrocyte clustering, and bonding to adjacent cartilage. In defects created in the medial condyle, there were statistically higher repair scores in the Col I/II hydrogels compared to the empty defects in matrix staining, hypocellularity, and adjacent cartilage (Figure 3-10). For all other scoring categories, there were no statistical differences between the three treatments of interest in a given defect location. The cartilage repair scores for empty defects was statistically higher in the medial condyle than the trochlear groove for the cellular morphology, matrix staining, and thickness categories. In contrast, the cartilage repair scores for the Col I/II treatment were statistically higher in the trochlear groove than the medial condyle for the cellular morphology, thickness, and chondrocyte clustering categories.

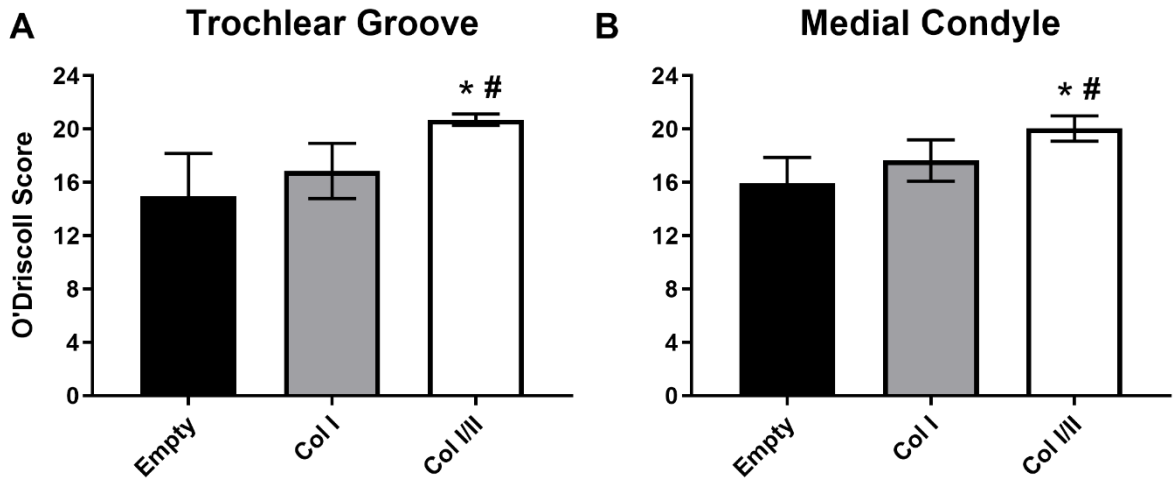

Figure 3-6. The Col I/II hydrogel repaired cartilage defects significantly better than either Col I or empty defects.

Histological evaluation using the O'Driscoll scoring criteria to assess cartilage repair within defects in the trochlear groove and medial condyle. The Col I/II hydrogel (n=8) repaired cartilage defects significantly better than either Col I (n=8) or empty defects (n=16). An ANOVA and Tukey's post hoc test were performed ($p < 0.05$). * indicates statistical difference from the empty defect within a defect location, and # indicates statistical difference from the Col I hydrogel within a defect location.

3.4 Discussion

Despite current advances in treatment options for patients suffering from osteoarthritis and other cartilage diseases, we lack a way to repair and regenerate articular cartilage. Collagen hydrogels have been widely utilized as a scaffold material for use in cartilage tissue engineering applications. Collagen type I, which is found in numerous places throughout the body including bone and scar tissue, continues to be the most utilized type of collagen in tissue engineered cartilage scaffolds even though it has also been shown to promote bone formation.[224] Previous studies have shown that when cultured on collagen type I hydrogels, osteoblasts maintain their phenotype and MSCs are able to undergo osteogenesis.[102,225]

On the other hand, collagen type II is found in native cartilage tissue and is a promising addition to a biomaterial to promote cartilage repair. For example, the addition of collagen type II to an alginate scaffold, when stimulated with TGF-β1 and dexamethasone, induced mesenchymal

stem cells differentiation into a chondrogenic lineage.[110] A few papers have investigated collagen type II scaffolds[111,118] despite the lack of robust hydrogels and inferior mechanical properties.[115,117,217] Lazarini *et al.* created collagen type II hydrogels with encapsulated adipose-derived stem cells (ASCs), but extremely high concentrations of collagen type II make this a costly option.[118] Lu *et al.* also created a collagen type II hydrogel with encapsulated ASCs and compared to a collagen type I hydrogel; however, this study was not able to decouple differences in the mechanical properties between the two formulations.[111] Building on the known benefits of collagen type II in MSC differentiation and maintenance of chondrocyte differentiation, our lab previously characterized the network structure and mechanical properties of blended hydrogel scaffolds made of a 3:1 collagen type I to collagen type II ratio with the goal of developing a self-assembling hydrogel containing collagen II for cartilage tissue engineering.[217] Our current study is the first to encapsulate mesenchymal stem cells (MSCs) in a collagen type I and II hydrogel and investigate both *in vitro* chondrogenic differentiation and *in vivo* cartilage repair potential.

The addition of collagen type II to a composite scaffold has been used in several previous studies as a cue to enhance chondrogenic potential of a tissue engineered scaffold.[110,113,135,226–228] In addition, collagen type I and II blend hydrogels with embedded chondrocytes were able to maintain a rounded morphology and secrete ECM specific to cartilage.[135] Our hydrogels contained encapsulated MSCs that we expected to secrete cartilage-specific ECM over the culture period. When cultured for 28 days, there was a statistical increase in the GAG production in the Col I/II hydrogels compared to the Col I hydrogels or pellets. The increase in normalized GAG levels for the Col I/II hydrogels suggested that the addition of collagen type II promoted GAG production. Such effects were not observed in a study where GAG content increased with increased collagen type I concentration in collagen type I and II hydrogels with encapsulated chondrocytes; however, it should be noted that the increased collagen type I concentration also increased the stiffness of the gels.[135] Our results are consistent with previous studies that establish the superiority of collagen type II for promoting chondrogenesis of MSCs compared to collagen type I.[110,133,229] For example, in alginate and collagen type II hydrogels with embedded MSCs, GAG production was upregulated when compared to alginate and collagen type I hydrogels with embedded MSCs.[110] At each time point of our current study, the Col I/II hydrogels had statistically lower AP activity than the pellets with TGF-β3 (Pel). There was also statistically lower AP activity in the Col I/II hydrogels compared to the Col I hydrogels at days 7,14, and 21. These results suggested that the

addition of collagen II suppressed AP activity. An increase in AP activity is undesirable for MSCs embedded within a tissue engineered cartilage scaffold since AP is a hypertrophic marker and indicates early bone formation. In agreement with our study, a previous study found that collagen type II added to the medium enhanced GAG synthesis but did not increase alkaline phosphatase activity of mesenchymal progenitor cells.[230]

There are several variables that affect the collagen hydrogel fabrication process, and we had to choose whether to keep the concentration of collagen prior to polymerization constant as opposed to the mechanical properties of our hydrogels post-polymerization (there is a ~3-fold difference in the average G' values of the Col I/II hydrogels (76.43 Pa) and Col I hydrogels (310.10 Pa) before cells are added). Because we chose to keep the former variable constant, we performed tests to ensure that our results could be attributed to the addition of collagen type II and were not due to changes in mechanical properties. To do so, we created an all collagen type I hydrogel that had mechanical properties that matched those of our Col I/II hydrogel (Table 3-6 and Figure 3-11). There was a statistically lower amount of GAG produced in the Col I hydrogel and the collagen type I mechanically matched (MM) hydrogel compared to the Col I/II hydrogel (Figure 3-12A). When compared to the Col I/II hydrogel, there was a statistical increase in AP activity at all time points for the MM hydrogel (Figure 3-12B). From these data we conclude that the addition of collagen type II promoted GAG production independent of mechanical properties.

Gene expression levels for cartilage-specific and collagen-related genes were measured using qRT-PCR in cells cultured in Col I/II hydrogels, Col I hydrogels, pellets with TGF-β3 (Pel), and pellets without TGF-β3 (Pel (-TGF)) after 14 days. There was an upregulation in two cartilage-specific genes, aggrecan and sox9, in the Col I/II gels compared to either pellets without TGF-β3 (Pel (-TGF)) or both the pellets without TGF-β3 (Pel (-TGF)) and Col I hydrogels, respectively. Sox9 is considered the master transcription factor involved in chondrogenesis since it is essential for both mesenchymal condensation and hypertrophy inhibition.[231] In addition, a number of different extracellular matrix genes found in proliferating chondrocytes, including collagen type II, collagen type IX, collagen type XI, and aggrecan, are activated by sox9.[232] Thus, the upregulation seen in sox9 was expected to correspond with an upregulation in collagen type II and a downregulation in collagen type X. An upregulation in collagen type II was seen, but there was no statistical difference in relative gene expression between the Col I/II and Col I hydrogels. Despite the upregulation in sox9, a slight upregulation in collagen type X was seen in the Col I/II

and Col I hydrogels. However, the low alkaline phosphatase activity for the Col I/II hydrogels, as well as previous studies indicating that collagen type X is a component of normal articular cartilage,[233] suggested that the cells may not become hypertrophic. Collagen type I expression in the Col I/II hydrogels and pellets with TGF-β3 (Pel) had statistically higher gene expression levels than the pellets without TGF-β3 (Pel (-TGF)). Collagen type I is a marker for fibrocartilage and chondrocyte dedifferentiation, both of which are undesirable in the context of articular cartilage defect repair. Overall, our results were consistent with those seen in alginate and collagen type II blend hydrogels with embedded MSCs where a number of chondrogenic genes and collagen type II synthesis were upregulated compared to alginate and collagen type I composite hydrogels with embedded MSCs or stem cells in monolayer.[110]

Our average modified O'Driscoll scores in both defect locations were consistent with average scores seen in other studies where cartilage defect repair was investigated while using scaffolds including collagen type II in a rabbit model. A modified O'Driscoll score of approximately 20 was seen in studies investigating dried collagen type I and II scaffolds combined with microfracture and chemically crosslinked polyethylene glycol and collagen type II scaffolds with implanted autologous chondrocytes.[131,138] Histological and immunohistochemical observations revealed that the Col I/II hydrogels, compared to Col I hydrogels and empty defects, provided a conducive environment for integration with surrounding tissue and allowed for favorable conditions in the process of cartilage repair. When the HE sections were analyzed, the empty defects contained a more fibrocartilage-like repair tissue with signs of fibrosis. A previous study has shown that the regenerated tissue that forms in empty cartilage defects is more fibrotic and deteriorates compared to defects with collagen matrices, and this finding is consistent with our observations.[234] In addition, the superficial region of the trochlear groove defects filled with the Col I hydrogel did not contain a smooth surface representative of native cartilage but instead had a fibrillated surface and fibrotic areas. The mixture of cartilage-like tissue and fibrotic areas suggested that the repair tissue in the defects filled with Col I scaffolds formed a more fibrocartilage-like tissue, which is known to be less durable than hyaline cartilage and only produces short-term repair. In the medial condyle defects filled with Col I hydrogels, the repair tissue did not completely fill the defect and had unorganized areas that contained both cartilage and bone tissue. These areas of bone tissue were poorly integrated with surrounding cartilage and are believed to be remnants from defect drilling.

Lack of integration with surrounding tissue has been a reason for many failed attempts to repair a cartilage defect with a tissue engineered construct.[235] Nonetheless, the combination of a collagen type I and II hydrogel promoted cell integration with surrounding tissue, including both the surrounding cartilage and underlying bone, and provided favorable conditions for cartilage repair. An increase in the degree of integration suggested that the addition of collagen type II to the scaffolds provided cues to better recruit chondrocytes from the surrounding tissue to the defect area or allowed cell migration out of the hydrogel. A similar degree of integration was seen in a study that encapsulated chondrocytes in collagen type I and II scaffolds that were used to repair cartilage defects in a rabbit model.[139]

A previous *in vivo* study that implanted a combination of collagen type II, fibrin sealant, and adipose-derived stem cells into rabbit knees observed the presence of chondrocyte-like cells throughout the tissue with increasing concentration in the deep zone, and the authors thus concluded that the defects were in an advanced healing stage.[118] Our data are in accordance with this study as we have shown that MSCs encapsulated within our Col I/II scaffold can either differentiate to a chondrocyte phenotype or recruit chondrocytes from the surrounding tissue to populate the defect site. Larger lacunar spaces in the deeper repair tissue and flattened cells in the superficial zone of the trochlear groove defects filled with Col I/II hydrogels showed that cells within the repair tissue are in different stages of development.

Including collagen type II in our hydrogel increased the amount of cartilage-specific ECM molecules produced by cells in the tissue. Although there was an increase in collagen type II staining for the Col I/II scaffold (Figure 3-13), it is difficult to interpret these results since collagen type II was added prior to polymerization. Picrosirius red was used to stain sections, which were imaged using polarized light microscopy to analyze collagen organization (Figure 3-14). Although slight differences between treatments were observed, little to no collagen fiber organization, as seen in native tissue, was observed. However, other important markers of cartilage matrix, like proteoglycan staining in the SOFG slides, were more intense in the Col I/II hydrogels than both the Col I and empty defects. In addition, increases in SOFG proteoglycan staining adjacent to the cells and in the surrounding matrix in the defects filled with Col I/II scaffolds supported the results from the *in vitro* GAG experiments. Taken together, these results suggested that the addition of collagen type II to a hydrogel with encapsulated MSCs is advantageous to promote cartilage matrix production.

3.5 Conclusions

The Col I/II construct used in this study induced and maintained the differentiation of MSCs into chondrocytes *in vitro,* and the cellular morphology and proteoglycan staining for the Col I/II hydrogels matched that of articular cartilage tissue surrounding the repair tissue *in vivo*. There was a greater degree of cartilage repair for the Col I/II hydrogels compared to the Col I hydrogels and the empty defect controls in both the medial condyle and the trochlear groove. Results from this study suggest that there is clinical value in the cartilage repair capabilities of our Col I/II hydrogel with encapsulated MSCs. However, a longer evaluation time frame must be investigated using a larger animal in future studies.

3.6 Acknowledgements

This work was supported by the Purdue Davidson School of Chemical Engineering, National Institutes of Health [NIAMS R21AR065644 and R01AR065398], Indiana Clinical and Translational Sciences [NIH TL1TR001107 to CEK], Purdue Office of Research and Partnerships, and Purdue Office of the Provost. This publication was further supported by the Indiana Clinical and Translational Sciences Institute, funded in part by grant #UL1 TR001108 from the National Institutes of Health, National Center for Advancing Translational Sciences, Clinical and Translational Sciences Award. The authors thank Victor Bernal-Crespo at the Purdue Histology Research Laboratory for performing all histology and immunohistochemistry. The authors also wish to thank Robyn McCain, Christa Crain, Kris Kazmierczak, Shery Park, and Cheryl Anderson of the Purdue Pre-Clinical Research Laboratory for their assistance with the rabbit study.

3.7 Chapter 3 Supplementary Information

3.7.1 Contraction

The degree of contraction over time was assessed by measuring the cross-sectional area of the hydrogel-cell constructs from images at each media change. The cross-sectional area was measure using ImageJ software (National Institutes of Health, Bethesda, MD) and presented as the percentage of original area. During the time of culture, pictures of the hydrogels were taken, and their surface area was measured at different time points to investigate contraction. Figure 3-7

shows that the hydrogels cultured with TGF-β3, for both Col I and Col I/II hydrogels, contracted more quickly than hydrogels cultured without TGF-β3 (Col I (-TGF) and Col I/II (-TGF)). However, after 28 days in culture, there was no statistical difference in contraction of the hydrogels regardless of media or hydrogel composition.

3.7.2 Rheology

Samples of 150 µL were polymerized on a Tekdon slide at 37°C for 12 hours in a humid incubator. Rheological analysis was done using an ARG2 rheometer (TA instruments, New Castle, DE) with a 20 mm cone geometry. Frequency sweeps were performed at 37°C from 0.01 to 1 Hz with a controlled stress of 0.5 Pa.

3.7.3 Macroscopic Scoring

After necropsy, the knees of the rabbits were dissected and photographed for macroscopic scoring. The images of the defects in the trochlear groove and the media condyle were scrambled so that scorers would be blinded to the treatments. The images were scored using categories adapted from Van den Borne *et al.*[223] In addition, the scores were totaled to give an overall macroscopic score. Three blinded observers scored the defects where n=8 defects were scored for the Col I/II and Col I defect and n=16 defects were scored for the empty defects. Kruskal-Wallis one-way ANOVAs and Dunn's multiple comparisons tests revealed that there were no statistical differences between the three treatments investigated in any of the macroscopic scoring categories (degree of defect repair, integration to border zone, and macroscopic appearance) for defects either in the trochlear groove and media condyle ($p < 0.05$). There were no statistical differences between the three treatments investigated when comparing overall repair assessment value for defects either in the trochlear groove and media condyle.

3.7.4 Collagen Type II Immunohistological Staining

Immunohistochemistry was performed with an antibody labeling type II collagen (Abcam; clone 2B1.5, ab185430, 0.2 mg/mL). Slides were deparaffinized in xylene and rehydrated to water through graded ethanol washes. The rest of the staining protocol was carried out in a Dako Autostainer (Agilent, Santa Clara, CA) at room temperature with Tris buffered saline/Tween washes. Slides were incubated in pepsin (Thermo Fisher Scientific, Waltham, MA) for 15 minutes,

and endogenous peroxidase was quenched with 3% hydrogen peroxide in water for 5 minutes. The samples were blocked for 20 minutes with 2.5% normal horse serum. Col II mouse monoclonal antibody at a dilution of 1:100 was applied for 60 minutes. A horse anti-mouse secondary (Vector Labs, Burlingame, CA) was applied for 30 minutes, and ImmPACT DAB (3,3'-diaminobenzidine) horseradish peroxidase (HRP) substrate (Vector Labs, Burlingame, CA) was applied for 5 minutes. Slides were then put in an XL Autostainer (Leica, Buffalo Grove, IL) for hematoxylin counterstaining and addition of a coverslip.

3.7.5 Picrosirius Red Staining and Imaging

Picrosirius red was used to stain tissue, and sections were imaged using polarized light microscopy to examine collagen fibril organization. Cartilage architecture was analyzed using the addition of a polarizer and analyzer to a light microscope to detect changes in the direction of polarized light, or birefringence.

3.7.6 Supplemental Figures and Table

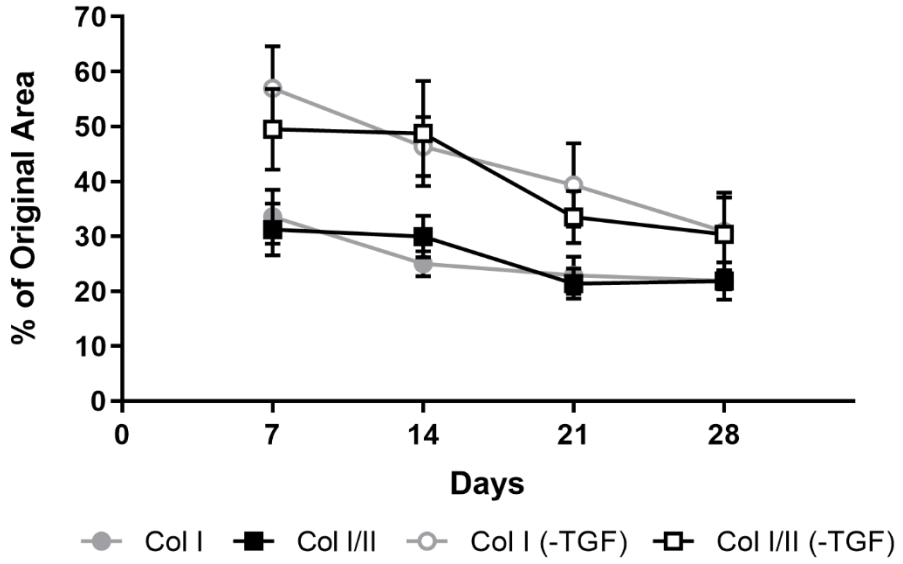

Figure 3-7. Comparison of the percentage of the original surface area of cell-hydrogel constructs over a 28-day period to examine the contraction of the cell-seeded hydrogels over time. Values are expressed as mean ± SD (n = 4).

Table 3-1. Primer sequences utilized for quantitative reverse transcription-polymerase chain reaction.

Gene of Interest	Accession number		5' → 3' sequence	Product length (bp)	Primer efficiency	Reference
Collagen Type I	NM 001195668.1	Forward	ATGGATGAGGAAACTGGCAACT	114	101.9%	Liao, 2010[236]
		Reverse	GCCATCGACAAGAACAGTGTAAGT			
Collagen Type II	NM 001195671.1	Forward	GCCACCGTGCCCAAGAAGAACT	160	103.1%	Yuan, 2016[135]
		Reverse	ACAGCAGGCGCAGGAAGGTCAT			
Collagen Type X	XM 002714724.3	Forward	GCCAGGACCTCCAGGACTATCA	103	100.0%	Zheng, 2009[237]
		Reverse	CCCAATGTCTCCTTTCGGTCCA			
Aggrecan	XM 008251723.2	Forward	CCTACCAGGACAAGGTCTCG	163	98.1%	Chen, 2016[238]
		Reverse	ACACCTTTCACCACCACCTC			
Sox9	XM 008271763.2	Forward	GGAAGCTCTGGAGACTGCTG	135	96.8%	Zhang, 2012[239]
		Reverse	CGTTCTTCACCGACTTCCTC			
GAPDH	NM 001082253.1	Forward	CGCCTGGAGAAAGCTGCTA	104	96.0%	Morigele, 2013[240]
		Reverse	ACGACCTGGTCCTCGGTGTA			

Table 3-2. Histological and histochemical grading scale adapted from O'Driscoll *et al.* [222]

	Score
Nature of the predominant tissue	
Cellular morphology	
Hyaline articular cartilage	4
Incompletely differentiated mesenchyme	2
Fibrous tissue or bone	0
Safranin-O staining of the matrix	
Normal or nearly normal	3
Moderate	2
Slight	1
None	0
Structural characteristics	
Surface regularity	3
Smooth and intact	2
Superficial horizontal lamination	1
Fissures - 0 to 25 percent of the thickness	0.5
Fissures - 25 to 100 percent of the thickness	0
Structural integrity	
Normal	2
Slight disruptions, including cysts	1
Severe disintegration	0
Thickness	
100 percent of normal adjacent cartilage	2
50 - 100 percent of normal adjacent cartilage	1
0 - 50 percent of normal adjacent cartilage	0
Bonding to the Adjacent Cartilage	
Bonded at both ends of graft	2
Bonded at one end and partially at one end	1.5
Bonded at one end or partially at both ends	1
Bonded partially at one end	0.5
Not bonded	0
Freedom from cellular changes of degeneration	
Hypocellularity	
Normal cellularity	3
Slight hypocellularity	2
Moderate hypocellularity	1
Severe hypocellularity	0
Chondrocyte clustering	
No clusters	2
<25 percent of the cells	1
25 - 100 percent of the cells	0
Freedom from degenerative changes in adjacent cartilage	
Normal cellularity, no clusters, normal staining	3
Normal cellularity, mild clusters, moderate staining	2
Mild or moderate hypocellularity, slight staining	1
Severe hypocellularity, poor or no staining	0

Table 3-3. Glycosaminoglycan (GAG), DNA, and dry weight (DW) values at 14 days of culture.

	Day 14		
Treatment	GAG (ng)	DNA (ng)	DW (mg)
Col I	59488.1 ± 29273.8	4086.4 ± 2110.4	0.50 ± 0.08
Col I/II	100765.6 ± 15239.6	6486.2 ± 992.8	0.62 ± 0.05
Pel	48746.7 ± 39052.2	5142.4 ± 3989.2	N/A
Col I (-TGF)	35451.2 ± 5756.1	8178.5 ± 828.6	0.53 ± 0.06
Col I/II (-TGF)	30402.5 ± 5484.1	7626.7 ± 558.2	0.65 ± 0.12
Pel (-TGF)	8489.1 ± 6356.3	4665.1 ± 3193.7	N/A

Table 3-4. Glycosaminoglycan (GAG), DNA, and dry weight (DW) values at 28 days of culture.

	Day 28		
Treatment	GAG (ng)	DNA (ng)	DW (mg)
Col I	59712.9 ± 7215.2	2903.8 ± 867.7	0.28 ± 0.1
Col I/II	78664.0 ± 14462.5	2183.7 ± 403.0	0.33 ± 0.2
Pel	38605.6 ± 8909.1	1900.8 ± 696.1	N/A
Col I (-TGF)	71891.5 ± 7821.2	4162 ±549.9	0.27 ± 0.1
Col I/II (-TGF)	66711.8 ± 10522.0	3438.9 ± 589.2	0.23 ± 0.0
Pel (-TGF)	2706.0 ± 960.4	1223.0 ± 345.1	N/A

Table 3-5. Macroscopic grading scale adapted from Van den Borne *et al.*[223]

	Score
Degree of Defect Repair	
In level with surrounding cartilage	4
75 % repair of defect depth	3
50% repair of defect depth	2
25% repair of defect depth	1
0% repair of defect depth	0
Integration to Border Zone	
Complete integration with surrounding cartilage	4
Demarcating border < 1 mm	3
3/4th of graft integrated, 1/4th with a notable boarder > 1 mm width	2
1/2th of graft integrated, 1/2th with a notable boarder > 1 mm width	1
From no contact to 1/4th of graft integrated	0
Macroscopic Appearance	
Intact smooth surface	4
Fibrillated surface	3
Small, scattered fissures or cracs	2
Several small, or few but large fissures	1
Total degeneration of grafted area	0

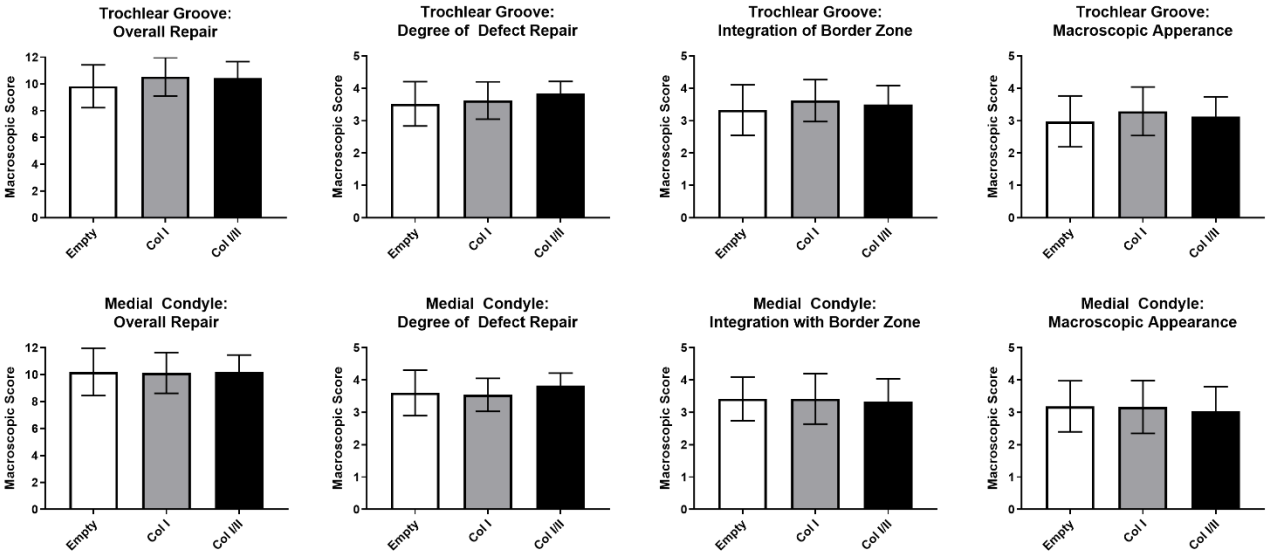

Figure 3-8. Macroscopic scoring of repaired cartilage left empty or filled with either a Col I or Col I/II hydrogel.

Kruskal-Wallis one-way ANOVAs and Dunn's post hoc tests were performed ($p < 0.05$) for macroscopic scoring analysis. Three blinded observers scored the defects where n=8 defects were scored for the Col I/II and Col I defect and n=16 defects were scored for the empty defects.

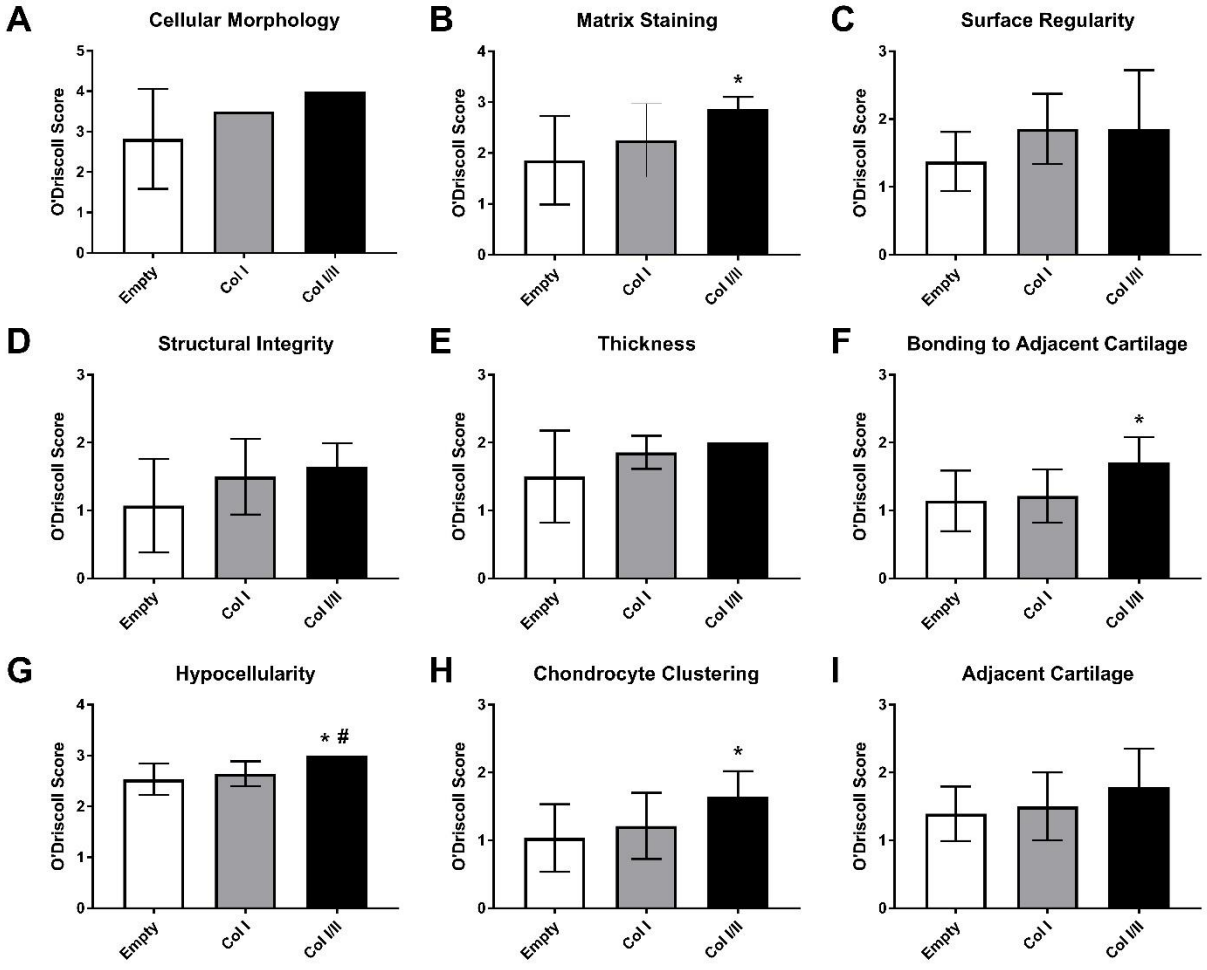

Figure 3-9. Histological evaluation of each O'Driscoll scoring category to assess cartilage repair within defects in the trochlear groove.

Single factor analysis of variance (ANOVA) and Tukey's post hoc tests were performed ($p < 0.05$) for histology scoring analysis. * indicates statistical difference from the empty defects, and # indicates statistical difference from the Col I hydrogels.

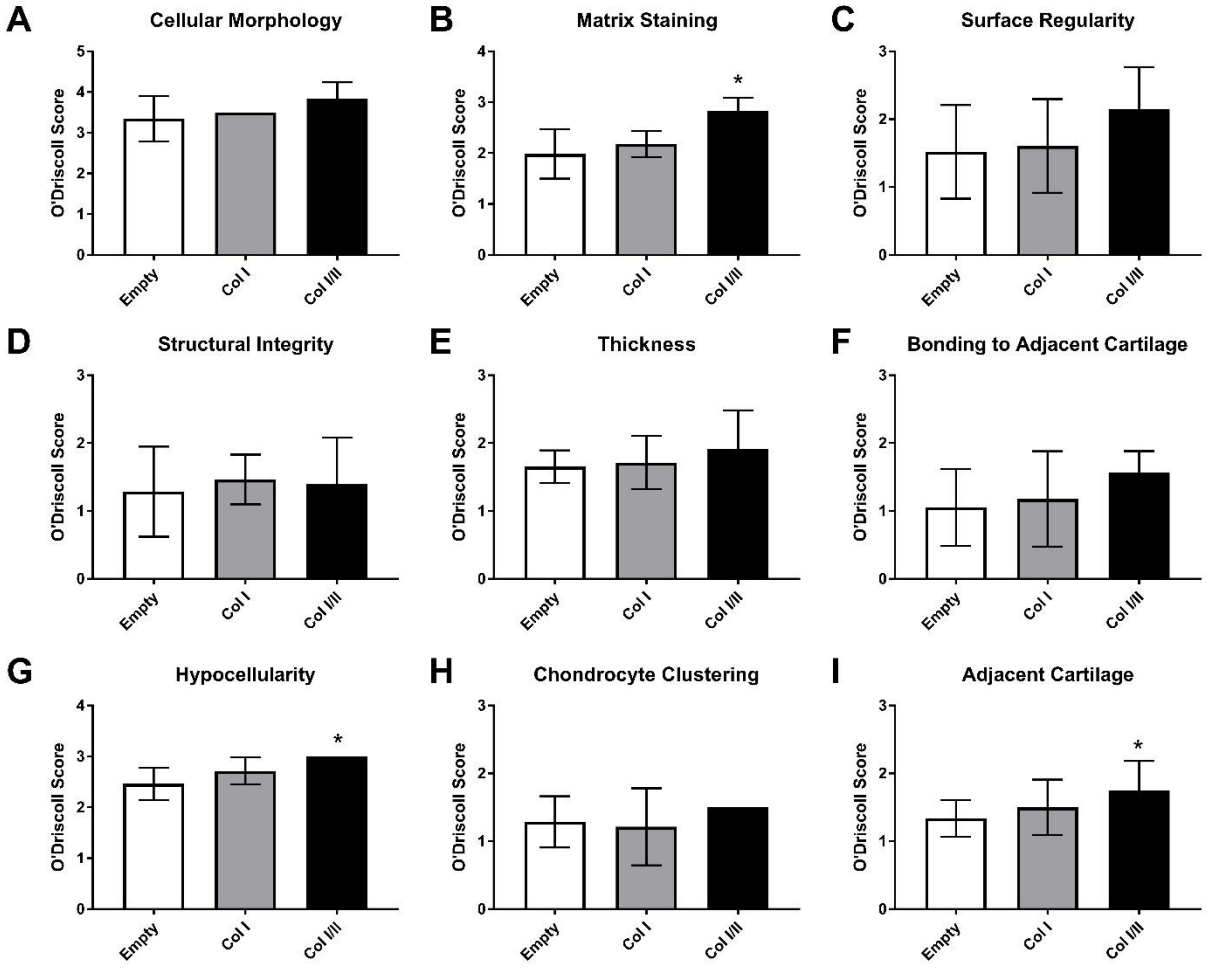

Figure 3-10. Histological evaluation of each O'Driscoll scoring category to assess cartilage repair within defects in the medial condyle.

An ANOVA and Tukey's post hoc tests were performed ($p < 0.05$) for histology scoring analysis. * indicates statistical difference from the empty defects, and # indicates statistical difference from the Col I hydrogels.

Table 3-6. Polymerization conditions to create a hydrogel with mechanical properties that match those of the Col I/II blend hydrogel.

Name	Pre-polymerization Ratio of Col I:II	Pre-polymerization concentration (mg/mL)	Post-polymerization concentration (mg/mL)
Collagen Type I/II (Col I/II)	3:1	4	3.00 ± 0.05
Mechanically Matched Col I (MM)	1:0	3.2	2.96 ± 0.01
Collagen Type I (Col I)	1:0	4	3.69 ± 0.04

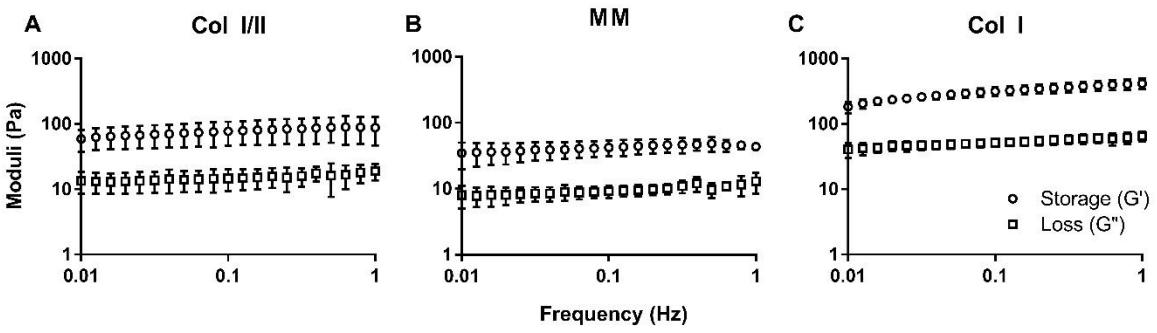

Figure 3-11. Frequency sweeps confirmed that the mechanical properties were statistically similar between the Col I/II and the Col I MM hydrogels (n=4).

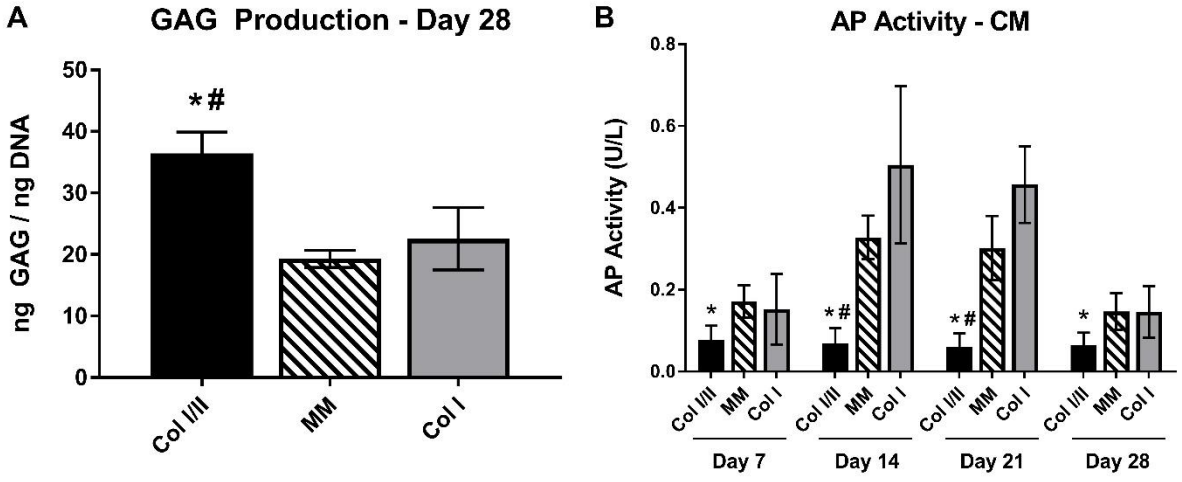

Figure 3-12. The addition of collagen type II promoted GAG synthesis and did not increase alkaline phosphatase activity, and these effects were independent of mechanical properties.

(A) GAG/DNA ratio of the cell-hydrogel constructs after a 4-week culture period. Values are expressed as mean ± SD (n = 4). An ANOVA and Tukey's post hoc test were performed ($p < 0.05$). * indicates statistical difference from the MM sample, and # indicates statistical difference from the Col I hydrogel. (B) AP activity of rabbit MSCs over time (n = 4). An ANOVA and Tukey's post hoc test were performed ($p < 0.05$). * indicates statistical difference from the MM sample within a time point, and # indicates statistical difference from the Col I hydrogel within a time point.

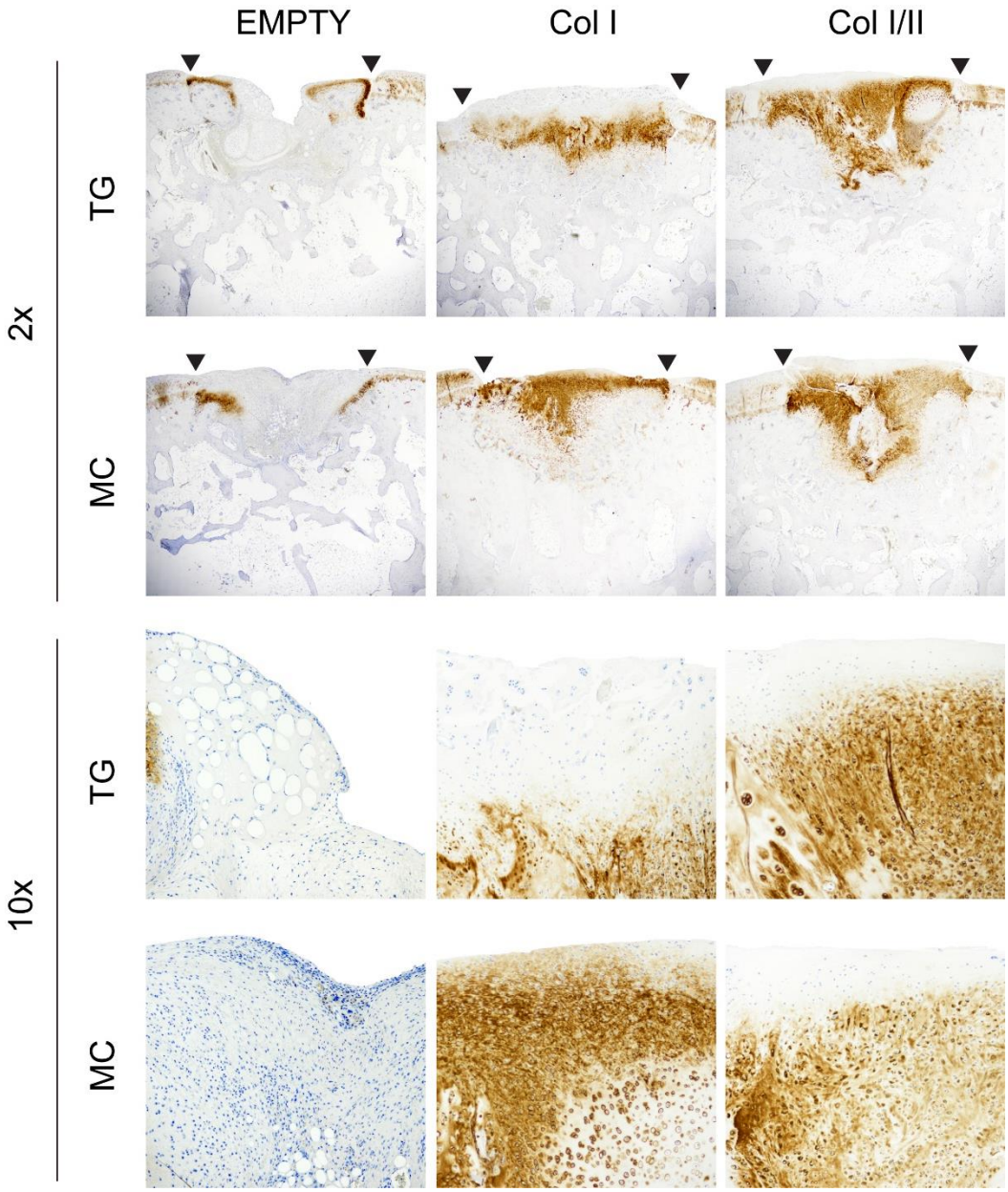

Figure 3-13. More collagen type II was labeled in defects that were filled with Col I/II hydrogels compared to defects that were filled with Col I hydrogels or left empty.

Collagen type II IHC of repaired cartilage left blank or filled with either a Col I or Col I/II hydrogel in the trochlear groove (TG) or the medial condyle (MC) at two different magnifications (2x and 10x). Immunohistochemical labeling of collagen type II revealed that collagen type II was present in all defects filled with hydrogel constructs. Brown labeling of collagen type II was present throughout the defect but was most intense adjacent to the bone compared to the tissue surface. This intensity differential was especially noticeable in defects with Col I scaffolds in the TG. The empty defects also contained some staining for collagen type II, but staining was localized to areas adjacent to surrounding tissue. Areas further away from surrounding tissue were void of collagen type II staining.

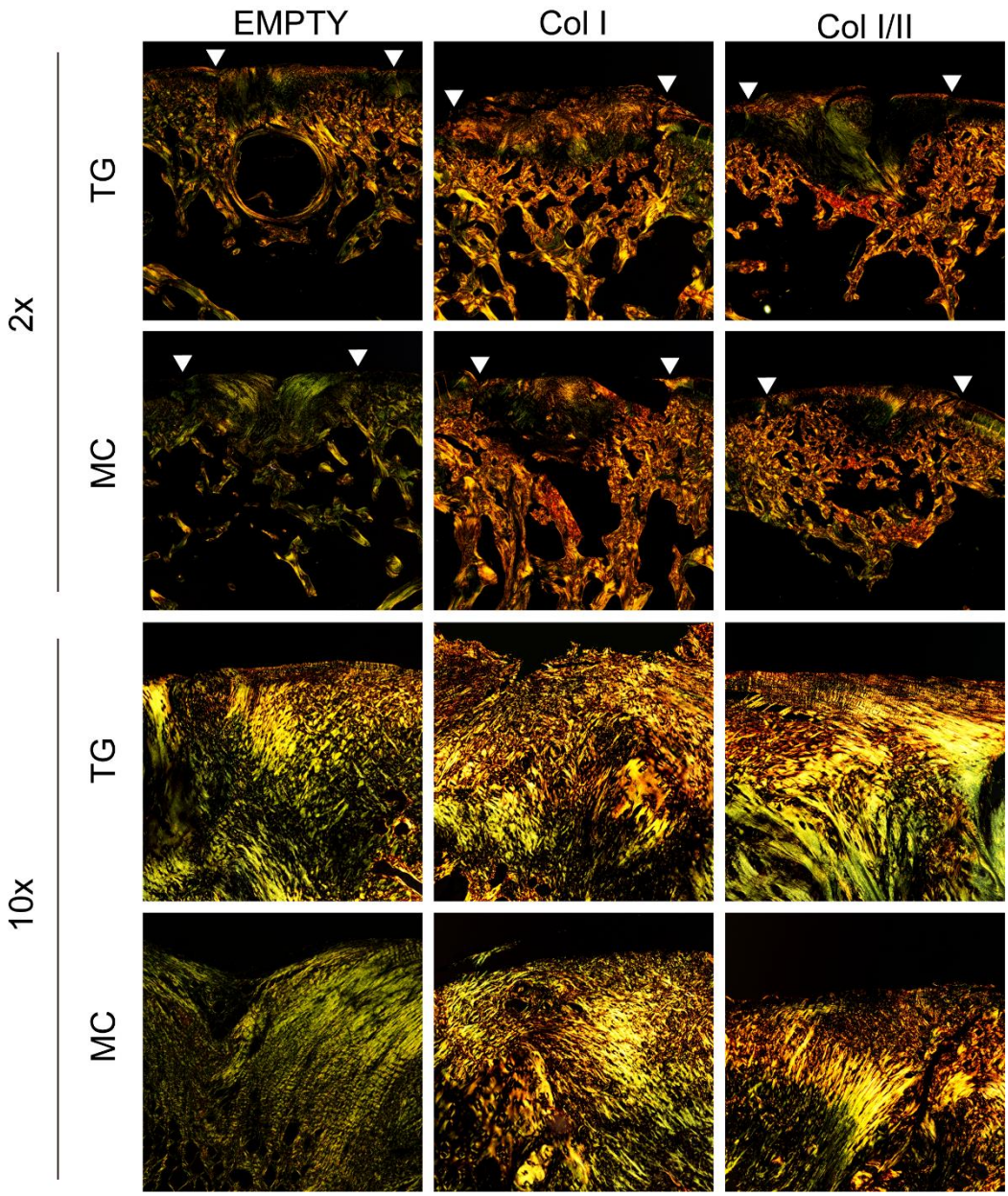

Figure 3-14. Picrosirius red staining of repaired cartilage left empty or filled with either a Col I or Col I/II hydrogel.

Cartilage repair in two different locations, the trochlear groove (TG) and the medial condyle (MC), was analyzed at 2x and 10x. Picrosirius red was used to stain sections and imaged using polarized light microscopy to analyze collagen organization. Although slight differences between treatments could be distinguished, little to no collagen fiber organization, as seen in native tissue, was observed.

4. INCORPORATION OF A CHONDROITIN SULFATE AND COLLAGEN-BINDING PEPTIDE MOLECULE TO A COLLAGEN TYPE I AND II BLEND HYDROGEL FOR CARTILAGE TISSUE ENGINEERING

4.1 Introduction

Osteoarthritis, a disease defined by the loss of articular cartilage, is a burden both, physically and financially, since half a million Americans undergo a total joint replacement due to the disease each year.[241] Due to the fact that articular cartilage is avascular and contains a low concentration of cells, it lacks the inherent ability for self-repair.[210] Therefore, patients with damaged cartilage seek out one of the many surgical treatment options for focal cartilage defects, including osteochondral grafts, autologous chondrocyte implantation, and marrow stimulation.[211,212] However, these options are invasive, incur long rehabilitation times, and usually promote the regrowth of fibrocartilage, which has mechanical properties inferior to native cartilage.[213] In order to better mimic native tissue, we take a tissue engineering approach to the repair of cartilage which combines cells, a scaffold, and bioactive factors that can be implanted into a cartilage defect.[6] The choice of scaffold and addition of extracellular matrix molecules are two ways to enhance the chondrogenesis of mesenchymal stem cells (MSCs), a promising cell source that differentiate into chondrocytes under certain environmental conditions.[215,216]

Articular cartilage is predominately made up of collagen type II fibrils, which make up the 3D architecture of the tissue, and monomers of aggrecan, which attach to a central filament of HA in a supramolecular complex known as a proteoglycan. Proteoglycans are negatively charged molecules that become trapped in a collagen network, and their negative charge results in water influx and retention in the tissue. [11,12] The retention of water gives cartilage a high compressive strength and aids in joint lubrication. Chondroitin sulfate (CS) is a sulfated glycosaminoglycan (GAG) that attaches to a link protein to form a molecule of aggrecan. [28]

For tissue engineered scaffolds, collagen hydrogels are an attractive option due to their biocompatibility and ubiquity in tissues.[96] Collagen type I, which is abundantly available, continues to be the most utilized type of collagen scaffolds for cartilage repair, even though collagen type II is the main component found in native cartilage tissue. Several studies have used collagen type I to repair cartilage defects, but better integration with surrounding tissue and surface

splitting, fibrillation, and thinning are some limitations that will need to be addressed as areas for improvement before clinic use.[107] Early studies investigating the differentiation of MSCs into chondrocytes in collagen type I based hydrogels saw promising repair.[106,107] However, other studies have shown that collagen type II hydrogels promote the differentiation of embedded MSCs to chondrocytes more efficiently than collagen type I hydrogels.[110,111] There are many examples of hydrogels with incorporated CS in which the addition of CS has been shown to improve scaffolds for articular cartilage tissue engineering. CS has been shown to stimulate the production of proteoglycans by chondrocytes when dosed extracellularly[242] and enhance the ability of MSCs to differentiation into chondrocytes when incorporated into hydrogels with encapsulated MSC.[243–245] CS is able to directly influence the fate of stem cells by acting as a biochemical cue or indirectly influence stem cell fate by binding with growth factors.[246]

A scaffold with a collagen type I to collagen type II ratio of 3:1 (this formulation is hereafter referred to as Col I/II gels) was developed and characterized previously by our laboratory to harness the biological activity of collagen type II and the superior gelation of collagen type I.[217] Although the blends were able to retain CS and HA post-polymerization, less than 45% of the original CS and 25% of the original HA added was incorporated in the Col I/II hydrogels. The Col I/II hydrogels were evaluated for chondrogenic differentiation of MSCs *in vitro* and cartilage repair potential *in vivo*. The Col I/II hydrogel showed potential for regeneration, as it promoted integration with surrounding tissue and provided favorable repair conditions for cartilage repair, but there was room for improvement. This study investigates strategies to better retain matrix molecules, like CS, in a scaffold material to better recapitulate aspects of native cartilage.

Previous studies have incorporated ECM molecules using different methods including physical entrapment[110,124] and chemical conjugation.[247,248] For example, a photopolymerized and crosslinked polyvinyl alcohol (PVA) and CS hydrogel was able to maintain the shape of encapsulated chondrocytes and be remodeled by chondroitinase ABC.[243] When in a dynamic loading condition, PEG based hydrogels with covalently incorporated methacrylated CS and encapsulated MSCs had a decrease in Col X and RUNX2 gene expression and collagen type I protein expression as compared to an all PEG based hydrogel.[244] A similar down regulation in hypertrophic genes, and upregulation of cartilage specific genes, was also seen in PEG and methacrylated CS hydrogels when compared to PEG based gels.[245] When CS was added to a hydrogel made of PEG-RGD, embedded chondrocytes produced the highest level of GAG

accumulation compared to PEG-RGD hydrogels alone and PEG-RGD hydrogels with added HA.[143] In ECM-based cryogels made of either methacrylated CS or methacrylated HA crosslinked to poly (ethylene glycol) diacrylate (PEGDA), the addition of methacrylated CS stimulated gene expression of aggrecan and GAG accumulation.[144] The addition of a thiolated CS to a PEG based hydrogel with encapsulated MSCs partnered with dynamic compression was able to support differentiation into chondrocytes and inhibit MSC hypertrophy.[249] Chondroitin sulfate has also been incorporated into natural hydrogels with encapsulated MSC or chondrocytes. Chondrocytes, that were cultured on a chitosan membrane modified with CS, were able to retain their phenotype and produce proteins that are specific to the matrix of cartilage.[250] Crosslinked chondroitin sulfate and collagen type II hydrogels with seeded MSCs were able to repair cartilage defects after one month in vivo with the formation of lacuna and newly synthesized collagen type II.[251]

Our laboratory has previously designed and characterized molecules, that contain relevant peptides attached the glycosaminoglycan backbones, to mimic aggrecan[181,252], lubricin[253], and decorin.[145–148,254] A collagen-binding peptide (RRANAALKAGELYKSILYGSG), or SILY, attached to dermatan sulfate (DS) backbone, has been used to design a mimic of decorin (DS-SILY), a small proteoglycan that is associated with collagen fibrils.[145–148] DS-SILY has been shown to bind to collagen, masking it from platelet activation in veins damaged from balloon angioplasty, and inhibiting MMP-1 and MMP-13 mediated collagen degradation.[145,147] Although the same SILY peptide was used previously, this study investigates a collagen binding peptidoglycan (CS-SILY) where different amounts of SILY peptide were conjugated to functional groups on CS to facilitate further incorporation of CS to our collagen type I/II blend hydrogels.

Overall, this study investigates how the addition of SILY peptides to a CS backbone enhances the retention of CS into a Col I/II blend hydrogel over time, and how this addition alters network structure and mechanical properties. The number of SILY peptides attached to a CS backbone, through an amide bond using 1-ethyl-3-(3-dimethylaminopropyl)carbodiimide hydrochloride (EDC) coupling, was varied to create 3 different molecules: CS-10SILY, CS-15SILY, and CS-20SILY, with 10, 15, and 20 denoting the number of SILY peptides attached to CS. The *in vitro* chondrogenic differentiation potential and gene expression of bone marrow-derived MSCs embedded within Col I/II gels and supplemented with CS or CS-SILY molecules was also examined.

4.2 Materials and Methods

4.2.1 Reagents

Unless otherwise specified, all materials used were purchased from Sigma-Aldrich (St. Louis, MO).

4.2.2 Molecule Preparation

The collagen-binding peptidoglycan was synthesized using EDC chemistry to conjugate the SILY peptide to a chondroitin-6-sulfate (CS) (Seikagaku, Tokyo, Japan) backbone with an amide bond. Using an 8 M urea solution and 0.05 mM EDC, the carboxyl groups on the CS backbone were activated for 20 minutes at room temperature and pH 4.5. The CS backbone was then functionalized by reacting 10% molar excess of the desired SILY peptide (either 10, 15 or 20) attachment overnight with shaking. The pH was then altered to 8 to stop the reaction. The molecules were purified using size exclusion chromatography on an AKTA FPLC (GE Healthcare, Piscataway, NJ) with Bio-Scale Mini Bio-Gel columns packed with polyacrylamide beads (Bio-Rad Laboratories, Hercules, CA) and then freeze dried. A Nanodrop 2000 spectrophotometer (Thermo Fisher Scientific, Waltham, MA) was used to confirm the final concentration of peptide attachment to the CS backbone using a standard curve based on peptide absorbance at 280 nm. Three different molecules were created including CS-10SILY, CS-15SILY, and CS-20SILY. All of these molecules had measured moles of SILY peptide within ±10% of the desired moles of SILY.

4.2.3 Hydrogel Preparation

The collagen type I and II blend hydrogels were prepared using a protocol described in detail in Kilmer *et al*. A stock solution of collagen type II from lyophilized chicken sternum (Sigma-Aldrich, Saint Louis, MO) was prepared at a concentration of 11 mg/mL in 20 mM acetic acid. The concentration of the collagen type II stock solution was measured after sterile filtration using a bicinchoninic acid (BCA) assay (Pierce, Rockford, IL). Using the post-sterilization concentration, the collagen type II was then diluted to a stock concentration of 8 mg/mL in 20 mM acetic acid prior to use. A 3:1 collagen type I to collagen type II (Col I/II) was created by combining acid-solubilized collagen type I from rat tail (Corning, Corning, NY) with the stock solution of collagen type II. A neutralization solution was prepared to rise the pH of the solutions to 7.4 with the addition of 10x PBS, 1 M NaOH, and 1x PBS and diluted to a final concentration

of 4 mg/mL total collagen. To the base hydrogel with no added CS (No Trt), 10 uM of CS, CS-10SILY, CS-15SILY, or CS-20SILY was added in the 1xPBS of the neutralization solution.

4.2.4 Chondroitin Sulfate Diffusion from Hydrogel

A dimethyl methylene blue (DMMB) assay was used to measure the amount of CS retained, in the form of CS or a CS-SILY molecule, over time. Hydrogels, which were allowed to polymerize for either 3 or 12 hours at 37°C, were created with 10 µM of either CS, CS-10SILY, CS-15SILY, or CS-20SILY. After polymerization, all hydrogels were washed with 1xPBS for 5 minutes, and hydrogels were sampled and freeze-dried each day from day 0 to 7. Hydrogels were digested at 60°C for 24 hours with 125 µg/mL of activated papain solution in a papain digestion buffer (5 mM ethylenediaminetetraacetic acid (EDTA), 5 mM L-cysteine (Alfa Aesar, Ward Hill, MA), and 100 mM NaH_2PO_4).[219] The digested product was then freeze-dried and resuspended in autoclaved water. A 20 µL aliquot of digested hydrogel construct was combined with 30 µL of water and 250 µL DMMB dye solution. The absorbance of the solution was then measured at 525 nm. A standard curve was created using either CS, CS-10SILY, CS-15SILY, or CS-20SILY depending on the molecule that was added prior to polymerization. The percentage of encapsulated CS was calculated by comparing the amount of CS retained in the gel with the amount of CS in the hydrogel over time.

4.2.5 Cryoscanning Electron Microscopy (Cryo-SEM)

The same hydrogel treatments used in the diffusion experiments were analyzed using Cryo-SEM (Nova NanoSEM, FEI, Hillsboro, OR), and 75 uL of each hydrogel was polymerized at 37°C on a machined stage. The stages with polymerized hydrogels were moved into a stage holder and then flash frozen in liquid nitrogen slush. The samples were fractured in a Gatan Alto 2500 prechamber (Gatan Inc., Pleasanton, CA). Samples were sublimated for between 10 and 15 minutes at -90°C and sputter-coated with platinum for 120 seconds. The samples were then imaged on the microscope cryostage at -140°C. Fibrils were measured with the FIJI image processing package (National Institutes of Health, Bethesda, MD) using a previously described protocol.[217] Fibril diameter measurements ($n \geq 270$) were analyzed by blinded observers who measured the fibril diameter of 10 fibers in 9 images of each treatment. The percent porosity and number of pores was calculated using the Diameter J plugin on FIJI to segment the image and calculate the void in 9 images per treatment.

4.2.6 Rheology

Frequency sweeps were performed on an ARG2 rheometer (TA instruments, New Castle, DE) using a 20 mm cone geometry. Hydrogels were polymerized on a Teflon coated microscope slide (Tekdon, Myakka City, FL) at a volume of 150 uL. The frequency was varied from 0.01 to 10 Hz with a controlled stress of 0.5 Pa.

4.2.7 Stem Cell Encapsulation

Mesenchymal stem cells were isolated from the bone marrow of New Zealand White rabbits. Bone marrow was collected from both femurs and humeri of skeletally mature New Zealand White rabbits (Covance, Princeton, NJ) following a protocol that was approved by the Purdue Animal Care and Use Committee (PACUC). Bone marrow was aspirated using an 18-gauge needle that was percutaneously inserted into the intertrochanteric fossa of the femur and the greater tubercle of the humerus. The marrow from each rabbit was pooled, centrifuged, and resuspended in maintenance medium (low-glucose Dulbecco's modified Eagle's medium (DMEM) supplemented with 10% fetal bovine serum (Lonza, Walkersville, MD) and 1% penicillin-streptomycin). Autoclaved water was added to lyse the red blood cells. Upon centrifugation, the cells were plated and incubated at 37°C with 5% CO_2. The first medium change was performed after four days of culture following a 1 xPBS wash step, and subsequent medium changes were every three days. The cells were subcultured after 2.5 weeks upon reaching 70% - 80% confluency.

MSCs were resuspended in collagen pre-polymerization solutions at a cell density of 5 x 10^6 cells/mL. The pre-polymerization solution contained either the neutralization solution discussed in the hydrogel preparation section the addition of CS in the form of 10 µM CS, CS-10SILY, CS-15SILY, or CS-20SILY. The hydrogels were allowed to polymerize at 37°C for 3 hours before the addition of chondrogenic medium. Defined chondrogenic medium (CM) was formulated with high-glucose DMEM supplemented with 1% ITS+Premix (BD Biosciences, San Jose, CA), 1% penicillin-streptomycin, 1 mM sodium pyruvate, 50 µM proline, 4 mM L-glutamine, 50 µg/mL ascorbic acid, 100 nM dexamethasone, and 10 ng/mL transforming growth factor-β3 (TGF-β3)(Peprotech, Rocky Hill, NJ). For GAG, DNA, and collagen analysis, cell-hydrogel constructs were cultured for up to 4 weeks with 3 medium changes each week. Hydrogels were maintained in free-floating conditions. Cell-hydrogel constructs were papain digested before DNA and GAG quantification.

4.2.8 GAG Production and DNA Analysis

Using a Hoechst dye, DNA was measured as previously described, and a standard curve of calf thymus DNA was created.[220] The cell-hydrogel construct was added to a Hoechst dye solution, and the fluorescence was read at an excitation wavelength of 340 nm and an emission wavelength of 465 nm. The DNA content of the cells encapsulated in hydrogels was measured as a way to normalize the GAG production. GAG content was measured using a dimethyl methylene blue (DMMB) assay where 20 µL of the papain digested hydrogel constructs were diluted with 30 µL of water and 250 µL DMMB dye solution (n = 4). The absorbance of the solution was read at 525 nm. A standard curve was created using chondroitin sulfate from shark cartilage (Seikagaku, Tokyo, Japan). The GAG values measured were normalized to the amount of DNA measured per sample.

4.2.9 Collagen Analysis

Using a Biocolor Soluble Collagen Assay kit (Carrickfergus, Northern Ireland), collagen was measured using a Sircol dye reagent and following the manufactures instructions. The cell-hydrogel constructs were freeze dried and resuspended in a 0.1 mg/mL solution of pepsin in 0.5 mM acetic acid. The samples scaffold samples were incubated overnight at 4°C in the acid-pepsin extraction solution. The acid-pepsin extraction step was not required for media aliquots. Once the collage-dye complex precipitated out from unbound dye, the pellet was resuspended. The absorbance was measured at a wavelength of 555 nm. A standard curve was created using collagen type I/II in either 20 mM acetic acid or chondrogenic media depending on the culture material.

4.2.10 Gene Expression

The hydrogels were washed with PBS then homogenized in lysis buffer and β-mercaptoethanol using a syringe needle. The NucleoSpin RNA kit from Macherey-Nagel (Bethlehem, PA) was used to isolate RNA. A High Capacity cDNA Reverse Transcription kit from Applied Biosystems (Foster City, CA) was used to synthesize complementary DNA from the isolated RNA. Relative expression levels were measured using qRT-PCR with the primer sequences (Table 4-1) for collagen type I, II, and X, aggrecan, Sox9, and glyceraldehyde-3-phosphate dehydrogenase (GAPDH) (Integrated DNA Technologies, Skokie, IL). The samples were heated for 10 minutes

at 95°C followed by 40 cycles for 15 seconds at 95°C, 15 seconds at 55 or 60°C, and 40 seconds at 68°C. All values were normalized to GAPDH levels. The differences in gene expression were calculated relative to negative controls using the ΔΔCt method.[221]

4.2.11 Statistics

All data is shown as a mean with error bars showing one standard deviation. Single factor analysis of variance (ANOVA) and Tukey post hoc tests were performed for the CS encapsulation, rheology experiments, GAG production, collagen content in cell culture media, and collagen content in cell-hydrogel constructs. A general linear model with nested factors and Tukey post hoc tests were performed to analyze the fibril diameter, percent porosity, and number of pore data. An alpha level of 0.05 was selected for statistical significance in all statistical tests. Single factor analysis of variance (ANOVA) and Tukey's post hoc tests were performed for gene expression analysis of collagen type II at 1 week, sox 9 at 1 week, aggrecan at 2 weeks, and sox 9 at 2 weeks. An ANOVA and a Games Howell post hoc test were performed for gene expression analysis of collagen type I and collagen type X at both timepoints. A Box-Cox transformation was used to analyze data for gene expression analysis of aggrecan at 1 week and collagen type II at 2 weeks.

4.3 Results

Addition of CS-SILY molecules enhanced CS retention.

Col I/II hydrogels were polymerized for 3 hours with either 10 µM of CS, CS-10SILY, CS-15SILY, or CS-20SILY. A DMMB assay was used to understand how much CS was encapsulated in the hydrogel from 0 to 7 days. Immediately after a 3-hour polymerization period and a PBS wash, there was a statistically higher amount of CS encapsulated in the CS-20SILY hydrogels (73.7 ± 6.6%) compared to the CS-10SILY (55.6 ± 9.0%) and CS (55.5 ± 6.0%) hydrogels (Figure 4-1). However, there was no statistical difference between the CS-20SILY and CS-15SILY (67.6 ± 4.9%) treatments. On day 2, the CS hydrogel was under 20% of the original amount encapsulated. The CS-10SILY contained under 20% of the original amount of CS encapsulated on day 4. The CS-15SILY and CS-20SILY did not contain under 20% of the original amount of CS encapsulated in the 7-day period analyzed. After 7 days in the hydrogels polymerized for 3 hours, both the CS-15SILY and CS-20SILY, which were not statistically different from one another, contained over 20% of the originally encapsulated CS. There was a

statistical difference in the amount of CS encapsulated in the hydrogel in the CS-15SILY (20.8 ± 4.8%) and the CS-20SILY (21.8 ± 3.9%) as compared to the CS-10SILY (10.0 ± 1.4%) or CS (0.8 ± 0.9%) hydrogels.

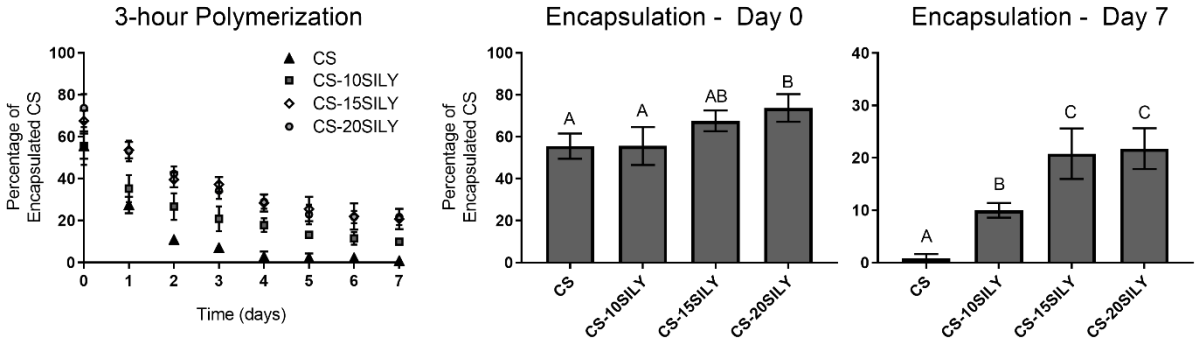

Figure 4-1. Percentage of encapsulated CS retained in the hydrogel over time after a 3-hour polymerization.

CS encapsulation after a wash (day 0) or 7-day period are shown. Single factor analysis of variance (ANOVA) and Tukey post hoc tests were performed (n=4). Different letters indicate groups with a significantly different percentage of encapsulated CS ($p < 0.05$). Data is represented as the mean ± the standard deviation.

Mechanical properties of the scaffold were altered with the addition of CS and CS-SILY molecules.

Frequency sweeps, to better understand how the mechanical properties of a Col I/II hydrogel are altered with the addition of CS-SILY molecules, were performed from 0.01 to 10 Hz (Figure 4-2). Hydrogels of only collagen (No Trt) were compared to hydrogels with added CS, CS-10SILY, CS-15SILY, or CS-20SILY. The frequency sweeps show that at 0.1 Hz, the Col, CS, CS-10SILY, CS-15SILY, and CS-20SILY hydrogels, respectively, had an average storage modulus (G') of 144.8 ± 58.3, 280.6 ± 180.3, 201.1 ± 47.6, 493.9 ±87.3, and 684.0 ± 63.2 Pa, and an average loss moduli (G") of 30.7 ± 2.1, 63.7 ± 44.4, 37.4 ± 7.5, 87.3 ± 19.0, and 139.76 ± 22.6 Pa (Figure 4-2). At 1 Hz, the Col, CS, CS-10SILY, CS-15SILY, and CS-20SILY hydrogels, respectively, had an average G' of 188.1 ± 73.0, 389.4 ± 262.0, 245.6 ± 74.0, 551.48 ± 132.3, and 763.5 ± 90.0 Pa, and an average G" of 37.5 ± 5.7, 80.6 ± 55.7, 44.1 ± 6.4, 105.5 ± 26.9, and 148.1 ± 27.1 Pa (Figure 4-2). When a CS-SILY molecule was added, we saw a trend of increasing G' when more SILY peptides were added on to the CS backbone. The G' value for CS-20SILY was statistically higher compared to the G' of all other treatments at 0.1 Hz.

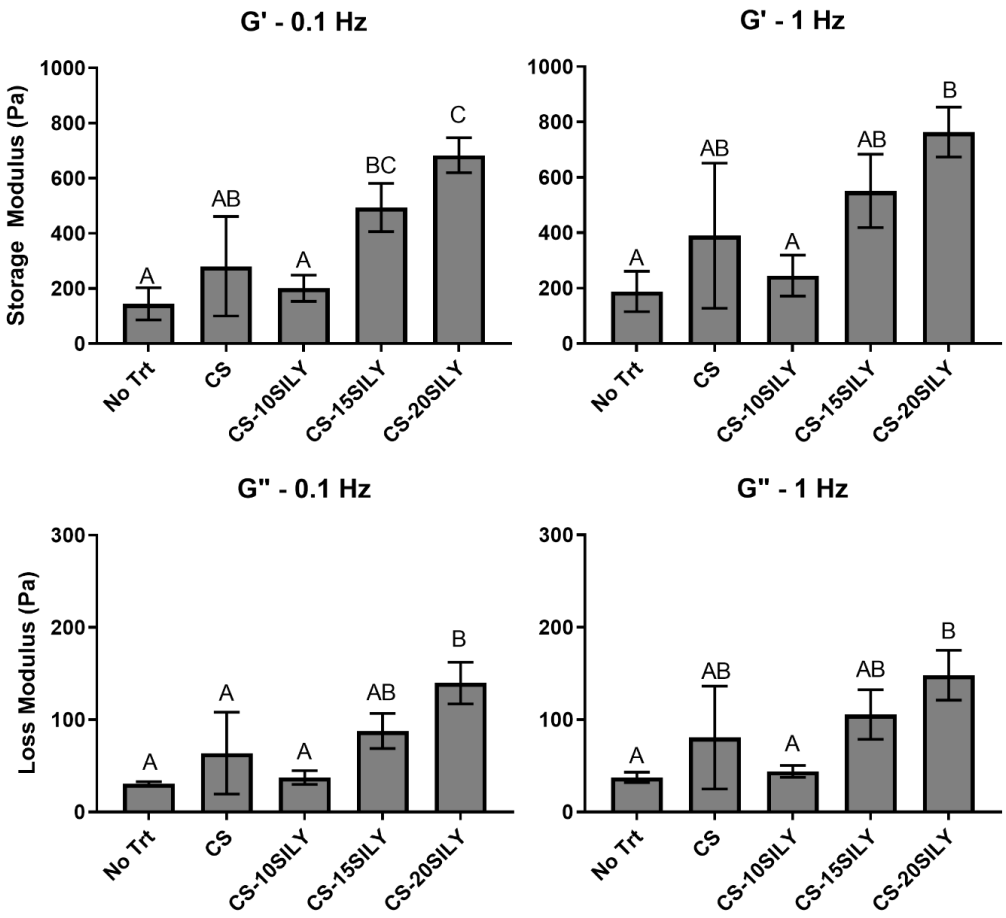

Figure 4-2.The storage modulus (G') and loss modulus (G") of hydrogels with the addition of CS or CS-SILY molecules.

Frequency sweeps from 0.01 to 10 Hz were performed. Single factor analysis of variance (ANOVA) and Tukey post hoc tests were performed (n=3) at 0.1 and 1 Hz. Different letters indicate groups with a significantly different G' ($p < 0.05$) or G" ($p < 0.05$). Data is represented as the mean ± the standard deviation.

Addition of CS-SILY decreases the average fibril diameter.

Cryo-SEM was performed to investigate the network structure of hydrogels polymerized in the presence of CS or CS-SILY molecules, and a representative cryo-SEM images of each treatment is shown in Figure 3A. The distribution of collagen fibrils was analyzed and presented normalized to the frequency of a certain fibril diameter measurement (Figure 4-3A). The Col and CS treatments had a wider distribution of fibril diameters from 50 nm to 300 nm for the Col hydrogels and 25 nm to 300 nm for the CS hydrogels (Figure 4-3B). In contrast, the fibril diameters

in the hydrogels with CS-SILY molecules added had a fibril diameter distribution with less variation from 75nm to 250 nm for the CS-10SILY hydrogels, 25 nm to 150 nm for the CS-15SILY hydrogels, and 50 nm to 200 nm for the CS-20SILY hydrogels. Qualitatively, the fibrils look much thinner in the images where CS-SILY molecules are added prior to polymerization. This was further investigated by measuring the collagen fibril diameters using ImageJ to calculate the average fibril diameter (Figure 4-3C). We saw a statistically smaller average fibril diameter in the CS-15SILY and CS-20SILY compared to the collagen only (No Trt), CS, and CS-10SILY hydrogels. The average fibril diameter of the No Trt and CS hydrogels was statistically similar. The average fibril diameter of the CS-10SILY was smaller than the No Trt and CS hydrogels but larger than the CS-15SILY and CS-20SILY hydrogels. We saw no trends between the treatment groups when the percent porosity was analyzed using ImageJ (Figure 4-3D), and the addition of CS-SILY molecules increased the number of pores found in the hydrogels (Figure 4-3D).

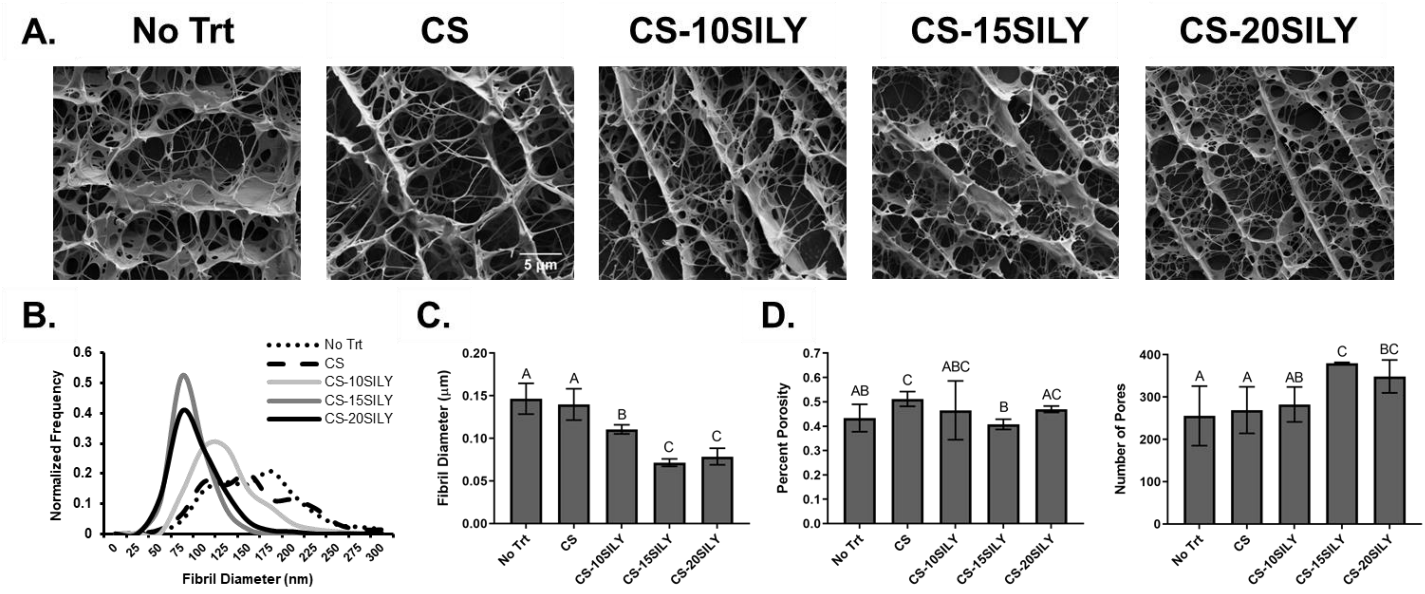

Figure 4-3. The effect of adding CS or CS related molecules on collagen network structure.

Representative cyroSEM images for collagen hydrogels with no additional molecules (No Trt) or the addition of CS, CS-10SILY, CS-15SILY, or CS-20SILY (a). The scale bar represents 5 μm. The fibril distributions are also represented as normalized frequency for each hydrogel formulation ($n \geq 270$) (B). Average fibril diameter in hydrogels with added CS related molecules (C). Different letters indicate groups with a significantly different average fibril diameter ($p < 0.05$). The percent porosity (n=9) and number of pores (n=9) based on cryoSEM images (D). Different letters indicate groups with a significantly different percent porosity ($p < 0.05$) or number of pores ($p < 0.05$). Data is represented as the mean ± the standard deviation.

Addition of CS-SILY molecules increased GAG production and had no change on collagen content.

The GAG and DNA content in each scaffold, with or without added CS or CS-SILY, and encapsulated MSCs was analyzed after a 21- or 28-day culture period with the results shown in Figure 4-4A and B. GAG production was normalized to DNA content in the cell-hydrogel constructs (Figure 4-10). Although all other treatments had a significant increase in GAG content compared to scaffold with no added CS, there were no statistical differences in the normalized GAG levels in scaffolds with added CS, CS-10SILY, CS-15SILY, or CS-20SILY when they were cultured for 21 days. After 28 days in culture, there was a statistically greater amount of normalized GAG in the scaffolds with one of the CS-SILY molecules add prior to fibrillogenesis as compared to the scaffolds with or without added CS. Similar trends were also seen when the GAG production data was analyzed on a per scaffold basis (Figure 4-11).

The collagen content normalized to DNA in each scaffold, with or without added CS or CS-SILY, and encapsulated MSCs was analyzed after a 21- or 28-day culture period with the results shown in Figure 4-4C and D. There was no statistical difference in the total collagen content when normalized to DNA in the hydrogels polymerized with or without CS or CS-SILY molecules. The data was also analyzed as collagen content on a per scaffold basis. After 21 days of culture, there was a statistically higher amount of collagen per scaffold when a CS-SILY molecule was added as compared when CS was added to the scaffold or no addition molecule was included (Figure 4-11). After 28 days in culture, there was a statistically higher amount of collagen per scaffold when a CS-SILY molecule was added into the scaffold compared to the scaffolds that had no added collagen (Figure 4-11). However, there was no statistical difference between the scaffolds that had a CS-SILY molecule or CS added.

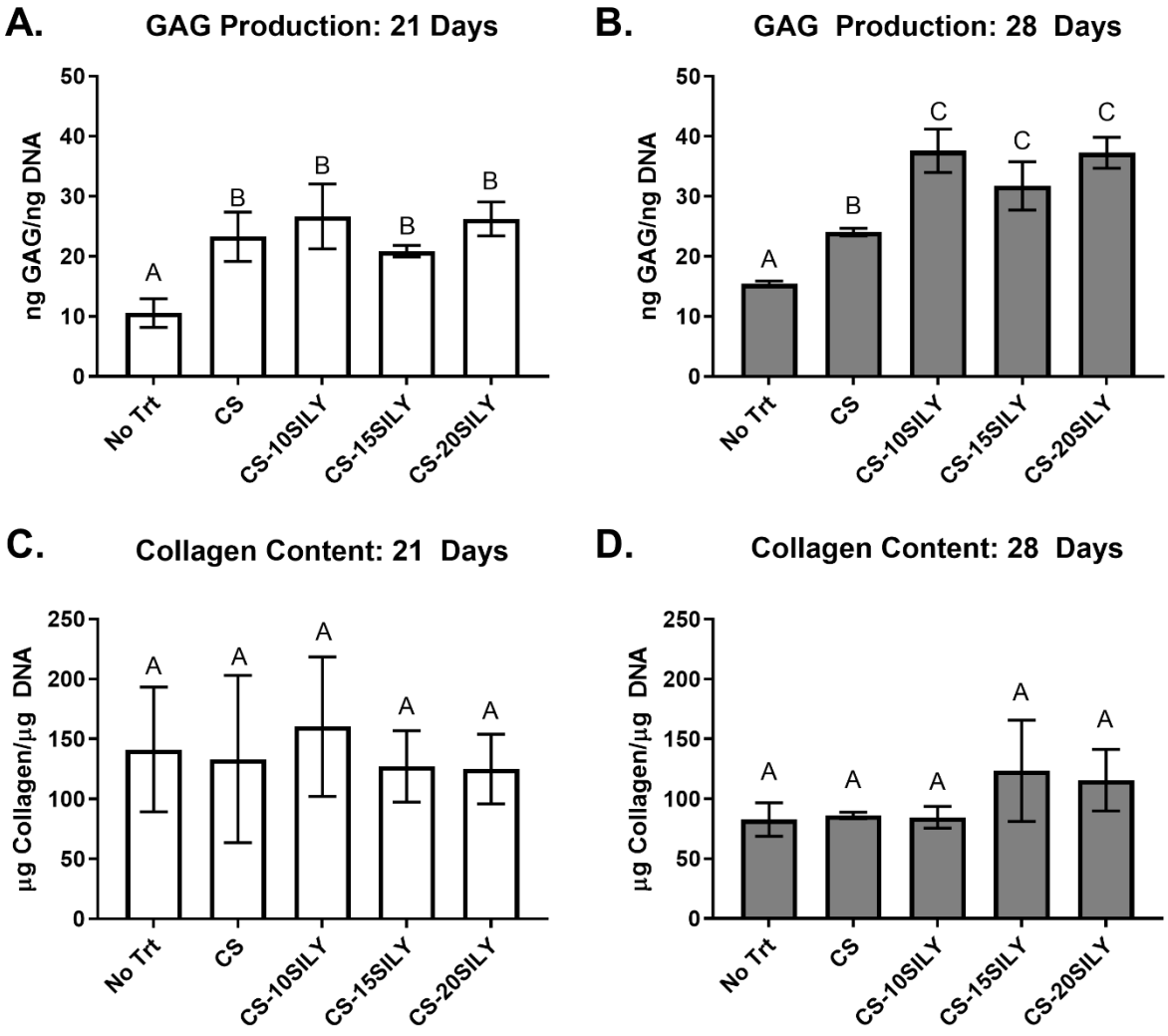

Figure 4-4. The addition of CS-SILY molecule increases GAG production after 28 days in culture and has no change on collagen content.

GAG/DNA ratio of the cell-hydrogel constructs with or with added CS or CS-SILY molecules after a (A) 21-day or (B) 28-day culture period. Values are expressed as mean ± SD (n = 4). Total collagen/DNA ratio of the cell-hydrogel constructs with or with added CS or CS-SILY molecules after a (C) 21-day or (D) 28-day culture period. Values are expressed as mean ± SD (n = 3). An ANOVA and Tukey's post hoc tests were performed. Different letters indicate groups with a significantly different GAG production or total collagen content at a certain timepoint ($p < 0.05$).

There was a lesser amount of collagen in cell culture media from scaffolds with CS-SILY molecules.

The mass of collagen in cell culture media was measured using a Sircol dye assay after a 7, 14, or 21 or 28-day culture period with the results shown in Figure 4-5. After 7 days in culture, there was statically less collagen in the cell culture media removed from cell-hydrogel constructs with CS-10SILY or CS-15SILY added to the scaffold prior to polymerization when compared to scaffolds with or without CS added. At all other timepoints, there was no statistical difference in the amount of collagen recovered from cell culture media in any of the treatments examined.

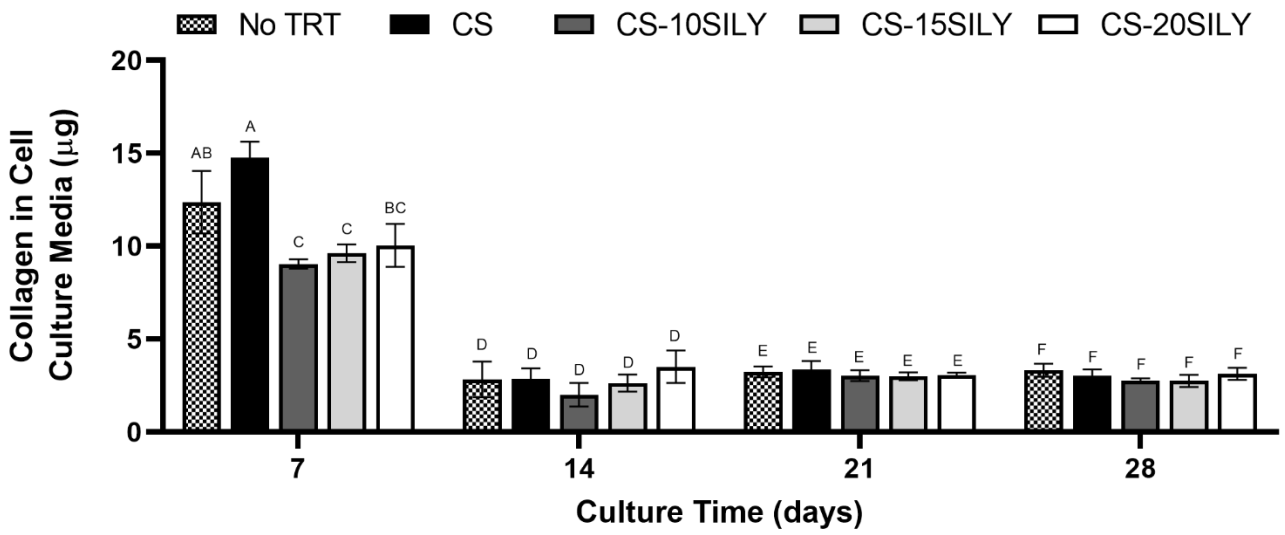

Figure 4-5. A lesser amount of collagen was recovered in cell culture media in the scaffolds where a CS-SILY molecule was added.

Collagen from media aliquots in which cell-hydrogel constructs, with or without added CS or CS-SILY molecules, were cultured. Media was sampled after 7, 14, 21, or 28 days, and collagen was measured using a sircol dye assay kit. Values are expressed as mean ± SD (n = 3). An ANOVA and Tukey's post hoc tests were performed. Different letters indicate groups with a significantly different mass of collagen in the measured cell culture media at a certain timepoint ($p < 0.05$).

Aggrecan gene expression was upregulated in the CS-10SILY hydrogels after 14 days.

Gene expression levels were measured at day 7 and 14 using qRT-PCR in MSCs cultured in Col I/II hydrogels with either no additional treatment or CS, CS-10SILY, CS-15SILY, or CS-20SILY added prior to polymerization as seen in Figure 4-6. There was a slight upregulation in sox9 gene expression with the addition of CS or CS-SILY molecules after 7 days in culture. There was statistical increase in sox9 expression in the scaffolds with CS-10SILY and CS as compared to the scaffolds with no added GAG treatment. After 7 days in culture, there was also a statistical increase in aggrecan expression in samples with CS, CS-10SILY, or CS-15SILY as compared to scaffolds with no added GAG or CS-20SILY. There was no statistical difference between treatments in collagen type II or collagen type X expression at 7 days. There was a slight upregulation at 14 days of sox9 expression in scaffolds with CS or CS-SILY added prior to polymerization. However, the only statistical difference was an increase in sox9 expression in scaffolds with CS and CS-15SILY compared to scaffolds with no added GAG. Aggrecan gene expression was upregulated in the CS-10SILY hydrogels after 14 days as compared to all other treatments. Scaffolds with added CS-20SILY had statistically higher collagen type II expression as compared to scaffolds with CS-10SILY, CS-15SILY, or no added GAG treatment. Finally, there was no statistical difference between treatments in collagen type I or collagen type X expression at 14 days.

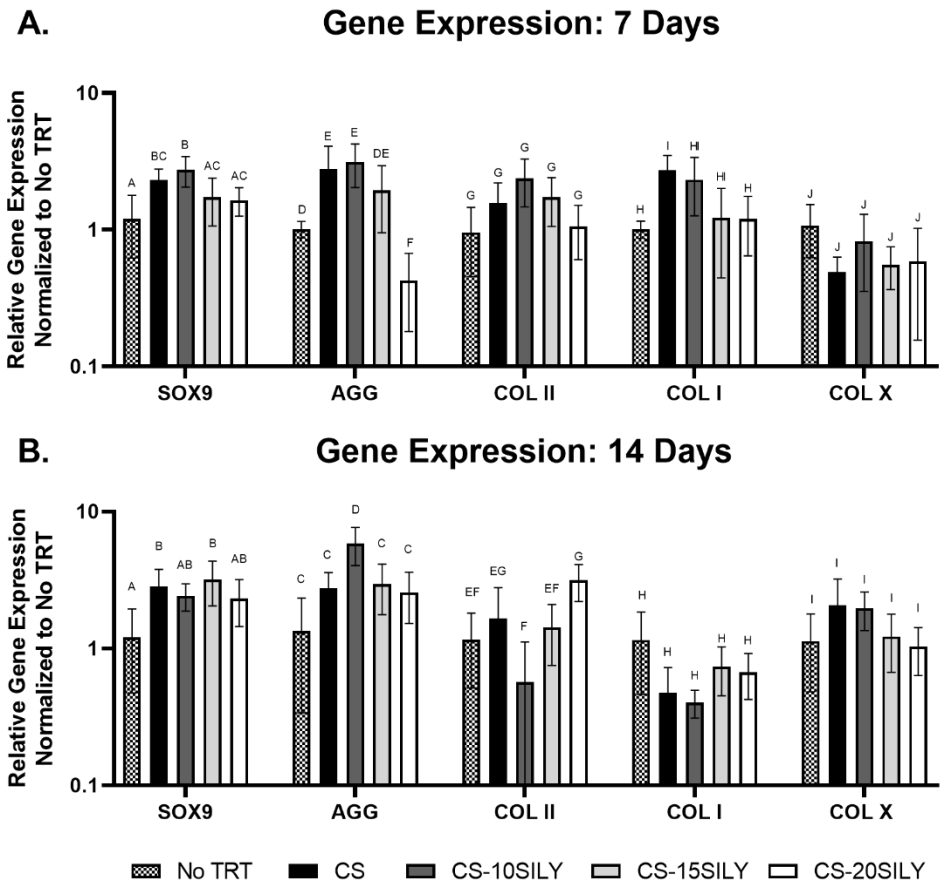

Figure 4-6. Relative gene expression of chondrogenic and collagen genes at days 7 and 14. Single factor analysis of variance (ANOVA) and Tukey's post hoc tests were performed for gene expression analysis of collagen type II at 1 week, sox 9 at 1 week, aggrecan at 2 weeks, and sox 9 at 2 weeks. An ANOVA and a Games Howell post hoc test were performed for gene expression analysis of collagen type I and collagen type X at both timepoints. A Box-Cox transformation was used to analyze data for gene expression analysis of aggrecan at 1 week and collagen type II at 2 weeks. Different letters indicate groups with a significantly different relative gene expression for a certain gene at a certain timepoint ($p < 0.05$).

4.4 Discussion

Due to the fact that CS is able to influence the fate of stem cells by acting as a biochemical cue and binding with growth factors,[246] studies have attempted to retain CS in their tissue engineered cartilage construct. This study investigates strategies to better retain, without the use of chemical crosslinking, matrix molecules, like CS, to a scaffold material to better recapitulate aspects of native cartilage. To date, this is the first study to retain CS in a collagen-based scaffold

by incorporating a CS molecule with attached collagen binding peptides. The addition of the collagen peptide, in the form of the CS-15SILY or CS-20SILY, allowed for over 20% of the original amount of CS to be retained after 7 days where as less than 1% of the free CS remained in the same time period. In addition, we investigate how the addition of these molecules alters the physical properties of a Col I/II based hydrogel. Furthermore, the CS retention, average fibril diameter, and mechanical properties can be tuned by adjusting the amount of SILY peptides attached to the CS backbone.

Previous studies note that the addition of HA or CS would hardly cause any change to mechanical properties of collagen matrices.[255] In a study of collagen type I hydrogels, there was actually a slight decrease in storage modulus when CS was added during polymerization.[256] In this study, there was an increasing trend in the G' value during rheological testing with the addition of CS-SILY molecules. When a CS-SILY molecule was added, we saw a trend of increasing G' when the number of SILY peptides on the CS backbone was increased. It is hypothesized that the increase in mechanical properties can be attributed to further crosslinking during fibrillogensis due to the binding of SILY molecules to collagen fibrils as seen in other studies investigated DS-SILY.[145] It is important to note that there are a number of other properties of hydrogels that can cause differences in gel stiffness including fibril branding, fibril length, and physical interactions between CS-CS, CS-collagen, and SILY-collagen.[257,258] Murphy *et al.* reported that in MSCs cultured in soft collagen-glycosaminoglycan scaffolds, with a compressive modulus of 0.5 kPa, were more likely to express cartilage specific genes and MSCs cultured in stiff collagen-glycosaminoglycan scaffolds, with a compressive modulus of 1.5 kPa, were more likely to express bone specific genes.[259] All of the scaffold formulations in this study were similar in stiffness to the soft hydrogels mentioned above, and the Col I/II hydrogels with added CS-15SILY (493.9 Pa) and CS-20SILY (684.0 Pa) molecules had stiffness that were similar to the 0.5 kPa hydrogel that prompted chondrogenesis.

Although the interactions of CS and proteins have been studied, there are discrepancies in the literature on how CS alters fibril size and rate of fibrillogenesis.[182,256,260] One study showed that the addition of CS to a collagen scaffold increased fibril diameter in a dose dependent matter.[260] In contrast, Douglas *et al.* found that the addition of CS to both collagen type I and II caused fibrils to become thinner and hypothesized that the more CS present the greater the hindrance of fibril growth.[182] This is consistent with our results, which found that the collagen

average fibril diameter was statistically smaller in the CS-15SILY and CS-20SILY, the scaffold with the highest amount of retained CS, compared to the collagen only (No Trt), CS, and CS-10SILY hydrogels. These results may be due to the fact that sugars have been shown to disrupt hydrogen-bonded water bridges between the helices of collagen which inhibits the fibrillogenesis of collagen.[261]

In our current study, statistical differences were seen between treatments in collagen content after 21 days, but it took 28 days to see differences in GAG production. There was a statistically greater amount of normalized GAG, after 28 days in culture, in the scaffolds with one of the CS-SILY molecules added prior to fibrillogenesis as compared to the scaffolds with or without added CS. The results suggest that the CS, introduced to the Col I/II in the form of a CS-SILY molecule, is still bioactive when crosslinked with a collagen-binding peptide. After 21 days of culture, there was a statistically higher amount of collagen per scaffold, but no statistical difference when collagen is normalized to DNA, when a CS-SILY molecule was added as compared when CS was added to the scaffold or no addition molecule was included. With respect to collagen content per scaffold at the same timepoint, there was no difference between the 3 different CS-SILY molecules. A decrease in the mass of collagen in each scaffold was seen from 21 to 28 days. These results suggest that cells are remodeling more collagen, seen by a decrease in collagen content, as they make more GAGs.

Previous studies have added CS to collagen-based scaffolds to help chondrocytes maintain their rounded morphology and provide cells biochemical cues. In the current study, slight differences in the gene expression of cartilage specific genes were seen. Aggrecan gene expression was upregulated in scaffolds with CS, CS-10SILY, or CS-15SILY as compared to samples with no added GAG or CS-20SILY after 7 days and in CS-10SILY hydrogels after 14 days as compared to all other treatments. There was statistical increase in sox9 expression in the scaffolds with CS-10SILY and CS compared to scaffolds with no added GAG which is consistent with the idea that CS is still bioactive when crosslinked with a collagen-binding peptide. Sox9 is considered the master transcription factor involved in chondrogenesis since it is essential for both mesenchymal condensation and hypertrophy inhibition. Mixed results were seen in a study by Van Susante et *al.* where no difference in gene expression was seen after 14 days of chondrocytes in collagen type I and CS hydrogels.[262] In contrast, there was more GAG production by the chondrocytes, after 14 days of culture, in the COL I and CS hydrogels as compared to the all collagen type I gels.[262]

Pieper *et al.* evaluated crosslinked collagen-based scaffolds with chondrocytes, but differences, in terms of gene expression and biochemical analysis, were only seen between different types of collagens in contrast to the absence or presences of CS. [123] Although the mechanism remains unclear, the addition of CS to scaffolds has been shown to prevents or delays the further differentiation of MSCs to a hypertrophic phenotype, represented with the gene expression of collagen type X.[245] However, we saw no difference in collagen type x expression between our treatments investigated at either timepoint.

An animal study would further elucidate in vitro results as an in vivo study could potentially provide more insight into discrepancies between protein production and gene expression. Additionally, the inclusion of other ECM molecules can further recapitulate native properties of cartilage. However, it is important to note we previously saw HA strongly interacted with CS preventing some CS incorporation, during polymerization, into a collagen hydrogel.[217] Finally, it is difficult to fully understand the collagen production, of the studied hydrogels, during the culture period due to the fact that scaffolds were designed to made from collagen. Since the scaffold is continually remodeled by the cells, it is difficult to distinguish which collagen was added prior to polymerization and what collagen has been newly produced.

4.5 Conclusions

This study investigated the use of CS with attached collagen binding peptides to retain, without the use of chemical crosslinking, matrix molecules and better recapitulate aspects of native cartilage. Since the CS retention, average fibril diameter, and mechanical properties are altered by the addition of different CS-SILY molecules, the properties of the desired Col I/II hydrogel can be tuned by adjusting the amount of SILY peptides attached to the CS backbone. Finally, the scaffolds that contained CS-10SILY, CS-15SILY, and CS-20SILY had higher glycosaminoglycan production which suggests better differentiation of MSCs into chondrocytes in scaffolds that contain a CS-SILY molecule. Taken together, these results suggested that the addition of a CS-SILY molecule to a collagen type II to a hydrogel with encapsulated MSCs has the potential to promote cartilage repair.

4.6 Chapter 4 Supplementary Information

Table 4-1. Primer sequences utilized for quantitative reverse transcription-polymerase chain reaction.

Gene of Interest	Accession number		5' → 3' sequence	Product length (bp)	Primer efficiency	Reference
Collagen Type I	NM 001195668.1	Forward	ATGGATGAGGAAACTGGCAACT	114	101.9%	Liao, 2010[236]
		Reverse	GCCATCGACAAGAACAGTGTAAGT			
Collagen Type II	NM 001195671.1	Forward	GCCACCGTGCCCAAGAAGAACT	160	103.1%	Yuan, 2016[135]
		Reverse	ACAGCAGGCGCAGGAAGGTCAT			
Collagen Type X	XM 002714724.3	Forward	GCCAGGACCTCCAGGACTATCA	103	100.0%	Zheng, 2009[237]
		Reverse	CCCAATGTCTCCTTTCGGTCCA			
Aggrecan	XM 008251723.2	Forward	CCTACCAGGACAAGGTCTCG	163	98.1%	Chen, 2016[238]
		Reverse	ACACCTTTCACCACCACCTC			
Sox9	XM 008271763.2	Forward	GGAAGCTCTGGAGACTGCTG	135	96.8%	Zhang, 2012[239]
		Reverse	CGTTCTTCACCGACTTCCTC			
GAPDH	NM 001082253.1	Forward	CGCCTGGAGAAAGCTGCTA	104	96.0%	Morigele, 2013[240]
		Reverse	ACGACCTGGTCCTCGGTGTA			

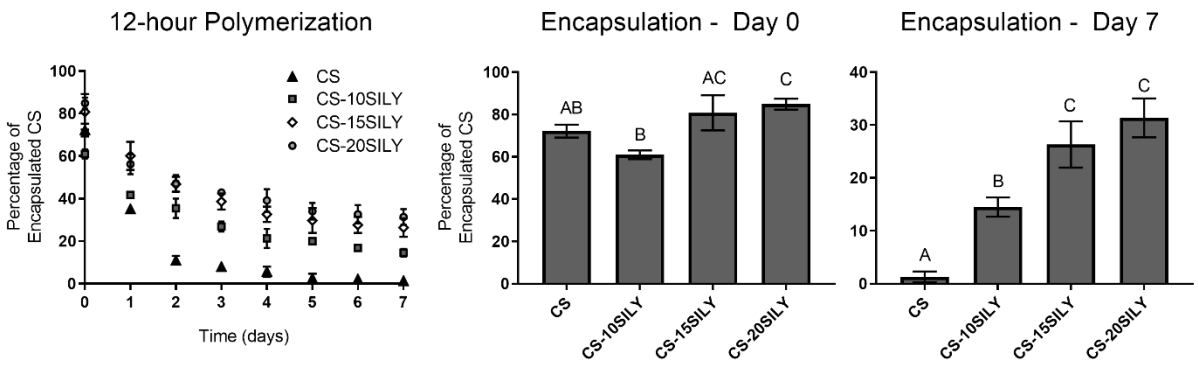

Figure 4-7. Percentage of encapsulated CS retained in the hydrogel over time after a 12-hour polymerization.

CS Encapsulation after a wash or 7-day period are shown. Single factor analysis of variance (ANOVA) and Tukey post hoc tests were performed (n=4). Different letters indicate groups with a significantly different percentage of encapsulated CS ($p < 0.05$). Data is represented as the mean ± the standard deviation.

Addition of CS-SILY molecules enhanced CS retention in scaffold polymerized for 12 hours.

Col I/II hydrogels were polymerized for 12 hours with either 10 µM of CS, CS-10SILY, CS-15SILY, or CS-20SILY. A DMMB assay was used to understand how much CS was encapsulated in the hydrogel from 0 to 7 days. Immediately after a 12-hour polymerization period (Figure 4-7) and a PBS wash, there was a statistically higher amount of CS encapsulated in the CS-20SILY hydrogels (84.9 ± 2.6%) compared to the CS-10SILY (61.0 ± 2.1%) and CS (72.2 ± 3.0%) hydrogels, but there was no statistical difference between the CS-20SILY and CS-15SILY (80.8 ± 8.3%) treatments. On day 2, the CS hydrogel was under 20% of the original amount encapsulated. The CS-10SILY contained under 20% of the original amount of CS encapsulated on day 5. Similarly, to the hydrogels polymerized for 3 hours, the CS-15SILY and CS-20SILY, which were not statistically different from one another, did not contain under 20% of the original amount of CS encapsulated in the 7-day period analyzed. After 7 days, the trend in CS encapsulation was similar for the hydrogels polymerized for 3 or 12 hours. There was a statistical difference in the amount of CS encapsulated in the hydrogel in the CS-15SILY (26.3 ± 4.4%) and the CS-20SILY (31.4 ± 3.7%) as compared to the CS-10SILY (14.5 ± 1.8%) or CS (1.3 ± 1.0%) hydrogels. The frequency sweeps show that at 0.1 Hz, the Col, CS, CS-10SILY, CS-15SILY, and CS-20SILY hydrogels, respectively, had an average complex modulus (G*) of 148.2 ± 57.8, 287.8 ± 185.6, 204.5 ± 48.2, 501.7 ± 89.0, and 659.2 ± 1.6 Pa. At 1 Hz, the Col, CS, CS-10SILY, CS-15SILY, and

CS-20SILY hydrogels, respectively, had an average G* of 192.1 ± 71.9, 397.6 ± 267.8, 249.6 ± 73.8, 561.5 ± 134.9, and 741.9 ± 30.7 Pa.

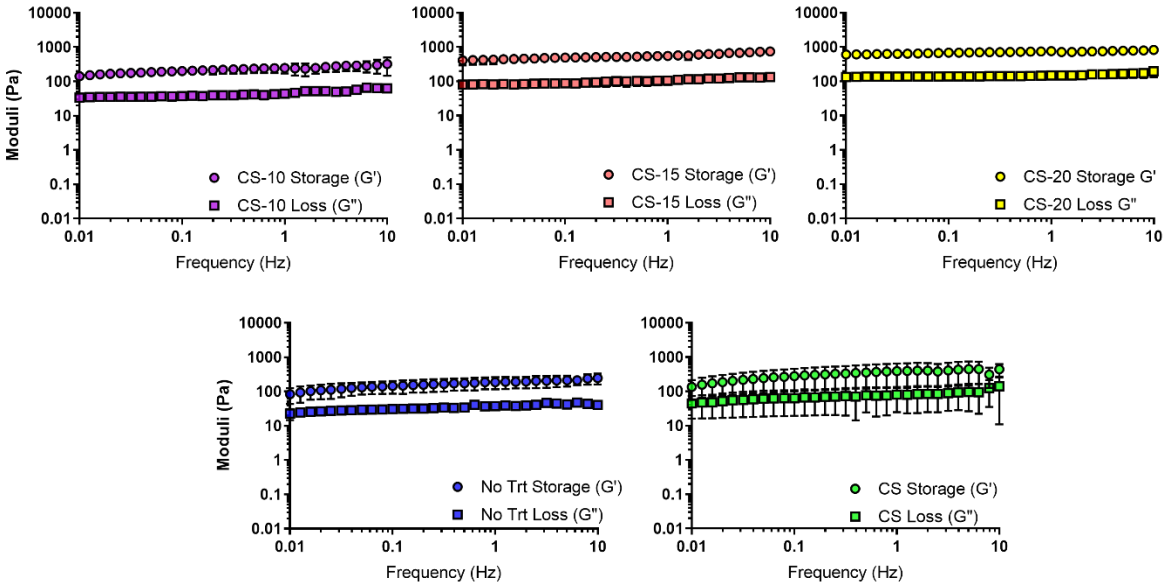

Figure 4-8. Storage and Loss Moduli of hydrogels with the addition of CS or CS-SILY molecules.

Frequency sweeps from 0.01 to 10 Hz were performed. Data (n=3) is represented as the mean ± the standard deviation.

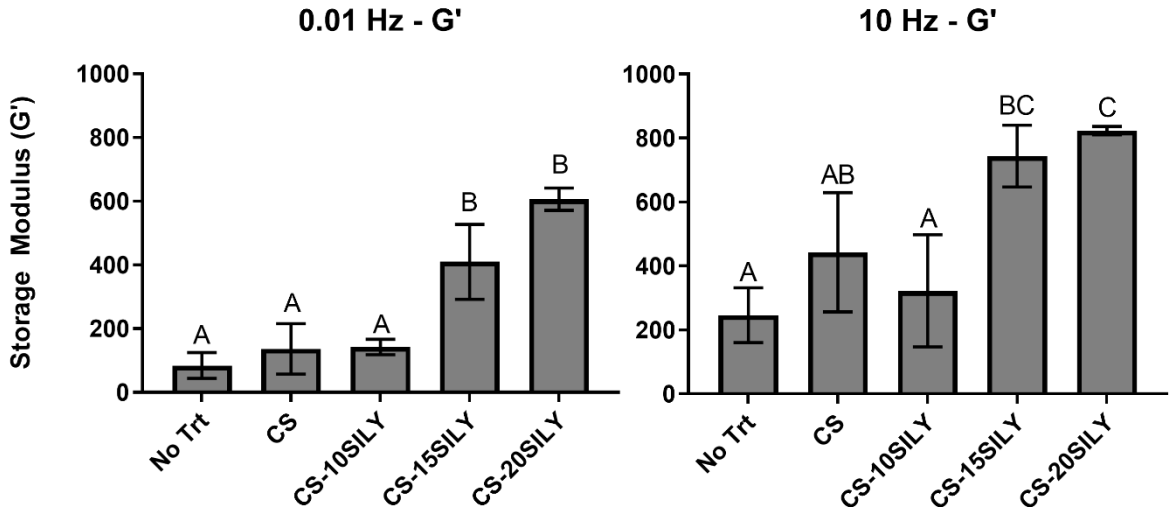

Figure 4-9. The storage modulus (G') of hydrogels with the addition of CS or CS-SILY molecules.

Frequency sweeps from 0.01 to 10 Hz were performed. Single factor analysis of variance (ANOVA) and Tukey post hoc tests were performed (n=3) at 0.01 and 10 Hz. Different letters indicate groups with a significantly different G' ($p < 0.05$). Data is represented as the mean ± the standard deviation.

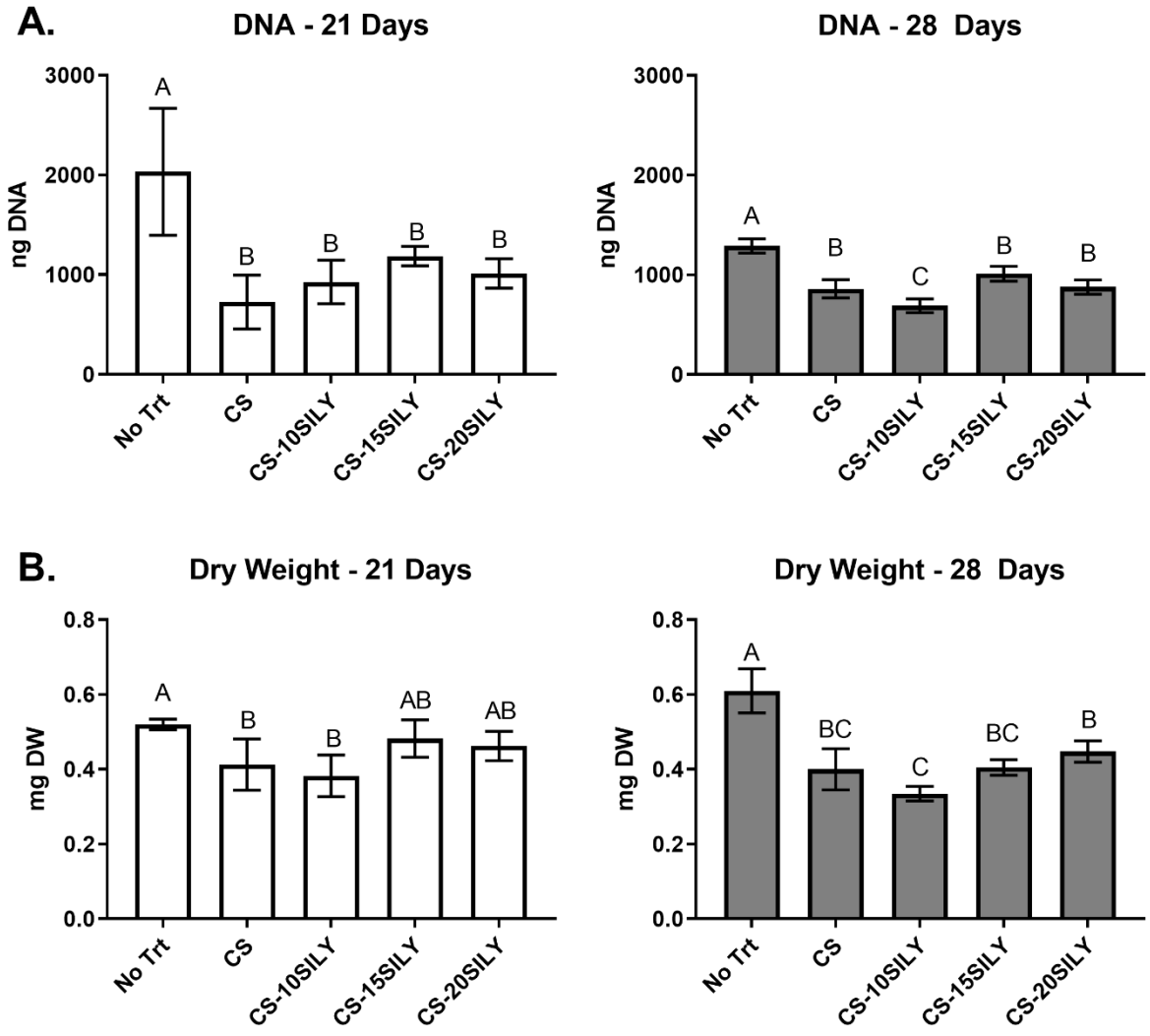

Figure 4-10. The mass of DNA or dry weight (DW) of the cell-hydrogel constructs with or with added CS or CS-SILY molecules after a (A) 21-day or (B) 28-day culture period.

Values are expressed as mean ± SD (n = 4). An ANOVA and Tukey's post hoc test were performed. Different letters indicate groups with a significantly different DNA or DW at a certain timepoint ($p < 0.05$).

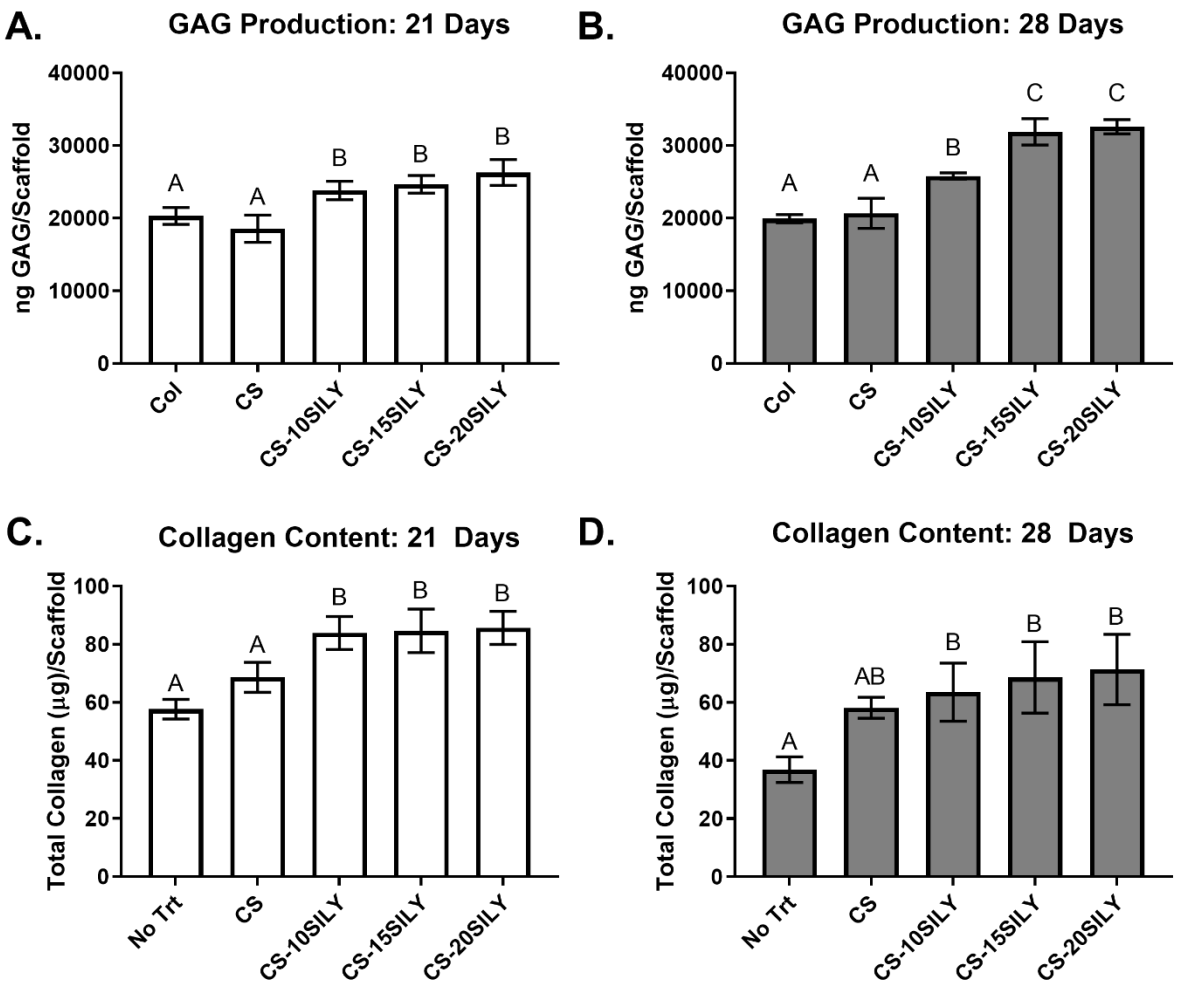

Figure 4-11. GAG production of the cell-hydrogel constructs with or with added CS or CS-SILY molecules after a (A) 21-day or (B) 28-day culture period.

Values are expressed as mean ± SD (n = 4). Total collagen of the cell-hydrogel constructs with or with added CS or CS-SILY molecules after a (C) 21-day or (D) 28-day culture period. Values are expressed as mean ± SD (n = 3). An ANOVA and Tukey's post hoc tests were performed. Different letters indicate groups with a significantly different GAG production or total collagen content at a certain timepoint ($p < 0.05$).

5. CONCLUSIONS AND FUTURE WORK

The goal of this thesis was to create and investigate a biomimetic scaffold to replace damaged articular cartilage. An introduction of the different components that make up cartilage tissue and the status of cartilage repair options was presented, and the shortcomings of current treatment options and collagen type I scaffold were identified.

In Chapter 1, we harnessed the biological activity of collagen type II and the superior mechanical properties of collagen type I by blending the two types together into a composite hydrogel. Compared to collagen type I, collagen type II has superior chondroinductive properties but does not form robust hydrogels on its own. Thus, recent work has focused on adding collagen type II to other materials (e.g., collagen type I). Hydrogels made of various blends of collagen type I and II were investigated to understand whether the addition of collagen type I to a collagen type II hydrogel altered the amount of protein incorporated into the hydrogels, the mechanical properties of the hydrogels, and the structure of the collagen network. We demonstrated that the addition of collagen type II alters gel formation, network structure, and mechanical properties. The collagen blend hydrogels successfully incorporated both types of collagen and retained chondroitin sulfate and hyaluronic acid. Cryo-scanning electron microscopy images showed that the 3:1 ratio of collagen type I to type II gels had a lower void space percentage than the 1:1 gels, and the complex modulus was larger for the 3:1 gels ($G^* = 5.0$ Pa) compared to the 1:1 gels ($G^* = 1.2$ Pa). We found that the 3:1 blend consistently formed gels with superior mechanical properties compared to the other blends, so all subsequent studies used the 3:1 ratio as our optimized collagen type I and II blend hydrogel.

Previous studies with collagen type I and II blend hydrogels have only encapsulated chondrocytes within the gels. Our study was the first to encapsulate MSCs in a collagen type I and II hydrogel and investigate them in cartilage defect repair using a rabbit model. In addition, the study was unique because it decouples an increase in chondrogenesis *in vitro* from differences in initial hydrogel stiffness. The chondrogenic potential of collagen type I and II blend hydrogels, both *in vitro* and *in vivo*, was explored. To evaluate the chondrogenic differentiation potential of bone marrow-derived MSCs embedded within a collagen type I and II blend gel *in vitro*, rabbit MSCs were isolated from bone marrow and embedded within hydrogels made up of either all collagen type I or a 3:1 blend of collagen type I to II (Col I/II). Our findings demonstrated that the

addition of collagen type II promotes the production of GAGs which is indicative of matrix deposition. After 4 weeks in culture, there was a statistical increase in the normalized GAG content in the Col I/II hydrogels compared to the all collagen type I hydrogels. The addition of collagen type II decreased alkaline phosphatase activity, which is a hypertrophic marker and is undesirable because it indicates early bone formation. Our results *in vitro* indicate that the addition of collagen type II to our hydrogel scaffold promotes the differentiation of MSCs to the desired cartilage phenotype. Analyzed and scored histology sections from the *in vivo* study indicate that there was a statistically higher overall cartilage repair score for the Col I/II hydrogels as compared to the all collagen type I hydrogel treatment and the empty defect control in both the medial condyle and the trochlear groove.

Finally, we investigated the use of CS conjugated with collagen binding peptides to retain, without the use of chemical crosslinking, matrix molecules and better recapitulate aspects of native cartilage. Since CS retention, average fibril diameter, and mechanical properties are altered by the addition of different CS-SILY molecules, the properties of the desired Col I/II hydrogel can be tuned by adjusting the amount of SILY peptides attached to the CS backbone. The scaffolds that contained CS-10SILY, CS-15SILY, and CS-20SILY had higher GAG production which suggests better differentiation of MSCs into chondrocytes in scaffolds that contain a CS-SILY molecule. Taken together, these results suggest that the addition of CS-SILY molecules to a collagen type I and II hydrogel with encapsulated MSCs has the potential to promote cartilage repair.

Results from this work have shown that there is clinical value in the cartilage repair capabilities of our Col I/II hydrogel with encapsulated MSCs. A proposed next step for expanding on the rabbit study includes investigating cartilage defect repair with a longer evaluation time frame in a larger animal. To validate cartilage repair, the Col I/II scaffold with encapsulated MSCs could be evaluated by implantation within a critical size cartilage defect in skeletally mature Hampshire Suffolk cross sheep. Several animal models of full thickness articular cartilage defects exist, but the sheep is a commonly used animal model for translating research into cartilage repair.[150–152] Sheep are easy to house and handle; their stifle is accessible for defect creation and repair; and they have low levels of spontaneous healing.[153,154] Furthermore, the sheep has been considered a scaled-down version of a human knee due to common anatomical characteristics.[155] Due to the age of skeletal maturity (2- to 3-years),[154] only female sheep will be used since current breeding practices are to maintain a large female population with relatively few males. Thus, male

sheep that have reached skeletal maturity are rare and would be difficult to obtain or would require us to raise and house them for a few years prior to our studies.

Some changes will be made to the MSC isolation procedure that was used when MSCs were isolated from rabbits. Bone marrow will be aspirated from the iliac crest of 2- to 3-year-old skeletally mature ewes[149] that are free of both lameness and radiographic evidence of stifle (knee) pathology. The bone marrow extraction sites will be clipped and scrubbed using chlorhexidine and standard techniques. Five to ten milliliters of bone marrow will be aspirated from the iliac crest of sheep using a Jamshidi-bone marrow aspiration needle into a heparinized syringe, in contrast to the previously used method of only a syringe and a needle.[263] In addition, mononuclear cells will be isolated using a Ficoll-Paque Plus density gradient. This technique separates cells into layers based on how quickly cells can move through the Ficoll-Paque solution during centrifugation. The cells harvested using this method should contain highly purified MSCs. Another change to the previous protocol will be to also confirm we have isolated MSCs using flow cytometry. Based on the recommendations of the International Society for Cellular Therapy and the limited availability of antibodies that recognize sheep surface markers, we will also use flow cytometry to verify that our MSCs have the following profile: $CD73^+$, $CD90^+$, $CD105^+$, $CD11b^-$, $CD45^-$, HLA-DR^-.[264–266]

In sheep, the most commonly recommended defect size is around 7 mm in diameter since it is reported as the critical size defect that does not heal spontaneously.[154,267] In addition, a 7-mm-diameter size is required to develop osteoarthritis in a stable joint.[268] We will thus create a defect with a diameter of 7 mm and depth of 2 to 3 mm, a size that is consistent with a full thickness cartilage defect.[154] After 21 weeks, the animals will be euthanized since this time point is consistent with similar studies in a sheep model.[154,269–271] The newly formed tissue will be evaluated for surface regularity, cartilage thickness, integration of donor with host cartilage, and cell morphology and proteoglycan staining using the O'Driscoll cartilage repair score.[272]

We are also interested in the mechanical properties of the repair tissue due to the fact that current treatment options promote the regrowth of fibrocartilage, which has mechanical properties inferior to native, hyaline cartilage.[213] For mechanical testing, a 3-mm diameter biopsy punch will be used to obtain cartilage plugs from all treatment groups and from healthy control tissue surrounding the defect sites. The plugs will be stored in protease inhibitors at -80°C prior to mechanical testing. Upon thawing, calipers will be used to measure the thickness of the plugs. Confined compression testing will be performed using a previously described experimental set

up.[273] Briefly, samples will be confined in a 3-mm diameter chamber and covered with a porous filter that allows water exchange. Samples will be compressed in steps of 5% strain with 10 minutes equilibration until a maximum of 40% strain. The aggregate modulus and hydraulic permeability will be calculated.[274]

We anticipate improved tissue architecture in terms of cellular morphology and matrix staining with our optimized and cellularized constructs compared to acellular constructs or no treatment controls. Although unlikely, we recognize that the gel constructs may not be retained in the defect. In this event, we will suture in place a biodegradable, collagen sheet to hold our scaffold in place. In addition, if obtaining bone marrow exclusively from the iliac crest does not yield the required amount of MSCs, we will also extract bone marrow from the femur and the humerus. Since we have experience with MSC isolation in two different animal models, we do not anticipate technical challenges with the proposed methods.

Proposed next steps for expanding on the CS-SILY study include studying the potential chondroprotective effects of adding CS-SILY to a Col I/II hydrogel encapsulated with MSCs when in the presence of collagenase or inflammatory molecules and investigating MSC differentiation. Previous studies have shown that supplementation of CS can mitigate the fact that chondrocytes cannot replace collagen and proteoglycan degraded by OA even with an increased rate of synthesis.[35] The addition of CS can increase chondrocyte metabolism to synthesize collagen and proteoglycans. CS has also been shown to increase the production of HA by human synovial cells, which increases the viscosity of synovial fluid.[142]

As previously discussed in Chapter 4, our laboratory has designed and characterized peptidoglycans to mimic aggrecan[181,252], lubricin[253], and decorin.[145–148,275] A collagen-binding peptide (RRANAALKAGELYKSILYGSG), or SILY, attached to dermatan sulfate (DS) backbone, another example of a glycosaminoglycan, has been used to design a mimic of decorin, a small proteoglycan that is associated with collagen fibrils.[145–148] The collagen binding peptidoglycan (DS-SILY) has been shown to bind to collagen, masking it from platelet activation in veins damaged from balloon angioplasty and inhibit collagen degradation by MMP-1 and MMP-13.[145,147]

We will culture scaffolds in either an inflamed or enzymatic degradation environment to optimize suppression of ECM degradation with CS-SILY molecules. As the Panitch lab has previously published, to mimic the inflammatory environment, scaffolds will be incubated in

chondrogenic media with 20 ng/mL of IL-1β or collagenase, and the culture media will be replaced every 2 days.[181] We will compare the how the addition of different CS-SILY molecules (CS-10SILY, CS-15SILY, and CS-20SILY) and various concentrations of the same molecules, in Col I/II hydrogels with encapsulated MSCs, retain collagen in the hydrogel when cultured with either IL-1β or collagenase. We will compare these treatments to hydrogels without any additional matrix molecules and encapsulated CS only. After 7 days in culture, the scaffold will be harvested to analyze how much collagen is retained in the gel. We anticipate that the addition of CS-SILY to our Col I/II hydrogel will protect the construct against collagenase degradation due to binding of the SILY peptide to our scaffold.

To investigate the chondrogenic enhancement effect of CS-SILY in an inflamed or enzymatic degradation environment, we will culture cell-hydrogel constructs in IL-1β or collagenase, with the treatments notated in the previous study, and measure the differentiation potential of MSCs to chondrocytes. Scaffolds will be grown for 3 or 4 weeks before the GAG values using a DMMB assay will be measured and normalized to the amount of DNA measured per sample. Hydrogels will also be created and harvested to understand gene expression of cartilage specific and inflammatory genes. At the completion of culture, mRNA will be isolated from the hydrogels and reverse transcribed for qRT-PCR. Gene expression levels for GAPDH, aggrecan, types I, II, and X collagen, MMP-13, aggrecanase (ADAMPS4/5), and IL-1β will be determined.

To study the enhancement of chondrogenesis due to the addition of CS-SILY in an osteoarthritic environment, we will add CS-SILY in a Col I/II hydrogels with encapsulated MSCs and subject them to synovial fluid. Synovial fluid will be aspirated from the knee joint of humans, from both healthy patients and patients with OA, using a syringe. Other published studies report the volumes of synovial fluid pulled from patients to be within 5 to 25 mL with an average of 9.4 mL.[276] The synovial fluid will be filtered and centrifuged to remove cells and debris from the fluid. Scaffolds will be harvested after 3 and 4 weeks. The amount of GAG will be quantified using a DMMB assay will be measured and normalized to the amount of DNA measured per sample. Hydrogels will also be created and harvested to understand gene expression of cartilage specific and inflammatory genes using qRT-PCR.

Altogether, information from the experiments discussed in this section will help researchers and clinicians work towards a tissue engineering option for repair cartilage defects. The large

animal study will allow us to further evaluate the efficacy of our constructs and move closer to the development of safe and effective tissue engineering-based cartilage repair therapy. The investigation into the use of CS-SILY for both the induction of chondrogenesis in an osteoarthritic model and the ability of the molecules to be chondroprotective will give us important information regarding the use of additional matrix molecules as biofactors within tissue engineered constructs for cartilage repair in a patient with osteoarthritis.

REFERENCES

(1) Lawrence, R. C.; Felson, D. T.; Helmick, C. G.; Arnold, L. M.; Deyo, R. A.; Gabriel, S.; Hirsch, R.; Hochberg, M. C.; Hunder, G. G.; Jordan, J. M.; et al. Estimates of the Prevalence of Arthritis and Other Rheumatic Conditions in the United States. Part II. *Arthritis Rheum* **2008**, *58* (1), 26–35. https://doi.org/10.1002/art.23176.Estimates.

(2) Gomoll, a. H.; Filardo, G.; de Girolamo, L.; Esprequeira-Mendes, J.; Marcacci, M.; Rodkey, W. G.; Steadman, R. J.; Zaffagnini, S.; Kon, E. Surgical Treatment for Early Osteoarthritis. Part I: Cartilage Repair Procedures. *Knee Surgery, Sport. Traumatol. Arthrosc.* **2012**, *20* (3), 450–466. https://doi.org/10.1007/s00167-011-1780-x.

(3) Wang, Z.; Peng, J. Articular Cartilage Tissue Engineering: Development and Future: A Review. *J. Musculoskelet. Pain* **2014**, *22* (28), 68–77. https://doi.org/10.3109/10582452.2014.883017.

(4) Goldring, M. B.; Goldring, S. R. Osteoarthritis. *J. Cell. Physiol.* **2007**, *213* (2), 626–634. https://doi.org/10.1002/JCP.

(5) Alford, J. W.; Cole, B. J. Cartilage Restoration, Part 1: Basic Science, Historical Perspective, Patient Evaluation, and Treatment Options. *Am. J. Sports Med.* **2005**, *33* (2), 295–306. https://doi.org/10.1177/0363546504273510.

(6) Matsiko, A.; Levingstone, T. J.; O'Brien, F. J. Advanced Strategies for Articular Cartilage Defect Repair. *Materials (Basel).* **2013**, *6* (2), 637–668. https://doi.org/10.3390/ma6020637.

(7) Abulhasan, J.; Grey, M. Anatomy and Physiology of Knee Stability. *J. Funct. Morphol. Kinesiol.* **2017**, *2* (4), 34. https://doi.org/10.3390/jfmk2040034.

(8) Souza, R. B.; Doan, R. Anatomy and Physiology of the Knee. In *ADVANCES IN MRI OF THE KNEE FOR OSTEOARTHRITIS*; Majumdar, S., Ed.; World Scientific Publishing Co. Pte. Ltd: San Francisco, 2010; pp 1–26. https://doi.org/10.1016/B978-0-323-01830-2.50077-8.

(9) Mirzayan, R. *Cartilage Injury in the Athlete.*; Gumpert, E., Ed.; Thieme Meidcal Publishers, Inc.: New York, 2006; Vol. 1.

(10) Tetteh, E. S. Basic Science and Surgical Treatment Options for Articular Cartilage Injuries of the Knee. *J. Orthop. Sports Phys. Ther.* **2012**, *42* (3), 243–253. https://doi.org/10.2519/jospt.2012.3673.

(11) Shimomura, K.; Moriguchi, Y.; Murawski, C. D.; Yoshikawa, H.; Nakamura, N. Osteochondral Tissue Engineering with Biphasic Scaffold: Current Strategies and Techniques. *Tissue Eng. Part B Rev.* **2014**, *20* (5), 468–476. https://doi.org/10.1089/ten.teb.2013.0543.

(12) Hardingham, T. E.; Fosang, A. J. Proteoglycans: Many Forms and Many Funtions. *J. Fed. Am. Soc. Exp. Biol.* **1992**, *6*, 861–870.

(13) Nukavarapu, S. P.; Dorcemus, D. L. Osteochondral Tissue Engineering: Current Strategies and Challenges. *Biotechnol. Adv.* **2013**, *31* (5), 706–721. https://doi.org/10.1016/j.biotechadv.2012.11.004.

(14) Nukavarapu, S. P.; Dorcemus, D. L. Osteochondral Tissue Engineering: Current Strategies and Challenges. *Biotechnol. Adv.* **2013**, *31* (5), 706–721. https://doi.org/10.1016/j.biotechadv.2012.11.004.

(15) Shirazi, R.; Shirazi-Adl, a. Deep Vertical Collagen Fibrils Play a Significant Role in Mechanics of Articular Cartilage. *J. Orthop. Res.* **2008**, *26* (5), 608–615. https://doi.org/10.1002/jor.20537.

(16) Khoshgoftar, M.; Wilson, W.; Ito, K.; Van Donkelaar, C. C. The Effect of Tissue-Engineered Cartilage Biomechanical and Biochemical Properties on Its Post-Implantation Mechanical Behavior. *Biomech. Model. Mechanobiol.* **2013**, *12* (1), 43–54. https://doi.org/10.1007/s10237-012-0380-0.

(17) Dubey, N.; Letourneau, P. C.; Tranquillo, R. T. Neuronal Contact Guidance in Magnetically Aligned Fibrin Gels: Effect of Variation in Gel Mechano-Structural Properties. *Biomaterials* **2001**, *22* (10), 1065–1075. https://doi.org/10.1016/S0142-9612(00)00341-0.

(18) Xie, J.; Liu, W.; Macewan, M. R.; Bridgman, P. C.; Xia, Y. Neurite Outgrowth on Electrospun Nano Fi Bers with Uniaxial Alignment : The E Ff Ects of Fiber Density , Surface Coating , and Supporting Substrate. **2015**, No. 2, 1878–1885.

(19) Sophia Fox, A. J.; Bedi, A.; Rodeo, S. a. The Basic Science of Articular Cartilage: Structure, Composition, and Function. *Sports Health* **2009**, *1* (6), 461–468. https://doi.org/10.1177/1941738109350438.

(20) Fox, A. J. S.; Bedi, A.; Rodeo, S. A. The Basic Science of Articular Cartilage: Structure, Composition, and Function. *Sports Health* **2009**, *1* (6), 461–468. https://doi.org/10.1177/1941738109350438.

(21) Knudson, W.; Knudson, C. B. Cartilage Proteoglycans. *Semin. Cell Dev. Biol.* **2001**, *12* (2), 69–78. https://doi.org/10.1006/scdb.2000.0243.

(22) Lafont, J. E. Lack of Oxygen in Articular Cartilage: Consequences for Chondrocyte Biology. *Int. J. Exp. Pathol.* **2010**, *91* (2), 99–106. https://doi.org/10.1111/j.1365-2613.2010.00707.x.

(23) Cremer, M.; Rosloniec, E.; Kang, H. The Cartilage Collagens: A Review of Their Structure, Organization, and Role in the Pathogenesis of Experimental Arthritis in Animals and in Human Rheumatic Disease. *J. Mol. Med.* **1998**, *76* (3–4), 275–288. https://doi.org/10.1007/s001090050217.

(24) Cen, L.; Liu, W. E. I.; Cui, L. E. I.; Zhang, W.; Cao, Y.; L, R. S. W.; People, S.; Tong, S. J. Collagen Tissue Engineering : Development of Novel Biomaterials. *Pediatr. Res.* **2008**, *63* (5), 492–496.

(25) Kadler, K. E.; Hill, A.; Canty-Laird, E. G. Collagen Fibrillogenesis: Fibronectin, Integrins, and Minor Collagens as Organizers and Nucleators. *Curr. Opin. Cell Biol.* **2008**, *20* (5), 495–501. https://doi.org/10.1016/j.ceb.2008.06.008.

(26) Li, F.; Liu, W. Collagen-Based Hydrogels and Applications in Regenreative Medicine. In *Handbook of Hydrogels: Properties, Preparation & Applications*; Stein, D. B., Ed.; Nova Science Publishers, Inc.: New York, 2009; pp 365–396.

(27) Mow, V. C.; Ratcliffe, A.; Poole, A. R. Cartilage and Diarthrodial Joints as Paradigms for Hierarchical Materials and Structures. *Biomaterials* **1992**, *13* (2), 67–97. https://doi.org/10.1016/0142-9612(92)90001-5.

(28) Darling, E. M.; Athanasiou, K. A. Biomechanical Strategies for Articular Cartilage Regeneration. *Ann. Biomed. Eng.* **2003**, *31* (9), 1114–1124. https://doi.org/10.1114/1.1603752.

(29) Kiani, C.; Chen, L.; Wu, Y. J.; Yee, A. J.; Yang, B. B. Structure and Function of Aggrecan. *Cell Res.* **2002**, *12* (1), 19–32. https://doi.org/10.1038/sj.cr.7290106.

(30) Carney, S.; Muir, H. The Structure and Function of Cartilage. *Physiol. Rev.* **1988**, *65* (3), 858–910. https://doi.org/vol012a11 [pii].

(31) Little, C. B.; Meeker, C. T.; Golub, S. B.; Lawlor, K. E.; Farmer, P. J.; Smith, S. M.; Fosang, A. J. Blocking Aggrecanase Cleavage in the Aggrecan Interglobular Domain Abrogates Cartilage Erosion and Promotes Cartilage Repair. *J. Clin. Invest.* **2007**, *117* (6), 1627–1636. https://doi.org/10.1172/JCI30765.

(32) Dudhia, J. Aggrecan, Aging and Assembly in Articular Cartilage. *Cell. Mol. Life Sci.* **2005**, *62* (19–20), 2241–2256. https://doi.org/10.1007/s00018-005-5217-x.

(33) Heingard, D.; Hascall, V. C. Aggregation of Cartilage Proteoglycans. *J. Biol. Chem.* **1974**, *249* (13), 4250–4256.

(34) Fraser, J. R. .; Laurent, T. C.; Laurent, U. B. . Hyaluronan: Its Nature, Distribution, Functions and Turnover. *J. Intern. Med.* **1997**, *242*, 27–33.

(35) Martel-Pelletier, J.; Boileau, C.; Pelletier, J. P.; Roughley, P. J. Cartilage in Normal and Osteoarthritis Conditions. *Best Pract. Res. Clin. Rheumatol.* **2008**, *22* (2), 351–384. https://doi.org/10.1016/j.berh.2008.02.001.

(36) Mow, V. C.; Holmes, M. H.; Lai, W. M. Fluid Transport and Mechanial Properties of Articular Cartilage: A Review. *J. Biomech.* **1984**, *17* (5), 377–394.

(37) Fosang, A. J.; Hardingham, T. E. Isolation of the N-Terminal Globular Protein Domains from Cartilage Proteoglycans. Identification of G2 Domain and Its Lack of Interaction with Hyaluronate and Link Protein. *Biochem. J.* **1989**, *261* (3), 801–809.

(38) Vertel, B. M. The Ins and Outs of Aggrecan. *Trends Cell Biol.* **1995**, *5* (12), 458–464. https://doi.org/10.1016/S0962-8924(00)89115-1.

(39) Kapoor, M.; Mahomed, N. N.; Medicine, P. *Osteoarthritis*.

(40) Dequeker, J.; Luyten, F. The History of Osteoarthritis-Osteoarthrosis. *Ann. Rheum. Dis.* **2008**, *67* (1), 5–10.

(41) Poole, A. R.; Guilak, F.; Abramson, S. B. Etiopathogenesis of Osteoarthritis. In *Osteoarthritis: Pathogenesis, Diagnosis, Available Treatments, Drug Safety, Regenerative and Precision Medicine*; 2007; pp 27–45.

(42) Tiku, M. L.; Sabaawy, H. E. Cartilage Regeneration for Treatment of Osteoarthritis: A Paradigm for Nonsurgical Intervention. *Ther. Adv. Musculoskelet. Dis.* **2015**, *7* (3), 76–87. https://doi.org/10.1177/1759720X15576866.

(43) Felson, D. T.; Gale, D. R.; Elon Gale, M.; Niu, J.; Hunter, D. J.; Goggins, J.; La Valley, M. P. Osteophytes and Progression of Knee Osteoarthritis. *Rheumatology* **2005**, *44* (1), 100–104. https://doi.org/10.1093/rheumatology/keh411.

(44) Aigner, T.; Schmitz, N. *Pathogenesis and Pathology of Osteoarthritis*, Fifth Edit.; Hochberg, M. C., Smolen, J., Silman, A., Weinblatt, M., Weisman, M., Eds.; Elsevier Inc.: Philadelphia, 2011; Vol. 5. https://doi.org/10.1159/000050478.

(45) Mathiessen, A.; Conaghan, P. G. Synovitis in Osteoarthritis: Current Understanding with Therapeutic Implications. *Arthritis Res. Ther.* **2017**, *19* (1), 1–9. https://doi.org/10.1186/s13075-017-1229-9.

(46) Zhang, W.; Ouyang, H.; Dass, C. R.; Xu, J. Current Research on Pharmacologic and Regenerative Therapies for Osteoarthritis. *Bone Res.* **2016**, *4* (December 2015). https://doi.org/10.1038/boneres.2015.40.

(47) Aigner, T.; Mckenna, L. Cellular and Molecular Life Sciences Molecular Pathology and Pathobiology of Osteoarthritic Cartilage. **2002**, *59*, 5–18.

(48) Tetlow, L. C.; Adlam, D. J.; Woolley, D. E. Matrix Metalloproteinase and Proinflammatory Cytokine Production by Chondrocytes of Human Osteoarthritic Cartilage: Associations with Degenerative Changes. *Arthritis Rheum.* **2001**, *44* (3), 585–594. https://doi.org/10.1002/1529-0131(200103)44:3<585::AID-ANR107>3.0.CO;2-C.

(49) Nagase, H.; Kashiwagi, M. Aggrecanases and Cartilage Matrix Degradation. *Arthritis Res. Ther.* **2003**, *5* (2), 94–103. https://doi.org/10.1186/ar630.

(50) Dean, D. D.; Martel-Pelletier, J.; Pelletier, J. P.; Howell, D. S.; Woessner, J. F. Evidence for Metalloproteinase Inhibitor Imbalance in Human Osteoarthritic Cartilage. *J. Clin. Invest.* **1989**, *84* (2), 678–685. https://doi.org/10.1172/JCI114215.

(51) García-Carvajal, Z.; Garciadiego-Cázares; Parra-Cid, C.; Aguilar-Gaytán, R.; Velasquillo, C.; Ibarra, C.; Carmona, J. S. C. Cartilage Tissue Engineering: The Role of Extracellular Matrix (ECM) and Novel Strategies. *Regen. Med. Tissue Eng.* **2013**, 365–398. https://doi.org/http://dx.doi.org/10.5772/55917.

(52) Bertrand, J.; Cromme, C.; Umlauf, D.; Frank, S.; Pap, T. Molecular Mechanisms of Cartilage Remodelling in Osteoarthritis. *Int. J. Biochem. Cell Biol.* **2010**, *42* (10), 1594–1601. https://doi.org/10.1016/j.biocel.2010.06.022.

(53) A.D., P.; Warren R.F. Rodeo, S. A. Basic Science of Articular Cartilage Repair. *Clin Sport. Med* **2005**, *24* (1), 1–12.

(54) Pratta, M. A.; Yao, W.; Decicco, C.; Tortorella, M. D.; Liu, R. Q.; Copeland, R. A.; Magolda, R.; Newton, R. C.; Trzaskos, J. M.; Arner, E. C. Aggrecan Protects Cartilage Collagen from Proteolytic Cleavage. *J. Biol. Chem.* **2003**, *278* (46), 439–445. https://doi.org/10.1074/jbc.M303737200.

(55) Bernhard, J. C.; Panitch, A. Synthesis and Characterization of an Aggrecan Mimic. *Acta Biomater.* **2012**, *8* (4), 1543–1550. https://doi.org/10.1016/j.actbio.2011.12.029.

(56) Han, E.; Wilensky, L. M.; Schumacher, B. L.; Chen, A. C.; Masuda, K.; Sah, R. L. Tissue Engineering by Molecular Disassembly and Reassembly: Biomimetic Retention of Mechanically Functional Aggrecan in Hydrogel. *Tissue Eng. Part C. Methods* **2010**, *16* (6), 1471–1479. https://doi.org/10.1089/ten.tec.2009.0800.

(57) Heinegard, D.; Sommarin, Y. For These Proteoglycans , Partly Due to Different Techniques Used in Their Characterization , Which for the Most Part Depends on Radiolabeled Compo- Nents . One Can Also Identify Somewhat Larger Chondroitin / Dermatan Sul- Fate Proteoglycans and Somewhat. *Methods Enzym.* **1987**, *144*, 319–372.

(58) Newman, A. P. Current Concepts Articular Cartilage Repair. **1998**, *26* (2).

(59) Hochberg, M. C.; Altman, R. D.; April, K. T.; Benkhalti, M.; Guyatt, G.; McGowan, J.; Towheed, T.; Welch, V.; Wells, G.; Tugwell, P. American College of Rheumatology 2012 Recommendations for the Use of Nonpharmacologic and Pharmacologic Therapies in Osteoarthritis of the Hand, Hip, and Knee. *Arthritis Care Res.* **2012**, *64* (4), 465–474. https://doi.org/10.1002/acr.21596.

(60) Henriksen, M.; Christensen, R.; Klokker, L.; Bartholdy, C.; Bandak, E.; Ellegaard, K.; Boesen, M. P.; Riis, R. G. C.; Bartels, E. M.; Bliddal, H. Evaluation of the Benefit of Corticosteroid Injection Before Exercise Therapy in Patients With Osteoarthritis of the Knee. *JAMA Intern. Med.* **2015**, *175* (6), 923–930. https://doi.org/10.1001/jamainternmed.2015.0461.

(61) Migliore, a.; Giovannangeli, F.; Granata, M.; Laganà, B. Hylan G-F 20: Review of Its Safety and Efficacy in the Management of Joint Pain in Osteoarthritis. *Clin. Med. Insights Arthritis Musculoskelet. Disord.* **2010**, *3*, 55–68.

(62) Cole, B. J.; Pascual-Garrido, C.; Grumet, R. C. Surgical Management of Articular Cartilage Defects in the Knee. *J. Bone Joint Surg. Am.* **2009**, *91* (7), 1778–1790. https://doi.org/10.1177/036354659602400302.

(63) Ah, G.; Farr, J.; Sd, G.; Kercher, J.; Minas, T. Instructional Course Lectures Surgical Management of Articular Cartilage Defects of the Knee. *J. Bone Jt. Surg.* **2010**, *92*, 2470–2490.

(64) Johnson, L. L. A Controlled Trial of Arthroscopic Surgery for Osteoarthritis of the Knee. *Arthroscopy* **2002**, *18* (7), 683–687. https://doi.org/10.1056/NEJMoa013259.

(65) Hangody, L.; Vásárhelyi, G.; Hangody, L. R.; Sükösd, Z.; Tibay, G.; Bartha, L.; Bodó, G. Autologous Osteochondral Grafting-Technique and Long-Term Results. *Injury* **2008**, *39* (1 SUPPL.), 32–39. https://doi.org/10.1016/j.injury.2008.01.041.

(66) Rand, J. A. Role of Arthroscopy in Osteoarthritis of the Knee. *J. Arthrosc. Relat. Surg.* **1991**, *7* (4), 358–363. https://doi.org/10.1016/0749-8063(91)90004-H.

(67) Langer, R.; Vacanti, J. P. Tissue Engineering. *Science (80-.).* **1993**, *260* (5110), 920–926. https://doi.org/10.1126/science.8493529.

(68) Jubel, A.; Andermahr, J.; Schiffer, G.; Fischer, J.; Rehm, K. E.; Stoddart, M. J.; Häuselmann, H. J. Transplantation of de Novo Scaffold-Free Cartilage Implants into Sheep Knee Chondral Defects. *Am. J. Sports Med.* **2008**, *36* (8), 1555–1564. https://doi.org/10.1177/0363546508321474.

(69) Ofek, G.; Revell, C. M.; Hu, J. C.; Allison, D. D.; Grande-Allen, K. J.; Athanasiou, K. A. Matrix Development in Self-Assembly of Articular Cartilage. *PLoS One* **2008**, *3* (7). https://doi.org/10.1371/journal.pone.0002795.

(70) Melrose, J.; Chuang, C.; Whitelock, J. Tissue Engineering of Cartilages Using Biomatricies. *J. Chem. Technol. Biotechnol.* **2008**, *83*, 444–463. https://doi.org/10.1002/jctb.

(71) Kock, L.; Van Donkelaar, C. C.; Ito, K. Tissue Engineering of Functional Articular Cartilage: The Current Status. *Cell Tissue Res.* **2012**, *347* (3), 613–627. https://doi.org/10.1007/s00441-011-1243-1.

(72) Steinert, A. F.; Ghivizzani, S. C.; Rethwilm, A.; Tuan, R. S.; Evans, C. H.; Nöth, U. Major Biological Obstacles for Persistent Cell-Based Regeneration of Articular Cartilage. *Arthritis Res. Ther.* **2007**, *9* (3), 213. https://doi.org/10.1186/ar2195.

(73) Dell'Accio, F.; De Bari, C.; Luyten, F. P. Molecular Markers Predictive of the Capacity of Expanded Human Articular Chondrocytes to Form Stable Cartilage in Vivo. *Arthritis Rheum.* **2001**, *44* (7), 1608–1619. https://doi.org/10.1002/1529-0131(200107)44:7<1608::AID-ART284>3.0.CO;2-T.

(74) Pittenger, M. F.; Mackay, A. M.; Beck, S. C.; Jaiswal, R. K.; Douglas, R.; Mosca, J. D.; Moorman, M. A.; Simonetti, D. W.; Craig, S.; Marshak, D. R. Multilineage Potential of Adult Human Mesenchymal Stem Cells. *Science* **1999**, *284* (5411), 143–147. https://doi.org/10.1126/science.284.5411.143.

(75) Awad, H. A.; Wickham, M. Q.; Leddy, H. A.; Gimble, J. M.; Guilak, F. Chondrogenic Differentiation of Adipose-Derived Adult Stem Cells in Agarose, Alginate, and Gelatin Scaffolds. *Biomaterials* **2004**, *25* (16), 3211–3222. https://doi.org/10.1016/j.biomaterials.2003.10.045.

(76) Yoshimura, H.; Muneta, T.; Nimura, A.; Yokoyama, A.; Koga, H.; Sekiya, I. Comparison of Rat Mesenchymal Stem Cells Derived from Bone Marrow, Synovium, Periosteum, Adipose Tissue, and Muscle. *Cell Tissue Res.* **2007**, *327* (3), 449–462. https://doi.org/10.1007/s00441-006-0308-z.

(77) Sakaguchi, Y.; Sekiya, I.; Yagishita, K.; Muneta, T. Comparison of Human Stem Cells Derived from Various Mesenchymal Tissues: Superiority of Synovium as a Cell Source. *Arthritis Rheum.* **2005**, *52* (8), 2521–2529. https://doi.org/10.1002/art.21212.

(78) Solchaga, L. a; Yoo, J. U.; Lundberg, M.; Dennis, J. E.; Huibregtse, B. a; Goldberg, V. M.; Caplan, a I. Hyaluronan-Based Polymers in the Treatment of Osteochondral Defects. *J. Orthop. Res.* **2000**, *18* (5), 773–780. https://doi.org/10.1002/jor.1100180515.

(79) Koga, H.; Muneta, T.; Nagase, T.; Nimura, A.; Ju, Y.-J.; Mochizuki, T.; Sekiya, I. Comparison of Mesenchymal Tissues-Derived Stem Cells for in Vivo Chondrogenesis: Suitable Conditions for Cell Therapy of Cartilage Defects in Rabbit. *Cell Tissue Res.* **2008**, *333* (2), 207–215. https://doi.org/10.1007/s00441-008-0633-5.

(80) Burdick, J. a; Vunjak-Novakovic, G. Engineered Microenvironments for Controlled Stem Cell Differentiation. *Tissue Eng. Part A* **2009**, *15* (2), 205–219. https://doi.org/10.1089/ten.tea.2008.0131.

(81) Higuchi, A.; Ling, Q. D.; Chang, Y.; Hsu, S. T.; Umezawa, A. Physical Cues of Biomaterials Guide Stem Cell Differentiation Fate. *Chem. Rev.* **2013**, *113* (5), 3297–3328. https://doi.org/10.1021/cr300426x.

(82) Pittenger, M. F.; Mackay, a M.; Beck, S. C.; Jaiswal, R. K.; Douglas, R.; Mosca, J. D.; Moorman, M. a; Simonetti, D. W.; Craig, S.; Marshak, D. R. Multilineage Potential of Adult Human Mesenchymal Stem Cells. *Science* **1999**, *284* (5411), 143–147. https://doi.org/10.1126/science.284.5411.143.

(83) Alberti, K.; Davey, R. E.; Onishi, K.; George, S.; Salchert, K.; Seib, F. P.; Bornhäuser, M.; Pompe, T.; Nagy, A.; Werner, C.; et al. Functional Immobilization of Signaling Proteins Enables Control of Stem Cell Fate. *Nat. Methods* **2008**, *5* (7), 645–650. https://doi.org/10.1038/nmeth.1222.

(84) Schugar, R. C.; Robbins, P. D.; Deasy, B. M. Small Molecules in Stem Cell Self-Renewal and Differentiation. *Gene Ther.* **2008**, *15* (2), 126–135. https://doi.org/10.1038/sj.gt.3303062.

(85) Ding, S.; Schultz, P. G. A Role for Chemistry in Stem Cell Biology. *Nat. Biotechnol.* **2004**, *22* (7), 833–840. https://doi.org/10.1038/nbt987.

(86) Wescoe, K. E.; Schugar, R. C.; Chu, C. R.; Deasy, B. M. The Role of the Biochemical and Biophysical Environment in Chondrogenic Stem Cell Differentiation Assays and Cartilage Tissue Engineering. *Cell Biochem. Biophys.* **2008**, *52* (2), 85–102. https://doi.org/10.1007/s12013-008-9029-0.

(87) Demoor, M.; Ollitrault, D.; Gomez-Leduc, T.; Bouyoucef, M.; Hervieu, M.; Fabre, H.; Lafont, J.; Denoix, J. M.; Audigié, F.; Mallein-Gerin, F.; et al. Cartilage Tissue Engineering: Molecular Control of Chondrocyte Differentiation for Proper Cartilage Matrix Reconstruction. *Biochim. Biophys. Acta - Gen. Subj.* **2014**, *1840* (8), 2414–2440. https://doi.org/10.1016/j.bbagen.2014.02.030.

(88) Discher, D. E.; Mooney, D. J.; Zandstra, P. W. Growth Factors. Matrices, and Forces Combine and Control Stem Cells. *Science (80-.).* **2009**, *324* (5935), 1673–1677. https://doi.org/10.1126/science.1171643.Growth.

(89) Grimaud, E.; Heymann, D.; Rédini, F. Recent Advances in TGF-Beta Effects on Chondrocyte Metabolism. Potential Therapeutic Roles of TGF-Beta in Cartilage Disorders. *Cytokine Growth Factor Rev.* **2002**, *13* (3), 241–257.

(90) Ducy, P.; Karsenty, G. The Family of Bone Morphogenetic Proteins. *Kidney Int.* **2000**, *57* (6), 2207–2214. https://doi.org/10.1046/j.1523-1755.2000.00081.x.

(91) Kwon, S.-H.; Lee, T.-J.; Park, J.; Hwang, J.-E.; Jin, M.; Jang, H.; Hwang, N. S.; Kim, B.-S. Modulation of BMP-2-Induced Chondrogenic versus Osteogenic Differentiation of Human Mesenchymal Stem Cells by Cell-Specific Extracellular Matrices. *Tissue Eng. Part A* **2012**, *19*, 121022130818004. https://doi.org/10.1089/ten.TEA.2012.0245.

(92) Yang, H. S.; La, W.-G.; Bhang, S. H.; Kim, H.-J.; Im, G.-I.; Lee, H.; Park, J.-H.; Kim, B.-S. Hyaline Cartilage Regeneration by Combined Therapy of Microfracture and Long-Term Bone Morphogenetic Protein-2 Delivery. *Tissue Eng. Part A* **2011**, *17* (13–14), 1809–1818. https://doi.org/10.1089/ten.tea.2010.0540.

(93) Sellers, R. S.; Peluso, D.; Morris, E. a. The Effect of Recombinant Human Bone Morphogenetic Protein-2 (RhBMP-2) on the Healing of Full-Thickness Defects of Articular Cartilage. *J. Bone Joint Surg. Am.* **1997**, *79* (10), 1452–1463.

(94) Hutmacher, D. W. Scaffolds in Tissue Engineering Bone and Cartilage. *Biomaterials* **2000**, *21* (24), 2529–2543. https://doi.org/10.1016/S0142-9612(00)00121-6.

(95) Chen, G., Ushida, T., & Tateishi, T. Scaffold Design for Tissue Engineering. *Macromol. Biosci.* **2002**, *2* (2), 67–77.

(96) Spiller, K. L.; Maher, S. A.; Lowman, A. M. Hydrogels for the Repair of Articular Cartilage Defects. *Tissue Eng. Part B Rev.* **2011**, *17* (4), 281–299. https://doi.org/10.1089/ten.teb.2011.0077.

(97) Zhu, S.; Yuan, Q.; Yin, T.; You, J.; Gu, Z.; Xiong, S.; Hu, Y. Self-Assembly of Collagen-Based Biomaterials: Preparation, Characterizations and Biomedical Applications. *J. Mater. Chem. B* **2018**, *6* (18), 2650–2676. https://doi.org/10.1039/c7tb02999c.

(98) Chajra, H.; Rousseau, C. F.; Cortial, D.; Ronzière, M. C.; Herbage, D.; Mallein-Gerin, F.; Freyria, a M. Collagen-Based Biomaterials and Cartilage Engineering. Application to Osteochondral Defects. *Biomed. Mater. Eng.* **2008**, *18* (1 Suppl), S33-45.

(99) Albrecht, C.; Tichy, B.; Nürnberger, S.; Hosiner, S.; Zak, L.; Aldrian, S.; Marlovits, S. Gene Expression and Cell Differentiation in Matrix-Associated Chondrocyte Transplantation Grafts: A Comparative Study. *Osteoarthr. Cartil.* **2011**, *19* (10), 1219–1227. https://doi.org/10.1016/j.joca.2011.07.004.

(100) Zak, L.; Albrecht, C.; Wondrasch, B.; Widhalm, H.; Vekszler, G.; Trattnig, S.; Marlovits, S.; Aldrian, S. Results 2 Years after Matrix-Associated Autologous Chondrocyte Transplantation Using the Novocart 3D Scaffold: An Analysis of Clinical and Radiological Data. *Am. J. Sports Med.* **2014**, *42* (7), 1618–1627. https://doi.org/10.1177/0363546514532337.

(101) Roessler, P. P.; Pfister, B.; Gesslein, M.; Figiel, J.; Heyse, T. J.; Colcuc, C.; Lorbach, O.; Efe, T.; Schüttler, K. F. Short-Term Follow up after Implantation of a Cell-Free Collagen Type I Matrix for the Treatment of Large Cartilage Defects of the Knee. *Int. Orthop.* **2015**, *39* (12), 2473–2479. https://doi.org/10.1007/s00264-015-2695-9.

(102) Mizuno, M.; Fujisawa, R.; Kuboki, Y. Type I Collagen-Induced Osteoblastic Differentiation of Bone-Marrow Cells Mediated by Collagen- Alpha2beta1. *J. Cell. Physiol.* **2000**, *213* (July 1999), 207–213. https://doi.org/10.1002/1097-4652(200008)184:2<207::AID-JCP8>3.0.CO;2-U.

(103) Bai, X.; Gao, M.; Syed, S.; Zhuang, J.; Xu, X.; Zhang, X. Bioactive Materials Bioactive Hydrogels for Bone Regeneration. *Bioact. Mater.* **2018**, *3* (4), 401–417. https://doi.org/10.1016/j.bioactmat.2018.05.006.

(104) Ochi, M.; Uchio, Y.; Kawasaki, K.; Wakitani, S.; Iwasa, J. Transplantation of Cartilage-like Tissue Made by Tissue Engineering in the Treatment of Cartilage Defects of the Knee. *J. Bone Jt. Surg.* **2002**, *84* (4), 571–578. https://doi.org/10.1302/0301-620X.84B4.0840571.

(105) Andereya, S.; Maus, U.; Gavenis, K.; Muller-Rath, R.; Miltner, O.; Mumme, T. First Clinical Experiences with a Novel 3D-Collagen Gel (CaRes(R)) for the Treatment of Focal Cartilage Defects in the Knee. *Z Orthrop Ihre Grenzgev* **2006**, *144*, 272–280. https://doi.org/10.1055/s-2006-933445.

(106) Wakitani, S.; Imoto, K.; Yamamoto, T.; Saito, M.; Murata, N.; Yoneda, M. Human Autologous Culture Expanded Bone Marrow-Mesenchymal Cell Transplantation for Repair of Cartilage Defects in Osteoarthritic Knees. *Osteoarthr. Cartil.* **2002**, *10* (3), 199–206. https://doi.org/10.1053/joca.2001.0504.

(107) Wakitani, S.; Goto, T.; Pineda, S. J.; Young, R. G.; Mansour, J. M.; Caplan, A. I.; Goldberg, V. M. Mesenchymal Cell-Based Repair of Large, Full-Thickness Defects of Articular Cartilage. *J. Bone Jt. Surg.* **1994**, No. 4. https://doi.org/10.2106/00004623-199404000-00013.

(108) Eyre, D. R.; Muir, H. Quantitative Analysis of Types I and II Collagens in Human Intervertebral Discs at Various Ages. *Biochim. Biophys. Act* **1977**, *492*, 29–42. https://doi.org/10.1016/0005-2795(77)90211-2.

(109) Fox, A. J. S.; Bedi, A.; Rodeo, S. A. The Basic Science of Human Knee Menisci. *Sport. Heal. A Multidiscip. Approach* **2012**, *4* (4), 340–351. https://doi.org/10.1177/1941738111429419.

(110) Bosnakovski, D.; Mizuno, M.; Kim, G. Chondrogenic Differentiation of Bovine Bone Marrow Mesenchymal Stem Cells (MSCs) in Different Hydrogels: Influence of Collagen Type II Extracellular Matrix on MSC Chondrogenesis. *Biotechnol. Bioeng.* **2006**, *93* (6), 1152–1163. https://doi.org/10.1002/bit.

(111) Lu, Z.; Doulabi, B. Z.; Huang, C.; Bank, R. a; Helder, M. N. Collagen Type II Enhances Chondrogenesis in Adipose Tissue-Derived Stem Cells by Affecting Cell Shape. *Tissue Eng. Part A* **2010**, *16* (1), 81–90. https://doi.org/10.1089/ten.TEA.2009.0222.

(112) Bajtner, E.; Nandakumar, K. S.; Engström, A.; Holmdahl, R. Chronic Development of Collagen-Induced Arthritis Is Associated with Arthritogenic Antibodies against Specific Epitopes on Type II Collagen. *Arthritis Res. Ther.* **2005**, *7* (5), R1148-57. https://doi.org/10.1186/ar1800.

(113) Freyria, A.-M.; Ronzière, M.-C.; Cortial, D.; Galois, L.; Hartmann, D.; Herbage, D.; Mallein-Gerin, F. Comparative Phenotypic Analysis of Articular Chondrocytes Cultured within Type I or Type II Collagen Scaffolds. *Tissue Eng. Part A* **2009**, *15* (6), 1233–1245. https://doi.org/10.1089/ten.tea.2008.0114.

(114) Farjanel, J.; Schürmann, G.; Bruckner, P. Contacts with Fibrils Containing Collagen I, but Not Collagens II, IX, and XI, Can Destabilize the Cartilage Phenotype of Chondrocytes. *Osteoarthr. Cartil.* **2001**, *9* (SUPPL. A). https://doi.org/10.1053/joca.2001.0445.

(115) Calderon, L.; Collin, E.; Velasco-Bayon, D.; Murphy, M.; O'Halloran, D.; Pandit, A. Type II Collagen-Hyaluronan Hydrogel--a Step towards a Scaffold for Intervertebral Disc Tissue Engineering. *Eur. Cell. Mater.* **2010**, *20*, 134–148. https://doi.org/vol020a12 [pii].

(116) Birk, D. E.; Silver, F. H. Collagen Fibrillogenesis in Vitro: Comparison of Types I, II, and III. *Arch. Biochem. Biophys.* **1984**, *235* (1), 178–185. https://doi.org/10.1016/0003-9861(84)90266-2.

(117) Dong, M.; Xu, S.; Bünger, M. H.; Birkedal, H.; Besenbacher, F. Temporal Assembly of Collagen Type II Studied by Atomic Force Microscopy. *Adv. Eng. Mater.* **2007**, *9* (12), 1129–1133. https://doi.org/10.1002/adem.200700220.

(118) Lazarini, M.; Bordeaux-Rego, P.; Giardini-Rosa, R.; Duarte, A. S. S.; Baratti, M. O.; Zorzi, A. R.; de Miranda, J. B.; Lenz Cesar, C.; Luzo, Â.; Olalla Saad, S. T. Natural Type II Collagen Hydrogel, Fibrin Sealant, and Adipose-Derived Stem Cells as a Promising Combination for Articular Cartilage Repair. *Cartilage* **2017**, *8* (4), 439–443. https://doi.org/10.1177/1947603516675914.

(119) Nehrer, S.; Breinan, H. a.; Ramappa, A.; Young, G.; Shortkroff, S.; Louie, L. K.; Sledge, C. B.; Yannas, I. V.; Spector, M. Matrix Collagen Type and Pore Size Influence Behaviour of Seeded Canine Chondrocytes. *Biomaterials* **1997**, *18* (11), 769–776. https://doi.org/10.1016/S0142-9612(97)00001-X.

(120) Levingstone, T. J.; Matsiko, A.; Dickson, G. R.; O'Brien, F. J.; Gleeson, J. P. A Biomimetic Multi-Layered Collagen-Based Scaffold for Osteochondral Repair. *Acta Biomater.* **2014**, *10* (5), 1996–2004. https://doi.org/10.1016/j.actbio.2014.01.005.

(121) Buma, P.; Pieper, J. S.; Van Tienen, T.; Van Susante, J. L. C.; Van Der Kraan, P. M.; Veerkamp, J. H.; Van Den Berg, W. B.; Veth, R. P. H.; Van Kuppevelt, T. H. Cross-Linked Type I and Type II Collagenous Matrices for the Repair of Full-Thickness Articular Cartilage Defects - A Study in Rabbits. *Biomaterials* **2003**, *24* (19), 3255–3263. https://doi.org/10.1016/S0142-9612(03)00143-1.

(122) Lee, C. R.; Grodzinsky, a. J.; Hsu, H. P.; Spector, M. Effects of a Cultured Autologous Chondrocyte-Seeded Type II Collagen Scaffold on the Healing of a Chondral Defect in a Canine Model. *J. Orthop. Res.* **2003**, *21* (2), 272–281. https://doi.org/10.1016/S0736-0266(02)00153-5.

(123) Pieper, J. S.; Van Der Kraan, P. M.; Hafmans, T.; Kamp, J.; Buma, P.; Van Susante, J. L. C.; Van Den Berg, W. B.; Veerkamp, J. H.; Van Kuppevelt, T. H. Crosslinked Type II Collagen Matrices: Preparation, Characterization, and Potential for Cartilage Engineering. *Biomaterials* **2002**, *23* (15), 3183–3192. https://doi.org/10.1016/S0142-9612(02)00067-4.

(124) Choi, B.; Kim, S.; Lin, B.; Wu, B. M.; Lee, M. Cartilaginous Extracellular Matrix-Modified Chitosan Hydrogels for Cartilage Tissue Engineering. *ACS Appl. Mater. Interfaces* **2014**, *6* (22), 20110–20121. https://doi.org/10.1021/am505723k.

(125) Yang, K.; Sun, J.; Wei, D.; Yuan, L.; Yang, J.; Guo, L.; Fan, H.; Zhang, X. Photo-Crosslinked Mono-Component Type II Collagen Hydrogel as a Matrix to Induce Chondrogenic Differentiation of Bone Marrow Mesenchymal Stem Cells. *J. Mater. Chem. B* **2017**, *5* (44), 8707–8718. https://doi.org/10.1039/c7tb02348k.

(126) Vickers, S. M.; Squitieri, L. E. E. S.; Spector, M. Effects of Cross-Linking Type II Collagen-GAG Scaffolds on Chondrogenesis in Vitro: Dynamic Porte Reduciton Promotes Cartilage Formation. *Tissue Eng.* **2006**, *12* (5). https://doi.org/10.1089/ten.2006.12.1345.

(127) Pulkkinen, H. J.; Tiitu, V.; Valonen, P.; Jurvelin, J. S.; Rieppo, L.; Toyras, J.; Silvast, T. S.; Lammi, M. J.; Kiviranta, I. Repair of Osteochondral Defects with Recombinant Human Type II Collagen Gel and Autologous Chondrocytes in Rabbit. *Osteoarthr. Cartil.* **2013**, *21* (3), 481–490. https://doi.org/10.1016/j.joca.2012.12.004.

(128) Muhonen, V.; Narcisi, R.; Nystedt, J.; Korhonen, M.; van Osch, G. J. V. M.; Kiviranta, I. Recombinant Human Type II Collagen Hydrogel Provides a Xeno-Free 3D Micro-Environment for Chondrogenesis of Human Bone Marrow-Derived Mesenchymal Stromal Cells. *J. Tissue Eng. Regen. Med.* **2017**, *11* (3), 843–854. https://doi.org/10.1002/term.1983.

(129) Báez, J.; Olsen, D.; Polarek, J. W. Recombinant Microbial Systems for the Production of Human Collagen and Gelatin. *Appl. Microbiol. Biotechnol.* **2005**, *69* (3), 245–252. https://doi.org/10.1007/s00253-005-0180-x.

(130) Kontturi, L. S.; Järvinen, E.; Muhonen, V.; Collin, E. C.; Pandit, A. S.; Kiviranta, I.; Yliperttula, M.; Urtti, A. An Injectable, in Situ Forming Type II Collagen/Hyaluronic Acid Hydrogel Vehicle for Chondrocyte Delivery in Cartilage Tissue Engineering. *Drug Deliv. Transl. Res.* **2014**, *4* (2), 149–158. https://doi.org/10.1007/s13346-013-0188-1.

(131) Funayama, A.; Niki, Y.; Matsumoto, H.; Maeno, S.; Yatabe, T.; Morioka, H.; Yanagimoto, S.; Taguchi, T.; Tanaka, J.; Toyama, Y. Repair of Full-Thickness Articular Cartilage Defects Using Injectable Type II Collagen Gel Embedded with Cultured Chondrocytes in a Rabbit Model. *J. Orthop. Sci.* **2008**, *13* (3), 225–232. https://doi.org/10.1007/s00776-008-1220-z.

(132) Lee, C. R.; Grodzinsky, A. J.; Spector, M. The Effects of Cross-Linking of Collagen-Glycosaminoglycan Scaffolds on Compressive Stiffness, Chondrocyte-Mediated Contraction, Proliferation and Biosynthesis. *Life Sci.* **2001**, *22* (23), 3145–3154.

(133) Almeida, H. V.; Sathy, B. N.; Dudurych, I.; Buckley, C. T.; O'Brien, F. J.; Kelly, D. J. Anisotropic Shape-Memory Alginate Scaffolds Functionalized with Either Type I or Type II Collagen for Cartilage Tissue Engineering. *Tissue Eng. Part A* **2017**, *23* (1–2), 55–68. https://doi.org/10.1089/ten.tea.2016.0055.

(134) Ragetly, G.; Griffon, D. J.; Chung, Y. S. The Effect of Type II Collagen Coating of Chitosan Fibrous Scaffolds on Mesenchymal Stem Cell Adhesion and Chondrogenesis. *Acta Biomater.* **2010**, *6* (10), 3988–3997. https://doi.org/10.1016/j.actbio.2010.05.016.

(135) Yuan, L.; Li, B.; Yang, J.; Ni, Y.; Teng, Y.; Guo, L.; Fan, H.; Fan, Y.; Zhang, X. Effects of Composition and Mechanical Property of Injectable Collagen I/II Composite Hydrogels on Chondrocyte Behaviors. *Tissue Eng. Part A* **2016**, *22* (11–12), 899–906. https://doi.org/10.1089/ten.tea.2015.0513.

(136) Mueller, S. M.; Shortkroff, S.; Schneider, T. O.; Breinan, H. A.; Yannas, I. V.; Spector, M. Meniscus Cells Seeded in Type I and Type II Collage-GAG Matricies in Vitro. *J Biomed Mater Res* **1997**, *38*, 95–104. https://doi.org/DOI: 10.1016/S0142-9612(98)00189-6.

(137) Lee, C. R.; Grodzinsky, A. J.; Spector, M. Biosynthetic Response of Passaged Chondrocytes in a Type II Collagen Scaffold to Mechanical Compression. *J. Biomed. Mater. Res. - Part A* **2003**, *64* (3), 560–569. https://doi.org/10.1002/jbm.a.10443.

(138) Enea, D.; Guerra, D.; Roggiani, J.; Cecconi, S.; Manzotti, S.; Quaglino, D.; Pasquali-Ronchetti, I.; Gigante, A. Mixed Type I and Type II Collagen Scaffold for Cartilage Repair: Ultrastructural Study of Synovial Membrane Response and Healing Potential *versus* Microfractures (A Pilot Study). *Int. J. Immunopathol. Pharmacol.* **2013**, *26* (4), 917–930. https://doi.org/10.1177/039463201302600410.

(139) Wang, K. H.; Wan, R.; Chiu, L. H.; Tsai, Y. H.; Fang, C. L.; Bowley, J. F.; Chen, K. C.; Shih, H. N.; Lai, W. F. T. Effects of Collagen Matrix and Bioreactor Cultivation on Cartilage Regeneration of a Full-Thickness Critical-Size Knee Joint Cartilage Defects with Subchondral Bone Damage in a Rabbit Model. *PLoS One* **2018**, *13* (5), 1–15. https://doi.org/10.1371/journal.pone.0196779.

(140) Jerosch, J. Effects of Glucosamine and Chondroitin Sulfate on Cartilage Metabolism in OA: Outlook on Other Nutrient Partners Especially Omega-3 Fatty Acids. *Int. J. Rheumatol.* **2011**, *2011*. https://doi.org/10.1155/2011/969012.

(141) Martel-Pelletier, J.; Tat, S. K.; Pelletier, J. P. Effects of Chondroitin Sulfate in the Pathophysiology of the Osteoarthritic Joint : A Narrative Review. *Osteoarthr. Cartil.* **2010**, *18*, S7–S11. https://doi.org/10.1016/j.joca.2010.01.015.

(142) David-Raoudi, M.; Deschrevel, B.; Leclercq, S.; Gaĺera, P.; Boumediene, K.; Pujol, J. P. Chondroitin Sulfate Increases Hyaluronan Production by Human Synoviocytes through Differential Regulation of Hyaluronan Synthases: Role of P38 and Akt. *Arthritis Rheum.* **2009**, *60* (3), 760–770. https://doi.org/10.1002/art.24302.

(143) Kim, H. D.; Heo, J.; Hwang, Y.; Kwak, S.; Park, O. K.; Kim, H.; Varghese, S.; Hwang, N. S.; Al, K. I. M. E. T. Photopolymerizing Hydrogels for Cartilage Tissue Engineering. *Tissue Eng Part A* **2015**, *21*, 757–766. https://doi.org/10.1089/ten.tea.2014.0233.

(144) Han, M.; Kim, S.; Kim, H. D.; Yim, H.; Bencherif, S. A.; Kim, T.; Hwang, N. S. Extracellular Matrix-Based Cryogels for Cartilage Tissue Engineering. *Int. J. Biol. Macromol.* **2016**, *93*, 1410–1419. https://doi.org/10.1016/j.ijbiomac.2016.05.024.

(145) Paderi, J. E.; Panitch, A. Design of a Synthetic Collagen-Binding Peptidoglycan That Modulates Collagen Fibrillogenesis. *Biomacromolecules* **2008**, *9* (9), 2562–2566. https://doi.org/10.1021/bm8006852.

(146) Paderi, J. E.; Stuart, K.; Sturek, M.; Park, K.; Panitch, A. The Inhibition of Platelet Adhesion and Activation on Collagen during Balloon Angioplasty by Collagen-Binding Peptidoglycans. *Biomaterials* **2011**, *32* (10), 2516–2523. https://doi.org/10.1016/j.biomaterials.2010.12.025.

(147) Stuart, K.; Paderi, J.; Snyder, P. W.; Freeman, L.; Panitch, A. Collagen-Binding Peptidoglycans Inhibit MMP Mediated Collagen Degradation and Reduce Dermal Scarring. *PLoS One* **2011**, *6* (7). https://doi.org/10.1371/journal.pone.0022139.

(148) Scott, R. a.; Paderi, J. E.; Sturek, M.; Panitch, A. Decorin Mimic Inhibits Vascular Smooth Muscle Proliferation and Migration. *PLoS One* **2013**, *8* (11), 1–12. https://doi.org/10.1371/journal.pone.0082456.

(149) Ahern, B. J.; Parvizi, J.; Boston, R.; Schaer, T. P. Preclinical Animal Models in Single Site Cartilage Defect Testing: A Systematic Review. *Osteoarthr. Cartil.* **2009**, *17* (6), 705–713. https://doi.org/10.1016/j.joca.2008.11.008.

(150) Goebel, L.; Müller, A.; Bücker, A.; Madry, H. High Resolution MRI Imaging at 9 . 4 Tesla of the Osteochondral Unit in a Translational Model of Articular Cartilage Repair. **2015**, 1–12. https://doi.org/10.1186/s12891-015-0543-0.

(151) Goebel, L.; Gao, L. Cartilage. **2017**, No. May. https://doi.org/10.1007/978-3-319-53316-2.

(152) Orth, P.; Duffner, J.; Zurakowski, D. Small-Diameter Awls Improve Articular Cartilage Repair After Microfracture Treatment in a Translational Animal Model. 209–219. https://doi.org/10.1177/0363546515610507.

(153) Xing, D.; Chen, J.; Yang, J.; Heng, B. C.; Ge, Z.; Lin, J. Perspectives on Animal Models Utilized for the Research and Development of Regenerative Therapies for Articular Cartilage. *Curr. Mol. Biol. Reports* **2016**, *2* (2), 90–100. https://doi.org/10.1007/s40610-016-0038-2.

(154) Ahern, B. J.; Parvizi, J.; Boston, R.; Schaer, T. P. Preclinical Animal Models in Single Site Cartilage Defect Testing: A Systematic Review. *Osteoarthr. Cartil.* **2009**, *17* (6), 705–713. https://doi.org/10.1016/j.joca.2008.11.008.

(155) Osterhoff, G.; Löf, S.; Steinke, H.; Feja, C.; Josten, C.; Hepp, P. The Knee Comparative Anatomical Measurements of Osseous Structures in the Ovine and Human Knee. **2011**, *18*, 98–103. https://doi.org/10.1016/j.knee.2010.02.001.

(156) An, Y. H.; Friedman, R. J. *Animal Models in Orthopaedic Research*; An, Y. H., Friedman, R. J., Eds.; CRC Press: Boca Raton, 1998.

(157) Chu, C. R.; Coutts, R. D.; Yoshioka, M.; Harwood, F. L.; Monosov, A. Z.; Amiel, D. Articular Cartilage Repair Using Allogeneic Perichondrocyte- Seeded Biodegradable Porous Polylactic Acid (PLA): A Tissue-Engineering Study ". **1995**, *29*, 1147–1154.

(158) Furukawa, B. Y. T. Biochemical Studies on Repair Cartilage Resurfacing Experimental Defects in the Rabbit Knee. *J. Bone Joing Surg.* **1980**, *62* (1).

(159) Im, G. I.; Kim, D. Y.; Shin, J. H.; Hyun, C. W.; Cho, W. H. Repair of Cartilage Defect in the Rabbit with Cultured Mesenchymal Stem Cells from Bone Marrow. *J. Bone Joint Surg. Br.* **2001**, *83* (2), 289–294. https://doi.org/10.1302/0301-620X.83B2.10495.

(160) Kawamura, S.; Wakitani, S. Articular Cartilage Repair: Rabbit Experiments with a Collagen Gel-Biomatrix and Chondrocytes Cultured in It. *Acta Orthop. Scand.* **1998**, No. August 2014. https://doi.org/10.3109/17453679809002358.

(161) Shapiro, F.; Koide, S.; Glimcher, M. Cell Origin and Differentiation in the Repair of Full-Thickness Defects of Articular Cartilage. *J. Bone Joi* **1993**, 532–553.

(162) Wakitani, S.; Goto, T.; Pineda, S. J.; Young, R. G.; Mansour, J. M.; Caplan, a I.; Goldberg, V. M. Mesenchymal Cell-Based Repair of Large, Full-Thickness Defects of Articular Cartilage. *J. Bone Joint Surg. Am.* **1994**, *76* (4), 579–592.

(163) Tamai, N.; Myoui, A.; Hirao, M.; Kaito, T.; Ochi, T. A New Biotechnology for Articular Cartilage Repair : Subchondral Implantation of a Composite of Interconnected Porous Hydroxyapatite , Synthetic Polymer (PLA-PEG), and Bone Morphogenetic Protein-2 (RhBMP-2). *Osteoarthr. Cartil.* **2005**. https://doi.org/10.1016/j.joca.2004.12.014.

(164) Trzeciak, T.; Kruczynski, J.; Jaroszewski, J.; Lubiatowski, P. Evaluation of Cartilage Reconstruction by Means of Autologous Chondrocyte Versus Periosteal Graft Transplantation : An Animal Study. *Transplant. Proc.* **2005**, No. 135, 305–311. https://doi.org/10.1016/j.transproceed.2005.12.028.

(165) Wei, X.; Gao, J.; Messner, K. Maturation-Dependent Repair of Untreated Osteochondral Defects in the Rabbit Knee Joint. **1997**, *34*, 63–72.

(166) Dell'Accio, F.; Vanlauwe, J.; Bellemans, J.; Neys, J.; Bari, C. De; Luyten, F. P. Expanded Phenotypically Stable Chondrocytes Persist in the Repair Tissue and Contribute to Cartilage Matrix Formation and Structural Integration in a Goat Model of Autologous Chondrocyte Implantation. **2003**, *21*, 123–131.

(167) Im, G. I.; Kim, D. Y.; Shin, J. H.; Hyun, C. W.; Cho, W. H. Repair of Cartilage Defect in the Rabbit with Cultured Mesenchymal Stem Cells from Bone Marrow. *J. Bone Jt. Surg.* **2001**, *83* (2), 289–294. https://doi.org/10.1302/0301-620X.83B2.10495.

(168) Rahman, R. A.; Radzi, M. A. A.; Sukri, N. M.; Nazir, N. M.; Sha'ban, M. Tissue Engineering of Articular Cartilage: From Bench to Bed-Side. *Tissue Eng. Regen. Med.* **2014**, *12* (1), 1–11. https://doi.org/10.1007/s13770-014-9044-8.

(169) Mafi, P.; Hindocha, S.; Mafi, R.; S. Khan, W. Evaluation of Biological Protein-Based Collagen Scaffolds in Cartilage and Musculoskeletal Tissue Engineering- A Systematic Review of the Literature. *Curr. Stem Cell Res. Ther.* **2012**, *7* (4), 302–309. https://doi.org/10.2174/157488812800793045.

(170) Basu, J.; Ludlow, J. W. Tissue Engineered and Regenerative Medicine Products; Woodhead Publishing Limited: Philadelphia, 2012; pp 23–24.

(171) Mafi, P.; Hindocha, S.; Mafi, R.; Khan, W. S. Evaluation of Biological Protein-Based Collagen Scaffolds in Cartilage and Musculoskeletal Tissue Engineering- A Systematic Review of the Literature. *Curr. Stem Cell Res. Ther.* **2012**, *7* (4), 302–309. https://doi.org/10.2174/157488812800793045.

(172) Lu, Z.; Doulabi, B. Z.; Huang, C.; Bank, R. a; Helder, M. N. Collagen Type II Enhances Chondrogenesis in Adipose Tissue-Derived Stem Cells by Affecting Cell Shape. *Tissue Eng. Part A* **2010**, *16* (1), 81–90. https://doi.org/10.1089/ten.tea.2009.0222.

(173) Bosnakovski, D.; Mizuno, M.; Kim, G.; Takagi, S.; Okumura, M.; Fujin. Chondrogenic Differentiation of Bovine Bone Marrow Mesenchymal Stem Cells (MSCs) in Different Hydrogels: Nfluence of Collagen Type II Extracellular Matrix on MSC Chondrogenesis. *Biotechnol. Bioeng.* **2006**, *93* (6), 1152–1163. https://doi.org/10.1002/bit.

(174) McBeath, R.; Pirone, D. M.; Nelson, C. M.; Bhadriraju, K.; Chen, C. S. Cell Shape, Cytoskeletal Tension, and RhoA Regulate Stem Cell Lineage Commitment. *Dev. Cell* **2004**, *6* (4), 483–495. https://doi.org/10.1016/S1534-5807(04)00075-9.

(175) Akkiraju, H.; Nohe, A. Role of Chondrocytes in Cartilage Formation, Progression of Osteoarthritis and Cartilage Regeneration. *J. Dev. Biol.* **2015**, *3* (4), 177–192. https://doi.org/10.3390/jdb3040177.

(176) Kuhn, K. The Classical Collagens: Types I,II, and II. In *Structure and function of collagen types*; 1987; pp 1–37.

(177) Wess, T. Collagen Fibril Form and Function. *Adv. Protein Chem.* **2005**, *70* (04), 341–374. https://doi.org/10.1016/S0065-3233(04)70010-8.

(178) Calderon, L.; Collin, E.; Velasco-Bayon, D.; Murphy, M.; O'Halloran, D.; Pandit, A. Type II Collagen-Hyaluronan Hydrogel: A Step towards a Scaffold for Intervertebral Disc Tissue Engineering. *Eur. Cell. Mater.* **2010**, *20*, 134–148. https://doi.org/vol020a12 [pii].

(179) Stuart, K.; Panitch, A. Characterization of Gels Composed of Blends of Collagen l, Collagen III, and Chondroitin Sulfate. *Biomacromolecules* **2009**, *10* (1), 25–31. https://doi.org/10.1021/bm800888u.

(180) Stuart, K.; Panitch, A. Influence of Chondroitin Sulfate on Collagen Gel Structure and Mechanical Properties at Physiologically Relevant Levels. *Biopolymers* **2008**, *89* (10), 841–851. https://doi.org/10.1002/bip.21024.

(181) Sharma, S.; Panitch, A.; Neu, C. P. Incorporation of an Aggrecan Mimic Prevents Proteolytic Degradation of Anisotropic Cartilage Analogs. *Acta Biomater.* **2013**, *9* (1), 4618–4625. https://doi.org/10.1016/j.actbio.2012.08.041.

(182) Douglas, T.; Heinemann, S.; Mietrach, C.; Hempel, U.; Bierbaum, S.; Scharnweber, D.; Worch, H. Interactions of Collagen Types I and II with Chondroitin Sulfates A-C and Their Effect on Osteoblast Adhesion. *Biomacromolecules* **2007**, *8* (4), 1085–1092. https://doi.org/10.1021/bm0609644.

(183) Keech, M. K. The Formation of Fibrils from Collagen Solutions. IV. Effect of Mucopolysaccharides and Nucleic Acids: An Electron Microscope Study. *J. Biophys. Biochem. Cytol.* **1961**, *9*, 193–209.

(184) Mathews, M. B. The Interaction of Collagen and Acid Mucopolysaccharides. A Model for Connective Tissue. *Biochem. J.* **1965**, *96* (3), 710–716.

(185) Obrink, B.; Wasteson, A. Nature of the Interaction of Chondroitin 4-Sulphate and Chondroitin Sulphate-Proteoglycan with Collagen. *Biochem. J.* **1971**, *121*, 227–233.

(186) Pieper, J. S.; Van Der Kraan, P. M.; Hafmans, T.; Kamp, J.; Buma, P.; Van Susante, J. L. C.; Van Den Berg, W. B.; Veerkamp, J. H.; Van Kuppevelt, T. H. Crosslinked Type II Collagen Matrices: Preparation, Characterization, and Potential for Cartilage Engineering. *Biomaterials* **2002**, *23* (15), 3183–3192. https://doi.org/10.1016/S0142-9612(02)00067-4.

(187) Borzacchiello, A.; Ambrosio, L.; Netti, P.; Nicolais, L. Rheology of Biological Fluids and Their Substitutes. In *Tissue Engineering And Novel Delivery Systems*; Yaszemski, M. J., Trantolo, D. J., Lewandrowski, K.-U., Hasirci, V., Altobelli, D. E., Wise, D. L., Eds.; CRC Press: Boca Raton, 2003; pp 268–283.

(188) Kato, Y.; Mukudai, Y.; Okimura, A.; Shimazu, A.; Nakamura, S. Effects of Hyaluronic Acid on the Release of Cartilage Matrix Proteoglycan and Fibronectin from the Cell Matrix Layer of Chondrocyte Cultures: Interactions between Hyaluronic Acid and Chondroitin Sulfate Glycosaminoglycan. *J. Rheumatol.* **1995**, *22*, 158–159.

(189) Brightman, A. O.; Rajwa, B. P.; Sturgis, J. E.; McCallister, M. E.; Robinson, J. P.; Voytik-Harbin, S. L. Time-Lapse Confocal Reflection Microscopy of Collagen Fibrillogenesis and Extracellular Matrix Assembly in Vitro. *Biopolymers* **2000**, *54* (3), 222–234.

(190) Stamov, D.; Grimmer, M.; Salchert, K.; Pompe, T.; Werner, C. Heparin Intercalation into Reconstituted Collagen I Fibrils: Impact on Growth Kinetics and Morphology. *Biomaterials* **2008**, *29* (1), 1–14.

(191) Lélu, S.; Pluen, A. Characterization of Composite Networks Made of Type I Collagen, Hyaluronic Acid and Decorin. *Macromol. Symp.* **2007**, *256* (1), 175–188. https://doi.org/10.1002/masy.200751020.

(192) Notbohm, H.; Mosler, S.; Müller, P. K.; Brinckmann, J. In Vitro Formation and Aggregation of Heterotypic Collagen I and III Fibrils. *Int. J. Biol. Macromol.* **1993**, *15* (5), 299–304.

(193) Kreger, S. T.; Bell, B. J.; Bailey, J.; Stites, E.; Kuske, J.; Waisner, B.; Voytik-Harbin, S. L. Polymerization and Matrix Physical Properties as Important Design Considerations for Soluble Collagen Formulations. *Biopolymers* **2010**, *8* (93), 690–707. https://doi.org/10.1126/scisignal.2001449.Engineering.

(194) Antoine, E. E.; Vlachos, P. P.; Rylander, M. N. Review of Collagen I Hydrogels for Bioengineered Tissue Microenvironments: Characterization of Mechanics, Structure, and Transport. *Tissue Eng. Part B* **2014**, *20* (6), 683–696. https://doi.org/10.1089/ten.TEB.2014.0086.

(195) Sivakumar, L.; Agarwal, G. The Influence of Discoidin Domain Receptor 2 on the Persistence Length of Collagen Type I Fibers. *Biomaterials* **2010**, *31* (18), 4802–4808. https://doi.org/10.1016/j.biomaterials.2010.02.070.

(196) Lake, S. P.; Barocas, V. H. Mechanical and Structural Contribution of Non-Fibrillar Matrix in Uniaxial Tension: A Collagen-Agarose Co-Gel Model. *Ann. Biomed. Eng.* **2011**, *39* (7), 1891–1903. https://doi.org/10.1007/s10439-011-0298-1.

(197) Lee, J. E.; Park, J. C.; Hwang, Y. S.; Kim, J. K.; Kim, J. G.; Sub, H. Characterization of UV-Irradiated Dense/Porous Collagen Membranes: Morphology, Enzymatic Degradation, and Mechanical Properties. *Yonsei Medical Journal*. 2001, pp 172–179.

(198) Shayegan, M.; Forde, N. R. Microrheological Characterization of Collagen Systems: From Molecular Solutions to Fibrillar Gels. *PLoS One* **2013**, *8* (8). https://doi.org/10.1371/journal.pone.0070590.

(199) Halloran, D. O.; Grad, S.; Stoddart, M.; Dockery, P.; Alini, M.; Pandit, A. S. An Injectable Cross-Linked Scaffold for Nucleus Pulposus Regeneration. *Biomaterials* **2008**, *29* (4), 438–447.

(200) Xu, B.; Zhang, Y.; Chow, M. J. Experimental and Modeling Study of Collagen Scaffolds with the Effects of Crosslinking and Fiber Alignment. *Int. J. Biomater.* **2011**, *2011*, 1–12.

(201) Sheu, M. T.; Huang, J. C.; Yeh, G. C.; Ho, H. O. Characterization of Collagen Gel Solutions and Collagen Matrices for Cell Culture. *Biomaterials* **2001**, *22* (13), 1713–1719.

(202) Lu, Z.; Doulabi, B. Z.; Huang, C.; Bank, R. A.; Helder, M. N. Collagen Type II Enhances Chondrogenesis in Adipose Tissue-Derived Stem Cells by Affecting Cell Shape. *Tissue Eng. Part A* **2010**, *16* (1), 81–90. https://doi.org/10.1089/ten.tea.2009.0222.

(203) Bosnakovski, D.; Mizuno, M.; Kim, G.; Takagi, S.; Okumura, M.; Fujinaga, T. Chondrogenic Differentiation of Bovine Bone Marrow Mesenchymal Stem Cells (MSCs) in Different Hydrogels: Influence of Collagen Type II Extracellular Matrix on MSC Chondrogenesis. *Biotechnol. Bioeng.* **2006**, *93* (6), 1152–1163. https://doi.org/10.1002/bit.

(204) Freyria, a M.; Ronzière, M. C.; Cortial, D.; Galois, L.; Hartmann, D.; Herbage, D.; Mallein-Gerin, F.; Ronziere, M. C.; Cortial, D.; Galois, L.; et al. Comparative Phenotypic Analysis of Articular Chondrocytes Cultured within Type I or Type II Collagen Scaffolds. *Tissue Eng Part A* **2009**, *15* (6), 1233–1245. https://doi.org/10.1089/ten.tea.2008.0114.

(205) Nehrer, S.; Breinan, H. A.; Ramappa, A.; Hsu, H. P.; Minas, T.; Shortkroff, S.; Sledge, C. B.; Yannas, I. V.; Spector, M. Chondrocyte-Seeded Collagen Matrices Implanted in a Chondral Defect in a Canine Model. *Biomaterials* **1998**, *19* (24), 2313–2328. https://doi.org/10.1016/S0142-9612(98)00143-4.

(206) Reboredo, J. W.; Weigel, T.; Steinert, A.; Rackwitz, L.; Rudert, M.; Walles, H. Investigation of Migration and Differentiation of Human Mesenchymal Stem Cells on Five-Layered Collagenous Electrospun Scaffold Mimicking Native Cartilage Structure. *Adv. Healthc. Mater.* **2016**, 1–8. https://doi.org/10.1002/adhm.201600134.

(207) Yuan, L.; Li, B.; Yang, J.; Ni, Y.; Teng, Y.; Guo, L.; Fan, H.; Fan, Y.; Zhang, X. Effects of Composition and Mechanical Property of Injectable Collagen I/II Composite Hydrogels on Chondrocyte Behaviors. *Tissue Eng. Part A* **2016**, *22* (11–12), 899–906. https://doi.org/10.1089/ten.tea.2015.0513.

(208) Cisternas, M. G.; Murphy, L.; Sacks, J. J.; Solomon, D. H.; Pasta, D. J.; Helmick, C. G. Alternative Methods for Defining Osteoarthritis and the Impact on Estimating Prevalence in a US Population-Based Survey. *Arthritis Care Res.* **2016**, *68* (5), 574–580. https://doi.org/10.1002/acr.22721.

(209) McCormick, F.; Harris, J. D.; Abrams, G. D.; Frank, R.; Gupta, A.; Hussey, K.; Wilson, H.; Bach, B.; Cole, B. Trends in the Surgical Treatment of Articular Cartilage Lesions in the United States: An Analysis of a Large Private-Payer Database over a Period of 8 Years. *J. Arthrosc. Relat. Surg.* **2014**, *30* (2), 222–226. https://doi.org/10.1016/j.arthro.2013.11.001.

(210) Huey, D. J.; Hu, J. C.; Athanasiou, K. A. Unlike Bone, Cartilage Regeneration Remains Elusive. *Science* **2012**, *338* (6109), 917–921. https://doi.org/10.1126/science.1222454.Unlike.

(211) de l'Escalopier, N.; Anract, P.; Biau, D. Surgical Treatments for Osteoarthritis. *Ann. Phys. Rehabil. Med.* **2016**, *59* (3), 227–233. https://doi.org/10.1016/j.rehab.2016.04.003.

(212) Madry, H.; Grün, U. W.; Knutsen, G. Cartilage Repair and Joint Preservation. *Dtsch. Aerzteblatt Online* **2011**, *108* (40). https://doi.org/10.3238/arztebl.2011.0669.

(213) Alford, J. W.; Cole, B. J. Cartilage Restoration, Part 1: Basic Science, Historical Perspective, Patient Evaluation, and Treatment Options. *Am. J. Sports Med.* **2005**, *33* (2), 295–306. https://doi.org/10.1177/0363546504273510.

(214) Seliktar, D. Designing Cell-Compatible Hydrogels for Biomedical Applications. *Science* **2012**, *336* (6085), 1124–1128. https://doi.org/10.1126/science.1214804.

(215) Makris, E. A.; Gomoll, A. H.; Malizos, K. N.; Hu, J. C.; Athanasiou, K. A. Repair and Tissue Engineering Techniques for Articular Cartilage. *Nat Rev Rheumatol* **2015**, *8* (12), 1699–1712. https://doi.org/10.1016/j.rasd.2014.08.015.Social.

(216) Pittenger, M. F.; Mackay, A. M.; Beck, S. C.; Jaiswal, R. K.; Douglas, R.; Mosca, J. D.; Moorman, M. A.; Simonetti, D. W.; Craig, S.; Marshak, D. R. Multilineage Potential of Adult Human Mesenchymal Stem Cells. *Science* **1999**, *284* (5411), 143–147. https://doi.org/10.1126/science.284.5411.143.

(217) Vázquez-Portalatín, N.; Kilmer, C. E.; Panitch, A.; Liu, J. C. Characterization of Collagen Type I and II Blended Hydrogels for Articular Cartilage Tissue Engineering. *Biomacromolecules* **2016**, *17* (10), 3145–3152. https://doi.org/10.1021/acs.biomac.6b00684.

(218) Penick, K. J.; Solchaga, L. a.; Welter, J. F. High-Throughput Aggregate Culture System to Assess the Chondrogenic Potential of Mesenchymal Stem Cells. *Biotechniques* **2005**, *39* (5), 687–690. https://doi.org/10.2144/000112009.

(219) Renner, J. N.; Kim, Y.; Liu, J. C. Bone Morphogenetic Protein-Derived Peptide Promotes Chondrogenic Differentiation of Human Mesenchymal Stem Cells. *Tissue Eng. Part A* **2012**, *18* (23–24), 2581–2589. https://doi.org/10.1089/ten.tea.2011.0400.

(220) Kim, Y. J.; Sah, R. L. Y.; Doong, J. Y. H.; Grodzinsky, A. J. Fluorometric Assay of DNA in Cartilage Explants Using Hoechst 33258. *Anal. Biochem.* **1988**, *174* (1), 168–176. https://doi.org/10.1016/0003-2697(88)90532-5.

(221) Bookout, A. L.; Cummins, C. L.; Mangelsdorf, D. J.; Pesola, J. M.; Kramer, M. F. High-Throughput Real-Time Quantitative Reverse Transcription PCR. In *Current Protocols in Molecular Biology*; Sons, J. W. &, Ed.; New York, 2006; Vol. 831, p 15.8.1–15.8.28. https://doi.org/10.1002/0471142727.mb1508s73.

(222) O'Driscoll, S. W.; Keeley, F. W.; Salter, R. B. Durability of Regenerated Articular Cartilage Produced by Free Autogenous Periosteal Grafts in Major Full-Thickness Defects in Joint Surfaces under the Influence of Continuous Passive Motion. A Follow-up Report at One Year. *J. Bone Jt. surgery.* **1988**, *70* (4), 595–606. https://doi.org/10.2106/00004623-198870040-00017.

(223) van den Borne, M. P. J.; Raijmakers, N. J. H.; Vanlauwe, J.; Victor, J.; de Jong, S. N.; Bellemans, J.; Saris, D. B. F. International Cartilage Repair Society (ICRS) and Oswestry Macroscopic Cartilage Evaluation Scores Validated for Use in Autologous Chondrocyte Implantation (ACI) and Microfracture. *Osteoarthr. Cartil.* **2007**, *15* (12), 1397–1402. https://doi.org/10.1016/j.joca.2007.05.005.

(224) Antoine, E. E.; Vlachos, P. P.; Rylander, M. N. Review of Collagen I Hydrogels for Bioengineered Tissue Microenvironments: Characterization of Mechanics, Structure, and Transport. *Tissue Eng. Part B Rev.* **2014**, *20* (6), 683–696. https://doi.org/10.1089/ten.teb.2014.0086.

(225) Lynch, M. P.; Stein, J. L.; Stein, G. S.; Lian, J. B. The Influence of Type I Collagen on the Development and Mainteance of the Osteoblast Phenotype in Primary and Passaged Rat Calvarial Osteoblast: Modification of Expression of Genes Supporting Cell Growth, Adhesion, and Extracellular Matrix Mineralization. *Exp. Cell Res.* **1995**, *216*, 35–45. https://doi.org/10.1006/excr.1995.1005.

(226) Rutgers, M.; Saris, D. B.; Vonk, L. A.; van Rijen, M. H.; Akrum, V.; Langeveld, D.; van Boxtel, A.; Dhert, W. J.; Creemers, L. B. Effect of Collagen Type I or Type II on Chondrogenesis by Cultured Human Articular Chondrocytes. *Tissue Eng. Part A* **2013**, *19* (1–2), 59–65. https://doi.org/10.1089/ten.tea.2011.0416.

(227) Nehrer, S.; Breinan, H. H.; Ashkar, S.; Ph, D.; Shortkroff, S.; Minas, T. O. M.; Sledge, C. B.; Yannas, I. V; Spector, M. Characteristics of Articular Chondrocytes Seeded in Collagen Matrices in Vitro. *Tissue Eng.* **1998**, *4* (2), 175–183. https://doi.org/10.1089/ten.1998.4.175.

(228) Nehrer, S.; Breinan, H. a.; Ramappa, A.; Shortkroff, S.; Young, G.; Minas, T.; Sledge, C. B.; Yannas, I. V.; Spector, M. Canine Chondrocytes Seeded in Type I and Type II Collagen Implants Investigated in Vitro. *J. Biomed. Mater. Res.* **1997**, *38* (2), 95–104. https://doi.org/10.1002/(SICI)1097-4636(199722)38:2<95::AID-JBM3>3.0.CO;2-B.

(229) Tamaddon, M.; Burrows, M.; Ferreira, S. A.; Dazzi, F.; Apperley, J. F.; Bradshaw, A.; Brand, D. D.; Czernuszka, J.; Gentleman, E. Monomeric, Porous Type II Collagen Scaffolds Promote Chondrogenic Differentiation of Human Bone Marrow Mesenchymal Stem Cells in Vitro. *Sci. Rep.* **2017**, *7* (March), 1–10. https://doi.org/10.1038/srep43519.

(230) Chen, C. W.; Tsai, Y. H.; Deng, W. P.; Shih, S. N.; Fang, C. L.; Burch, J. G.; Chen, W. H.; Lai, W. F. Type I and II Collagen Regulation of Chondrogenic Differentiation by Mesenchymal Progenitor Cells. *J. Orthop. Res.* **2005**, *23* (2), 446–453. https://doi.org/10.1016/j.orthres.2004.09.002.

(231) Giuliani, N.; Lisignoli, G.; Magnani, M.; Racano, C.; Bolzoni, M.; Dalla Palma, B.; Spolzino, A.; Manferdini, C.; Abati, C.; Toscani, D.; et al. New Insights into Osteogenic and Chondrogenic Differentiation of Human Bone Marrow Mesenchymal Stem Cells and Their Potential Clinical Applications for Bone Regeneration in Pediatric Orthopaedics. *Stem Cells Int.* **2013**, *2013*. https://doi.org/10.1155/2013/312501.

(232) Jo, A.; Denduluri, S.; Zhang, B.; Wang, Z.; Yin, L.; Yan, Z.; Kang, R.; Shi, L. L.; Mok, J.; Lee, M. J.; et al. The Versatile Functions of Sox9 in Development, Stem Cells, and Human Diseases. *Genes Dis.* **2014**, *1* (2), 149–161. https://doi.org/10.1016/j.gendis.2014.09.004.

(233) Rucklidge, G. J.; Milne, G.; Robins, S. P. Collagen Type X : A Component of the Surface of Normal Human, Pig, and Rat Articular Cartilage. **1996**, *302* (224), 297–302. https://doi.org/10.1006/bbrc.1996.1024.

(234) Frenkel, S. R.; Toolan, B.; Menche, D.; Pitman, M. I.; Pachence, J. M. Chondrocyte Transplantation Using a Collagen Bilayer Matrix for Cartilage Repair. *J. Bone Joint Surg. Br.* **1997**, *79* (5), 831–836. https://doi.org/10.1302/0301-620X.79B5.7278.

(235) Khan, I. M.; Gilbert, S. J.; Singhrao, S. K.; Duance, V. C.; Archer, C. W. Cartilage Integration: Evaluation of the Reasons for Failure of Integration during Cartilage Repair. A Review. *Eur. Cells Mater.* **2008**, *16* (0), 26–39. https://doi.org/10.22203/eCM.v016a04.

(236) Liao, J.; Guo, X.; Grande-Allen, K. J.; Kasper, F. K.; Mikos, A. G. Bioactive Polymer/Extracellular Matrix Scaffolds Fabricated with a Flow Perfusion Bioreactor for Cartilage Tissue Engineering. *Biomaterials* **2010**, *31* (34), 1–15. https://doi.org/10.1016/j.biomaterials.2010.07.110.BIOACTIVE.

(237) Zheng, L.; Sun, J.; Chen, X.; Wang, G.; Jiang, B.; Fan, H.; Zhang, X. In Vivo Cartilage Engineering with Collagen Hydrogel and Allogenous Chondrocytes after Diffusion Chamber Implantation in Immunocompetent Host. *Tissue Eng. Part A* **2009**, *15* (8), 2145–2153. https://doi.org/ ? .

(238) Chen, C. H.; Kuo, C. Y.; Wang, Y. J.; Chen, J. P. Dual Function of Glucosamine in Gelatin/Hyaluronic Acid Cryogel to Modulate Scaffold Mechanical Properties and to Maintain Chondrogenic Phenotype for Cartilage Tissue Engineering. *Int. J. Mol. Sci.* **2016**, *17* (11). https://doi.org/10.3390/ijms17111957.

(239) Zhang, L.; Yuan, T.; Guo, L.; Zhang, X. An in Vitro Study of Collagen Hydrogel to Induce the Chondrogenic Differentiation of Mesenchymal Stem Cells. *J. Biomed. Mater. Res. - Part A* **2012**, *100 A* (10), 2717–2725. https://doi.org/10.1002/jbm.a.34194.

(240) Morigele, M.; Shao, Z.; Zhang, Z.; Kaige, M.; Zhang, Y.; Qiang, W.; Yang, S. TGF-B1 Induces a Nucleus Pulposus-like Phenotype in Notch 1 Knockdown Rabbit Bone Marrow Mesenchymal Stem Cells. *Cell Biol. Int.* **2013**, *37* (8), 820–825. https://doi.org/10.1002/cbin.10109.

(241) Krasnokutsky, S.; Samuels, J.; Abramson, S. B. Osteoarthritis in 2007. *Bull. NYU Hosp. Jt. Dis.* **2007**, *65* (3), 222–228. https://doi.org/17922674.

(242) Huang, D. Effect of Extracellular Chondroitin Sulfate on Cultured Chondrocytes. *J. Cell Biol.* **1974**, *62* (3), 881–886. https://doi.org/10.1083/jcb.62.3.881.

(243) Bryant, S. J.; Arthur, J. A.; Davis-Arehart, K. A.; Luo, N.; Shoemaker, R. K.; Anseth, K. S. Synthesis and Characterization of Photopolymerized Multifunctional Hydrogels: Water-Soluble Poly(Vinyl Alcohol) and Chondroitin Sulfate Macromers for Chondrocyte Encapsulation. *Macromolecules* **2004**, *37* (18), 6726–6733. https://doi.org/10.1021/ma0499324.

(244) Steinmetz, N. J.; Bryant, S. J. Chondroitin Sulfate and Dynamic Loading Alter Chondrogenesis of Human Mscs in Peg Hydrogels. *Biotechnol. Bioeng.* **2012**, *109* (10), 2671–2682. https://doi.org/10.1002/bit.24519.

(245) Varghese, S.; Hwang, N. S.; Canver, A. C.; Theprungsirikul, P.; Lin, D. W.; Elisseeff, J. Chondroitin Sulfate Based Niches for Chondrogenic Differentiation of Mesenchymal Stem Cells. *Matrix Biol.* **2008**, *27* (1), 12–21. https://doi.org/10.1016/j.matbio.2007.07.002.

(246) Nandini, C. D.; Sugahara, K. Role of the Sulfation Pattern of Chondroitin Sulfate in Its Biological Activities and in the Binding of Growth Factors. *Adv. Pharmacol.* **2006**, *53* (05). https://doi.org/10.1016/S1054-3589(05)53012-6.

(247) Wang, T.; Lai, J. H.; Han, L.; Tong, X.; Yang, F. Chondrogenic Differentiation of Adipose-Derived Stromal Cells in Combinatorial Hydrogels Containing Cartilage Matrix Proteins with Decoupled Mechanical Stiffness. **2014**, *20*. https://doi.org/10.1089/ten.tea.2013.0531.

(248) Yu, F.; Xiaodong, C.; LI, Y.; Zeng, L.; Yuan, B.; Chen, X. An Injectable Hyaluronic Acid/PEG Hydrogel for Cartilage Tissue Engineering Formed by Integrating Enzymatic Crosslinking and Diels–Alder "Click Chemistry." *Polym. Chem.* **2014**, *5*, 1082–1090. https://doi.org/10.1039/c3py00869j.

(249) Aisenbrey, E. A.; Bryant, S. J. The Role of Chondroitin Sulfate in Regulating Hypertrophy during MSC Chondrogenesis in a Cartilage Mimetic Hydrogel under Dynamic Loading. *Biomaterials* **2019**, *190–191* (June 2018), 51–62. https://doi.org/10.1016/j.biomaterials.2018.10.028.

(250) Sechriest, V. F.; Miao, Y. J.; Niyibizi, C.; Westerhausen-Larson, A.; Matthew, H. W.; Evans, C. H.; Fu, F. H.; Suh, J. K. GAG-Augmented Polysaccharide Hydrogel: A Novel Biocompatible and Biodegradable Material to Support Chondrogenesis. *J. Biomed. Mater. Res.* **2000**, *49* (4), 534–541. https://doi.org/10.1002/(SICI)1097-4636(20000315)49:4<534::AID-JBM12>3.0.CO;2-#.

(251) Chen, W.-C.; Wei, Y.-H.; Chu, I.-M.; Yao, C.-L. Effect of Chondroitin Sulphate C on the in Vitro and in Vivo Chondrogenesis of Mesenchymal Stem Cells in Crosslinked Type II Collagen Scaffolds. *J. Tissue Eng. Regen. Med.* **2013**, *7*, 665–672. https://doi.org/10.1002/term.

(252) Bernhard, J. C.; Panitch, A. Synthesis and Characterization of an Aggrecan Mimic. *Acta Biomater.* **2012**, *8* (4), 1543–1550. https://doi.org/10.1016/j.actbio.2011.12.029.

(253) Lawrence, A.; Bible, M. D.; Xu, X.; Calve, S.; Panitch, A.; Neu, C. P. Synthesis and Characterization of a Lubricin Mimic (MLub) to Reduce Friction and Adhesion on the Articular Cartilage Surface. *Biomaterials* **2015**, *73*, 42–50. https://doi.org/10.1016/j.biomaterials.2015.09.012.

(254) Scott, R. a.; Panitch, A. Decorin Mimic Regulates Platelet-Derived Growth Factor and Interferon-Beta Stimulation of Vascular Smooth Muscle Cells. *Biomacromolecules* **2014**, *15* (6), 2090–2103. https://doi.org/10.1021/bm500224f.

(255) Matsiko, A.; Levingstone, T. J.; O'Brien, F. J.; Gleeson, J. P. Addition of Hyaluronic Acid Improves Cellular Infiltration and Promotes Early-Stage Chondrogenesis in a Collagen-Based Scaffold for Cartilage Tissue Engineering. *J. Mech. Behav. Biomed. Mater.* **2012**, *11*, 41–52. https://doi.org/10.1016/j.jmbbm.2011.11.012.

(256) Stuart, K.; Panitch, A. Influence of Chondroitin Sulfate on Collagen Gel Structure and Mechanical Properties at Physiologically Relevant Levels. *Biopolymers* **2008**, *89* (10), 841–851. https://doi.org/10.1002/bip.21024.

(257) Scott, J. E.; Parry, D. A. D. Control of Collagen Fibril Diameters in Tissues. *Int. J. Biol. Macromol.* **1992**, *14* (5), 292–293. https://doi.org/10.1016/S0141-8130(05)80043-1.

(258) ÖBrink, B.; Sundelöf, L. -O. Light Scattering in the Study of Associating Macromolecules: The Binding of Glycosaminoglycans to Collagen. *Eur. J. Biochem.* **1973**, *37* (2), 226–232. https://doi.org/10.1111/j.1432-1033.1973.tb02979.x.

(259) Murphy, C. M.; Matsiko, A.; Haugh, M. G.; Gleeson, J. P.; O'Brien, F. J. Mesenchymal Stem Cell Fate Is Regulated by the Composition and Mechanical Properties of Collagen-Glycosaminoglycan Scaffolds. *J. Mech. Behav. Biomed. Mater.* **2012**, *11*, 53–62. https://doi.org/10.1016/j.jmbbm.2011.11.009.

(260) Bierbaum, S.; Doublas, T.; Hanke, T.; Scharnweber, D.; Tippelt, S.; Monsees, T. K.; Funk, R. H. W.; Worch, H. Collagenenous Matrix Coatings on Titatnium Implants Modified with Decorin and Chondroitin Sulfate: Characterization and Influence on Osteoblastic Cells. *J. Biomed. Mater. Res.* **2006**, *67* (8), 1180–1185. https://doi.org/10.1002/jbm.a.

(261) Kuznetsova, N.; Chi, S. L.; Leikin, S. Sugars and Polyols Inhibit Fibrillogenesis of Type I Collagen by Disrupting Hydrogen-Bonded Water Bridges between the Helices. *Biochemistry* **1998**, *37* (34), 11888–11895. https://doi.org/10.1021/bi980089+.

(262) Van Susante, J. L. C.; Pieper, J.; Buma, P.; Van Kuppevelt, T. H.; Van Beuningen, H.; Kraan, P. M. Van Der; Veerkamp, J. H.; Berg, W. B. Van Den; Veth, R. P. H. Linkage of Chondroitin-Sulfate to Type I Collagen Scaffolds Stimulates the Bioactivity of Seeded Chondrocytes in Vitro. *Biomaterials* **2001**, *22* (17), 2359–2369.

(263) Al Faqeh, H.; Nor Hamdan, B. M. Y.; Chen, H. C.; Aminuddin, B. S.; Ruszymah, B. H. I. The Potential of Intra-Articular Injection of Chondrogenic-Induced Bone Marrow Stem Cells to Retard the Progression of Osteoarthritis in a Sheep Model. *Exp. Gerontol.* **2012**, *47* (6), 458–464. https://doi.org/10.1016/j.exger.2012.03.018.

(264) Dominici, M.; Le Blanc, K.; Mueller, I.; Slaper-Cortenbach, I.; Marini, F. .; Krause, D. S.; Deans, R. J.; Keating, A.; Prockop, D. J.; Horwitz, E. M. Minimal Criteria for Defining Multipotent Mesenchymal Stromal Cells. The International Society for Cellular Therapy Position Statement. *Cytotherapy* **2006**, *8* (4), 315–317. https://doi.org/10.1080/14653240600855905.

(265) Godoy, R. F.; Alves, A. L. G.; Gibson, A. J.; Lima, E. M. M.; Goodship, A. E. Do Progenitor Cells from Different Tissue Have the Same Phenotype? *Res. Vet. Sci.* **2014**, *96* (3), 454–459. https://doi.org/10.1016/J.RVSC.2014.02.013.

(266) Khan, M. R.; Chandrashekran, A.; Smith, R. K. W.; Dudhia, J. Immunophenotypic Characterization of Ovine Mesenchymal Stem Cells. *Cytom. Part A* **2016**, *89* (5), 443–450. https://doi.org/10.1002/cyto.a.22849.

(267) Cook, J. L.; Hung, C. T.; Kuroki, K.; Stoker, A. M.; Cook, C. R.; Pfeiffer, F. M.; Sherman, S. L.; Stannard, J. P. Animal Models of Cartilage Repair. *Bone Joint Res.* **2014**, *3* (4), 89–94. https://doi.org/10.1302/2046-3758.34.2000238.

(268) Schinhan, M.; Gruber, M.; Vavken, P.; Dorotka, R.; Samouh, L.; Chiari, C.; Gruebl-, R.; Nehrer, S. Critical-Size Defect Induces Unicompartmental Osteoarthritis in a Stable Ovine Knee. **2012**, No. February, 214–220. https://doi.org/10.1002/jor.21521.

(269) Burks, R. T.; Greis, P. E.; Arnoczky, S. P.; Scher, C. The Use of a Single Osteochondral Autograft Plug in the Treatment of a Large Osteochondral Lesion in the Femoral Condyle: An Experimental Study in Sheep. *Am. J. Sports Med.* **2006**, *34* (2), 247–255. https://doi.org/10.1177/0363546505279914.

(270) Frosch, K. H.; Drengk, A.; Krause, P.; Viereck, V.; Miosge, N.; Werner, C.; Schild, D.; Stürmer, E. K.; Stürmer, K. M. Stem Cell-Coated Titanium Implants for the Partial Joint Resurfacing of the Knee. *Biomaterials* **2006**, *27* (12), 2542–2549. https://doi.org/10.1016/j.biomaterials.2005.11.034.

(271) Mrosek, E. H.; Chung, H.-W.; Fitzsimmons, J. S.; ODriscoll, S. W.; Reinholz, G. G.; Schagemann, J. C. Porous Tantalum Biocomposites for Osteochondral Defect Repair: A Follow-up Study in a Sheep Model. *Bone Jt. Res.* **2016**, *5* (9), 403–411. https://doi.org/10.1302/2046-3758.59.BJR-2016-0070.R1.

(272) O'Driscoll, S. W.; Keeley, F. W.; Salter, R. B. Durability of Regenerated Articular Cartilage Produced by Free Autogenous Periosteal Grafts in Major Full-Thickness Defects in Joint Surfaces under the Influence of Continuous Passive Motion. A Follow-up Report at One Year. *J. Bone Joint Surg. Am.* **1988**, *70* (4), 595–606.

(273) Griffin, D. J.; Ortved, K. F.; Nixon, A. J.; Bonassar, L. J. Mechanical Properties and Structure-Function Relationships in Articular Cartilage Repaired Using IGF-I Gene-Enhanced Chondrocytes. *J. Orthop. Res.* **2016**, *34* (1), 149–153. https://doi.org/10.1002/jor.23038.

(274) Mow, V. C.; Kuei, S. C.; Lai, W. M.; Armstrong, C. G. Biphasic Creep and Stress Relaxation of Articular Cartilage in Compression: Theory and Experiments. *J. Biomech. Eng.* **1980**, *102* (1), 73. https://doi.org/10.1115/1.3138202.

(275) Scott, R. A.; Panitch, A. Decorin Mimic Regulates Platelet-Derived Growth Factor and Interferon-γ Stimulation of Vascular Smooth Muscle Cells. *Biomacromolecules* **2014**, *15* (6), 2090–2103. https://doi.org/10.1021/bm500224f.

(276) Zhang, S.; Muneta, T.; Morito, T.; Mochizuki, T.; Sekiya, I. Autologous Synovial Fluid Enhances Migration of Mesenchymal Stem Cells from Synovium of Osteoarthritis Patients in Tissue Culture System. *J. Orthop. Res.* **2008**, *26* (10), 1413–1418. https://doi.org/10.1002/jor.20659.

(277) Schmitt, B.; Ringe, J.; Haupl, T.; Notter, M.; Manz, R.; Burmester, G. R.; Sittinger, M.; Kaps, C. BMP2 Initiates Chondrogenic Lineage Development of Adult Human Mesenchymal Stem Cells in High-Density Culture. *Differentiation* **2003**, *71* (9–10), 567–577. https://doi.org/10.1111/j.1432-0436.2003.07109003.x.

(278) Renner, J. N.; Kim, Y.; Liu, J. C. Bone Morphogenetic Protein-Derived Peptide Promotes Chondrogenic Differentiation of Human Mesenchymal Stem Cells. *Tissue Eng. Part A* **2012**, *18* (23–24), 2581–2589. https://doi.org/10.1089/ten.TEA.2011.0400.

(279) Saito, A.; Suzuki, Y.; Ogata, S. I.; Ohtsuki, C.; Tanihara, M. Activation of Osteo-Progenitor Cells by a Novel Synthetic Peptide Derived from the Bone Morphogenetic Protein-2 Knuckle Epitope. *Biochim. Biophys. Acta* **2003**, *1651* (1–2), 60–67. https://doi.org/10.1016/S1570-9639(03)00235-8.

(280) Lee, J. S.; Lee, J. S.; Murphy, W. L. Modular Peptides Promote Human Mesenchymal Stem Cell Differentiation on Biomaterial Surfaces. *Acta Biomater.* **2010**, *6* (1), 21–28. https://doi.org/10.1016/j.actbio.2009.08.003.

(281) Mitchell, E. a; Chaffey, B. T.; McCaskie, A. W.; Lakey, J. H.; Birch, M. a. Controlled Spatial and Conformational Display of Immobilised Bone Morphogenetic Protein-2 and Osteopontin Signalling Motifs Regulates Osteoblast Adhesion and Differentiation in Vitro. *BMC Biol.* **2010**, *8* (Il), 57. https://doi.org/10.1186/1741-7007-8-57.

(282) He, X.; Ma, J.; Jabbari, E. Effect of Grafting RGD and BMP-2 Protein-Derived Peptides to a Hydrogel Substrate on Osteogenic Differentiation of Marrow Stromal Cells. *Langmuir* **2008**, *24* (21), 12508–12516. https://doi.org/10.1021/la802447v.

(283) Torbet, J.; Malbouyres, M.; Builles, N.; Justin, V.; Roulet, M.; Damour, O.; Oldberg, Å.; Ruggiero, F.; Hulmes, D. J. S. Tissue Engineering of the Cornea: Orthogonal Scaffold of Magnetically Aligned Collagen Lamellae for Corneal Stroma Reconstruction. *Annu. Int. Conf. IEEE Eng. Med. Biol.* **2007**, *28*, 6399. https://doi.org/10.1109/IEMBS.2007.4353820.

(284) Guo, C.; Kaufman, L. J. Flow and Magnetic Field Induced Collagen Alignment. *Biomaterials* **2007**, *28* (6), 1105–1114. https://doi.org/10.1016/j.biomaterials.2006.10.010.

(285) Novak, T.; Voytik-Harbin, S. L.; Neu, C. P. Cell Encapsulation in a Magnetically Aligned Collagen-GAG Copolymer Microenvironment. *Acta Biomater.* **2014**, *11* (1), 274–282. https://doi.org/10.1016/j.actbio.2014.09.031.

APPENDIX A. BMP PEPTIDE ADDED AT FEEDING

MSCs can be directed to differentiate at a certain time and to a specific phenotype based on a number of different biological and physical cues.[80] It is well known that many different biological cues, including growth factors, hormones, extracellular matrix, and other small chemicals, can direct the fate of stem cells to a certain differentiation lineage.[81–83] A number of both natural and synthetic molecules have been shown to be useful for guiding stem cells through chondrogenesis.[84,85] For example, soluble growth factors secreted by the cell direct stem cell differentiation in vivo, but they can also be added to a culture in vitro and similarly affect the cells.[84] The most popular growth factors that stimulate chondrogenesis are insulin-like growth factor (IGF) and the transforming growth factor beta (TGF-β) family.[86–88] The TGF-β family is known for inducing differentiation to chondrocytes while preventing differentiation to osteocytes. Collagen type II expression and proteoglycan synthesis are increased in systems cultured with TGF-β3, a potent inducer of chondrogensis.[89] A subgroup of the TGF-β family, the bone morphogenetic proteins (BMPs), also plays a crucial role in cartilage repair.

Bone morphogenetic protein-2 (BMP-2) is expressed during mesenchymal condensation, an important step in cartilage and embryonic development.[90] We are interested in BMP-2 due to the fact that it is a growth factor that is a proven to be a very powerful stimulator of chondrogenesis in MSCs.[277] The ability to stimulate differentiation to chondrocytes can be amplified when BMP-2 is combined with TGF-β3.[87] However, as dosage is increased, the protein begins to promote differentiation to osteocytes.[87] Previous work has shown that when MSCs are grown in a matrix that is rich in proteoglycans and collagen type II, they favor differentiation to cartilage over bone when stimulated with BMP-2.[91] BMP-2 has also been used *in vivo* where it has been shown to regenerate hyaline-like cartilage and aid in the cartilage healing process.[92,93] Growth factors are long, complex molecules that are difficult to incorporate into a scaffold. In contrast, peptide sequences are much smaller than the full-length growth factors making them much easier to incorporate into scaffolds while being simpler and cheaper to synthesize.[278] A BMP peptide (KIPKASSVPTELSAISTLYL) was created using residues 73-92 from the BMP-2 knuckle epitope.[279] Dr. Liu's lab has previously shown that the BMP peptide can stimulate human MSCs to undergo chondrogenesis without including additional growth factors.[278] The BMP peptide was also shown to direct MSCs to increase collagen production and promote GAG production. When

compared to BMP-2, the peptide also showed little increase in the gene expression of hypertrophic markers like AP activity and collagen type X.[278] Even when grafted to the surface of a scaffold, the peptide has shown the ability to remain active.[280–282] We added different concentrations of BMP-2 peptide at feedings to MSCs encapsulated in Col I/II hydrogels. Either 10 ng/mL of TGF-β3, no added growth factor (No GF), a 100 µg/mL treatment of BMP peptide (BMP (H)), a 50 µg/mL treatment of BMP peptide (BMP (M)), a 10 µg/mL treatment of BMP peptide (BMP (L)), or a 100 µg/mL treatment of BMP peptide and 10 ng/mL of TGF-β3 (BMP+TGF) were added to the base CM- media. We hypothesized that the BMP peptide would help promote the differentiation of MSCs to chondrocytes in a dose dependent manor. After 14 days in culture, the scaffolds were analyzed for AP Activity. After a 21- and 28-day culture period, the scaffolds were lyophilized and analyzed for GAG production, DNA, and dry weight (DW).

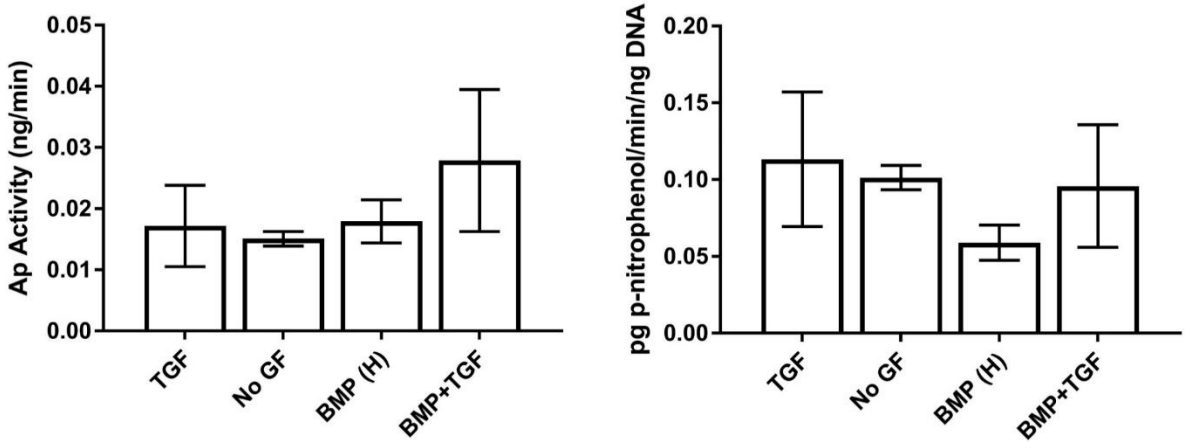

Figure 5-1. AP activity at 14 days per scaffold and AP Activity at 14 normalized to DNA.

Either 10 ng/mL of TGF-β3, no added growth factor (No GF), a 100 µg/mL treatment of BMP peptide (BMP (H)), or a 100 µg/mL treatment of BMP peptide and 10 ng/mL of TGF-β3 (BMP+TGF) were added at feeding in the base CM- media.The analysis of AP activity was done directly on the gels.

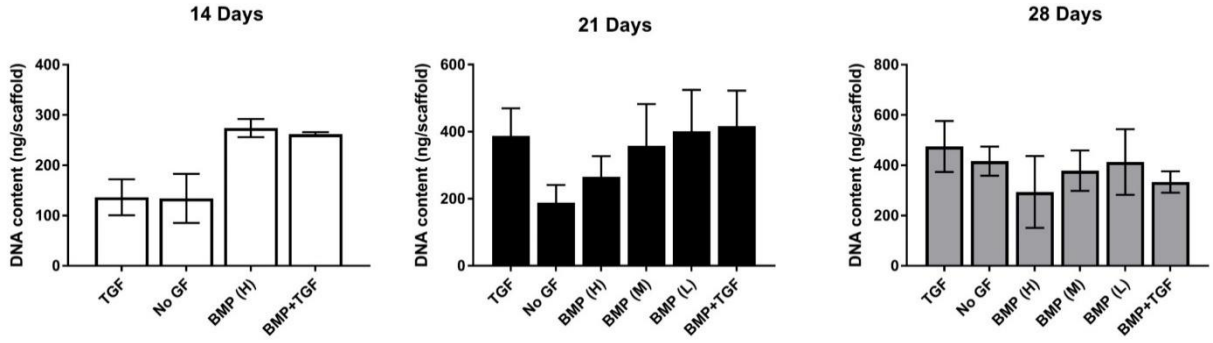

Figure 5-2. DNA content at 3 different timepoints (14, 21, and 28 days) using a Hoescht dye.

Either 10 ng/mL of TGF-β3, no added growth factor (No GF), a 100 µg/mL treatment of BMP peptide (BMP (H)), a 50 µg/mL treatment of BMP peptide (BMP (M)), a 10 µg/mL treatment of BMP peptide (BMP (L)), or a 100 µg/mL treatment of BMP peptide and 10 ng/mL of TGF-β3 (BMP+TGF) were added at feeding in the base CM- media.

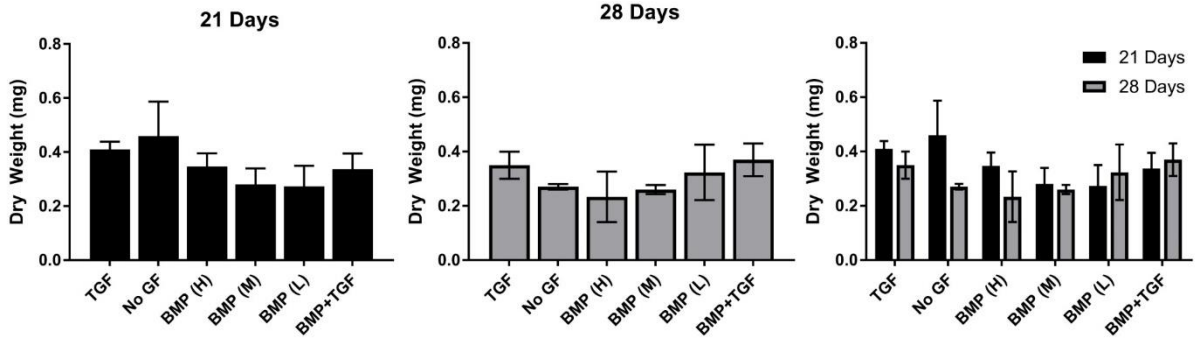

Figure 5-3. Dry weight (DW) of the scaffolds at 21 and 28 days of culture.

Either 10 ng/mL of TGF-β3, no added growth factor (No GF), a 100 µg/mL treatment of BMP peptide (BMP (H)), a 50 µg/mL treatment of BMP peptide (BMP (M)), a 10 µg/mL treatment of BMP peptide (BMP (L)), or a 100 µg/mL treatment of BMP peptide and 10 ng/mL of TGF-β3 (BMP+TGF) were added at feeding in the base CM- media.

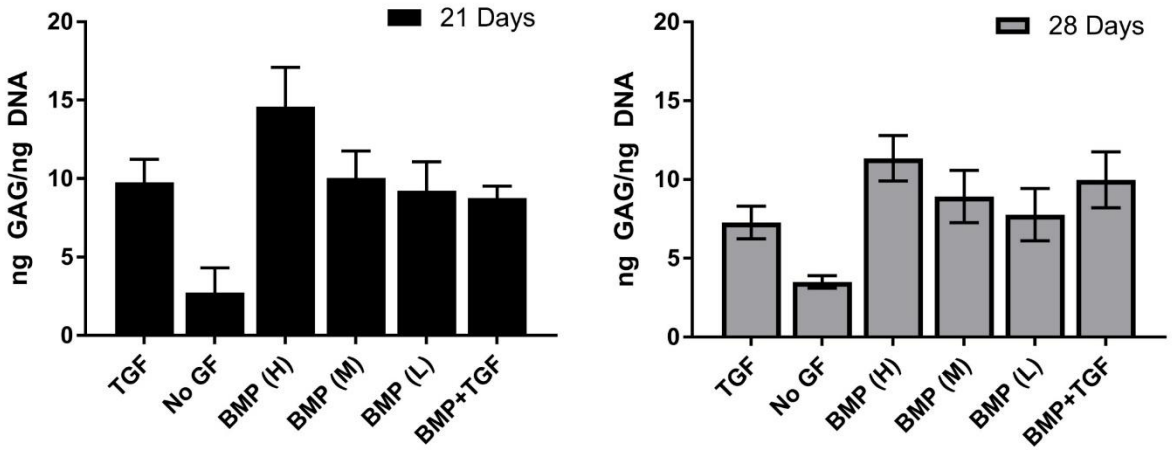

Figure 5-4. GAG/DNA ratio of the cell-hydrogel constructs with different treatments added at feeding in the base CM- media.

Either 10 ng/mL of TGF-β3, no added growth factor (No GF), a 100 µg/mL treatment of BMP peptide (BMP (H)), a 50 µg/mL treatment of BMP peptide (BMP (M)), a 10 µg/mL treatment of BMP peptide (BMP (L)), or a 100 µg/mL treatment of BMP peptide and 10 ng/mL of TGF-β3 (BMP+TGF) were added at feeding.

APPENDIX B. ALIGNED COLLAGEN HYDROGEL

The orientation of collagen fibers changes throughout the different zones of cartilage. In the deep zone, vertical collagen fibers protect against large strains experienced at the junction of bone and cartilage.[15] The middle zone has randomly aligned collagen fibers, and horizontal fibers in the superficial tangential zone resist tensile stresses parallel to the surface of articular cartilage.[16] Collagen fibril alignment also plays a fundamental role in cell biosynthesis of ECM components and phenotype.[17,18] Previous studies have shown that noninvasive magnetic alignment can be used to control the orientation of collagen fibers.[283,284] When chondrocytes were embedded in a scaffold with aligned collagen, the gene expression of aggrecan and collagen type II were enhanced when compared to scaffolds with unaligned collagen fibers.[181] The increase in aggrecan and collagen type II expression was further amplified in the presence of the aggrecan mimic.[181]

Col I and Col I/II scaffolds were aligned by adding the unpolymerized solution to an ibidi slide that placed in the isocenter of a magnet (Figure 5-5). To induce alignment in the presence of a 7T magnetic field of a small animal Magnetic Resonance Imaging (MRI), the hydrogel was incubated in the bore of the magnet for 1 hour at 37°C. Alignment was confirmed by analyzing images take on a confocal microscope with a 2-D fast fourier transform based birefringence calculation using ImageJ as described in Novak *et al.*[285] We were able to successfully align collagen fibers in both Col I and Col I/II scaffolds using a 7T small animal MRI (Figure 5-6).

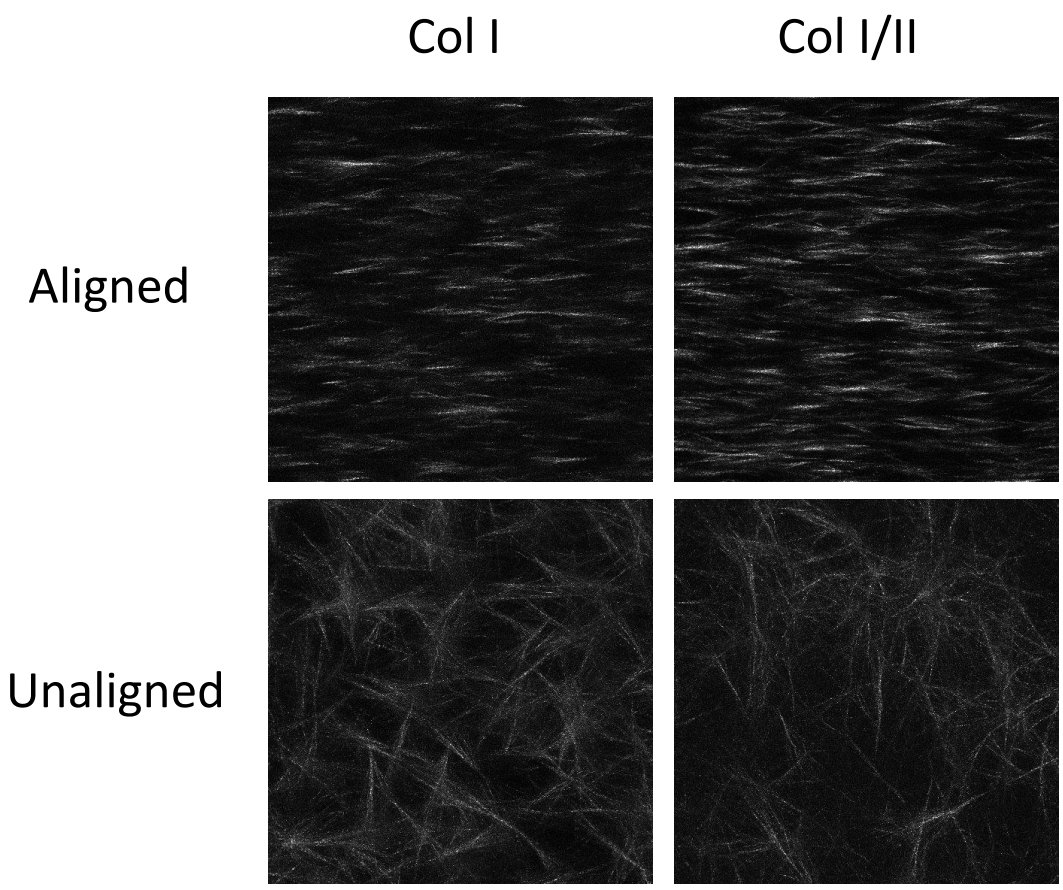

Figure 5-5. Confocal reflectance microscopy images of aligned and unaligned collagen fibers in Col I and Col I/II blend hydrogels.

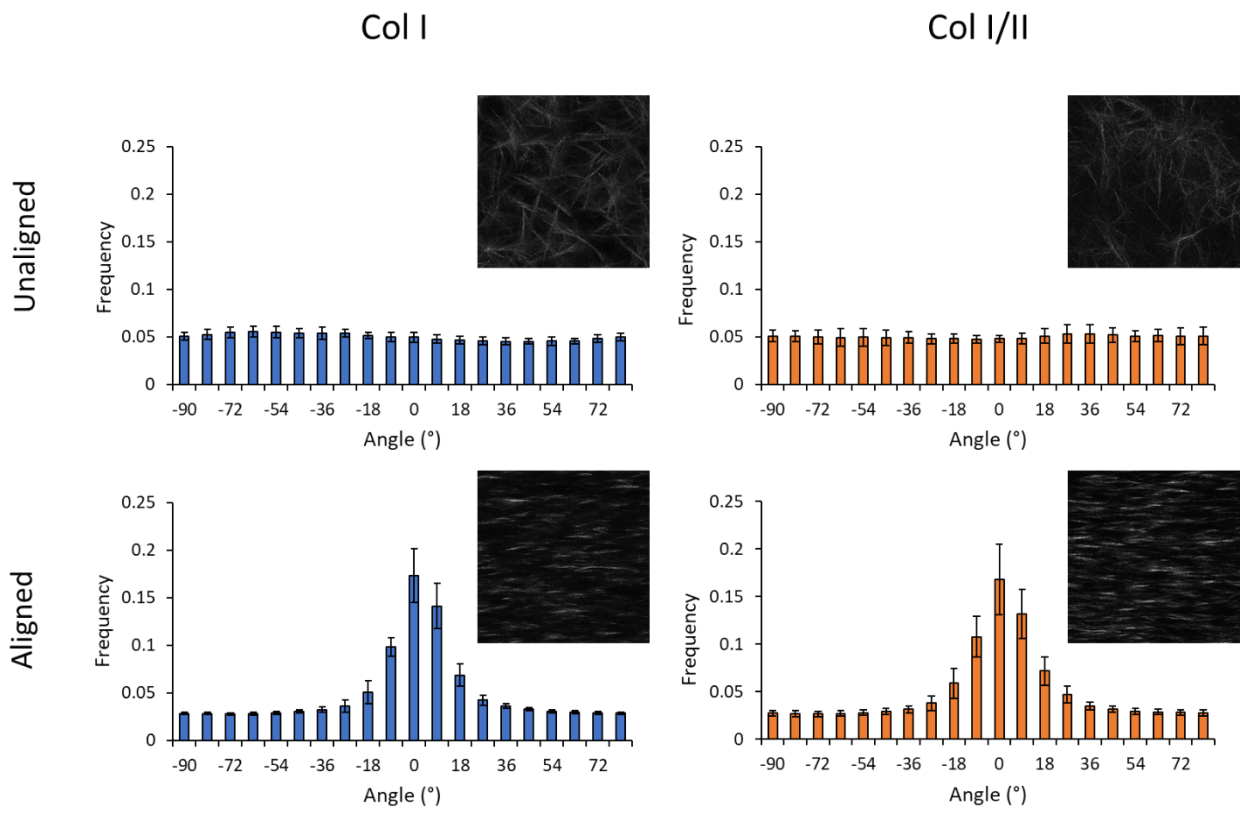

Figure 5-6. Confocal reflectance microscopy images of aligned and unaligned collagen fibers in Col I and Col I/II blend hydrogels and graphs with the frequency of collagen fibers at certain angles to confirm alignment.

APPENDIX C. OSTEOGENIC DIFFERENTIATION

We evaluated the 2D *in vitro* bone marrow differentiation potential of the rabbit MSCs that were isolated to encapsulate in the Col I/II hydrogels. The cells were cultured on tissue culture polystyrene 24 well plates in growth medium. Growth medium (GM) was prepared using low glucose DMEM, 10% FBS, and 1% P/S. When the cells reached about a confluency of about 70%, samples were either switched to an osteogenic medium or continued to be cultured in growth medium. osteogenic medium (ODM) contained low glucose DMEM, 10% FBS, 1% pen-strep, 100 nM dexamethasone, 50 µM ascorbic acid 2-phosphate, and 10 mM glycerol-2 phosphate disodium salt hydrate. After 3 weeks in culture, the samples were stained with Alizarin Red S (ARS)(Figure 5-7) for calcium deposits and alkaline phosphatase (Figure 5-8). More calcium deposits stained by ARS were observed in MSCs that were cultured in ODM than MSCs that were cultured in GM after 3 weeks in culture. More staining for alkaline phosphatase was observed in MSCs that were cultured in ODM than MSCs that were cultured in GM after 3 weeks in culture.

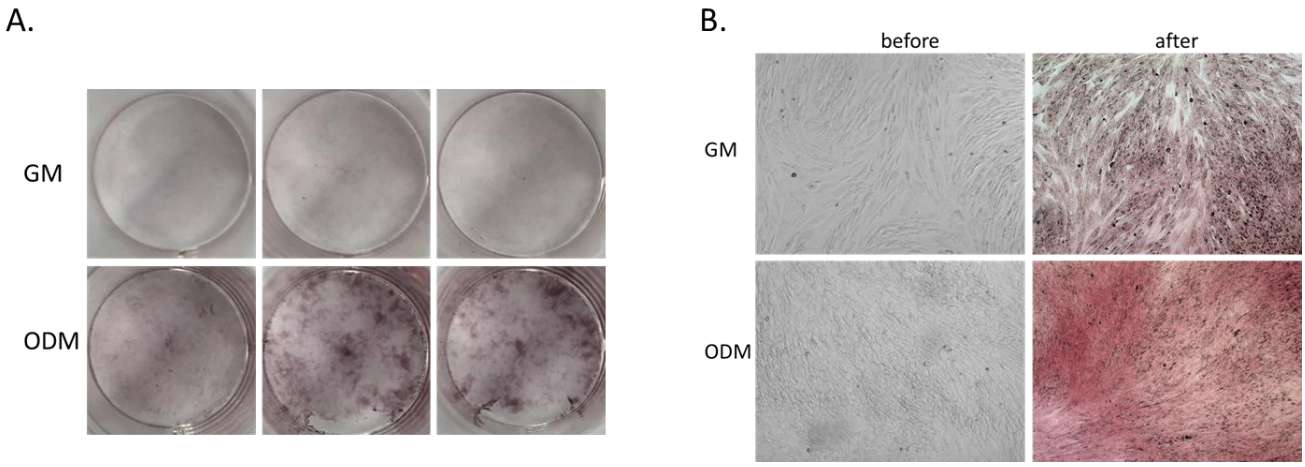

Figure 5-7. More calcium deposits stained by ARS were observed in MSCs that were cultured in an osteogenic medium (ODM) than MSCs that were cultured in growth medium (GM) after 3 weeks in culture.

The whole image of the well where the cells were cultured is shown in panel A and microscope images at 4x of the center of the well are shown in panel B.

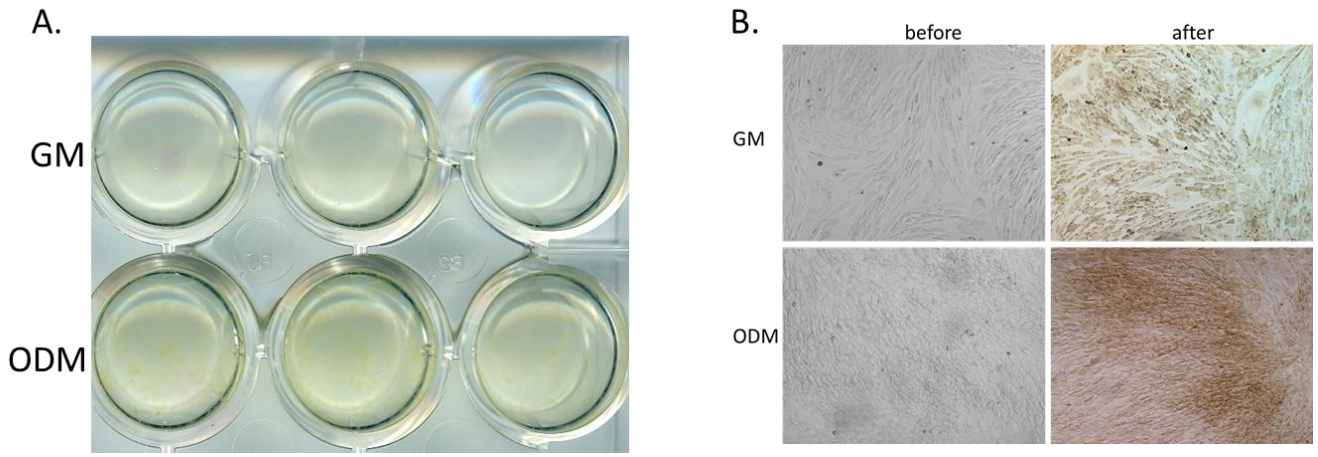

Figure 5-8. More staining for alkaline phosphatase was observed in MSCs that were cultured in an osteogenic medium (ODM) than MSCs that were cultured in growth medium (GM) after 3 weeks in culture.

The whole image of the well where the cells were cultured is shown in panel A and microscope images at 4x of the center of the well are shown in panel B.

APPENDIX D. PROTOCOLS

Collagen Hydrogel Gelation Procedure

1. Determine the final volume of solution required and your desired concentration. For almost all studies in this thesis, a final concentration of collagen of 4 mg/mL was used. The final volume was often altered based on how many hydrogels were needed for a desired experiment.
2. Place stocks of collagen type I on ice collagen type II
3. Prepare stocks of 10x PBS, 1x PBS, and 1M NaOH.
4. Adjust the pH of the 10x PBS and 1x PBS to 7.4.
5. Divide the required final volume of hydrogel (in mL) by 10. This number is the amount of 10x PBS required (in mL).
6. Multiply the required final volume of hydrogel (in mL) by the final desired collagen concentration (in mg/mL) then divide that number by the concentration of collagen type I in the bottle. The calculated value is the volume of total collagen to be added (in mL).
   Note: The concentration of collagen type I value alters by stock. The collagen type II will be diluted down to the same concentration as the stock collagen type II concentration.
7. Multiply the volume of collagen to be added by 0.023. This value is the volume of 1M NaOH (in mL).
8. Subtract the calculated total collagen volume, the calculated 10x PBS, and the volume of 1M NaOH from the final volume of hydrogel required. This value is the required volume of 1x PBS (in mL).
9. Mix together the required volumes of 10x PBS, 1x PBS, and 1M NaOH to create a neutralization solution.
10. Add the calculated volume of collagen with a positive displacement pipette and slowly mix. To create an all collagen type I, all of the volume of collagen added will be collagen type I. To create an all collagen type I and II blend hydrogel, a 3:1 ratio of collagen type I to collagen type II will be added at this step. In our original characterization studies, different ratios of collagen type I to collagen type II were used.
11. The hydrogels were then allowed to polymerize for between 2 and 24 hours at 37°C. **Note:** The collagen type I comes sterilized and can be considered sterile as long as it is always opened in a biosafety cabinet. The collagen type II is received in a lyophilized form. An 11 mg/mL stock solution of collagen type II from lyophilized chicken sternum (Sigma-Aldrich) was prepared in 20 mM acetic acid. Take out an aliquot of the 11 mg/mL solution and sterile filter the rest of the collagen type II. Upon sterile filtration, the concentration of the collagen type II stock solution was measured using a bicinchoninic acid (BCA) assay (Pierce) following the manufacturer's protocol with the 11 mg/mL collagen type II aliquot as the standard. The stock solution of collagen type II was then diluted to the same concentration as the stock collagen type I in 20 mM acetic acid prior to use.
12. When checking the pH of the solution or making a neutralization solution, add all of the require 10x PBS, 75% of the required NaOH, 50% of the required 1x PBS, and all of the required collagen. Measure the pH of the solution using the micro-pH meter and adjust the pH by adding additional NaOH. Keep track of the added NaOH. When the solution pH is at 7.4, add the rest of the 1x PBS adjust for the amount of NaOH added. Check the fnal pH

of the solution. Repeat this protocol until results are constant after 5 replicates of the same NaOH addition. This neutralization solution can now be used in a sterile environment without the need for pHing every time.

Maintenance Media Preparation (Modified from Dr. Julie Renner)

Recipe:

- Lg-DMEM
- 10% Fetal Bovine Serum (FBS)
- 1% Pen-Strep

For a 500 mL Lg-DMEM bottle:

- Add 55.6 mL FBS
- Add 5.6 mL Pen-Strep

Note: If this is being used to culture mesenchymal stem cells add 10 ng/mL FGF-2 at feeding. Do not just simply add the FGF-2 to the stock 500 mL bottle. This value has been optimized for rabbit mesenchymal stem cells and it may need to be adjusted for other cell types.

To Prepare Fibroblast Growth Factor – 2 (FGF-2) Stocks (Modified from Peprotech):

1. If you order 10 ug of FGF-2, stock solutions should be made of 20 ug/mL.
2. Prep Tris Buffer (5 mM) for FGF-2 reconstitution:

- Dissolved 121.14 g (MW=121.14) of Tris in 800 mL of Milli-Q and adjust the pH to 7.6. This is a 1 M solution of Tris buffer. Note: this will take about 60 mL of concentrated HCl. Adjust the final volume to 1 L and recheck the pH.
- Dilute the solution down to 5 mM. Note: this is 2.5 mL of 1 M Tris Buffer and 497.5 mL of Milli-Q. This solution should then be autoclaved and sterile filtered prior to adding to the FGF-2.

3. Prepare 0.1% (w/v) BSA for FGF-2:

- Add 100 mg of BSA to 100 mL of PBS.
- Sterile Filter.
- The addition of the BSA acts as a carrier protein which helps to prolong shelf-life during storage conditions.

4. FGF-2 Reconstitution:

    - Centrifuge the FGF-2 container before opening. This is extremely important as some of the contents can get stuck into the top of the tube during shipping.
    - Add 10 uL of the 5 mM autoclaved and sterile filtered Tris Buffer to the FGF-2.
    - Add 490 uL of 0.1% BSA.
    - This recipe makes 25 tubes of 20 uL aliquots. Tubes should be stored in the -80°C freezer.

Thawing Bone Marrow Derived-Mesenchymal Stem Cells (Adapted from Julie Renner)

1. Warm up maintenance media (approximately 10 mL) in 100 mm (diameter) tissue culture dishes after calculating the desired number. Allow the plates to temperature (37°C) and CO_2 (5%) equilibrate in a humified cell culture incubator for about 30 minutes. For calculations, plate between 300,000 and 350,000 cells per 100 mm tissue culture dish.
2. Retrieve cryovial of cells from liquid nitrogen dewer and spray a kimwipe with ethanol to wipe the cryovial. Place cryovial in the cell culture hood and turn the cryovial cap to relieve pressure. Tighten the cap again.
3. Thaw the cryovial in the water bath at 37°C on a foam raft. Watch until the last sliver of ice melted. Note: this will take around 2 minutes. Sterilize the cryovial with ethanol and place back in the cell culture hood.
4. Add the contents of the cryovial into 5 mL of maintenance media that has been temperature equilibrated. Centrifuge at 300*g* for 5 minutes.
5. Resuspend in temperature equilibrated maintenance media. Count cells using a hemocytometer.
6. When cell density is determined, calculate the amount of cell slurry to add to plate between 300,000 and 350,000 cells per 100 mm tissue culture dish. (Aim to add about 2 to 1 mL of cell slurry). Shake the plate in a cross pattern to disperse cells.
7. Move the plates in a humid cell culture incubator at 37°C and 5 % CO_2.
8. Replace the media the following day as frozen cells are stored in DMSO.
9. Depending on the planned experiment, feed cells every 2 to 3 days which is about 10 mL of maintenance media in a 100 mm dish.

Subculturing Bone Marrow Derived-Mesenchymal Stem Cells

1. MSCs will need to be passaged when they reach between 70 and 80% confluent. It is important to check the status of the cells and there confluency every day. Note: Some cell types will need to passaged at a different confluency than MSCs.
2. Remove media in the cell culture dishes. Wash the plates with temperature equilibrated PBS and then discard.
3. Add 3 mL of Trypsin-EDTA to the 100 mm cell culture dish. Place the plate back in the incubator and start a stop watch for 1.5 minutes. Using a microscope, check on the detachment of the cells after the 1.5-minute wait time.
4. Transfer the plate back into the cell culture hood if about 90% are detached and floating in the cell culture media. If less than 90% of the cells are detached, put the place back in the incubator check for the detachment of cells, every 30 seconds, using the microscope. Do not incubate for more than 8 minutes. Note: These instructions are for MSCs. There are cell types that will need much more rigorous detachment methods.
5. To the trypsin-EDTA-cell slurry, add in the same amount of temperature equilibrated maintenance media as trypsin-EDTA that was added. In the 100 mm plate example above this would be 3 mL of maintenance media.
6. The trypsin-EDTA will now need to be removed from the cell slurry. Centrifuge at 300*g* for 5 minutes.
7. Resuspend in temperature equilibrated maintenance media. Count cells using a hemocytometer.

8. When cell density determined, calculate the amount of cell slurry to add to plate between 300,000 and 350,000 cells per 100 mm tissue culture dish. (Aim to add about 2 to 1 mL of cell slurry). Shake the plate in a cross pattern to disperse cells.

Bone Marrow Mesenchymal Stem Cell Freezing Solution (Modified from Dr. Julie Renner)

For 10 mL using maintenance media:

- Add 2.28 mL FBS
- Add 0.5 mL DMSO
- Add 7.22 mL of MM

For 10 mL using Lg-DMEM:

- Add 3 mL FBS
- Add 0.5 DMSO
- Add 6.5 Lg-DMEM

1. Follow the subculture procedure listed above.
2. Count cells using a hemocytometer.
3. Resuspend cells in freezing solution noted above. Resuspend at a cell density of 1,000,000 cells/mL. You will be aiming to place 1,000,000 cells in each cryovial you freeze.
4. Label a cryovial with your name, cell type, date, passage number, and initials.
5. Aliquot 1 mL of cell slurry into a cryovial.
6. Place the cryovial in the cell freezing container. Make sure that the isopropyl alcohol has been replaced. Some labs only replace this every 5 uses, but I feel more comfortable replacing it every time. This container will help freeze the cells at a specific rate. Place the freezing container in the -80°C freezer overnight.
7. Remove vials from freezing container and place the cryovials in the liquid nitrogen dewar from long term storage.

Mesenchymal Stem Cell Isolation (Cut Bone - Rabbit)

1. Prepare 2 plates of temperature and CO_2 adjusted maintenance media.
2. Warm a 50 mL of Maintenance Media.
3. Ethanol and UV sterilize clippers.
4. Euthanize rabbit with an overdose of barbiturate following guidelines from the American Veterinary Medical Association Panel on Euthanasia.
5. Dissect femurs and clean connective tissue attached to the bone. Pat bone with Kimwipe sprayed with ethanol and place femur in the cell culture hood. Cut the cap of the femurs.
6. Use a 10 mL syringe and 18-gauge needle, flush out marrow from the long bone and caps into 10 mL of warm maintenance media (for each femur). Place the cell suspension from both femurs into one 50 mL tube. Break up any clumps by pipetting up and down.
7. Centrifuge the marrow suspension for 10 minutes at 500*g*. Resuspend pellet in 10 mL of maintenance media. Place 5 mL of cell suspension into two 50 mL tubes.

8. To each 50 mL tube, add 15 mL of warmed and autoclaved Milli-Q. Mix by inverting for 30 seconds. Then make up the volume of the solution to 45 mL with maintenance media.
9. Centrifuge for 10 minutes at 500*g*. The pellet should be fairly white at this point. If the pellet is not white, repeat the water step to lyse the red blood cells.
10. Count cells (time permitting). Place approximately 10 million cells per 100 mm dish in maintenance media with 10 ng/mL added FGF-2.
11. Wash with PBS and change media after 4 days in culture. Change media (maintenance media with 10 ng/mL added FGF-2).
12. Cells will become confluent between 1.5 and 3 weeks.

Mesenchymal Stem Cell Isolation (Pooled Bone Marrow)

1. Rabbits were anesthetized by intramuscular injection with a mixture of ketamine, xylazine, and butorphanol (35 mg/kg, 5 mg/kg, and 0.01 mg/kg respectively) and were maintained on isoflurane and oxygen with a mask.
2. Bone marrow was collected from four sites including both the left and right proximal femurs and proximal humeri.
3. The bone marrow extraction sites were clipped and scrubbed with chlorhexidine using standard techniques.
4. Bone marrow was aspirated using an 18-gauge needle that was percutaneously inserted into the intertrochanteric fossa of the femur and the greater tubercle of the humerus.
5. After the needle penetrated through the bone into the medullary cavity, the bone marrow was aspirated.
6. The marrow from each rabbit was pooled by rabbit, centrifuged for 10 minutes at 500*g* and resuspended in maintenance medium (low-glucose Dulbecco's modified Eagle's medium (DMEM) supplemented with 10% fetal bovine serum (Lonza, Walkersville, MD) and 1% penicillin-streptomycin.
7. Autoclaved water was added to lyse the red blood cells. The marrow was gently mixed for 30 seconds before adding additional maintenance medium, and the suspension was centrifuged for 10 minutes at 500*g*.
8. After the pellet was resuspended in maintenance medium with 10 ng/mL added FGF-2, the cells were counted, plated on 100-mm plates at a density of 10^7 cells per plate, and incubated at 37°C with 5% CO_2.
9. The first medium change was performed after four days of culture following a phosphate buffered saline (1x PBS) wash step, and subsequent medium changes were every three days.
10. The cells were subcultured after 2.5 weeks upon reaching 70% - 80% confluency.

Mesenchymal Stem Cell Encapsulation in a Collagen Type I and II Blend Hydrogel

1. An 11 mg/mL stock solution of collagen type II from lyophilized chicken sternum was prepared in 20 mM acetic acid. Upon sterile filtration, the concentration of the collagen type II stock solution was measured using a bicinchoninic acid (BCA) assay following the manufacturer’s protocol. The stock solution of collagen type II was then diluted to 8 mg/mL in 20 mM acetic acid prior to use.
2. The stock solution of collagen type II was combined with acid-solubilized collagen type I from rat tail (Corning, Corning, NY).

3. The pH of the solutions was raised to 7.4 with the addition of 10x PBS, 1 M NaOH, and 1x PBS and diluted to a final concentration of 4 mg/mL total collagen. The gels were prepared with a 3:1 collagen type I to collagen type II ratio (Col I/II) or all collagen type I (Col I).
4. Cells were resuspended in collagen pre-polymerization solutions at a cell density of 5×10^6 cells/mL. The hydrogels were allowed to polymerize at 37°C for 2 or 3 hours before the addition of medium.
5. After polymerization, chondrogenic medium with or without added growth factor was added to the scaffolds.
6. Defined chondrogenic medium (CM) was formulated with high-glucose DMEM supplemented with 1% ITS+Premix (BD Biosciences, San Jose, CA), 1% penicillin-streptomycin, 1 mM sodium pyruvate, 50 µM proline, 4 mM L-glutamine, 50 µg/mL ascorbic acid, 100 nM dexamethasone, and 10 ng/mL transforming growth factor-β3 (TGF-β3) (Peprotech, Rocky Hill, NJ).
7. Defined chondrogenic medium without added growth factor (CM^-) was formulated the same way as CM but lacked TGF-β3. For *in vitro* analysis, cell-hydrogel constructs were cultured for up to 4 weeks with 3 medium changes each week.

Chondrogenic Media Recipe

Chondrogenic Base Media without AA, DEX, and TGF-β3 (CM^{--})

- High Glucose DMEM
- 1% ITS Premix
- 1% Pen-Strep
- 1 mM Sodium Pyruvate
- 50 µM Proline
- 4 mM L-Glutamine
- Note: weight out sodium pyruvate and proline together in ratio of 1:19.3 mg of proline to sodium pyruvate. Sterile filter. Ensure all things are sterile before adding them to the Hg DMEM.

Chondrogenic Base Media without TGF-β3 (CM^-)

- 1% ITS Premix
- 1% Pen-Strep
- 50 µg/mL L-ascorbic acid-2-phosphate (AA)
- 0.1 µM dexamethasone (DEX)
- 1 mM Sodium Pyruvate
- 50 µM Proline
- 4 mM L-Glutamine
- Note: This recipe is very similar to the CM^{--}, but AA an DEX must be added at feeding.
- DEX Stock: Make a 0.4 mg/mL solution of DEX in Ethanol. Sterile Filter. This solution will be considered the freezer stock. Store this solution in the -80°C freezer. The addition of 10 uL of freezer stock to 500 uL of CM^{--} prepares a fridge stock (good for 1 week). The fridge stock is a 7.48 ng/µL. When adding into CM^{--} to prepare CM^-, add 5 µL per mL of CM^{--}.

- AA Stock: Make a 10 mg/mL solution of AA in CM^{--}. Vortex. If you are having a hard time getting the AA into solution, place it briefly in the water bath. Sterile filter. This will need to be done at each feeding. Add 5 µL per mL of CM^{--}.

Chondrogenic Base Media with TGF-β3

- This is the same recipe as the CM^{-} except with 10 ng/mL TGF-β3 added at each feeding. For 2 µg/mL, add 5 µL per mL of CM^{--}.

Initiation of Pellet Culture (Adapted from Dr. Julie Renner)

1. To form the pellets, MSCs were centrifuged, washed, pelleted at a density of 2.5 x 10^5 cells/pellet, and cultured in a high-throughput culture system in a conical-bottom plate (this can also be done in 15 mL tubes). Note: Pellets are maintained in free-floating conditions.
2. Pull cells off the 100 mm dishes using the standard subculture protocol. Prior to counting, resuspend in CM^{--}.
3. Count cells using a hemocytometer. Alter the volume of cell sulurry so that you are plating 2.5 x 10^5 cells in 200 µL of CM^{-} (for negative pellets) or CM (for positive pellets). This may require another centrifugation step if the cells are too dilute for this density or the addition of more media.
4. Aliquot 200 µL of cell slurry into each well of a conical-bottom plate (NUNC).
5. Centrifuge at 300*g* for 5 minutes.
6. Move the plate in a humid cell culture incubator at 37°C and 5 % CO_2.
7. Depending on the planned experiment, feed pellets every 2 to 3 days which is about 200 µL of media per well. Negative pellets are feed with CM^{-} media, and positive pellets are fed with CM.

Papain Digestion

1. Papain (Papain from papaya latex) is used since it solubilizes GAGs and DNA, but degrades collagen.
2. Make a 10 mg/mL papain solution in MilliQ. This can be stored in the fridge at 4°C.
3. Prepare a papain digestion buffer (5 mM L-Cystiene, 100 mM NaH_2PO_4, and 5 mM EDTA in autoclaved MQ). The pH of the final solution was altered to 6.5. Store at 4°C.
4. Make a fresh 125 µg/mL of activated papain solution by mixing the fridge stock with papain digestion buffer.
5. Take media off of pellets, hydrogels, or cells.
6. Add 50 µL of activated papain solution to the pellets, hydrogels, or cells.
7. Place solution into PCR tubes.
8. Place tubes into the thermocycler. Use the Papain temperature ramp to digest gels (incubate at 60°C for 24 hours and 100°C for 10 minutes). The 100°C will inactivate the papain.
9. Centrifuge for 5 minutes at 500*g* then freeze.
10. Poke holes in the caps and freeze dry.

Alkaline Phosphatase Staining

1. Prepare cacodylic buffer by making a 0.2 M solution of cacodylic acid (Sodium cacodylate trihydrate) in milli-Q. Alter the pH to 7.4 and store at 4°C.
2. Prepare 4% paraformaldehyde in cacodylic buffer. Heat 7.5 mL of water to 65°C and add 0.6 g of paraformaldehyde (always use in a fume hood once dissolved) while stirring in the hood. Add a few drops of 10N NaOH until the solution turns clear. Alter the pH to 7.4 with concentrated HCl. Add 7.5 mL of 0.2 M cacodylic buffer.
3. Prepare a tris acid maleate stock solution. Add 12.1 g of Tris(hydroxymethyl) amino methane (THAM) and 11.6 g of maleic acid to 500 mL of Milli-Q.
4. Prepare 0.2N NaOH. Add 4g of NaOH to 500 mL of MilliQ.
5. Prepare tris maleate buffer. Add 25 mL of tris acid maleate stock solution, 40.5 mL of 0.2N NaOH, and 34.5 mL of Milli-Q.
6. Weigh materials to make the staining solution, but do not mix until added the cells. For 10 mL of staining solution, weigh out 5 mg of Napthol As-Mx Phosphate Disodium Salt and 10 mg of Fast Red. To these contents, 0.28 mL of DMF will be added. 4.72 mL of Milli-Q will be combined with 5 mL of the tris maleate buffer. Combine the Milli-Q/buffer solution with the DMF/Fast Red/Napthol solution. Sterile Filter. (Do this mixing right before you add it to the plate.)
7. Remove cell culture media and rinse cells two times with cacodylic buffer. Be careful to run the solution down the side of the plate.
8. Add 2 mL of 4% paraformaldehyde in cacodylic buffer by running the solution down the side of the plate.
9. Incubate the plate at 4°C for 10 to 20 minutes.
10. Remove the solution with a pipette and rinse cells 3 times with the cacodylic buffer.
11. Add 1 mL of the staining solution to each well.
12. Incubate the plate at 37°C for 30 minutes
13. Remove staining solution and rinse with cacodylic buffer.
14. Visualize alkaline phosphatase staining with an inverted microscope.

Collagen Incorporation into a Hydrogel (BCA Assay adapted from Pierce)

1. The collagen type II is received in a lyophilized form. An 11 mg/mL stock solution of collagen type II from lyophilized chicken sternum (Sigma-Aldrich) was prepared in 20 mM acetic acid. Take out an aliquot of the 11 mg/mL solution and sterile filter the rest of the collagen type II. Upon sterile filtration, the concentration of the collagen type II stock solution was measured using a bicinchoninic acid (BCA) assay with the 11 mg/mL collagen type II aliquot as the standard (the top of the working range of the assay is 2 mg/mL meaning the samples will be need to diluted).
2. Prepare a 2 mg/mL standard and serial dilute down to 0.03125 mg/mL in 20 mM acetic acid (2, 1, 0.5, 0.25, 0.125, 0.0625, 0.03125 mg/mL).
3. Make a working reagent (WR) solution that was a 50:1 (Reagent A:B) ratio.
4. Combine 25 µL of standard or sample to a 96 well plate.
5. 200 µL of WR was added to each well.
6. The samples were incubated for 30 minutes at 37°C and then cooled to room temperature.
7. The absorbance of the plates were read at 562 nm on the plate reader taking into consideration the dilution of samples.

8. The stock solution of collagen type II was then diluted to same concentration as the stock collagen type I in 20 mM acetic acid prior to use.

Collagen Assay (Sircol Dye Assay adapted from Biocolor)

1. The Sircol assay kit (catalog #: CLRS1111) should be purchased from Accurate Chemical & Scientific Corporation as they are the supplier of the kit in the US.
2. Freeze dry cell-hydrogel constructs and resuspended in a 0.1 mg/mL solution of pepsin in 0.5 mM acetic acid.
3. Incubated overnight at 4°C in the acid-pepsin extraction solution. Note: The acid-pepsin extraction step is not required for media aliquots.
4. The acid-pepsin solution was then neutralized using the provided acid neutralizing reagent.
5. Prepare a standard of collagen in either 20 mM acetic acid or cell culture medium. A low or high concentration standard can be made. The high concentration standard should contain the points 0.5, 0.4, 0.3, 0.2, and 0.1 ug collagen/uL. A blank of either 20 mM acetic acid or cell culture medium should also be included. The low concentration standard should contain the points 0.125, 0.1, 0.075, 0.05, 0.025, 0.014, 0.01, and 0.005 ug collagen/uL. A blank of either 20 mM acetic acid or cell culture medium should also be included for the low standard as well. For the standard use a 3:1 ratio of collagen type I to collagen type II.
6. Add 100 µL of standard or sample to a low bind microcentrifuge tube.
7. Add 1 mL of Sircol dye reagent. Invert the tubes to mix.
8. Place samples in a microcentrifuge tube rack and shake for 30 minutes,
9. Centrifuge samples at 12,000 rpm for 10 minutes.
10. Carefully remove supernatant. The collagen should bind to the dye and form a pellet in the bottom of the microcentrifuge tube.
11. Add 750 µL of acid-salt wash reagent that has been stored on ice to solubilize any unbound dye. It is important that this reagent is diluted in water upon receiving the kit. There should be 20 mL of acid-salt wash reagent in the bottle when the kit is received, and 80 mL of water should be added to dilute the reagent.
12. Once the collage-dye complex is precipitated out from unbound dye, the pellet should be resuspended in 250 µL of alkali reagent for the low concentration standard or 1000 µL of alkali reagent for the high concentration standard.
13. Measure the absorbance at a wavelength of 555 nm.

Chondroitin Sulfate Incorporation into a Hydrogel or GAG Production (DMMB Assay)

1. Prepare dimethyl methylene blue (DMMB) reagent. Add 3.04 g/L glycine, 2.37 g/L NaCl, 16 mg/L dimethyl methylene blue, and 0.1 M HCl. Mix for 2 hours.
2. Check the pH and alter as needed (pH = 3).
3. Read the absorbance at 525 nm. It should be around 0.31.
4. Store in an amber or light protected bottle. This solution is only good for about 3 months. Check the pH and absorbance before use if you are approaching that length of time.
5. A standard curve was created using chondroitin sulfate (CS) from shark cartilage (Seikagaku, Tokyo, Japan). Using a 10 mg/mL stock solution of CS, a standard curve

from 0.04 mg/mL to 0 was created (0.04, 0.02, 0.01, 0.005, 0.0025, 0.00125, and 0 mg/mL).

6. Take freeze dried samples and reconstitute in warmed and autoclaved milli-Q. 20 µL of the digested pellets or cell-hydrogel constructs were combined with 30 µL of water and 250 µL DMMB dye solution in a 96 well plate.
7. The absorbance of the solution was read at 525 nm as soon as the DMMB solution was added.
8. The GAG values measured were normalized to the amount of DNA measured per sample.

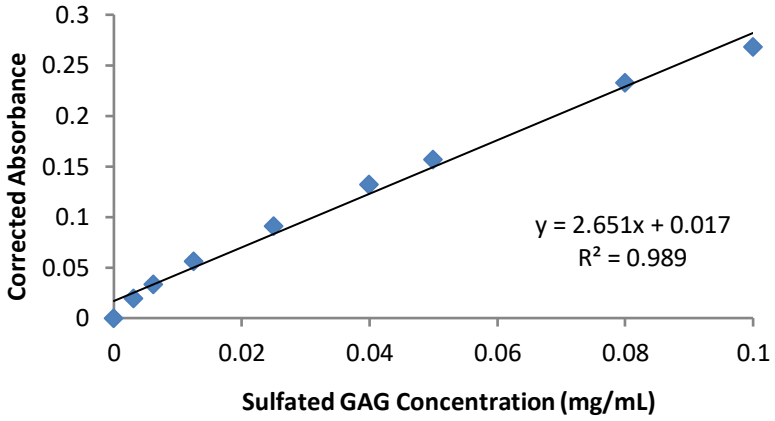

Figure 5-9. An example standard curve of sulfated glycosaminoglycans (GAGs) using DMMB Assay.

Measurement of DNA

1. Prepare TE buffer. TE buffer is 1 mM EDTA and 10 mM Tris-Cl. For a 100 mL of solution, add 0.2 mL of EDTA 90.5 M, pH 8.0) and 1 mL of Tris-Cl (1M, pH 8.0) then add autoclaved Milli-Q water to 100 mL (98.8 mL). Autoclave after preparation.
2. Calf thymus DNA was purchased lyophilized in the bottom of a vial. The DNA was reconstituted in TE buffer at 10 µg/mL. Place the calf thymus DNA vial in an ice box and shake on the shaker overnight. This part of the protocol sounds strange, but this was a suggestion from Sigma when I contacted them during the trouble shooting process. The 10 µg/mL DNA stocks will be stored at -20°C after reconstitution. Make standards by diluting stocks down with TE buffer. I have found the best standard range 2 µg/mL, 1 µg/mL, 0.5 µg/mL, 0.25 µg/mL, 0.125 µg/mL, and 0 µg/mL as a TE blank. I have seen some literature suggest a 4 µg/mL point in the standard, but I have found this point usually saturates out. I like to run this standard prior to running my samples because sample material is usually hard to come by (Low volume and long timepoints).
3. Add 50 µL of standard to the plate. When running samples, place 50 µL of sample in the plate. This does not have to be the pure sample. From my experience, sample on its own will saturate out on this assay. I have used between 5 µL - 20 µL of samples with the volume made up to 50 µL total with Milli-Q. When assaying for GAG, 20 µL of sample and 30 µL of water is my typical dilution, but make sure to make extra samples to test this out before running samples.

4. Prepare the TNE 1xBuffer. This will be used to prep the Hoechst dye stock. Dissolved 1.211 g Tris-Base (MW=121.14), 0.372 g EDTA, disodium salt, dehydrate (MW=372.2, and 11.689 g sodium chloride (MW=58.44) to 800 mL of Milli-Q. Autoclave after preparation.
5. Prepare a 1 mg/mL stock of Hoechst Dye (store at -20°C) in autoclaved Milli-Q. This stock can be frozen. For the assay itself, dilute down the previously dissolved Hoechst dye to a fresh stock of 0.7 µg/mL dye in TNE 1xBuffer. Add 3.5 µL of 1 mg/mL stock solution to 5 mL of TNE 1xBuffer. Make sure you understand when in this assay TE buffer is used (standard and blanks) and when the TNE 1xBuffer (dye preparation) is used since they can be easily confused.
6. Add 50 µL of the 0.7 µg/mL Hoechst dye to the samples and standards. Turn off the lights while plating the dye.
7. Read fluorescence at an excitation wavelength of 340 nm and an emission wavelength of 465 nm.
8. Subtract standard blank from all of the samples and standards. Plot RFU vs. known concentrations. Use a linear equation to calculate the concentration of samples. Adjust values based on utilized dilutions.

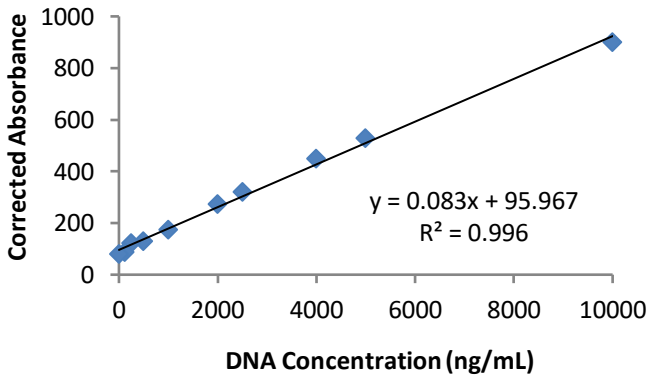

Figure 5-10. An example standard curve of DNA using a Hoechst Dye Assay.

AP Activity Assay (Hydrogels or Cell-Hydrogel Constructs)

1. Harvest scaffolds and wash with PBS. **Note:** This protocol was used to analyze alkaline phosphatase in 25 µL collagen type I and II blend hydrogels with encapsulated rabbit MSCs at a cell concentration of $5x10^6$ cells/mL or 250,000 cells per scaffold. Samples may need to be diluted if using other cell concentrations.
2. Prepare the collagenase buffer that is made up of 100 mM Tris and 1 mM $CaCl_2$ with the pH adjusted to 7.4. For a 15 mL stock, this is 181.7 mg of Tris, 1.7 mg of $CaCl_2$, and 15 mL of Milli-Q.
3. Collagenase digest the samples for 24 hours by adding 50 µL of 3 mg/mL collagenase solution in collagenase buffer.

4. Prepare the lysis buffer that is made up of 25 mM Sodium Carbonate and 1% v/v Triton x100 with the pH adjusted to 10.3. For a 15mL stock, this is 39.8 mg of sodium carbonate, 150 µL of Triton x100, and 14.85 mL of Milli-Q.
5. Prepare the para-nitrophenyl phosphate (pNPP) solution buffer. For a 15 mL stock, add 1.4 mg of $MgCl_2$, 0.1 mg of glycine, and 15 mL of Milli-Q. Make two stocks of this solution. To one the $MgCl_2$ and glycine are all that needs to be added to the water. To the second, ad 0.15 g of pNPP to the pNPP solution buffer. **Note:** This is stored at -20°C and this solution should be clear. If this solution is yellow, you will need to remake due to contamination by alkaline phosphatase or a time delay. Try to use this solution as soon as possible, but you do have more than 2 hours to work.
6. Prepare the standard solution buffer by add ¼ of the total volume of the solution as lysis buffer, ¼ of the total volume of the solution as collagenase buffer, and ½ of the solution as pNPP solution buffer without pNPP added. This solution will match the standards with the sample conditions. **Note:** This is stored at room temperature on the chemical shelf and this solution should be bright yellow. If this solution is not bright yellow, there is probably and issue with the pH of your standard solution buffer.
7. Use the standard solution buffer to make a 3 mg/mL stock of p-nitrophenol (MW = 139.11). Dilute this p-nitrophenol stock to 0.25 – 0 mg/mL. I suggest 0.25 mg/mL, 0.125 mg/mL, 0.0625 mg/mL, 0.03125 mg/mL, 0.15625 mg/mL, 0.0078125 mg/mL, 0.00390625 mg/mL, 0.001953125 mg/mL, and 0 mg/mL (all standard solution buffer). This is an extended standard because you will see that the higher concentrations tend to saturate out.
8. Add 100 µL of standard solution to a half-well 96-well plate. The original assay uses a full well 96-well plate with all plated values doubled. However, I have had success with this half-well protocol which leaves 25 µL to analyze the DNA content which can be used to normalize the AP activity data. **Note:** Since p-nitrophenol is a product of the reaction when pNPP is catalyzed by alkaline phosphatase, the standard wells are completed when 100 µL of standard is added to the plate.
9. Add 25 µL of the lysis buffer to all sample wells.
10. Add 25 µL of the digested samples and wait 2 min for the lysing of cells.
11. Add 50 µL of the pNPP solution buffer with the added pNPP to all the sample wells. The total volume in the solution well is now 100 µL and matches those of the standards.
12. Measure absorbance at 405 nm every minute for 2 hours (kinetic) on the plate reader.
13. Analyze the data.

Quantitative Real-time Polymerase Chain Reaction (PCR) Protocol

RNA Isolation (Adapted from the Macherey-Nagel NucleoSpin RNA kit)

1. Wash hydrogels, pellets, or cells with PBS. Add 350 uL of Lysis Buffer (RA1). Disrupt with a large gauge needle. Vortex. For best results, combine 3 50 µL hydrogels (each hydrogel has 250,000 cells so the combination should be 750,000 cells). At this point, the samples can be frozen until they will be further processed.
2. Add 3.5 µL of β-mercaptoethanol and step through the rest of the MN Nucleospin RNA protocol (740955) as the handbook states until the elution step.

3. Prior to the 9th step of the protocol (Elution step), warm the heat block to 65°C. Warm DEPC water (RNase and DNase free). Elute RNA from the column with 40 µL of the warmed water. Allow the water to sit on the column for 1 minute before centrifuging the column at 11,000*g* for 1 minute. Place the flow through on the top of the column to pass through a second time. Again, Allow the water to sit on the column for 1 minute before centrifuging the column at 11,000*g* for 1 minute. At this point, keep samples on ice at all times.

Reverse Transcription (adapted from Applied Biosystems)

1. Prior to starting the protocol from the Applied Biosystems High-Capacity cDNA Reverse Transcription Kit (4368814 – 200 reactions), use the nanodrop to measure the RNA concentration of your samples (above 7 ng/uL is ideal). You should see a peak at 260, and your A260/A280 value should be around 2 for purified RNA. You will need to record all of these values so you can dilute all samples prior to qPCR.
2. Make sure to take out all of the tubes, except the reverse transcriptase, ahead of use (more than 2 hours) to thaw on ice. The random primers take a long time to thaw. Thaw the reverse transcriptase right before use.
3. Step through the protocol in the kit (all steps are done on ice). Prepare 2xRT Master Mix (recipe is in the kit). Add 10 uL of Master Mix to 10 uL of isolated RNA and mix the two solutions together. Also prepare samples with all of the same contents except the reverse transcriptase. This sample will be your -RT sample. Aim to have at least one -RT sample for each reverse transcription run. I usually choose two of the samples I run in the thermocycler to have a -RT sample. I usually have to do more than one group of reverse transcriptions for an experiment though so I will have more than those original two -RT samples. Replace the reverse transcriptase with water. I aim to have 2 or 3 samples for each treatment (+RT).
4. Centrifuge the samples briefly.
5. Place tubes into the thermocycler.
6. Set the thermocycler to 25°C for 10 minutes, 37°C for 120 minutes, 85°C for 5 minutes, and 4°C forever. There is a protocol on the thermocycler for this sequence called RT.

qPCR

1. Using the RNA concentration measured earlier (assuming 100% transcription to cDNA) figure out how to dilution the samples to 1 ng/uL and account for the facts that the measured samples were also diluted in master mix during the reverse transcription. Dilute samples with DEPC water (RNase and DNase free).
2. Centrifuge forward and reverse primers prior to opening. Reconstitute forward and reverse primers (100 uM) in DEPC water (RNase and DNase free) using protocol by Integrated DNA Technologies (IDT).
3. For each sample, 7.5 uL of 2x iQ SYBR green supermix, 1.5 uL of 5 uM Forward Primer, 1.5 uL of 5 uM Reverse Primer, 2.1 uL of DEPC water (RNase and DNase free), and 2.4 uL of Template will be used for a total of 15 uL. However, these samples are run in duplicate and extra should be made to allow for pipetting error of such small samples. It is best to make one tube with 2.25 times the original recipe. The recipe for the 2.25x is, 16.875

uL of 2x iQ SYBR green supermix, 3.375 uL of 5 uM Forward Primer, 3.375 uL of 5 uM Reverse Primer, 4.725 uL of DEPC water (RNase and DNase free), and 5.4 uL of Template will be used for a total of 33.75 uL.

4. Label tubes and add either 5.4 uL of +RT, -RT, or no template control (NTC). A no template control has 5.4 uL of water in place of the DNA template.
5. Turn off the lights in the lab before thawing the SYBR.
6. To prepare the Master Mix, calculate the number of samples you have. This number should reflect the number of treatments you have (each which will be multiplied for 2.25x). Add 1 or 2 extra samples to account for pipetting error. Mix the required amount of 2x iQ SYBR green supermix, Forward Primer, Reverse Primer, and DEPC water (RNase and DNase free). Always add the SYBR last.
7. Add 28.35 uL of master mix to each tube (+RT, -RT, or NTC) and mix well.
8. Centrifuge samples at 500*g* for 1 minute at 4°C.
9. Add 15 uL of each sample to a PCR plate and cover the plate with a plate sealer that is specific for qPCR.
10. Use the centrifuge in the cell culture room to centrifuge samples at 500*g* for 7 minutes at 4°C.
11. Put plate in the qPCR thermocycler. Follow instructions on the thermocycler. Assign a plate layout. Run the machine at 95°C for 10 minutes, 40 cycles of 95°C for 15 seconds (denaturation), 60°C for 15 seconds (annealing)* and 68°C for 20 seconds (extension), and then a melt curve analysis. *This number will need to be optimized for each primer. All treatments with a gene should be ran on one plate. Run the housekeeping gene first. Standard curves will need to run on all primers by run a dilution series on cDNA.

Peptide Synthesis (Adapted from Dr. Jenny Lin and Celina Twitchell)

1. Weigh out the appropriate amount of 2-Cl-Trt-CL (aim for 1g) resin into a 50 mL peptide synthesis vessel. It is careful not to get the resin stuck on the edges of the synthesis vessel. In addition, it is also important to store the resin at 4°C in a desiccator. Wash the resin with dimethylformamide (DMF) for 3 times for 10 seconds (5 mL) then do the same with dichloromethane (DCM). Finally repeat again with DMF.
2. Swell the resin in 5 mL of DCM and 5 mL of DMF for 1 hour and then drain.
3. Add 10 mL of 10.8% v/v hydrazine hydrazide 50-60% (NH_2NH_2) and 100 µL of N,N-Diisoproprylethaylamine (DIPEA). React for 2 hours, at room temperature, with bubbling of N_2 to agitate the resin.
4. Repeat, but react for 1 hour.
5. Wash resin with DMF for 3 times for 5 minutes (5 mL) with bubbling. Drain between each wash.
6. Add 10 mL of 10% v/v of methanol in DMF. Wait for 30 minutes.
7. Drain and collect some resin for Ninhydrin test.
8. Wash resin with DMF for 3 times for 5 minutes (5 mL) with bubbling. Drain between each wash.
9. Dissolve Glycine (or first amino acid to couple), hydroxybenzoltriazole (HOBt), and N,N,N′,N′-Tetramethyl-O-(1H-benzotriazol-1-yl)uronium hexafluorophosphate (HBTU) in DMF. (ex: 1.832 g glycine, 0.83 g HOBt, and 2.33 g HBTU. An excel in Liu Share

contains all of the information to calculate these amounts for amino acid required.) Some amino acids will require shaking to dissolve completely. Add the mixture to the resin.
10. Add 2.68 mL of DIPEA to the resin. Let it react for more than 3.5 hours with bubbling. This can be left overnight. This protocol is for Fmoc amino acids.
11. When the next amino acid is ready to be added. Add 33% piperidine and let it react with the resin for 30 minutes. The piperadine mixture should be made fresh after 1 week of use.
12. Wash resin with DMF for 3 times for 5 minutes (5 mL) with bubbling. Drain between each wash.
13. Dissolve the next amino acid, HOBt, and HBTU in DMF. Add the mixture to the resin.
14. Add 2.68 mL of DIPEA to the resin. Let it react for more than 3.5 hours with bubbling.
15. Wash resin with DMF for 2 times for 5 minutes (5 mL) with bubbling. Wash resin with DCM for 2 times for 5 minutes (5 mL) with bubbling. Wash resin with IPA for 1 times for 5 minutes (5 mL) with bubbling. Wash resin with DMF for 2 times for 5 minutes (5 mL) with bubbling. Drain between each wash.
16. Repeat for each subsequent amino acid.
17. Deprotect last amino acid with piperidine.
18. Wash resin with DMF for 3 times for 5 minutes (5 mL) with bubbling. Wash resin with DCM for 3 times for 5 minutes (5 mL) with bubbling. Drain between each wash.
19. Add 15 mL of cleavage cocktail composed of 88% trifluoroacetic acid, 5% phenol, 5% dH2O, and 2% triisopropylsilane to the resin. Let the solution bubble for 1 to 1.5 hours.
20. Collect the flow through.
21. Add 35 mL diethyl ether to precipitate out peptide.
22. Pellet the peptide (centrifuge at 900*g* for 10 minutes) and resuspend in between 30 and 40 mL of Milli-Q. Freeze overnight and freeze dry the peptide.
23. Purify the peptides using a Vydac C18 column on an ÄKTA Explorer 100 FPLC with a 0.1% TFA and acetonitrile gradient.
24. Confirm the molecular weight of peptide using matrix-assisted laser desorption ionization time-of-flight (MALDI TOF) mass spectrometry on a Voyager DE PRO analyzer.

Molecule Preparation and Purification

1. The collagen-binding peptidoglycan was synthesized using EDC (1-ethyl-3-[3-dimethylaminopropyl] carbodiimide hydrochloride) chemistry to conjugate the SILY peptide to a CS backbone with an amide bond.
2. Prepare a solution of 8 M urea and 0.05 mM EDC to activate the carboxyl groups on the CS backbone for 20 minutes at room temperature after the pH was adjusted to 4.5.
3. Functionalize the CS backbone by reacting 10% excess moles of the desired SILY peptide (either 10, 15 or 20) attachment for 2 hours with shaking.
4. Alter the pH to 8 to stop the reaction.
5. Purify the molecules using size exclusion chromatography on an AKTA FPLC (GE Healthcare, Piscataway, NJ) with Bio-Scale Mini Bio-Gel columns packed with polyacrylamide beads (Bio-Rad Laboratories, Hercules, CA) and then freeze dried.
6. Confirm the final concentration of peptide attachment to the CS backbone using a Nanodrop 2000 spectrophotometer (Thermo Fisher Scientific, Waltham, MA).
7. Create a standard of only the peptide you wish to attach.

8. Read the known concentration (actual) and record the measured concentration from the nanodrop. Prepare a 1 mg/mL solution of your molecule and read the measured concentration. Back calculate the actual amount of peptide attached.

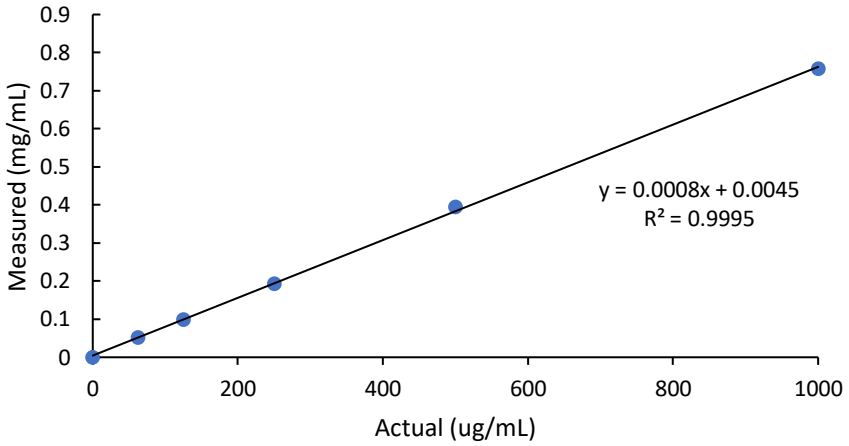

Figure 5-11. An example standard curve of hydrazide-SILY using a nanodrop.